Declaration

The presented thesis and the work contained in its contents has, unless otherwise indicated or referenced, has not been submitted previously for a degree at this or any other institution. All work included in this thesis has been performed entirely by the author.

Signed: _____

Date: _____

The investigation of germanium based compounds, transition metals and isoflavones within foods

By:

Stephen Dowling

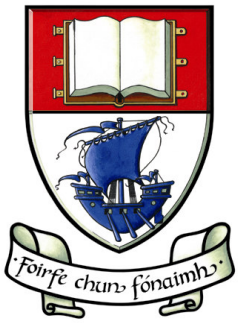

A dissertation submitted to the WIT for the degree of Doctor of Philosophy

November 2010

Under the supervision of

Dr. Helen Hughes, Waterford Institute of Technology and Prof. Fiona Regan, Dublin City University

Pharmaceutical and Molecular Biotechnology Research Centre

Waterford Institute of Technology

Waterford

Ireland

PMBrc

Acknowledgements:

I would like to thank all those who have contributed to this body of work. The tireless efforts of my two supervisors, Dr. Helen Hughes and Professor Fiona Regan. The support from my family, friends and all my colleagues from WIT and DCU over the years.

I would also like to thank Strand I and Enterprise Ireland for the funding for this project. Their funding was essential for all aspects of the work presented in this thesis.

This project has taught me much but also how little I truly know. Life is but a continually learning process.

To quote Oscar Wilde:
"Experience is simply the name we give our mistakes."

Abstract

The body of work here looks not only at how germanium was present in foods but also the ascertainment of chelation behaviour of germanium compounds and also transition metals with flavonoids. The chelation of germanium with flavonoids, or particularly isoflavones, is a completely novel area and gave some interesting results for chelation with isoflavones with transition metals, an area of research that was completely underexploited until recently. (refer to appendix 1)

The Fourier Transform Infrared (FTIR) analysis of foodstuffs for the presence germanium sesquioxide in food and soil and assigning interference bands from biomolecules that can hinder its' detection were carried out. Results found that the IR band from the carbon oxygen network (C-O-C) band in cellulose can interfere with determination of the germanium oxygen network (Ge-O-Ge) band from germanium sesquioxide. This interference hindered the detection of germanium sesquioxide in a food sample matrix. The Si-O band from silicates present in soil interfered with the determination of the Ge-O-Ge band also. The interferences found in this study make the detection of germanium sesquioxide difficult using FTIR spectroscopy.

Atomic Absorption Spectroscopy (AAS) of Cu, Pb, Fe and Ge in soil and food samples showed the variances of content of these elements in a biological matrix. The Ge levels in soil and food were 46.54 - 117.84 µg/g and 1.65 - 642.60 µg/g respectively. Fe, Pb and Cu levels in soil were 16062.03 - 21151.35 µg/g, 32.14 - 247.11 µg/g and 26.98 - 93.21 µg/g respectively. The soil samples are not significantly contaminated in relation to these elements and were within acceptable content limits. Fe, Pb and Cu levels in food were 11.88 - 841.75 µg/g, 0.95 -15.50 µg/g and 2.72 - 18.76 µg/g respectively. The Pb levels in food were mainly quite low and did not pose any hazard to human health. The iron and copper levels were found to be within acceptable nutritional parameters.

UV/Vis spectroscopy of isoflavone metal chelates revealed that biochanin A and gensitein chelated with both Cu(II) and Fe(III). Daidzein did not chelate with any of the studied metals. None of the studied isoflavones chelated with Ge(IV) compounds, germanium dioxide or germanium sesquioxide. The Metal/Ligand (M/L)

stoichiometries of Fe(III) chelates with genistein and biochanin A were 1:2 and 2:1 from pH of 4.0-9.0. The Metal/Ligand (M/L) stoichiometries of Cu(II) isoflavone chelates with genistein and biochanin A were 1:2, 2:1 and 2:3 at a pH of 4.0-9.0.

The copper and iron chelates were synthesised and characterised by elemental analysis, FTIR, thermogravimetric analysis (TGA), proton NMR spectroscopy and electrospray ionisation mass spectrometry (ESI-MS). These studies indicated a 1:2 M/L stoichiometry and suggested the isoflavones bind with the metals at the 4-keto and the 5-OH site. The NMR results were inconclusive with noisy signals observed for the iron chelates and no shifting in the proton peaks themselves.

2,2-diphenyl-1-picrylhydrazyl (DPPH) inhibition assays showed that copper isoflavone chelates have higher antioxidant activity than free isoflavones while the iron isoflavone chelates showed pro-oxidant activity compared to the free isoflavone. Synergistic DPPH studies with 0.02 mM ascorbic acid revealed copper chelates exhibit reduced antioxidant activity versus free isoflavones whereas the iron chelates showed lower pro-oxidant activity except at a concentration of 1.0 mM.

Chapter 1: Introduction:

The investigation of flavonoid metal chelates in foods.

1.1 Introduction

Traditional Chinese medicine has been in existence for several thousand years. The advent of scientific method saw developments in Chinese medicine using the logic and thoroughness provided by scientific evaluation of a medicinal substance [1]. Chinese herbs such as Panax Ginseng have seen sales of $98 million alone in the US per annum. Panax Ginseng has been associated with immunomodulatory activity such as anti-cancer, anti-microbial and blood sugar reduction. These claims have been substantiated in a small number of studies such as improvement in cognitive functions and reduced blood sugar levels in type II diabetics [2].

Antioxidants are used in the body to mediate damage caused by oxidative stress caused by free radicals, leading to conditions such as cancer. Antioxidants can be obtained from the diet, such as in vitamin C and vitamin E, or they can form key parts in the activity of an enzyme such as selenium in glutathione peroxidase [3,4]. Antioxidants have the ability to mediate a range of oxidative stress in induced disorders such as diabetes, hypertension, influenza and pneumonia to mention a few [5].

Cancer is a disease that is responsible for the development of tumours due to abnormal cell growth and differentiation in human tissue. The cause of the disease is a multitude of factors such as diet, toxic material exposure, irradiation, genetic predisposition and carcinogenic chemicals. The disease itself results from multiple genomic modifications including the recessive tumour suppressor genes and changes in the dominant oncogenes [6]. The oncogene is the gene responsible for the transcription of the oncoprotein that causes a disruption in cell self-regulation. This creates an abnormal stationary site that leads to initiation of malignant tumour creation [7].

Flavonoids are benzo-γ-pyrone derivatives or polyphenol compounds that have shown the ability to chelate with a number of metal ions including copper, iron and aluminium. Flavonoids show a variety of different stoichiometries with these metals with potential metal/ligand ratios in the region of 1:1, 1:2 and 2:3. The chelation of

these metals with the flavonoids has a number of applications including potential chelation therapy for Wilson's disease (copper overload disorder), the remediation of iron-induced lipid peroxidation and enhanced antioxidants [8-10].

1.2 Antioxidants

An antioxidant can be defined as 'any substance that when present at low concentrations compared with those of an oxidisable substrate, significantly delays or prevents oxidation [11]. Antioxidants are the body's defence against free radicals. They can be enzymes or high and low molecular weight molecules. They neutralize free radicals by donation of one of their own electrons i.e. they act as a reducing agent. This does not lead to the antioxidant itself becoming a free radical as it is stable in either an oxidised or a reduced state e.g. if during a cyclic voltammetry that both oxidation and reduction potential peaks of equal magnitude were noted. The range of antioxidants available can be classed as carotenoids, ascorbic acid, flavonoids and polyphenols [12]. Germanium can be viewed as an antioxidant in the form of germanium sesquioxide. Otherwise, germanium is regarded as a non-essential nutrient in the body [13].

Antioxidants have been used in the treatment of a range of diseases such as cancer, cardiovascular disease and diabetes to mention but a few. Research has shown that fruit and vegetables are rich in antioxidants and can lower cancer risk in the host. The relationship of cancer risk is inverse to that of fruit and vegetable consumption. [14]

1.2.1 Carotenoids

Carotenoids are non-polar compounds that can be sub-divided into two classes: a) carotenes that only possess carbon and hydrogen and b) xanthophylls that are oxygenated hydrocarbon derivatives that have an oxygen function such as keto, hydroxy etc. Their structural formula is normally a conjugated double bond system (see fig. 1.1). This influences their chemical and physical properties [15].

Carotenoids are important in the human diet as they are used as pigmentation, immuno-stimulants and antioxidants. A lack of carotenoids can be caused by environmental stress causing loss of colour in the host e.g. greying hair [16]. Carotenoids have also shown photoprotective properties by enhancing the epidermal defence against UV-induced damages such as erythema. Cesarini *et al.* [17] reported the oral intake of carotenoids like β-carotene increased skin resistance to erythema by 20% ($P = 0.01$). This has the benefit of slowing UV-induced aging and reducing the risk of skin cancer.

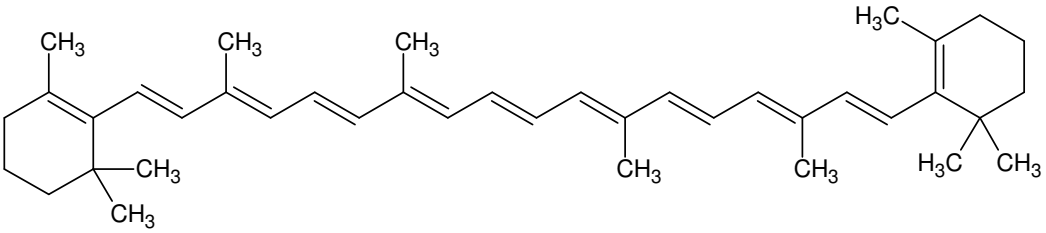

Fig. 1.1 Beta-carotene structure, a typical carotenoid.

Marco *et al.* [18] reported using carotenoids in the improvement of growth and development of crustaceans such as crayfish *Cherax quadrucarinatus.* Their diet was enhanced with supplements of carotenoids and retinoids such as β-carotene and vegetable oil.

Colgan *et al.* [19] used fruit and vegetables in a low fat diet to establish this effect on plasma lipoprotein and carotenoid metabolism. The study was done to establish if fruit and vegetable intake with a plant sterol enriched diet can prevent loss of carotenoids in blood plasma. It was found that plant sterol enriched diets had no effect on carotenoid concentrations such as retinol and α-carotene.

1.2.2 Polyphenols

Polyphenols are a large group of natural and synthetic small molecules that are composed of one or more aromatic phenolic rings (see fig. 1.2). They are found in high concentrations in substances such as wine, tea, nuts, berries and cocoa. Polyphenols can be subclassed into groups like vitamins, phenolic acids and flavonoids to name but a few [20]. Polyphenols act as reducing agents due to their hydrogen donating ability (as a result of their hydroxyl groups) and their chelating abilities. This ensures high reactivity with free radicals such as superoxide anions O_2^-,

hydroxyl anions and other free radical species. This facilitates phytochemical properties such as anti-inflammatory, antiallergic and antimicrobial effects [21].

Yahiro *et al.* [22] used polyphenols for inhibition of *helicobacter pylori,* a bacteria that is responsible for gastric damage by increasing acidity levels in the stomach. Hop bract extract was used to inhibit the microbe. It was concluded that the hop bract extract may suppress the helicobacter microbe making it potentially viable as an agent for treating the disease.

Madhan *et al.* [23] have reported collagen stabilization using plant polyphenol, catechin (see fig. 1.2). The studies show improvement in collagen thermal stability with a shrinkage temperature of 70 ^{0}C when treated with catechin. It was hypothesised that the catechin increased the degree of hydrogen bonding between the fibres. Ivanova *et al.* [24] examined the use of plant polyphenols on suppressing phagocytes in influenza infected mice. The polyphenol complex was extracted from the plant *geranium sanguinem* L. The application of the polyphenol extract suppressed the activity of the influenza phagocytes and other macrophages for 3 hours in the infected mice.

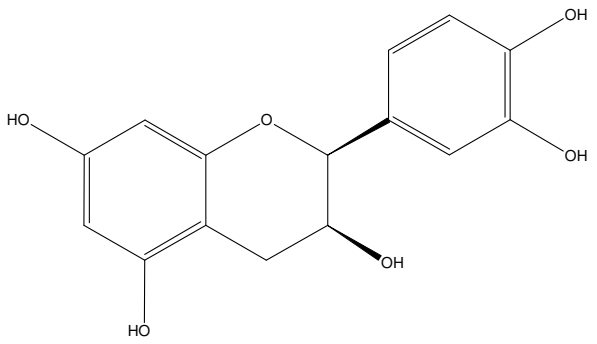

Fig. 1.2 Catechin, a plant polyphenol.

1.2.3 Flavonoids

Flavonoids are "a group of hydroxylated benzo-γ-pyrone derivatives widely distributed throughout the plant kingdom." They take their name from the latin term *flavus* meaning yellow. An example of a flavonoid would be quercetin, as shown in Fig. 1.3. They have a range of effects that are similar to other polyphenolic based

molecules such as antimicrobial, antioxidant and cytotoxic. Their properties are dependant on their level of free radical scavenging or metal chelation [25].

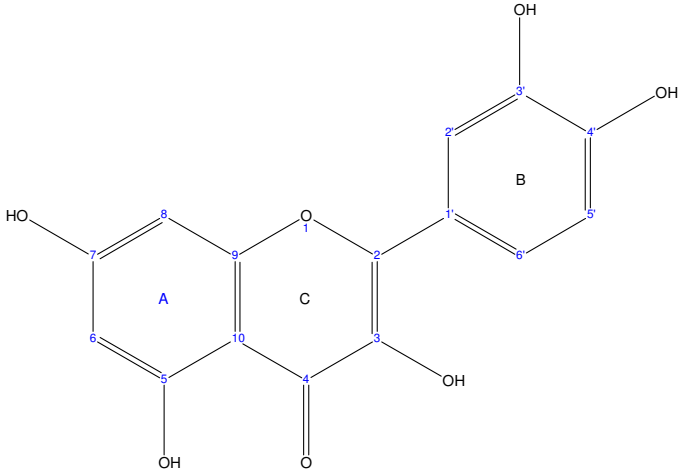

Fig. 1.3 Structure of quercetin.

There are many different types of flavonoid based upon modification of the flavonoid nucleus by processes such as polymerization, substitution of functionalities on the nucleus (see fig. 1.3) and photochemical reactions. The main structural variations of flavonoids are anthocyanidins, catechins, flavones, flavonols, flavanones and isoflavones. The next biggest modification of the flavonoid nucleus is the attachment of sugar moieties or glycosides to the structure. Flavonoids without this sugar group are called aglycones but these are rarely found in nature with the exception of catechins. The glycoside group has the ability to increase the hydrophilicity of the flavonoid. It is commonly found on the C-3 position of the flavonoid molecule [26].

The electron scavenging abilities of flavonoids can be attributed to the following groups in their structure; 1) an ortho-dihydroxy (catechol) structure in the molecule creates delocalization, 2) a double bond in conjunction with a ketone group, and 3) hydroxy groups in the ring structure can provide hydrogen bonding with the ketone group [27]. These groups also have the ability to chelate with metals such as copper, iron and aluminium. The chelation with these metals can lead to increases in the antioxidant ability of certain flavonoid species moreso than their uncomplexed counterparts [10,28].

Bucki *et al.* [29] looked at the flavonoid inhibition of platelet procoagulation activity for cardiovascular protection. Quercetin and catechin were used to reduce the phosphatidylserine levels in the blood stream responsible for platelet procoagulation. These flavonoids work by inhibition of the phosphoinositide kinases that create phosphatidylserine.

Kostyuk *et al.* [28] looked at flavonoid protection against asbestos-related cell injury. In his study, he used Fe^{2+}, Fe^{3+}, Cu^{2+} and Zn^{2+} metals in combination with rutin, and green tea epicatechins among others to see if they could protect peritoneal macrophages from asbestos damage. It was found that the metal complexes of the studied flavonoids in most of the studies had better free radical scavenging abilities than their free flavonoid counterparts. They later speculated that considering foods contain the same types of elements and flavonoids, it would be reasonable to assume that the nutritional quality of the foods would be enhanced with the flavonoid metal complexes present.

1.2.4 Germanium

Germanium can be found in nature in a variety of plants, such as tomatoes, and onions and animals in trace quantities. In the host it has beneficial effects such as immuno-enhancement, oxygen enrichment, anti-inflammatory and anti-tumour properties. The diseases it is effective against are cancer and arthritis among others [30]. The active agent in these foodstuffs is referred to as carboxyethylgermanium sesquioxide or Ge-132 (see fig. 1.4). This compound is linked to production of interferon, killer T cells and augmentation of Natural Killer (NK) cells [31].

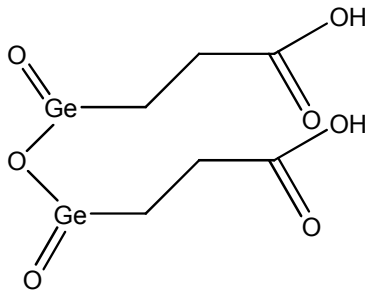

Fig 1.4 Germanium Sesquioxide or Ge-132

Organogermanium has also been shown to enhance the health/growth of some plant species. Yu *et al.* [32] reported seeing enhanced crop growth in ginseng, a plant that contains Ge-132. With just 60 ppm of organogermanium, a fresh biomass accumulation of 565 ± 6g was achieved.

Germanium antioxidants, such as propagermanium (refer to fig. 1.5), induce interferon production in the body. It also activates natural killer cells, macrophage, and neutrophiles as observed by Tsutsumi *et al.* [33] in the 10 patients studied.

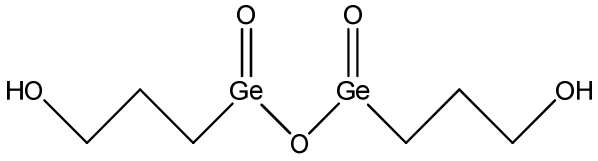

Fig. 1.5 Propagermanium structure

LeMaster *et al.* [34] reported the use of Ge-132 for treatment of osteoporosis in rats. The observations found were that the rats' transverse strength in the femur bone was enhanced when given Ge-132. It was concluded that Ge-132 prevents decreased bone strength and maintains bone mineral mass.

Lee *et al.* [35] also investigated the anti-inflammatory activity of germanium concentrated yeast and found it could inhibit prostaglandin E_2 and arachidonic acid in rat paw oedema. The results of the study showed that the anti-inflammatory activity of germanium concentrated yeast was partly responsible for arachidonic acid release.

1.3 Antioxidants in foodstuffs

Many foods such as fruit and vegetables are rich in antioxidants such as flavonoids and carotenes. Current nutritional theory agrees that a healthy diet is based on a balanced intake of fruit and vegetables to enhance health and well-being in the human body [19,36,37]. Plants form the basis of herbal remedies such as ginseng. The world health organisation has estimated that ~80 % of the earth's inhabitants rely on herbs as medication [38].

Antioxidants come from various substances in the soil that make their way into the food chain through uptake of nutrients by plants consumed by animals and so forth. Selenium occurs commonly in the Earth's crust and is taken up by plants as selenate or organic selenium. In animals where there is a selenium deficiency in the soil, diseases such as muscular dystrophy and hepatosis dieticia occur. It can also prevent cancer in animal species that exist in selenium rich environments. Human heart disease is also down in these areas [39].

The British nutrition foundation did a study in 2001 to evaluate antioxidants in food. The objectives were to determine signs/biomarkers of oxidative stress in the subjects, bioavailability and metabolism of the antioxidants and their mechanism of action. The results of this study were that there was no conclusive improvement in cardiovascular disease when the subjects were given antioxidants such as β-carotene and ascorbic acid. It also showed a number of uncertainties in relation to establishment of biomarkers for these diseases [35,40].

1.3.1 Ginseng

Some claim that ginseng is an herb that is beneficial to health in terms of restoring energy and increasing mental and physical abilities [41]. It was used by the Chinese in medicinal remedies for thousands of years and has recently become more popular in the West. The pharmacological mechanism of ginseng is unclear but it may have to do with the ginsenosides (a steroid like molecule) activating steroid receptors in the body [2].

Ginseng can be found in a variety of places like in parts of Asia, America and even Siberia. This positive impact on health has been recognised when it is used as a dietary supplement and a food additive. Its growth is dependent on age, location/population, light, soil conditions and root dry weight [42].

The pharmacological effects are attributed to ginsenosides, a diverse group of steroidal saponins. This gives it a wide variety of pharmacological effects including neuron protection, tumour inhibition and immunomodulatory effects. Attele *et al.* [41] reported seeing ginsenosides creating an enhancement in memory and learning in rats leading to an increase in production of acetylcholine from the hippocampus. The enhancement in memory was also symptomatic in the form of an increase in membrane fluidity in the cortical cells and a reduction in [Ca^{2+}] levels in the brain which is shown to increase with the onset of age in rats.

The ginsenosides (steroidal compounds) or active agents within ginseng were investigated by Lei *et al.* in relation to how they can restimulate the growth of ginseng callus. The group was trying to address the agrotechnical issue known as the "replant problem" where a 30 year wait was required for soil involved in growth of ginseng callus. The group looked at total ginsenosides, panaxadiol ginsenosides, panaxatriol ginsenosides and ginsenosides-Re in terms of their superoxide dismutase (SOD) activity, growth and also their effect on malondialdehyde (MDA) content, a primary constituent for healthy soil. The groups found the use of increasing concentrations of ginsenosides had an inhibitory effect on growth whereas increasing levels of ginsenosides up to 100 mg/L had an enhancing effect on SOD activity. The group concluded that the ginseonosides used in this study were inhibitory towards ginseng callus growth overall [43].

1.3.2 Tomatoes

Tomato is a key vegetable for daily dietary intake as it possesses antioxidants such as lycopenes. The consumption of lycopene is inversely related to the risk of cancer development such as prostate and pancreatic cancer. Other antioxidants in tomatoes are vitamin C and E but also beta-carotene, flavonoids and phenolic substances [44].

Toor *et al.* [45] performed a study of the different fractions of tomatoes to assess their levels of antioxidants such as lycopene. The skin, seeds and pulp of the tomato were analysed to this effect after being grown in a hydroponic facility in New Zealand. Based on actual fresh weights of the tomato, they found that most of the antioxidants were present in the seeds and the skin of the tomato. The greatest ascorbic acid content alone can be found in these areas of the tomato. Thus the level of antioxidant content is dependant on the fraction consumed.

Tomatoes were assessed for their total antioxidant activity during thermal processing by Dewanto *et al.* The study looked at the effect of thermal processing on antioxidant activity not just on vitamin C, which only accounted for part of the antioxidant activity, thereby taking into account the rest of the phytochemicals present in the tomatoes. At 88 ^{0}C for 2, 15 and 30 min periods, they found that the lycopene antioxidants became more bioavailable making them better for human consumption. Overall the study found that the total antioxidant activity went from 28.1 to 62.2 % over the 2 to 30 min thermal processing period [46].

Antioxidant activities of tomatoes vary from species to species with respect to their colour as was determined by Melendez-Martinez *et al.* The group examined tomato species such as *S. pimpinelifolium* and *S. lycopersicum*. The levels of rutin, chalcone naringenin and chlorogenic acid were assessed as these were the most potent antioxidants present within the tomatoes. They found the antioxidant concentration levels varied according to the degree of ripeness of the fruit e.g. chalcone naringenin. The in vitro antioxidant activities for the extracts were found to be highest with the methanol extracts and from the ripest tomatoes. Other extracts at other degrees of ripening were found not to have the same activity [47].

1.3.3 Garlic

Garlic has been used in herbal medicine for centuries to treat a variety of ailments such as hypoglycaemia, hypertension and microbial infections. [48] Garlic has been found to contain phenyl propanoids, diallyl sulphide, s-ethyl cysteine and n-acetylcysteine [49].

Balasenthil *et al.* [50] studied the effects of garlic on dimethylbenzanthracene (DMBA) induced Hamster Buccal Pouch Carcinogenesis. Garlic was used for its' cancer inhibition properties. The DMBA was smeared onto the buccal pouches of the hamsters and left for 14 weeks so as to develop oral tumours. One group of hamsters were administered 250 mg/kg body weight doses of garlic extract. The garlic fed hamsters had suppression of the oral cancer caused by DMBA. This highlighted the chemopreventive properties of garlic.

Another application of garlic is the use of garlic oil in the treatment of dyspeptic patients as reported by McNulty *et al.* [51] Helicobacter pylori, the cause of dyspepsia, was shown to have resistance to garlic oil in an in vitro study. It was tested in vivo using dyspeptic patients who had helicobacter pylori. However, the study found that the garlic oil was not effective at a dosage regimen of one garlic oil capsule 4 times daily to eradicate H. Pylori. The study recommended use of alternative dosage regimens or forms of administration for the garlic oil in light of these findings.

The antioxidant functions of E- and Z-ajoene from Japanese Garlic were assessed by Naznin *et al.* The group determined that the antioxidant activity of the Z-form was higher than the E- form. This was confirmed via DPPH inhibition studies from the concentration range of 0.2 to 1.0 mM. It was noted that during the incubation of the E and Z diastereomers, with nitro blue tetrazolium (NBT) superoxide anion, that after 80 min, no antioxidant activity could be observed whatsoever. The optimal time for the superoxide anion incubation was found to be 40 min with inhibition values of 1.9 and 4.8 % respectively for NBT [52].

1.3.4 Onion

Shon *et al.* [53] have studied the "antimutagenic antioxidant and free radical scavenging activity of ethyl acetate extracts in white, yellow and red onions". Flavonoids and phenolic acids were found to be the main substances. They were found to be the most potent in antimutagenic activity. This is due to the phenolic hydroxyl group in all species having a strong electron scavenging ability.

Onion extract has been used in the treatment of scar tissue in a series of scar treatment products. Onion extract is supposed to have anti-inflammatory, bacteriostatic and

collagen enrichment properties. This information is in dispute after studies performed to investigate the dermal regenerative properties of onion extract. One such study involved the double blind trial of evaluating 97 patients with new and old scar tissue. The patients did not see any healing of their scar tissue in particular but did notice a softening of their scars after 2 months of topical administration [54].

The antioxidant and antimicrobial activity of crude onion (Allium cepa, L.) extracts was assessed by Santas *et al.* Three Spanish onion types were extracted using 75 % methanol, evaporated to dryness and then further extracted into ethyl acetate and water. It was found that the ethyl acetate (hydrophobic) subfraction possessed the higher amounts of flavonoid. The antioxidant activities for both the 3 onion varieties showed no major difference in antioxidant capacity except for the Grano de Oro variety where it showed Trolox Equivalent Antioxidant Capacity (TEAC) of 74.86±1.77 μmol Trolox g^{-1} D.W. The rest of the antioxidant capacties for the onion extracts were in the range of 0.38 ± 0.01 to 74.86 ± 1.77 μmol Trolox g^{-1} D.W. [55].

1.3.5 Soybean

Soybean is a leguminous type of plant that is the most abundant source of phytoestrogens known as isoflavones. It is also a rich source of protein and fat and is the primary constituent of the Asian diet. 20-80 g of soy products are consumed by Asians on a daily basis. Soy products come in many different forms including soymilk, soya mince and soya flour. Soy products have been associated with reducing the risk of a number of hormonally induced cancers such as breast and prostate cancer. The biological activity within soybean is mainly attributed to isoflavones [56-58].

Soybean products were examined for extraction efficiencies by Achouri *et al.* The group compared the extraction of soybean products with acetonitrile-HCl, methanol and ethanol. The extraction efficiencies for the isoflavones as determined via HPLC were 74 %, 69 % and 65 % respectively for the solvents. Sonication versus sequential extraction was also evaluated and it was found that 15 min of sonication gave comparatively the same yield as 5 sequential extractions [59].

The antioxidant activity of the soybean matrix can be enhanced using food additives as was examined by Singh *et al.* This study involved the comparison of trichoderma

harzianum NBRI-1055-fermented soybean to that of unfermented soybean. The group extracted the trichoderma fermented soybean and unfermented soybean using water and methanol solvents. They found that the trichoderma soybean water extracts had the highest free radical scavenging ability along with other factors such as total flavonoid content and lipid peroxidation [60].

Soybean has also been used in infant foodstuffs and their isoflavone content was evaluated by P.A. Murphy *et al.* The group looked at a range of infant formulas from the Balitmore (east coast), Ames (Midwestern) and San Francisco (west coast) areas of the USA. The group found that the total amount of isoflavone content within the foodstuff was determined to be 214 to 285 μg/g [57].

1.4 Extraction of flavonoids from food

Extraction of antioxidants is determined by the antioxidant molecules that need to be extracted. Selection of an optimal extraction procedure can increase antioxidant concentration relative to the material it was extracted from [61]. This makes the selection of the extraction procedure most important. The conditions that can be varied include the use of solvent mixtures, temperature modification and even ultrasonic treatment [62].

Commonly used extraction techniques for flavonoids from foods can include solvent extraction, enzyme extraction, preparative HPLC and solid phase extraction [63-66]. A collective appraisal of these methods will allow a decision on the optimal one for flavonoid extraction from foods.

1.4.1 Solvent extraction of flavonoids

The extraction of flavonoids from defatted soya product, namely isoflavones can be achieved by the use of solvent extraction by a variety of solvents such as acetonitrile, acetone, ethanol and methanol mixed with either 0.1N HCl or deionised water or both [57,63].

Juntachote *et al.* [67] reported response surface methodology to the production of phenolic extracts in herbs such as lemon grass and rosemary. Response surface methodology is a chemometric technique using a sequence of designed experiments based upon mathematical and statistical techniques based on the fit of a polynomial equation to the experimental data [68]. This involved using different solvent ratios of ethanol and water, adjustment of extraction temperature and extraction time. The group found that the ethanol:water ratio had a significant impact on extraction yield of phenolics. Extraction time also had an impact on the extraction yield. It was found that the optimal conditions for total phenolic extraction in lemon grass and rosemary were an ethanol:water ratio of 3:1 at 75 ^{0}C. The extraction time was 30 min for rosemary and lemon grass and 90 min for galangal and holy basil. The extraction yields for the total phenolics tended to vary between 20 – 40 %.

Santoso *et al.* [69] used methanol extraction of anti-oxidants from Indonesian seaweeds in a fish oil emulsion system. The methanol extracts of the seaweeds were analysed in relation to their antioxidant abilities using a peroxide value (POV) system via an iron catalyst. The iron catalyst was used to stimulate lipid induced peroxidation in the fish oil emulsion. The polyphenol antioxidants from the seaweeds would be used to mediate this process. The POV tended to vary among different species of Indonesian seaweed. The methanol extraction itself was not modified to obtain optimal yields of polyphenols from seaweed but instead to evaluate the antioxidant ability.

Row *et al.* [70] reported the use of solvent extraction for catechin compounds in Korean tea. They focused on optimising parameters such as extraction solvent composition, extraction time and temperature. They found that the recovery was much improved when the extraction temperature was 80 ^{0}C. The extraction time was set at 15 min as anything beyond this time resulted in epimerisation of the catechins,

compromising their structure. The solvent extraction was chosen to be the best method as it achieved higher catechin purities than supercritical extraction. Water was the solvent for solvent extraction as it was more environmentally friendly and stable at a number of different operating temperatures.

1.4.2 Enzyme extraction

Li *et al.* [64] experimented with the extraction of phenolic antioxidants from citrus peels using enzymes. The citrus peels were derived from grapefruit, mandarin, Yen Ben lemon, Meyer lemon and orange. Conditions affecting the phenolic yield during enzyme extraction were peel condition, reaction temperature, enzyme type and citrus species. Extraction yield was highest using Celluzyme MX in water at about 65.5 %. The total phenolic content was found to be greatest at 80 ^{0}C. This was attributed to the heating of the cell walls of the citrus peels releasing more phenolics than enzyme degradation. It was speculated that the enzymes did have an effect at the lower temperatures of 19 – 37 ^{0}C and can aid extraction until inactivation past 37 ^{0}C. The optimal extraction time was 6 h with no improvement in recovery observed beyond this time.

Ferruzzi *et al.* [71] applied enzyme extraction to the analysis of catechins by enzyme assisted extraction. Pepsin was the enzyme used for the extraction and showed the highest recovery rate of catechins at 89 – 102 %. This recovery was the best in comparsion to acid precipitation (20 – 74 %) and methanol extraction (78 – 87 %). Milk content in the milk tea solutions also affected the % recovery with the highest recovery, 100 %, being seen in samples with 0 % milk i.e. an inverse relationship between milk content and recovery.

1.4.3 Preparative HPLC

Sudjaroen *et al.* [72] performed semi-preparative HPLC on Tamarind seeds that contained phenolic antioxidants in tandem with organic solvent extraction. The method involved 5 g of freeze-dried Tamarind seeds that were extracted with hexane over a 3 h period to remove lipid interferents. The extract was fed onto an Agilent 1100 liquid chromatograph fitted with an octadecyl preparative LC column. The extraction solvent systems that were utilised were methanol and an acetone methanol:acetic acid mixture using a soxhlet extraction system. The methanol

extraction system was found to have the higher yield of procyanidins while the acetone methanol:acetic acid system gave a lower yield of procyanidins but an enhanced yield of their oligomers. The preparative column gave enhanced purity of the phenolic components in the extract.

Owen *et al.* [65] studied how to isolate and analyse phenolic and flavonoid compounds in brined olive drupes. The isolation of these antioxidants involved purification by semi-preparative HPLC. The analysis made use of methanol extraction following input onto a preparative column. The study was able to evaluate that there was 1.64 % and 0.448 % dry weight phenolic content in black and green olive drupes. The extracts revealed contents of a number of phenolic compounds such as simple phenols and a variety of flavonoids such as procyanidin. They also ascertained that 3 to 10 mg of each compound was extracted for every 100 g of black olive pericarp seed in a very high purity.

Salo-Vaananen *et al.* [73] developed a method that allowed simultaneous HPLC analysis of lipophilic vitamins in animal products after small-scale extraction. Vitamins present in these meat products were tocopherols, retinols and cholecalciferol. In the case of fish extracts, purification would take place using normal-phase HPLC. The recoveries of samples spiked with the vitamins were found to be 80 – 111 %. The repeatability was found to be between 5 – 7 %. The best preparative column for the separation of the lipid-soluble vitamins was a µPorasil column with 10 µm particle size as it proved the most stable for vitamin separation and showed the lowest variation of 0.6 - 2.7 %.

1.4.4 Solid Phase Extraction

Dopico-Garcia *et al.* [66] utilised solid phase extraction of phenolic and phosphate antioxidants present in aqueous food simulants. The solid phase extraction of the antioxidants from the simulants was performed with a silica C_{18} cartridge. These extracts were later identified and quantitated by high performance liquid chromatography with a diode array detector. The antioxidants were derivatised so as to improve adsorption of the antioxidants in SPE. Phenol acetylation with acetic anhydride in the presence of carbonate/hydrogencarbonate is an example of one of the

derivatisations performed. Antioxidant recovery was in the range of 69 – 88 %. This was concluded to be due to the variable nature of the derivatisation reactions.

Solid phase extraction of antioxidants using Molecularly Imprinted Polymers or MIPs was performed by Bruggemann *et al.* [74] This involved the creation of MIPs from antioxidants butylated hydroxyanisole (BHA), butylated hydroxytoluene (BHT) and propyl gallate (PG). The PG-MIP column in particular was applied for the solid phase extraction of antioxidant spiked apple juice. The selectivity factor (α) for BHA from the control polymer (CP) was found to be in the region of 1.12 with highest selectivity seen in the BHT-MIP with 1.47. The PG MIP showed selectivity of 1.24. This highlights the effectiveness of MIP technology for isolation and purification of antioxidants from fruit juices.

Rochfort *et al.* reported the isolation and purification of glucoraphanin [75] from broccoli seeds by solid phase extraction and preparative HPLC. The group used hot aqueous extraction coupled with SPE followed by preparative HPLC. The crude glucoraphanin solution was passed through 2 types of SPE cartridge, a C18 and an amino propyl cartridge. The C18 column removed the organic impurities and the amino propyl cartridge retained the glucosinolates until it was eluted with 2 % ammonia in methanol. This was followed by preparative HPLC purification. The pure glucoraphanin yielded from the broccoli seeds was 0.6 % relative to the seed mass. The recovery of the glucoraphanin was not stated as there were no appropriate reference standards for their determination.

1.4.5 Selection of extraction method suitable for flavonoids

The extraction techniques reviewed vary in terms of extraction yield, degree of complexity and equipment required. Catechin compounds for example can exhibit high recoveries with solvent extraction where Row *et al.* managed to get very close to 7.65% content of catechins in green tea [70]. The extraction method for this project would most likely be solvent extraction utilising techniques such as stirring and sonication of sample at a set temperature for a fixed period of time that would allow the maximum yield of extract for flavonoids and potentially any metal complexes they had formed within the foodstuff matrix. Another advantage of using this technique is

the equipment needed is inexpensive and a large number of extractions can be conducted at the same time [57,63,67,69,70].

This technique could then be coupled with preparative liquid chromatography at a later stage when extraction yields have been optimised with each fraction being assessed for flavonoid and metal content along with mass spectrometry of the fractions. Using this methodology and a comparison to literature mass spectrometry values for flavonoid metal complexes, it should be possible to establish what percentage of the foodstuff is attributable to the flavonoid metal complexes [65,72,73].

1.5 Analysis of Flavonoid Metal Chelates

1.5.1 ESI-MS analysis

The ESI-MS of isoflavones has been quite well established with the HPLC analysis of isoflavone extracts from plants and other biological samples through ESI-MS systems [65,76,77]. What has not been as well documented is the analysis of flavonoid metal chelates via ESI-MS. These normally involve looking at flavonoid metal chelates of Cu(II), Fe(III), Fe(II) and Al(III). They also have to bypass the normal HPLC parameter in favour of utilising non-HPLC column methodologies such as direct sample injection at small µL/min concentrations to avoid destabilisation of the complex on the column.

The M/Z values in ESI-MS spectra are useful in identifying fragmentation ions but also in identifying fragmentation patterns associated with flavonoid ligands and metals chelated to them or adducts on the metals other than the ligand as was found by Pereira *et al.* [78] in their extensive characterisation of Cu(II)naringin complex. They compiled the following table of M/Z ions and corresponding compounds that might explain what was seen in the Mass Spectrum. (See Table 1.1)

Table 1.1 A table of M/Z values from ESI-MS analysis of Cu(II)Naringin Complex [78].

Nominal *M/Z*	**Structure**
581	Naringin+H^+
603	Naringin+Na^+
619	Naringin+K^+
641	Naringin-H^++$^{63}Cu^{2+}$
643	Naringin-H^++$^{65}Cu^{2+}$
673	Naringin-H^++$^{63}Cu^{2+}$+CH_3OH
675	Naringin-H^++$^{65}Cu^{2+}$+CH_3OH
705	Naringin-H^++$^{63}Cu^{2+}$+2CH_3OH
707	Naringin-H^++$^{65}Cu^{2+}$+2CH_3OH
933	Doubly charged: 3 Naringin-2H^++2$^{63}Cu^{2+}$
1183	2 Naringin+Na^+
1222	Doubly charged: 4 Naringin – 2H^++ $^{63}Cu^{2+}$+Na^++K^+

M/Z ratios can also be used to ascertain the stoichiometry of a flavonoid metal complex as dictated by Deng *et al.* [79] who performed an extensive study on aluminium(III)-isoflavone metal chelates with the flavonoids kaempferol, biochanin A and quercetin. The M/Z ratios proved most useful in the case of ascertaining the validity of 1:2 or 1:1 stoichiometries with the stated flavonoids. (see fig. 1.5).

As can be seen in fig. 1.6, the peak with the greatest relative intensity was found to be the M/Z 593 peak for the biochanin A:Al(III) 1:2 metal complex or $[AlL_2]^+$. This clearly dwarfed the other peak for the 1:1 complex $[AlH(L)]^+$. The same can be said of the other Al(III) flavonoid metal complexes. The chelation site cannot be inferred from UV/Vis spectra, only the stoichiometry. This makes ESI-MS a better choice for structural analysis [79]. The parameters for the analyses normally involve the preparation of the flavonoid having a molar excess of metal salt when the complex solution is mixed [9,78,80].

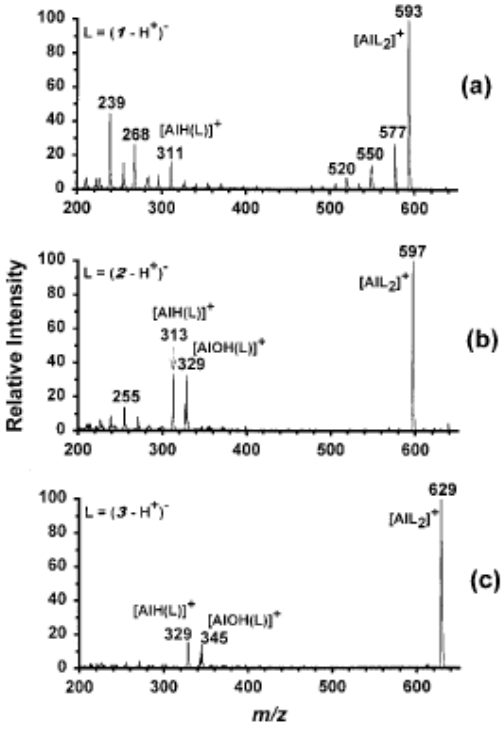

Fig. 1.6 ESI-MS chromatograms of biochanin-A (a), kaempferol (b) and quercetin (c) which were all obtained via chelation with Al(III) [79].

1.5.2 Vibrational analysis

Infrared (IR) spectroscopy is an analytical technique that can be applied to structural determination/categorisation of a wide variety of substances such as organic and inorganic substances. The principle behind IR spectroscopy is the measurement of and amount of IR radiation absorbed/transmitted at a given wavelength. This absorption/transmittance is dependant on the molecular vibrations of the molecule in question. The molecular vibrations are dictated by the atomic mass, bond strengths and intra- and inter-molecular interactions in the molecule. This translates into an IR spectrum when the absorption data is collated and plotted across the wavelength range. The IR wavelength is broken up into bands of NIR, 12500 – 4000 cm^{-1}, MID-IR, 4000 – 100 $cm^{-1}$and FAR-IR, 100 - 10 cm^{-1}. IR spectroscopy can be used for quantitative as well as qualitative purposes using a variant of Beer's Law. It has the advantage of being non-destructive, can be applied to real time monitoring systems and requires minimal sample preparation [81].

IR analysis of metal flavonoid complexes has also been used successfully. The IR analysis normally involves the preparation of the metal flavonoid complex by preparing both the metal salt and the flavonoid at nominal stoichiometries in methanol i.e. 0.5 or 2 M/L (Metal/Ligand) [82]. Two types of IR analysis have been used in previous studies: Fourier Transform (FT) IR and Raman spectroscopy [82-87].

The raman spectra of the metal-flavonoid compounds are complex but do bear recurring features that make them easy to identify as seen in figure 1.7 [87] for free catechin and metal-catechin systems.

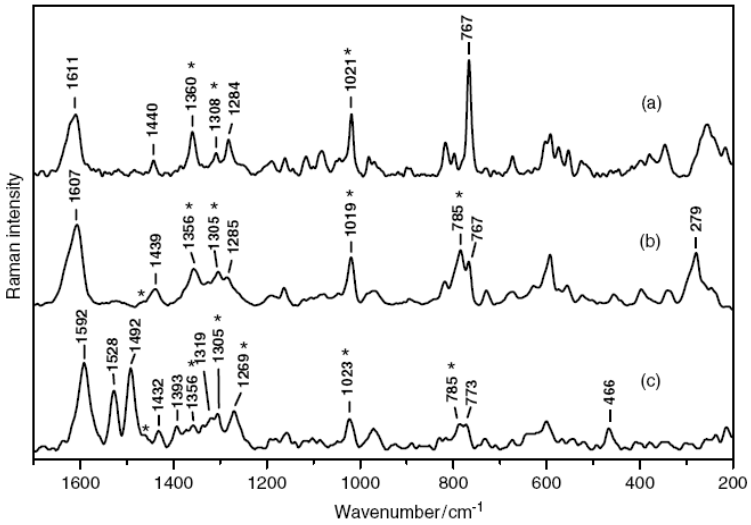

Fig. 1.7 Raman spectra of (a) free catechin, (b) catechin-Zn complex and (c) catechin-Cu complexes [87].

The above figure reflects that it is vital that a free flavonoid such as catechin must be analysed first prior to analysis of the actual metal flavonoid complexes themselves. The common Raman bands for flavonoids will always be attributable to the ring systems A and B which are the large peaks at 1607 - 1620 cm^{-1}. The next major set of bands at 1360 – 1308 cm^{-1} and 1021 cm^{-1} were due to the B ring specifically, due to OH from catechol groups and C-C bands on the aromatic ring itself. In the study, it was found that the intensity of the bands due to the B-ring were reduced with increasing metal concentration but a more pronounced M-O band at 279 and 486 cm^{-1} was observed respectively for Zn-catechin and Cu-catechin complexes. This indicated that copper and zinc were binding with the catechol moiety on the B-ring [87]. This type of structural information is invaluable in determining the chelation site of the

flavonoid with the metal and cannot be deduced by UV/Vis spectroscopy or molecular fluoresecence.

Other features that can be deduced by Raman spectroscopy are M/L ratios for flavonoid metal complexes and chelation sites associated with them. This can be accomplished by UV/Vis spectroscopy quite easily and is still the preferred method of determination, but Raman spectroscopy can give an extra degree of confirmation. This has been done by Toreggiani *et al.* [85] but in a different context related to Zn(II) quercetin complexes. Looking at M/L ratios of 0.5, 1 and 2 at pH 10 (see fig. 1.8), the group was able to deduce the ideal stoichiometry from looking at modifications in intensity of the C=O bands and the M-O bands. The main bands for the B ring C-C and C-O groups at 1650 cm^{-1} and 1425 cm^{-1} were unchanged past the M/L ratio of 1. This indicated that the spectrum was not effected by increased metal concentration and as such, Zn(II) was not chelating to any other site apart from the OH groups or catechol site on the B-ring i.e. it behaves as a unidentate ligand. This highlights that Raman analysis can be used to identify the optimal stoichiometry of the metal flavonoid complex in combination with UV/Vis spectroscopy.

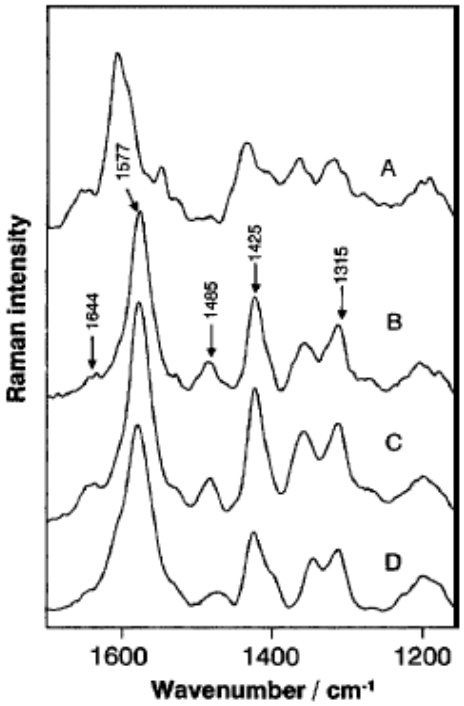

Fig. 1.8 The Raman spectra of free quercetin (A) and Zn-quercetin complexes at M/L ratios of 0.5,(B) 1.0,(C) and 2.0 (D) [85].

1.5.3 NMR analysis

Nuclear Magnetic Resonance or NMR spectroscopy is also used to assess the various structural features of flavonoid metal complexes in quite a number of studies where other inferences have been made by mass spectrometry, UV/Vis spectroscopy etc. The main features it can deduce are the shifting in electron density or deshielding of the hydrogen atoms upon metal complexation with the flavonoid. This causes the delta values of the proton peaks to shift downfield and can be used as a means to assess whether complexation was successful or not. It can also assess the planarity of a complex molecule and thus give additional conformational information about the structure that cannot be afforded by electronic and vibrational spectroscopy [8,78,86].

In a study undertaken by Pereira *et al.* [78] where he looked at the H^1 NMR spectra of Cu(II) naringin metal complexes, the following NMR data set was taken (see Table 1.2).

Table 1.2 The H^1 NMR data of free naringin and the Cu(II)naringin complex(Complex 1) [78]

Group	Naringin (δ, J)	Complex 1(δ, J)
OH	11.88 (s, 4'-OH s,); 9.51 (s, 5-OH)	12.05 (s, 5-OH)
H2', H6'	7.17(d, J=8.0 Hz)	7.02 (brd, J=6.6 Hz)
H3', H5'	6.64 (d, J=8.0 Hz)	6.52 (d, J=7.0 Hz)
H8	5.94 (d, $J_{H6/H8}$=7.0 Hz)	5.78 (d, $J_{H6/H8}$=5.5 Hz)
H6	4.97 (d, $J_{H6/H8}$=7.0 Hz)	4.79 (br s)
H2	5.13(dd, $J_{H2\text{-}H3A}$= 4.5 Hz)	5.13(m)
H3A	4.70 (dd, $J_{H3A\text{-}H3B}$=12.0 Hz; $J_{H2\text{-}H3A}$=4.5 Hz)	4.70 (brdd, $J_{H3A\text{-}H3B}$ = 12.0 Hz; $J_{H2\text{-}H3A}$ = 4.5 Hz)
H3B	4.8 (dd, $J_{H3A\text{-}H£B}$ = 12.0 Hz; $J_{H2\text{-}H3A}$ = 3.0 Hz)	4.8 (ddbr, $J_{H3A\text{-}H3B}$ = 12.0 Hz; $J_{H2\text{-}H3A}$ = 3.0 Hz)

Naringin and the Cu(II) complex have very pronounced differences between each other; namely the δ values are shifted downfield quite heavily for most cases of the hydrogens on complexation. Another observation is the absence of the 5-OH group suggesting that the hydrogen has been lost from this group. This is normally associated with a coordination bond of a metal to a hydroxyl group creating a M-O

group. The group recommended the use of DMSO as a solvent as opposed to methanol when conducting H^1 NMR analysis [78].

1.5.4 HPLC

HPLC analysis of flavonoid metal chelates has been a relatively underexploited field of research with many studies not investigating flavonoid metal chelates in foods as opposed to free flavonoids via methods such as GC and HPLC analysis [88,89].

The main reason is that conventional Reverse Phase-HPLC methods simply do not work effectively when it comes to analysis of metal-flavonoid complexes due to adsorption complications associated with the silica based stationary phase. This can affect complex stability and thus limits the usefulness of silica-based columns for this kind of analysis. This issue can be solved using specialised stationary phases such as polystyrenedivinylbenzene (PS/DVB). This stationary phase does not suffer from problems such as metal cation adsorption and thus would not experience any metal complex destabilisation issues [90].

A way around this issue is the use of a sodium acetate buffer: methanol mobile phase system to stabilise the metal flavonoid complex when passed through a silica C18 column as was done by G. Weber for iron, copper and aluminium quercetin-glycoside complexes. This method proved successful when tested at pH 2.5 and 4.0 with 4.0 being the more favourable pH for chelation site activation in quercetin glycoside [91].

1.5.5 Atomic Spectroscopy

Zhang *et al.* [92] reported separation and determination of trace, ng quantities, of inorganic germanium in Ge-132 via filtration chromatography and hydride generation-graphite furnace atomic absorption spectrometry (HGAAS). Filtration chromatography was performed on a cation exchange column for Ge-132 oral liquor. This was found to have a detection limit of less than $\mu g ml^{-1}$. To achieve this with HGAAS specialised conditions such as the construction of a palladium coated graphite furnace tube and the generation of GeH_4 via a HG-100 hydride generator was used.

McMahon *et al.* [31] used graphite furnace atomic absorption spectroscopy (GFAAS) to determine the total germanium content in real food samples. The limit of detection was determined as 3.37 μg L^{-1} and the limit of quantification was 20 μg L^{-1}. In the end, 24 food samples were tested such as aloe vera tablets and ginseng root. The study concluded that fresh food samples like tomatoes had the same concentration as fresh Chinese vegetables, in the range of 0.29 - 2.78 μg g^{-1}.

1.6 Flavonoid Metal Complexes

Flavonoids have the capability of forming a number of different complexes with various transition metals such as copper and iron as depicted in fig. 1.8. It has been suggested that the chelation sites responsible for the formation of these complexes are down to 4-keto and 5-OH groups, the 4-keto and 3-OH groups and the 3'-OH and 4'-OH groups present in the phenyl part of the flavonoid nucleus (see fig. 1.9). The typical complex metal:ligand ratio is dependant on pH and type of solvent but a lot of the flavonoid complexes show 1:1 or 1:2 complex formation with metals without pH variation. This was confirmed by ESI-MS studies that reviewed the chelation of transition metals with flavonoids [93]. The chelation of the flavonoids say in the case of a flavonoid glycoside can be seen in fig. 1.9.

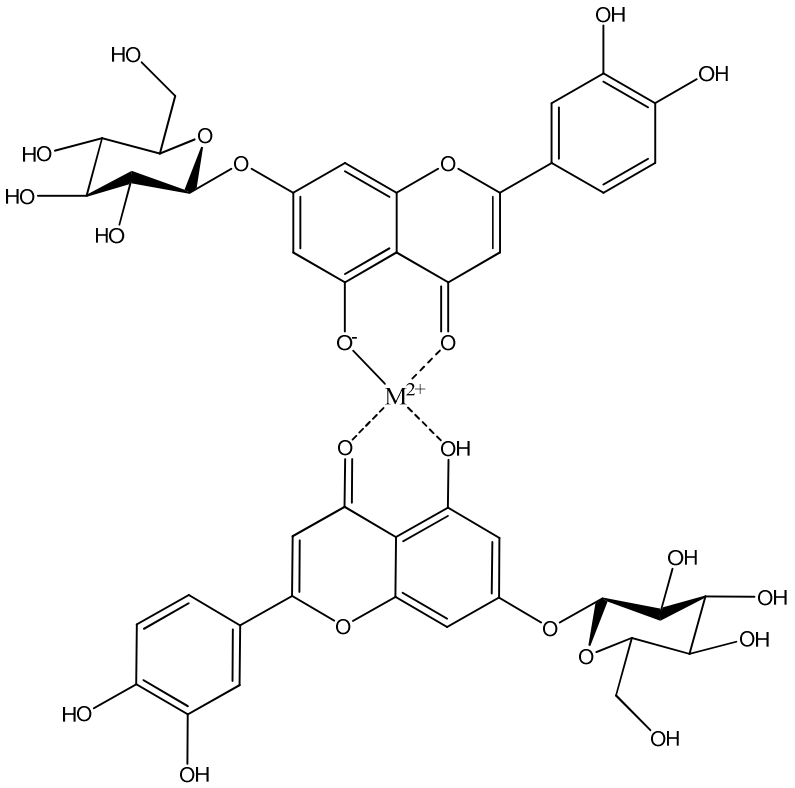

Fig. 1.9 Transtion metal (M^{2+}) flavonoid complex [94]

The ability of flavonoids to chelate with metals holds a number of therapeutic benefits among which is the mediation of metal overload disorders such as Wilson's disease caused by copper excess and iron-induced lipid peroxidation that is stimulated by iron overload [80]. They have been shown to have enhanced antioxidant abilites that can increase antioxidant potential 10 fold in some instances [78].

1.6.1 Chelation characteristic of flavonoid metal complexes

Flavonoids possess functionalities that allow them chelate with other metals like Fe(II), Fe(III) and Cu(II). These chelation sites normally contain hydroxyl and keto groups that work together in some combination. There are 3 possible areas where the metal ions can chelate on a flavonoid, the 3',4'-dihydroxy group on the B-ring, the 3-hydroxy or 5-hydroxy and the 4-carbonyl group in the C ring [10] (see Fig. 1.10).

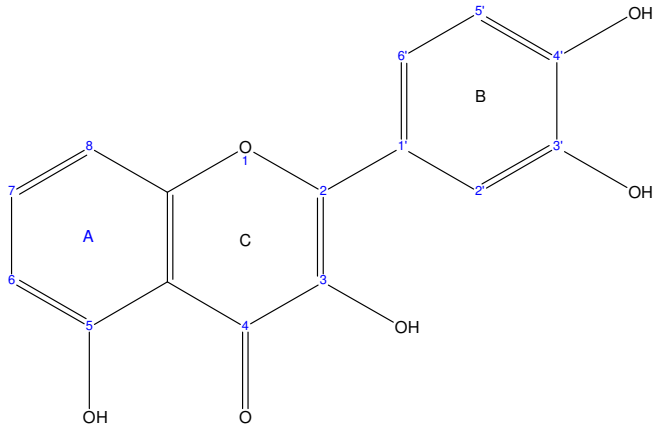

Fig. 1.10 Most common chelation sites for metal ions on flavonoid.

Quercetin has been investigated in relation to its chelation behaviour with iron. Leopoldini *et al.* [95] did such an investigation using a combination of UV/Vis spectroscopy and molecular modelling to show that iron was capable of having Metal/Ligand (M/L) ratios of 1:1 and 1:2. He theorised that 1:1 complexes were possible with all 3 chelation domains specified in the previous paragraph. The 1:2 complex was suggested to occur mainly at the sites on rings A and C at the 4-OH or 3-OH and 4-keto groups on quercetin.

A more comprehensive study of flavonoid complexation behaviour was undertaken by Lurdes Mira *et al.* [9] They studied a range of different flavonoid classes including flavones, flavonols, flavanones and isoflavones. They found that the stoichiometries of the flavonoids at pH 5.5 or less showed Metal/Ligand ratios of 1:2 and 1:1 with Cu(II) and Fe(III).They again found that the primary chelation sites were the 3',4'-OH group site and the 4-oxo, 5-OH group site.

The synthesis of isoflavone metal complexes has been undertaken by Chen *et al.* where they synthesised a number of transition metal complexes of isoflavones using Mn(II), Co(II), Cu(II), Zn(II), Ni(II) mainly with biochanin A. The groups found the common stoichiometry for the samples was 1:2 M/L stoichiometry. The binding based upon characterisation was theorised to take place with the 4-oxo and the 5-OH functionalities. The group also tested the synthesised complexes on cancer cell lines with comparison to cisplatin as a control. The group found that in most instances biochanin A showed enhanced performance in IC_{50} relative to that of cisplatin and the

metal complexes were not as effective relative to biochanin A although they generally outperformed cisplatin [96].

1.6.2 Antioxidant effects

The antioxidant capabilities of isoflavones have been well documented in the case of genistein, the most biologically active of the isoflavones, and also daidzein and their glycosylated counterparts [97,98]. Common health benefits are antimicrobial, anticancer (particularly in hormone related cancers) and antioxidant [99,100]. They have also been found to be beneficial in the case of menopausal women as an alternative to Hormone Replacment Therapy (HRT) in the form of isoflavone extract from soy products. This is related to its phytoestrogenic nature and its ability to have estrogen like effects on body regulatory functions [101].

The idea that this radical scavenging property of flavonoids can be enhanced by metals can be found in work carried out by Moridani *et al.* [102] This study looked at iron flavonoid complexes and their ability to have cytoprotection against superoxide radicals. Looking at rat hepatocytes, the superoxide radical scavenging activity was found to be at an optimum of 2:1 flavonoid:Fe^{3+}. The antioxidant capabilities of the complexes were greater than those seen in the uncomplexed forms of the flavonoids studied.

The results for a Cu(II)naringin complex used the same methodology to ascertain the extent of DPPH inhibition (an antioxidant assay) relative to naringin, the Cu(II)naringin complex, rutin and vitamin C. (see fig. 1.11)

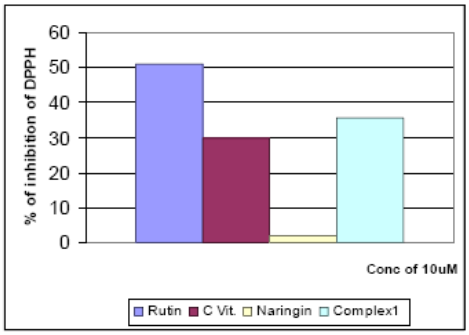

Fig. 1.11 A comparison of the %inhibition of DPPH (antioxidant assay) compared with rutin, vitamin C, naringin and the Cu(II) naringin complex all maintained at 10µM quantities [78].

The % inhibition of DPPH was greatest with the uncomplexed rutin as a positive control and was weakest with the uncomplexed naringinin. The % inhibition of DPPH for the Cu(II)naringin complex was somewhere in the region of 10 times higher than that of the uncomplexed naringin. This is a pronounced increase in antioxidant power and certainly gives more credibility to the theory that flavonoids are better antioxidants when complexed with metals [78].

The use of electrochemistry is also another way in which to evaluate the antioxidant abilities of the flavonoid metal complex. This is achieved by evaluating the electrochemical properties or the redox potential of the flavonoid metal complex. This is achieved through cyclic voltammetry. The oxidation peak is examined in relation to the antioxidant ability of the complex and free flavonoid. Souza *et al.* [86] looked at galangin and the complexes it formed with Al(III) and Zn(II) (see fig. 1.12).

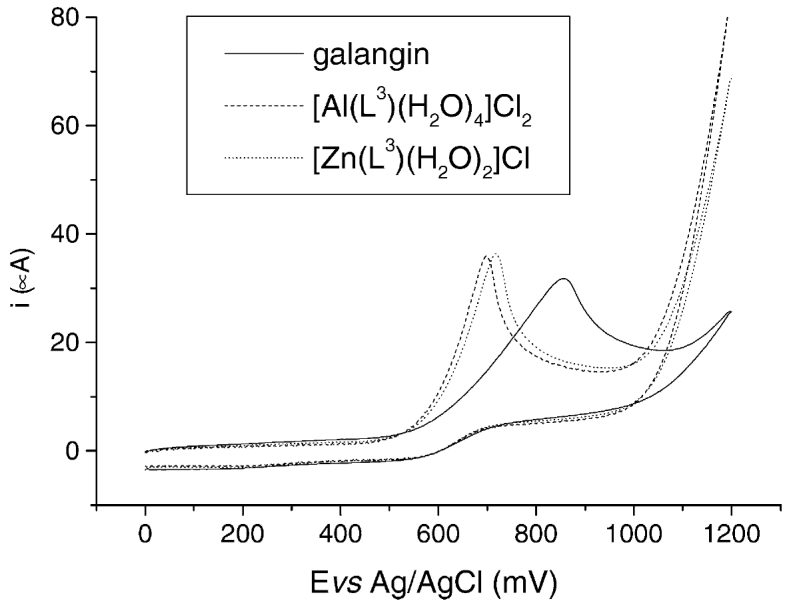

Fig. 1.12 Cyclic voltammograms of galangin and metal-galangin complexes formed with Al(III) and Zn(II) in a 0.1 M $LiClO_4$/MeOH at a scan rate of 0.1 Vs^{-1}. [86]

In this study, it was found that the galangin complex had a higher oxidation potential peak at +0.856 V. The Aluminium and Zinc complex were at a lower oxidation potential of +0.696 and +0.715 V respectively. Souza stated the lower the oxidation potential of the compound, the higher the antioxidant activity and thus this further proved that metal flavonoid complexes have better antioxidant abilities than flavonoids on their own [86].

Metal complexes of dietary flavonoids were examined by Kostyuk et al. when looking at free radical scavenging properties in vivo. The group utilised a number of in vivo evaluation techniques including mice experimentation, serum enzyme assays and GSH/GSSG assays. Their findings concluded that the radical scavenging IC_{50} values were 90 % lower than that of the free flavonoids. The mice trials revealed that metallothionein production in the liver was doubled with preventative administration of metal flavonoid complexes before the thioacetamide hepatotoxic agent was introduced. In all they found that the biological activity of the flavonoids was enhanced with the use of metal complexation [103].

1.7 Organic Germanium

1.7.1 Introduction

Organic Germanium is an organometallic compound that is of interest to this research group and has embodied many aspects of previous research such as the differentiation of organic and inorganic germanium as well as studying its interaction with biomolecules in food such as flavonoids [104]. The appreciation of germanium as a non-essential and toxic element has resulted in it being stigmatised. This is enforced by the collective FDA ban of germanium supplement imports in America due to toxicity issues with impure organic germanium products tainted with inorganic germanium reactants [105]. This represents an underdeveloped area of antioxidant research as a result.

Germanium was discovered in 1886 by Clemens Winkler. It has an atomic number of 32 and is a group IV element. Germanium is present in the earth's crust at 7 ppm and is 8 ppt in normal water. Its electronic configuration, [Ar] $4s^2$ $3d^{10}$ $4p^2$, is between that

of a metal and a non-metal which makes it quite unusual [106]. Germanium found its first major application in the form of semiconductor diode doping in the early 1930s with the help of E-P and Otavi Minen [107]. This allowed a revolution in the way electronics were done such as in power transistors and telecommunications. The germanium doping process of silicon in semiconductors is responsible for the microcomputer boom of the 1980s.

Clemens Winkler also developed the first organic compounds using the reaction of zinc diethyl and germanium tetrachloride in efforts to further explore its chemistry. This was followed by Eugene G. Rochow who synthesised organic germanium compounds directly from elemental germanium in reaction with methyl chloride. This formed the products dimethylgermanium dichloride and methylgermanium trichloride [108].

Germanium sesquioxide was originally discovered by VF Mironov in 1966 but the main developer of germanium sesquioxide in terms of synthesis and therapeutic application was Kazuhiro Asai. Asai established a coal research institute in Japan in 1945. As part of its research, it was instrumental in determining the levels of germanium in coal. Asai broadened this study into quantification of the levels of germanium in plants. For example, he found that germanium in aloe vera was 754 ppm and germanium in garlic was 77 ppm. This eventually lead to the synthesis of bis-2-(carboxyethyl) germanium sesquioxide or Ge-132 in November 1967.

Asai viewed the body as “a mass of minute electrical particles” with each organ of the body having a certain concentration of these particles. He hypothesized that the body has an optimum potential for healthy cells. If disease occurred, the potential would be upset. He regarded germanium as having a semi-conductive effect upon high potential cancerous tissue restoring it to a healthy potential. This was, in his view, the logic behind germanium sesquioxide’s immunomodulatory effects and hence the mechanism behind its therapeutic effects [13].

Germanium supplements have been associated with health hazards such as renal failure and in some instances death. Nagata *et al.* [109] reported in detail the acute renal failure of a middle aged housewife taking 600 mg of germanium in an elixir.

The germanium was present in the form of germanium dioxide. The renal failure led on to symptoms such as myopathy and skin rash. The post mortem revealed an abundance of germanium in the patient with 183 times the norm in the spleen and 175 times the norm in the thyroid gland. Okuda and his group [110] were responsible for treating 4 patients who developed renal dysfunction after chronic intake of germanium compounds. The abstinence of the patients from germanium containing compounds stopped deterioration of the renal system but renal dysfunction continued. Germanium excretion persisted 5-12 months after discontinuation of consumption. There were no reported urinary anomalies associated with the dysfunction leading Okuda to judge germanium dioxide was the cause of the problem.

1.7.2 Structural data on germanium sesquioxide

Solid dry germanium sesquioxide is classed as a material with a network of oxide polymers. As such, it has a range of states known as primary, secondary and tertiary structures. As suggested in the compound name, the germanium shares 3 oxygen atoms with other germanium centres or sesquioxide.

The primary structure is regarded as being a monomer subunit with carboxyethyl germanium sesquioxide attached to 3 shared oxygen atoms in dimeric formula or $(GeCH_2CH_2COOH)_2O_3$ (see fig. 1.12). The secondary structure is a little more complicated with 8 and 12 member rings of germanium oxygen being theorized. A low molecular weight 3D adamantane cage structure of $[(GeCH_2CH_2COOH)_2O_3]_n$ could possibly exist where n=2. Essentially infinite β-pleated sheets of variable molecular weight are the rule. Tertiary structures are aqueous solutions of Ge-132 and products have been shown to have transitory structures in aqueous solutions. The basic monomer represents a member of a polymeric chain best shown in the form of $[(GeCH_2CH_2COOH)_2O_3]_n$ where n depends on the way the solid crystallises out of solution. Thus multiple polymorphs are possible [111].

The crystalline structure of carboxyethylgermanium sesquioxide was investigated by Minoru *et al.* [112] His group synthesised germanium sesquioxide using a reaction of trichlorogermane with acrylonitrile and subsequent hydrolysis of the transition product to make germanium sesquioxide. This determined that the complexity of the hydrolysis products was influenced by the number of halogen atoms present on the

organogermanium halides. The hydrolysis products upon dehydration formed polymeric solids of general composition $(RGe)_2O_3$. The basic unit of the infinite sheet network was a 12 membered ring made up of germanium tetrahedrons bridged by oxygen atoms (See fig. 1.13).

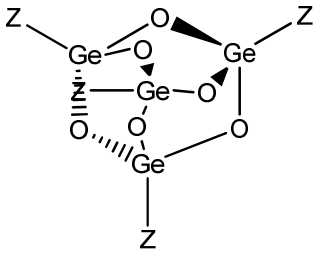

Fig. 1.13 Adamantane cage structure of germanium sesquioxide.

The carboxylate chains were arranged alternatively above and below. Sheets are bound vertically by hydrogen bonds between carboxyl groups attached to each sheet (See fig. 1.14) [112].

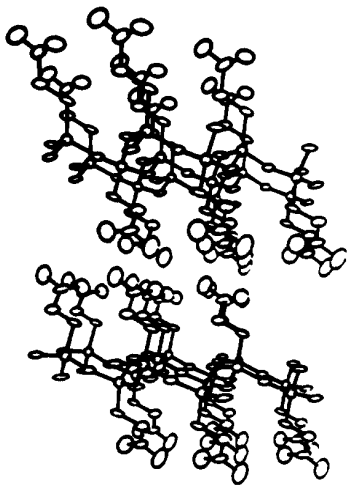

Fig. 1.14 Infinite β-sheet arrangement of germanium sesquioxide.

The interesting thing about the crystalline structure of carboxyethyl germanium sesquioxide is that it resembles the infinite sheet structure in crown ether. These compounds have novel metal ion and amino acid complexation abilities. Dr. Minoru believed this accounted for the biological activity exhibited by germanium sesquioxide.

1.8 Scope of Research

This project investigates germanium based compounds in foods and also takes into account the interactions of biomolecules like flavonoids with more prominent elements such as iron and copper. Foods have extremely complex biological sample matrices and this has to be considered when they are being analysed. It is also important to consider that no one molecule in foods is contributory to health but should be viewed in how they are all present in the food sample matrix and how they collectively contribute to health.

The inclusion of soils in the scope of research may give some insight into how soil components influence the sample makeup of vegetables. This has the potential to suggest a relationship between metals in soils and the metals in foods. The potential is also there to identify the presence of organic and inorganic germanium additionally in soil samples.

The research is broken down into the following areas:

1. The FTIR analysis of germanium compounds, germanium sesquioxide and germanium dioxide, in foods and soils using non-destructive techniques.
2. The quantitative determination of metals in soils and foods via atomic spectroscopy after acid digestion of samples.
3. The study of how metals complex with flavonoids in foods and their effects on the flavonoids stoichiometric or metal/ligand ratio.
4. The synthesis and characterisation of chelated flavonoids using techniques such as NMR, mass spectrometry, FTIR and UV/Vis.
5. Assessment of antioxidant activity of these flavonoid metal chelates in relation to antioxidant properties.

These areas of research are achieved through the use of analytical techniques like vibrational spectroscopy for the identification of germanium sesquioxide in food and soils as well as trying to characterise possible interferences associated with its determination from biomolecules in the matrix (Refer to Chapter 2). This will be to enhance knowledge of how germanium compounds can be interfered with in relation to common food and soil components such as proteins, lipids, carbohydrates and

minerals. This will verify if FTIR analysis is a viable spectroscopic technique for determining germanium compounds in foods and soils. The novelty lies with it being a development of previous work done by McMahon *et al.* with germanium compound determination in foods but not taking into account bands with sample matrix interferences in foods.

The investigation of metals, Fe, Cu, Pb and Ge in foods and soils will give an indication of how these elements relate to each other. This can be achieved through the use of Atomic Absorption Spectrometry (Refer to Chapter 3). This is being performed as an addition to the work performed by McMahon *et al.* where germanium content in foods was exclusively determined via graphite furnace AAS method. The enhancement of the study by analysis of soils and the analysis of 3 additional elements will be beneficial for the broader elemental content of the samples analysed.

The investigation of how biomolecules interact with metals can be observed using stoichiometry studies at varying pH's and metal solutions including Ge(IV), Cu(II) and Fe(III) metals with isoflavone molecules (Refer to Chapter 4). This will be done so as to enhance the little knowledge of the aforementioned elements chelation with isoflavones, genistein, daidzein and biochanin A. This represents an area of research that has been underexploited in flavonoid metal chemistry and could be very publishable. The pH adjustment is to look for variances of stoichiometry with protonation/deprotonation of hydroxyl groups in the isoflavones.

The synthesis and characterisation of successfully chelated biomolecules are explored later using Cu(II) and Fe(III) chelated with isoflavones (Refer to Chapter 5). This will be done as there has been only a handful of isoflavone metal chelate compounds synthesised in literature. This makes any synthesis of isoflavone metal chelates very novel. Also, there will be a view to perform some antioxidant assay work on synthesised compounds.

The assessment of the biological activities of the biomolecules in relation to antioxidant properties can be seen in DPPH inhibition studies with the isoflavone metal chelates (Refer to Chapter 6). This will be done with the purpose of seeing how antioxidant properties of isoflavones metal chelates compare with their free

isoflavones. This would confirm current observations about flavonoid metal chemistry where flavonoid metal chelates show enhanced antioxidant activity (Refer to section 1.6.2). This area is novel as isoflavone metal chelates were never directly assessed for their antioxidant properties when chelated to metals via an antioxidant assay.

Chapter 2: FTIR analysis of foodstuffs and soil for the presence of germanium(IV) compounds and the identification of protein, lipids, carbohydrates and mineral interferences

2.1 Introduction

Fourier Transform Infrared Spectroscopy (FTIR) is a frequently used method of analysis for samples in industrial, agricultural and nutritional science fields. FTIR is a non-destructive means of analysis that offers a range of advantages such as well-resolved absorption bands that can be used for identification of a compound based on the vibrational bands for a particular sample. It also offers high signal to noise ratio and a rapid means of spectral acquisition [113].

FTIR spectroscopy has been applied as a means of analysis for both food and soil alike for determination of a variety of factors. It has been applied to food for the analysis of moieties such as component identification, classification and moisture content determination [114-116]. It has also been applied to soil samples for the analysis of nitrate and carbonate levels and for classification [117,118].

Using this methodology, it is possible to identify soil types using combinations of sophisticated mathematical modelling programs that can trend the IR band inferences of an IR spectrum to give a complete picture of the components present in soil [119]. This can also be applied to foods in the form of quality control systems for foods as well as for the online analysis of constituents in foods that can allow simultaneous monitoring of bands due to polysaccharides, fats and water. This is combined with the fact that IR spectroscopy is non-destructive and will not compromise the sample integrity [115].

Michael McMahon worked previously to performed FITR analysis on germanium sesquioxide and germanium dioxide in foods. He assigned the IR bands associated with these compounds functionalities such as the germanium oxygen network (Ge-O-Ge) having a band at 927, 1047 and 1240 cm^{-1}. The assumption in the study was that all relevant IR bands were attributable to the germanium compounds and not those associated with common components in food such as lipids, carbohydrates and proteins. The purpose of this chapter is to re-examine

FTIR will be used in this work to identify the presence of germanium sesquioxide and dioxide in foods and soils. This will be accomplished by focusing specifically on the

fingerprint region at 1600 – 400 cm^{-1} where bands attributable to functional groups of these molecules will be found. The study will look at the viability of using FTIR spectroscopy for germanium(IV) compound detection and the ascertainment of possible interferences for germanium(IV) compounds.

The novelty of this body of work with germanium analysis is that is has not been looked at in the context for soils and foods. The only studies that have looked at germanium content within foods were undertaken by Kakimoto *et al.* in 1989 [120] and this work was only assessed from an elemental analysis standpoint. The FTIR analysis of germanium compounds within the foodstuffs is novel and has not been undertaken in the literature to date.

2.1.1 Soil

Soil has been categorised in the literature through advanced analytical techniques involving IR spectroscopy coupled with sophisticated statistical software capable of matching vibrational bands to certain characteristics inherent in soil. Among these characteristics are carbonate content, clay content and sand content. An example of a system that was developed specifically for the analysis of soil is the Soil Interference System (SINFERS). SINFERS uses diffuse reflectance FTIR spectroscopy for measurement of variables such as clay and organic carbon content. This system would not be as accurate as established techniques such as estimation of organic carbon content using the dichromate oxidation method set out by Walkley and Black [119] in 1934. It does, however, have the advantage of being quicker, cheaper and more efficient for large scale soil sampling but with the limitation that it cannot account for all the physical, chemical and biological properties of the soil. The advantage of using FTIR is that it is a spectroscopic technique that analyses the sample non-destructively rather than altering the sample makeup like in other experiments such as cation exchange capacity determinations using a reagent like sodium acetate [118].

R. Linker *et al.* [121] used attenuated total reflectance Mid-infrared spectroscopy (ATR-Mid-IR) for the detection of nitrate levels in soil. The focus was to utilise a reference IR spectrum library to determine soil type in the fingerprint region i.e. 1200 – 800 cm^{-1}. Following this identification, the nitrate content was determined by an

appropriate analytical model for this soil type in relation to ATR-Mid-IR. The data was subjected to cross-correlation with a reference library followed by principal component analysis through a neural feed-forward network. The method wasn't effective in terms of soil identification with the PCA analysis unable to clearly distinguish between different soil types such as Mediterranean red soil and calcareous (high calcium carbonate content) clay soil. More success was obtained for the nitrate determinations of soils, particularly non-calcareous soils. The main complication with this method was the interference of the carbonate IR band with the nitrate IR band that could account for the errors observed in this method. The lack of proper identification of the soils makes it suitable only to soils that exhibit very low carbonate content.

Calderon *et al.* [122] performed a study on manure and its decomposition in soil over a 10 week period. The manure was taken from four different types of beef and dairy cattle. The manure was kept in incubation with the soil and it was analysed at various intervals. The study noted that there was a decrease in the intensity of the IR bands associated with primary amides in proteins (1653 cm^{-1}) and bands from esters (1734 cm^{-1}) and C-H bands (2870 cm^{-1}) attributable to fatty acids during the decomposition of the manure. The intensity of the lignin bands (1510 cm^{-1}) increased over the decomposition period. The changes of the intensity values for nitrogen containing pyrozolates tended to fluctuate from manure to manure. This technique was assessed as having potential for decomposition analysis but needed further work.

Manure characterisation was also performed by Changwen *et al.* in relation to manure samples collected from various regions of China using FTIR-PAS (Photoacoustic spectroscopy). This characterisation process involved the use of intense laser light accompanied by the detection of acoustic emanations from the manure sample caused by the heating effect of the laser light photons where the sample would be in a resonant photoacoustic sample cell purged with dry helium (See fig. 2.1). The sounds would then be detected via microphone and amplified for generating analytically viable signals. The group deduced that if they used the full Mid-IR spectral acquisition range for quantification of organic matter levels, they received better R^2 values in the region of 0.93 up from 0.83 [123].

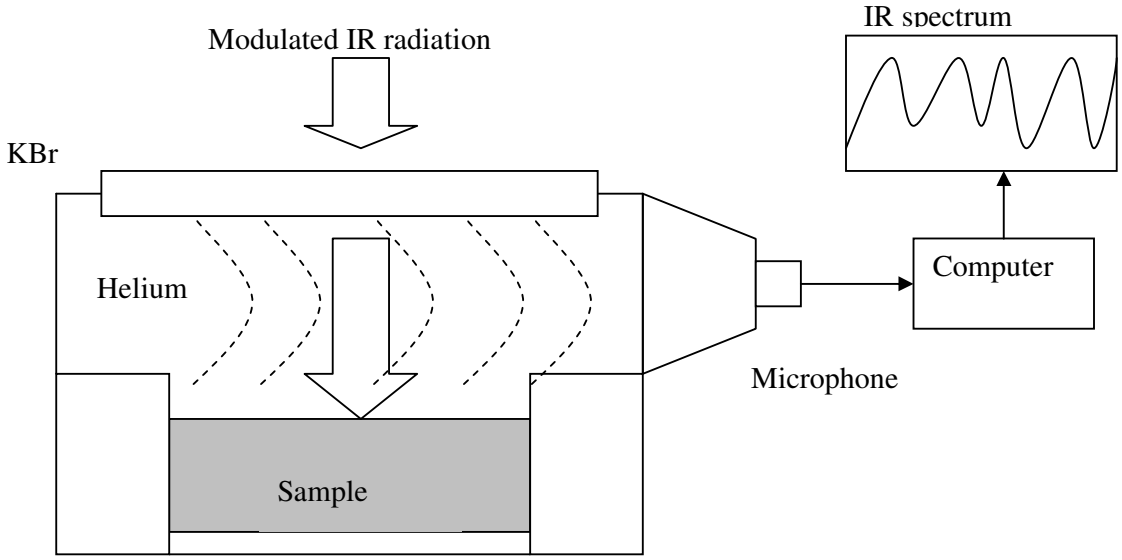

Fig. 2.1 Typical FTIR-PAS setup for sample characterisation [124].

FTIR is also increasingly finding application in forensic analysis of soil from crime scenes according to Cox *et al.* [125]. The group looked at the soil samples in terms of colour before and after dessication using the Munsell Colour Chart system. They also highlighted that the FTIR spectra showed mainly inorganic components as was confirmed by their organic content studies that revealed a range of 8.4 - 18.3%. The bands assignable to organic components were mainly due to Si-O stretch at 1050 cm^{-1} and other organic functionalities at 3400 and 1730 cm^{-1} from the soil humus. Using a series of inferences based upon soil type, soil colour and post-colour, density gradient, % organic content and the FTIR spectra, it was possible for the analyst to correctly identify the organic component of the soil and give viable forensic evidence.

2.1.2 Food

The analysis of food via FTIR has been applied successfully to food components such as proteins, carbohydrates and lipids [126-128]. The range of techniques that can be used in combination with FTIR for sample preparation/containment are Diffuse Reflectance Infrared Fourier transform systems (DRIFTS), photoacoustic (PAS) FTIR and attenuated total reflectance (ATR) (see fig. 2.3). The first two sampling techniques are mainly suitable for solid food samples and have overall good sensitivity and low interference. The last technique is mainly suitable for liquid/paste

food samples like juices. It is increasingly being used for analysis of liquid foodstuffs but does need a lot more sample for analysis purposes [129].

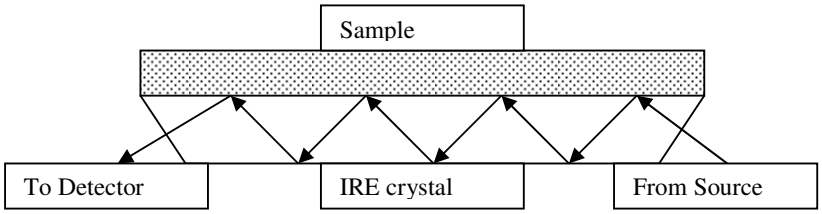

Fig. 2.3 A conceptual diagram of ATR sampling system in FTIR. [129]

Dogan *et al.* [116] were responsible for the development of a method for the FTIR characterisation of irradiated hazelnut. The concept was that foodstuffs are irradiated for the purpose of food preservation from factors such as microbial contamination. The study was trying to monitor the effects of ionizing radiation on structural and compositional properties of the hazelnut such as lipids and proteins. The hazelnut samples were subjected to doses ranging from 1.5 kGy to 10 kGy. The samples were then prepared for FTIR. Structural variations were observed increased presence of N-H and O-H bands at about 3345 cm^{-1} for the 10 kGy samples with little change for the lower dose samples. The study showed that the level of unsaturation increased from low dose to high dose irradiation of the food samples indicating some form of dehydrogenation process taking place for the lipids. This was further reaffirmed by an increase in the intensity of the C=O band at 1746 cm^{-1} for triacylglycerols. FTIR also showed a breakdown of the α-helical areas of the protein at a high dose of 10 kGy when monitoring the band at 1652 cm^{-1}. This band showed signs of decrease while the random coils at 1642 cm^{-1} show signs of increase suggesting some denaturation effect was taking place.

FTIR has also been applied in the quality control and identification of beers and spirits as was studied by Lachenmeier *et al.* [115]. He utilised an instrument called the Winescan FT120 specifically developed for the analysis of alcoholic beverages. The analysis sought to create a reference spectrum based upon 1060 FTIR data points with the subtraction of water absorption from bands 1447-1887 cm^{-1} and 2971-3696 cm^{-1}.

The results were promising for spirits and beer drinks with most spirits having R^2 values greater than 0.90 when compared to reference materials for alcoholic beverages. The FTIR analysis proved more suitable for multicomponent analysis than its rival, Near Infrared (NIR), as it gave more finely resolved bands and better accuracy. This form of classification is also cheaper than proton NMR analysis also used for this analysis.

Classification of food constituents has been achieved in FTIR for components such as vegetable oil authentication. Lai *et al.* [113] were responsible for using FTIR for the authentication of vegetable oils such as virgin olive oil and sunflower oil in food. PCA (Principle Component Analysis) was applied to the spectral results with special focus on spectral bands of 3100 – 2800 cm^{-1} and 1800 - 1000 cm^{-1}. This study managed to obtain a high signal to noise ratio for the oils investigated. This may have been attributed to the 256 interferograms taken for each spectrum and the fact that the FTIR had a dessicated and sealed sample compartment preventing any buildup of carbon dioxide or moisture. The method was relatively successful with a total of 57 out of 61 spectra being correctly identified by the discrimination model created by the group with a probability of 0.007% of unlikeliness. The 4 incorrect identifications were discovered to be refined virgin olive oil purchased from a supermarket. It was later determined that it was a mixture of vegetable and virgin olive oil which would have thrown off the discriminant analysis model. Thus, it seems that this model is quite suitable for authentication of vegetable oils in vegetable oil samples.

Another successful application of FTIR in food analysis is the analysis of polysaccharide food additives. This study was undertaken by Cerna *et al.* [130] for the characterisation of a number of different polysaccharide constituents such as starch and pectins which are commonly used as thickening agents in soups or jams. A quick and non-destructive method for the ascertainment of the polysaccharides by looking at various spectral markers in the fingerprint region of the IR spectrum between 1200 - 800 cm^{-1} using PCA (principal component analysis) was developed. The study sought to achieve a screening technique for the saccharides by identification of specific wavenumbers for fructose, mannose and sucrose which are components of polysaccharide species. In conclusion, no distinction could be made between monosaccharide, disaccharide and polysaccharide species. Only very slight

distinction could be made between glucose with a negative band at 998 cm^{-1} and galactose with a positive band at 1068 cm^{-1}. Identification could be made for sucrose at 995 cm^{-1} and mannose at 1072 and 1033 cm^{-1}. This gave a certain level of identification for some carbohydrate species in foodstuffs but not all.

FTIR analysis has also been used for characterisation of alcoholic products such as wine and brandy for ageing. This study was achieved by Palma *et al.* who used a dedicated FTIR instrument for FTIR analysis called the winescan FT-120 to obtain the IR spectra capable of filtration and temperature control of the sample. The study primarily focused on 2 principal components being absorptions due to water and alcohol. The aging was investigated by applying the previous PCA parameters with some brandy batches that were in the order of 6 months, 1 year and 3 years of aging. The samples were then grouped in terms of pin number or PN values that were based on 1000 wavenumber values selected from the 926-5012 cm^{-1} range. The study found 3 distinct groupings of these values for the differently aged brandies. Thus, they established a correlation between IR absorption signals and aging of brandy [131].

2.1.3 Gemanium compound determinations in food and soil via FTIR

The germanium(IV) sesquioxide functionalities can be broken down into Ge-C, Ge=O, Ge-O-Ge, Ge-O and C=O as dedtermined by Kakimoto *et al.* [132] when they synthesised germyl derivatives and determined their structure via infrared analysis. The bands found for the synthesised germanium sesquioxide are at 3050, 1690, 1409, 1240 and 790 cm^{-1} respectively.

Work carried out by McMahon *et al.* [104] on the FTIR analysis of germanium sesquioxide and germanium dioxide in foodstuffs, found that the main distinguishing factor between them were bands for the germanium oxygen network (Ge-O-Ge) that are solely found in germanium sesquioxide and not germanium dioxide. The common functionalities between the two are Ge-O and Ge=O. It was also proposed that the Ge-O-Ge network was an interference free band that could be seen in food IR spectra. This can be seen in a comparison of the IR spectra for germanium sesquioxide and germanium dioxide.

The purpose of determining the presence of germanium sesquioxide presence within foods and, to an extent, soil is for the benefits that germanium imparts upon these foodstuffs. Kakimoto *et al.* used the application of organic and inorganic germanium treatment of vegetables for the purpose of enhancing their shelf life without the need for expensive refrigeration systems. The research looked at radish sprouts, alfalfa, chives, parsley , shallots and tomatoes. Overall there was improvement in the shelf life of the vegetables with germanium exposure for tomatoes, lasting 10 days at room temperature conditions [120].

The advantage of having these substances present within the foodstuffs and soils could lead to a modification of their shelf life and impart enhanced biological properties such as better antioxidant activity. The assessment of germanium content (refer to chapter 3) would follow and then give a correlation with inorganic and organic germanium presence within food.

The study lacked IR data from major food components such as proteins, lipids, and carbohydrates so the results were not verified [126-128]. The work of Schulz *et al.* [127] looked at a means of identification of plant substances via FTIR in a review article. A complete table of common IR bands for functionalities associated with proteins, lipids and carbohydrates were compiled. This table will be used to great effect to compare primary FTIR functional bands for food constituents relative to the bands for germanium dioxide and germanium sesquioxide yielding a better account of interferences for their determination.

2.2 Aims

- To characterise germanium sesquioxide, germanium dioxide, a select group of foodstuffs and soils from different sites around the northside Dublin area.
- To compare the FTIR spectra to common bands found in literature for germanium sesequioxide and germanium dioxide
- To ascertain interferences from primary constituents in food and soil such as proteins, carbohydrates, lipids and minerals

2.3 Experimental

2.3.1 Instrument

Perkin-Elmer Spectrum GX FTIR with Helium-Neon Laser and DTGS detector and diffuse reflectance sample cup.

2.3.2 Chemicals

Germanium (IV) Oxide 99.9999% purity, Sigma Aldrich, Ireland.
Bis(2-carboxyethylgermanium sesquioxide), Sigma Aldrich, Ireland.
Dry Merck IR grade KBr used without further purification.

2.3.3 Method

2.3.3.1 Preparation of food for IR analysis

The vegetables were peeled and washed with deionised water. They were then chopped into fine pieces. Samples were placed into an oven at 103 ^{0}C until a constant dry weight was achieved. Samples were subsequently ground into a fine powder via mortar and pestle. This powder was transferred to a screw top container. The samples were left in a dessicator for storage until needed (see table 2.1 for full sample set).

Table 2.1 Food samples that were prepared for IR analysis

Foodstuff:	Producer/Supplier	Source
Green Pepper	Tesco	Tesco, Omni Centre, Santry, D9
Yellow Pepper	Tesco	Tesco, Omni Centre, Santry, D9
Red Pepper	Tesco	Tesco, Omni Centre, Santry, D9
Fresh Carrot	Tesco	Tesco, Omni Centre, Santry, D9
Potato	Tesco	Tesco, Omni Centre, Santry, D9
Ginger tablet	Good 'n natural	Clinic for alternative medicine, Limerick
Soya Flour	Nancys	Nancys Healthfood Store, Limerick
Tvp Soya Mince	Nancys	Nancys Healthfood Store, Limerick
Pearl Barley	Holland & Barett	Nancys Healthfood Store, Limerick
Ginseng tablet	Ortitis	Nancys Healthfood Store, Limerick
Apple	Tesco	Tesco, Omni Centre, Santry, D9
Cauliflower	Tesco	Tesco, Omni Centre, Santry, D9
Cucumber	Tesco	Tesco, Omni Centre, Santry, D9
Garlic	Tesco	Tesco, Omni Centre, Santry, D9
Lettuce	Tesco	Tesco, Omni Centre, Santry, D9
Mushroom	Tesco	Tesco, Omni Centre, Santry, D9
Parsnip	Tesco	Tesco, Omni Centre, Santry, D9
Peach	Tesco	Tesco, Omni Centre, Santry, D9
Scallion	Tesco	Tesco, Omni Centre, Santry, D9
Turnip	Tesco	Tesco, Omni Centre, Santry, D9

2.3.3.2 Preparation of soil for IR analysis

100 g quantities of the soil samples were dessicated to constant dry weight in an oven at a temperature of 110 ^{0}C followed by grinding to fine powder via mortar and pestle. This was followed by sieving the samples with a 20 mesh sieve. The samples were stored in 30 ml polypropylene containers until needed (refer to table 2.2 for soil sample sites).

Table 2.2 Summary of soil samples prepared for FTIR analysis

Site	Location	General Description
1	Gullivers Retail Pk., Santry, D9	Recent retail development. Surrounding area still being developed. Soil collected from freshly overturned site.
2	Gerralstown House, Santry Avenue, Santry, D9	Well-established area. Houses seem to date from fifties and sixties. Rundown alleyway towards back. Lots of rubbish e.g. domestic construction, industrial, etc.
3	Santry Demesne/Park East Side, Santry Avenue, Santry, D9	Taken from an area around tree with large overhanging bough. Area is well maintained and is relatively litter free.
4	Santry Demesne/Park West Side, Santry Avenue, Santry, D9	Taken from an area around tree on west side of park. Area is again well-maintained and is litter free.
5	Queensway Furniture Store, Swords Road, Santry, D9	Heavy Traffic, constant smell of dioxins and smoke in the air. Mild littering. Taken from tree on roadside beside queensway furniture superstore
6	Shanliss Park, Santry, D9	Quiet suburban area, mild litter, free from traffic. Good ratio of green area to concrete. Healthy looking environment. Old housing estate from seventies
7	Northeast DCU Campus, Collins Avenue, Glasnevin, D9	Beside Invent Building, taken beside holly plants. Mild litter. Healthy environment.
8	Southeast DCU Campus, Collins Avenue, Glasnevin, D9	Soil Heap just by tennis courts. Assorted construction waste e.g. concrete blocks , torn up path, cones etc.
9	Albert College Park, East Side, Ballymun Road, Glasnevin, D9	Well maintained park, abundant plant life in the form of trees and bushes, clean air. Not close to any major traffic.
10	Albert College Park, West Side, Ballymun Road, Glasnevin, D9	Same as east side only closer proximity to ballymun road. More pronounce smell of pollutants such as car exhaust.
11	Southwest DCU Campus, Collins Avenue, Glasnevin, D9	Old part of campus, abundant plantlife with trees, bushes and shrubberies. Relatively litter free. Far from Ballymun Road. Little Traffic
12	Northwest DCU Campus, Collins Avenue, Glasnevin, D9	Beside car park next to Helix, good plantlife abundance. Relatively clean smell. Sample taken next to hedge.

2.3.3.3 Preparation of tablet formulations for IR analysis

5 tablets were ground and crushed via mortar and pestle. In the case of capsules, the powder was ground and the plastic capsules were discarded. The powder was dried in an oven at 103 ^{0}C until a constant dry weight was achieved. Samples were then transferred to a screw top container and stored in a dessicator until required.

2.3.3.4 Analysis by FTIR

The samples were ground with dry KBr in the ratio of 19:1 KBr:Sample. The IR was calibrated against KBr to obtain a background spectrum. The samples were analysed in diffuse reflectance cups in the IR spectrophotometer according to the following parameters:

Parameters	Values
Resolution	4 cm^{-1}
Scan number	32 scans per spectrum
Wavenumber range	4000 cm^{-1} – 400 cm^{-1}
Mode	Absorbance

2.4 Results and Discussion

2.4.1 FTIR analysis of foodstuffs

2.4.1.1 Germanium (IV) compounds

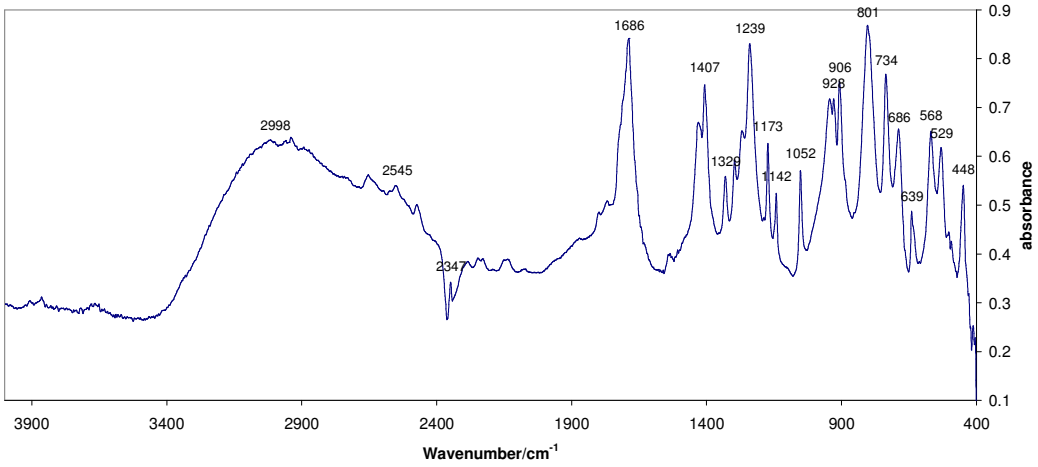

Fig 2.4 FTIR spectrum of Germanium Sesquioxide(Ge-132)

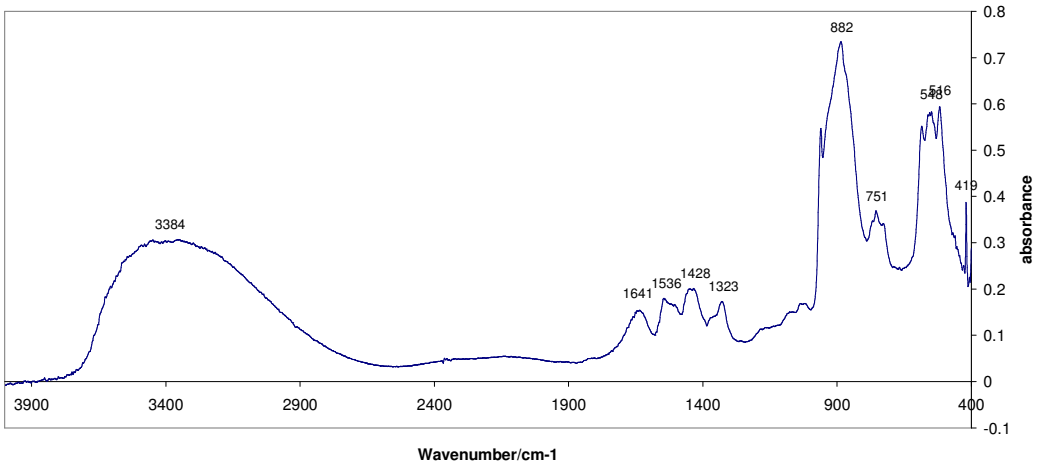

Fig 2.5 FTIR spectrum of Germanium(IV)Oxide

Combining the tables from McMahon *et al.* and that of Schulz *et al.*, it is possible to come up with the following table of IR bands for successful identification of functionalities in germanium sesquioixde, germanium dioxide and foods (see table 2.3).

Table 2.3: IR bands for functionalities in foods for Ge(IV)compounds components. [104,127,133]

Assignment	Functional Group	Model IR bands /cm^{-1}
Germanium Sesquioxide	Ge=O	555
	Ge-C	612
	Ge=O	798
	Ge-O-Ge	927
		1047
		1240
	Ge=O	1413
	C=O	1691
	GeO	2346
		2946

Using the bands present in table 2.3, it is possible to compare the germanium bands against the relevant bands that were in the foodstuff FTIR spectra (refer to table 2.4). The results expressed in table 2.4 are for bands that are most comparable. Some bands are not visible (N/V) but this maybe due to other sample matrix constituents such as lipids, carbohydrates and protein, which will be elaborated on later in this chapter. The following sections 2.3.1.1.1 to 2.3.1.1.5 deal with IR absorptions attributable to Ge=O, Ge-C, Ge-O-Ge, C=O and Ge-O.

Table 2.4 Results for IR bands of Germanium(IV) compounds in food (Note: N/V refers to Not Visible band)

	Germanium (IV) compound Functional Groups/cm^{-1}									
Sample	**Ge=O**	**Ge-C**	**Ge=O**	**Ge-O-Ge**			**Ge=O**	**C=O**	**Ge-O**	
Model IR bands	555	612	798	927	1047	1240	1413	1691	2346	2946
Ge-132com	568	639	734	928	1052	1239	1407	1686	2545	2998
GeO_2	548	N/V	751	N/V	N/V	N/V	1428	1641	N/V	N/V
Apple	N/V	N/V	783	929	1052	N/V	N/V	1729	N/V	2911
Carrot	585	N/V	778	925	1046	1238	N/V	1660	N/V	2927
Cauliflower	N/V	N/V	777	932	1038	1236	1403	1667	N/V	2900
Cucumber	N/V	N/V	771	N/V	1055	1227	1401	1663	N/V	2936
Garlic	583	N/V	N/V	930	N/V	N/V	1404	1662	N/V	2942
Ginger Tablet	N/V	N/V	763	923	N/V	N/V	N/V	1660	N/V	N/V
Ginseng Tablet	567	N/V	N/V	N/V	1031	1222	1413	1660	N/V	2927
Green Pepper	N/V	N/V	775	N/V	1044	1217	1403	N/V	N/V	2944
Lettuce	N/V	608	N/V	N/V	N/V	1225	1388	1666	N/V	2933
Mushroom	549	622	N/V	930	1020	1295	N/V	1684	N/V	2961
Parsnip	559	N/V	764	925	996	1319	N/V	N/V	N/V	2923
Peach	523	N/V	748	N/V	992	N/V	1421	1714	N/V	2929
Pearl Barley	499	628	N/V	931	1012	1336	1427	1644	N/V	2925
Potato	520	664	753	936	992	1333	N/V	1680	N/V	2872
Red Pepper	521	N/V	779	922	1014	1232	1405	N/V	N/V	2931
Scallion	491	N/V	779	N/V	1014	1245	1413	1663	N/V	2902
Soya Flour	513	706	N/V	N/V	1048	1231	1438	1656	N/V	2923
Soya Mince	546	706	N/V	N/V	993	1235	N/V	1687	N/V	2970
Turnip	552	696	779	918	1007	1234	1345	1594	N/V	2930
Yellow Pepper	547	668	778	N/V	N/V	1243	1393	1582	N/V	2982

2.4.1.1.1 Germanium oxygen bands, Ge-O and Ge=O

Ge=O is the bond that is associated with being in some germanium compounds but is not specific to Ge-132 alone. For example it can be found alternatively in germanium (IV) oxide also. So it can only be used as an indication of the presence of a germanium compound. The presence of a Ge-O bond might give an indication of organogermanium as it is not present in the inorganic germanium oxide. Ge-132 is used as the reference spectrum to establish the characteristic bands to be found in the foodstuffs analysed via IR spectroscopy.

Ge=O has absorptions assigned to 555, 798, and 1413 cm^{-1}. These absorptions are weak apart from the band at 1400 cm^{-1} which is strong relative to the interferents. Most of the foodstuff spectra only show 2 out of 3 of these bands. This is normally the case as the 555 cm^{-1} band is in the near infrared region where there is a lot more interference observed. The full list can be seen in Table 2.4. Results seem to indicate the presence of Ge=O bonds e.g. carrot has bands that may be assigned to Ge=O at 778 and 585 cm^{-1}. Green pepper bands visible at 775 and 1403 cm^{-1} indicate that the visibility of these bands can be dependant on the composition of the foodstuff analysed.

Ge-O has two characteristic bands at 2346 and 2946 cm^{-1}. In the case of all the foodstuffs analysed, the 2946 cm^{-1} band was readily observed in most of the foodstuffs but the band at 2346 cm^{-1} wasn't visible or if visible, it was too weak to be distinguished from noise. Carbon dioxide interference proved the greatest problem as it tends to absorb at about 2300 - 2100 cm^{-1} so it would have obscured this band. This was found to be the case by Belton *et al.* [134] who indicated that atmospheric carbon dioxide could dissolve when the sample is being dried and carboxylic acid components in the food matrix can be converted to carboxylates.

It can be postulated that if the 2946 cm^{-1} band is present, there is an indication of Ge-O in all the foodstuffs studied except the ginger tablet and, therefore, there may be the possible presence of inorganic or organic germanium complexes in the samples.

2.4.1.1.2 Germanium oxygen network (Ge-O-Ge)

The germanium oxygen network has three bands assigned to 927, 1047 and 1240 cm^{-1}. It was suggested [104] that the presence of this network in the IR spectrum of a food sample would mean that germanium sesquioxide rather than germanium oxide existed in the foodstuff. The samples that showed the presence of this network were garlic, cauliflower and the ginger tablet among other vegetables studied as indicated in Table 2.4.

The problem with the Ge-O-Ge band is that the food matrix can easily cause interference or in some cases it was quite weak and indistinguishable from noise even with spectral enhancement at 1100 – 700 cm^{-1}. There are also a series of other bands

that can be associated with this germanium oxygen network at 1047 and 1240 cm^{-1}. These bands can also be easily interfered with because C-O groups absorb around 1300 -1000 cm^{-1} and would be present in carbohydrates in foods.

2.4.1.1.3 Germanium carbon bands

These bands can be seen at ~ 612 cm^{-1}. This band is close to the near-IR end of the spectrum where there is a lot of interference. As such there were only a few occasions where it was observed in the foodstuffs such as lettuce and mushroom. This doesn't mean there was no Ge-C bond present in the food sample when the band was not visible but rather that it was hard to clarify with the noise of the spectrum in the 700 – 400 cm^{-1} range as can be seen in the spectrum for lettuce (fig. 2.7). It also may indicate the presence of other organic germanium compounds, such as sanumgerman/germanium lactate citrate [135], which also possess a Ge-C functionality.

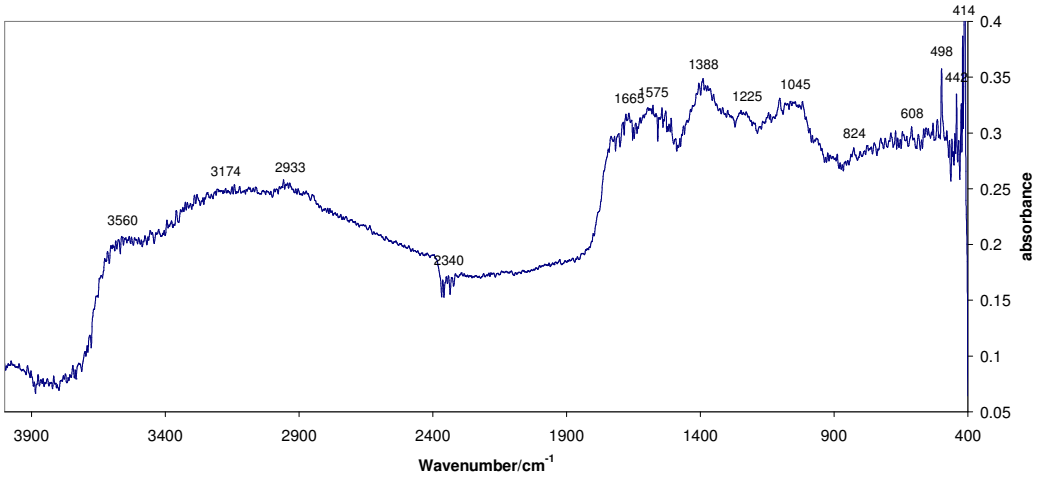

Fig. 2.7 FTIR spectrum of Lettuce.

2.4.1.1.4 Carbonyl bands

The carbonyl bond can be observed at 1691 cm^{-1}. It is a sharp band and is readily observable but does not give definitive proof of Ge-132 in the foodstuff sample as it can be found in a variety of other molecules such as lipids and carbohydrates [128,136]. This cannot be used as an indicator but it was included as it is part of the Ge-132 structure.

It was observed in carrot, cauliflower, cucumber and garlic and others as indicated in Table 2.4. It was not observed in green pepper and red pepper. It was unusual that it was not visible in the afforementioned foodtuffs as they do contain sugars in their food matrix which in turn have carbonyl groups. There was a peak observed at approximately 1720 cm^{-1} for some of the peppers but the peaks were weak and noisy.

2.4.1.1.5 Foods that contain Germanium(IV) compounds

The presence of germanium sesquioxide in foods is a possibility with some of the foods studied in Table 2.4. Foods that possess the Ge-C and the Ge-O-Ge network are most likely to contain germanium sesquioxide as inorganic germanium does not possess these bands. The foods that possess a Ge-C and a Ge-O-Ge band are mushroom, pearl barley, potato, soya flour, soya mince and turnip.

Inorganic germanium or germanium dioxide cannot be readily determined from the FTIR spectrum as the Ge=O band is also present in the germanium sesquioxide structure making it difficult to distinguish the presence of inorganic germanium in food.

2.4.1.2 Food matrix interference for Germanium (IV) compound determination

Previous research done by McMahon *et al.* [104] used FTIR spectroscopy to determine germanium sesquioxide presence in foods. The previous FTIR analyses failed to take into account the broad variety of biomolecules that are present in foodstuffs. Germanium is also present in trace amounts in the region of 0-10 µg/g in most food. A fraction of this is attributable to germanium sesquioxide making it present at very low concentrations [31,104]. The primary constituents in food that contribute to their biological makeup are lipids, carbohydrates and proteins [127]. These constituents are present in quantities that would be much greater than that of germanium sesquioxide and it is very possible that they have more intense IR bands for their functionalities. The following sections for protein, lipids and carbohydrates will try to assess the degree of this interference.

2.4.1.3 Proteins

Proteins are polypeptide chains that are composed of 20 different amino acids in various combinations and lengths. Proteins form the majority of tissue in plants and animals alike. They have a variety of biological roles in the body including structural molecules i.e. cell wall, enzymes and hormones [137]. This abundance in foods would make them a primary interferent in the determination of germanium sesquioxide in foods.

Proteins have three different types of aspects to their structures that are classified as primary, secondary and tertiary. The primary classification refers to the arrangement of the amino acids in the polypeptide chain and has distinctive functionalities like C-N at regular intervals on the protein chain and C-S and S-H with components such as cysteine and methionine. The secondary structure refers to how the polypeptide chains in the protein tend to arrange themselves such as in an α-helix or a β-pleated sheet. The secondary conformation is also mediated by effects such as disulphide linkages or S-S interactions between S-H groups of certain amino acids. The tertiary conformation is known as the 3-D arrangement of all the atoms in a protein [138]. Knowing this information about protein structure, it is possible to come up with a table of IR bands that are specific to proteins (see Table 2.5).

Table 2.5 IR bands associated with protein functional groups and conformational properties [127].

Assignment	Functional Group	Ideal/cm^{-1}
Proteins	C-Nprotein	1300-1230
	S-Sprotein(cysteine)	512
		525
		540
	C-Sprotein(methionine)	630-745
	S-Hprotein(methionine)	2550-2580
	d-ring(tryptophan)	1360
		880
		760
	(C=O)O$^-$ Aspartic and glutamic acids	1400-1430
	(C=O)OH Aspartic and glutamic acids	1700-1750
	a-helix	1655
		1275
	anti-parallel B-sheet	1670
		1235

2.4.1.3.1 Carbon-nitrogen bands (C-N)

This band absorbs at a range of 1300-1230 cm^{-1} at a medium intensity. The C-N bond is intrinsic to all protein molecules and gives a good indication of its presence along with other associated bands. Proteins are found in a variety of plant and meat products so they would be a common interferent in foodstuffs. Foodstuffs found to contain this group were carrot, cauliflower and cucumber among others indicated in table 2.6.

It is also found in soy products, soya mince and soya flour. This is to be expected as the soybean that they are derived from is protein based [97] and as such is most likely to possess the C-N band.

Table 2.6 Results for IR bands of Protein molecules in food (Note: N/V refers to No Visible band)

	Protein Functional Groups/cm^{-1}																			
	C-H	S-S			C-S	S-H	d-ring			(C=O)O$^-$		(C=O)OH	α-helix			anti-parallel β-sheet		
Ideal	1300-1230	512	525	540	630-745	2550-2580	1360	880	760	1400-1430		1700-1750	1655	1275	1670	1235		
Apple	N/V	N/V	N/V	544	N/V	N/V	N/V	N/V	N/V	N/V		1729	1658	N/V	N/V	N/V		
Carrot	1238	514	N/V	541	N/V	N/V	N/V	N/V	N/V	1429		1735	1660	1238	1660	1238		
Cauliflower	1236	498	N/V	N/V	666	N/V	N/V	N/V	777	1403		N/V	1667	N/V	1667	1236		
Cucumber	1227	515	N/V	550	N/V	N/V	N/V	N/V	771	1401		1720	1663	N/V	1663	1227		
Garlic	N/V	N/V	N/V	N/V	666	N/V	N/V	N/V	N/V	1404		N/V	1662	N/V	1662	N/V		
Ginger Tablet	N/V	514	N/V	N/V	N/V	N/V	N/V	N/V	763	1430		N/V	1660	N/V	1660	N/V		
Ginseng Tablet	1222	531	531	567	678	N/V	1364	N/V	N/V	1413		1736	1660	N/V	1660	1222		
Green Pepper	1217	N/V	N/V	N/V	N/V	N/V	N/V	N/V	N/V	1403		1714	N/V	N/V	N/V	1217		
Lettuce	1225	N/V	N/V	N/V	N/V	N/V	1388	N/V	N/V	1388		N/V	1666	1225	1666	N/V		
Mushroom	N/V	549	N/V	549	N/V	N/V	N/V	887	741	N/V		N/V	1684	N/V	1694	N/V		
Parsnip	1141	559	N/V	559	N/V	N/V	1319	N/V	730	N/V		N/V	N/V	N/V	N/V	1141		
Peach	N/V	N/V	523	N/V	N/V	N/V	N/V	885	748	1421		1714	N/V	N/V	1714	N/V		
Pearl Barley	1142	N/V	N/V	N/V	628	N/V	1336	859	N/V	1427		N/V	1644	N/V	N/V	1142		
Potato	1149	N/V	520	N/V	664	N/V	1333	860	731	N/V		1680	N/V	N/V	1680	1149		
Red Pepper	N/V	N/V	521	N/V	N/V	N/V	N/V	853	779	1405		1717	N/V	N/V	1717	N/V		
Scallion	N/V	604	491	N/V	N/V	N/V	1351	N/V	723	1413		1734	1663	1245	1734	1245		
Soya Flour	1139	N/V	513	N/V	N/V	N/V	1231	N/V	N/V	1438		1744	1656	1231	1744	1231		
Soya Mince	1163	663	N/V	546	663	N/V	N/V	N/V	N/V	1456		1687	1687	1235	1687	1235		
Turnip	1131	628	486	552	628	N/V	1234	868	706	N/V		N/V	1594	1234	N/V	1234		
Yellow Pepper	N/V	624	475	547	624	N/V	1243	868	N/V	1582		1732	1582	1243	N/V	1243		

2.4.1.3.2 Disulphide linkages (S-S)

Disulphide linkages or S-S bands are resultant from weak covalent interactions between thiol groups in cysteine amino acids. This linkage causes folds in the structure of the protein chain giving it a curled conformation. This would be used as a further indicator of the presence of a protein in a sample. It shows bands at a range of 540-512 cm^{-1} in the IR [138].

These bands were observed for about half the samples analysed. It was also hampered by the fact that there was a lot of noise around 500 cm^{-1}. They were observed for cucumber, carrot and mushroom among others. The disulphide linkages are very sensitive to heat so it is possible that the disulphide linkages split during oven drying or the bands were lost in the noise at the end of the spectrum.

2.4.1.3.3 Carbon-Sulphide band (C-S)

This band would be seen at 630-745 cm^{-1} with a weak absorption. This particular band would be seen if methionine is present in a protein chain. The presence of this band was only seen in a few samples including cauliflower, garlic and ginseng tablets. Its weak absorption is prone to noise and this might explain why it hasn't been seen in some of the other spectra.

2.4.1.3.4 Sulphur-Hydrogen band (S-H)

This band would be found commonly in the 2550-2580 cm^{-1} region of the spectrum. In this instance, there was no sign of this band in any of the FTIR spectra for the food samples. This could mean that there is no thiol group in the proteins in the food samples and hence no methionine or there could be a major interfering band blocking this band from showing. It is possible that it is hydroxyl band interference causing this as it is present in greater abundance in saccharides, proteins and lipids alike. The hydroxyl band also absorbs in a broader region at about 3600 -3000 cm^{-1}. [122] This might account for why it is not apparent on the FTIR spectra.

2.4.1.3.5 Carbonyl bands ((C=O)O$^-$, (C=O)OH)

(C=O)O$^-$ band is associated with the aspartic and glutamic acids and has a weak absorption at 1400-1430 cm^{-1}. This form normally occurs when the molecule is solvated allowing the dissociation of the H^+ ions in the solution. This also gives it a lower frequency absorption as stated due to the loss of the hydrogen and hence less hydrogen bonding that normally strengthens the intermolecular bonds resulting in higher vibrational frequency [139]. The absorption can be seen in food samples such as lettuce, ginger tablet and carrot (see Table 2.5).

(C=O)OH band is also associated with aspartic and glutamic acids and has a weak absorption at 1700-1750 cm^{-1}. The vibrational frequency is higher than the (C=O)O$^-$ for reasons discussed previously. This band was observed in food samples such as ginseng tablet and cucumber. The afforementioned bands are not specific to proteins as they can also be found in lipids to an extent or in their degradation products but if they are present they give an indication of the presence of aspartic and glutamic acids in protein [127].

2.4.1.3.6 Secondary structure of proteins

The α-helix is a secondary structural arrangement of amino acids in a protein. It resembles a corkscrew in terms of its spiral conformation [140]. The bands for the absorptions are at 1655 cm^{-1} and 1275 cm^{-1}. These bands were observed in foodstuffs such as lettuce and cucumber among others (see Table 2.5).

The β-sheet is another secondary structural arrangement of proteins. As the name suggests, the protein chains are arranged in zig-zag sheets that can either be parallel or anti-parallel [140]. The anti-parallel β-sheets can be found at 1670 and 1275 cm^{-1}. These are similar to the bands reported for the α-helix. These bands were found in carrot, cucumber and lettuce. With the noise of the FTIR spectra though, it is difficult to distinguish between the 2 structural arrangements.

2.4.1.3.7 Foods that contain Protein

Protein should be present in a number of food samples such as apple and soya based products. Protein presence can be identified by key functionalities such as C-N band and the bands due to the α-helix and the β-pleated sheets. Other functionalities, such as C=O, can be attributed to other food components such as carbohydrates. The C-S band is a weak absorption and is not as common as the C-N band because it is only associated with methionine while C-N is intrinsic to every amino acid.

The foods in table 2.6 that have the C-N, α-helix and the β-pleated sheets bands are carrot, cauliflower, cucumber, ginseng tablet, lettuce, potato, soya flour, soya mince and turnip. The rest of the foods either showed no presence of C-N bands or did not possess 3 out of 4 of the bands for α-helix and the β-pleated sheets.

Protein analysis has been conducted by groups such as Lacroix *et al.* where they looked at films of whey and soya protein. They found substantial N-H absorptions at 3293 cm^{-1} was indicative of protein presence. They were also able to detect the presence of α and β conformations of proteins at 1653 and 1638 cm^{-1}[141].

The interferences associated with germanium based compounds and proteins has only been documented by Sewell *et al* [142]. Their study involved the use of biomimetic templates for the formation of GeO_2 crystals where they used polyamidoamine (PAMAM) and polypropyleneimine (PPI) dendrimer peptides. Under analysis by FTIR, they noted a Ge-O-Ge band for the GeO_2 crystal (as it would be in a polymerised format within the crystal) around the 790 to 890 cm^{-1} range. The peptide amide stretching frequencies I and II were in the range of 1650 and 1450 cm^{-1}. This however is a controlled germanium dioxide synthesis experiment in the presence of selected peptides so the lack of interference is due to the simpler nature of the peptides compared to those of proteins which are polypeptides and thus more complicated and IR band rich [142].

Germanium sesquioxide has been analysed within biological matrices before in the form of Jurkan cells with the protein bands taken into consideration by Gaudenzi *et al.* The group found that in the presence of Ge-132 that they noted amide II absorption intensity decreased a small amount after 5.5 to 7 hours of exposure in the Jurkan cell

spectrum. peak shifts went up to 1550 cm^{-1} for the α-helix shift. They also noted the appearance of spectral features at 1000 and 1450 cm^{-1} [143].

Taking into consideration the FTIR bands that are attributable to proteins and those of the germanium compounds (result comparison in table I) there is little distinction to determine whether there is any absorption taking place due to germanium based compounds or due to protein absorption e.g. Gaudenzi *et al.* make reference to a band forming at 1450 cm^{-1} with sufficient exposure to Ge-132 but this band is also found in proteins from $(C=O)-O^-$ band as a result of deprotonation and is not necessarily confined to proteins.

2.4.1.4 Lipids

Lipids are biological hydrocarbons in plants and animals that have a diverse range of functions from energy storage to cell wall composition in the case of phospholipids membranes. They are normally soluble in organic solvents. Their structure is normally one that is divided between that of saturated lipids, that are normally found in lard and unsaturated lipids such as in sunflower oil. The unsaturated lipids normally contain the C=C and C-C bands. These lipids also possess bands such as =C-H, CH_2, and CH_3. The saturated lipids contain only the C-C, CH_2 and CH_3 bands. In triacylglycerols, the lipids contained are fatty acid esters of glycerol that possess C=O bands [138].

Knowing these aspects of lipid structure, it is possible to collate a table of functionalities and respective IR bands so as to establish the presence of lipids in the studied foodstuffs (see Table 2.7).

Table 2.7 IR bands associated with lipid functional groups [127].

Assignment	Functional Group	Ideal/cm^{-1}
Lipids	v(=C-H)	3008
	$v(CH_3)$	2970
	$v(CH_2)$	2940
	v(C=O)	1750
	$v(C=C)_{trans}$	1670
	$d(CH_2)$	1444
	v(C-C)	1100-800

Table 2.8 uses the values from table 2.7 with the foodstuffs studies and the results are compiled into a format that is quite similar to that observed for table 2.5. Sections 2.3.1.4.1. to 2.3.1.4.5 detail the absorptions due to =C-H, CH_3, CH_2, C=O, C=C and C-C bands.

Table 2.8 Results for IR bands of lipid molecules in food (Note: N/V refers to No Visible band)

	Lipid Functional Groups/cm^{-1}						
Functional Group	v(=C-H)	$v(CH_3)$	$v(CH_2)$	v(C=O)	v(C=C)trans	$d(CH_2)$	v(C-C)
Model IR bands	3008	2970	2940	1750	1670	1444	1100-800
Apple	N/V	2920	2911	1729	1658	1415	1045
Carrot	N/V	2927	2900	1735	1660	1429	1046
Cauliflower	N/V	N/V	2900	N/V	1667	N/V	1037
Cucumber	N/V	2936	N/V	1720	1663	N/V	1044
Garlic	N/V	2942	N/V	N/V	1662	N/V	N/V
Ginger Tablet	N/V	N/V	N/V	N/V	1660	N/V	N/V
Ginseng Tablet	N/V	N/V	2927	1736	1660	N/V	1031
Green Pepper	N/V	2944	N/V	1714	N/V	N/V	1044
Lettuce	N/V	2933	2933	N/V	1666	N/V	1045
Mushroom	N/V	2961	N/V	N/V	1684	N/V	1020
Parsnip	N/V	2923	N/V	1717	N/V	1417	996
Peach	N/V	N/V	2929	1714	N/V	1421	969
Pearl Barley	N/V	2925	2925	N/V	1644	1427	1012
Potato	N/V	2872	2872	N/V	1680	N/V	N/V
Red Pepper	N/V	2931	2931	1717	N/V	1405	1055
Scallion	N/V	2902	2902	1734	1663	1413	1050
Soya Flour	N/V	2923	2923	1744	1656	1438	1048
Soya Mince	N/V	2970	2970	N/V	1686	1456	N/V
Turnip	N/V	2930	2930	N/V	1594	N/V	1057
Yellow Pepper	N/V	2939	2882	1732	1582	N/V	1061

2.4.1.4.1 Sp^2 carbon-hydrogen band(=C-H)

This band is visible at 3008 cm^{-1}. It is found in unsaturated lipids such as olive oil. This particular band was not observed in any of the foodstuffs analysed suggesting that there are either no unsaturated fats in the foodstuffs or it is being interfered with by the broad hydroxyl band.

It is also possible that the mentioned groups are present in aromatic amino acids such as phenylalanine [138]. The commonalities of this band in other biomolecules like protein can mean that it is not suited for the sole determination of unsaturated lipids in foods.

2.4.1.4.2 Sp^3 carbon-hydrogen band(CH_3) and Sp^2 carbon-hydrogen band(CH_2)

The CH_3 band is visible at 2970 cm^{-1}. It is found in saturated, unsaturated lipids, proteins and sugars. This band was seen in a range of foodstuffs including apple, carrot and cucumber, indicating that there is saturated fat in these foodstuffs or sugar or proteins are present. The CH_2 band is visible at 2940 cm^{-1}. It can be found in the same types of molecules as CH_3. This was found in carrot, apple and ginseng tablet amongst others.

These cannot be used to determine a specific interferent as they can be assigned to a wide range of biomolecules such as carbohydrates and proteins [137] and therefore cannot be solely attributed to lipids.

2.4.1.4.3 Carbonyl group (C=O)

This band is apparent at 1750 cm^{-1}. It is normally found in the ester group of the lipid but can be found in sugars such as ketoses and proteins such as aspartic and glutamic acid as discussed earlier [137]. The band was found in a wide range of foodstuffs including peach, red pepper and scallions.

2.4.1.4.4 Carbon-carbon double bond (C=C) and carbon-carbon single bond (C-C)

The C=C band is found at 1670 cm^{-1}. These groups are normally associated with unsaturated lipids such as spreadable butter. It was found in foodstuffs such as potato, pearl barley and soya flour amongst others.

The C-C band is assigned to the range of 1100 – 800 cm^{-1}. It is found in any organic molecule such as protein and sugars. It doesn't give a definitive idea of the presence of lipids as it is such a common band. It was found in most of the foodstuffs analysed as a result including parsnip, yellow pepper and turnip.

2.4.1.4.5 Foods that contain lipids

The presence of lipids in foods can be ascertained by the presence of C=C bands from unsaturated lipids. These are quite common in vegetables and thus should be the most prominent. The other bands, such as CH_3 and C=O, can be found in carbohydrates and proteins so they cannot directly confirm the presence of lipids. The =C-H band is not a viable means of determining lipid presence as it is normally interfered with by OH groups at 3600 – 3000 cm^{-1}. This explains why the =C-H band is not visible in the IR spectra of the samples studied.

Table 2.8 shows that the C=C band is present in most foods studied with the exception of green pepper, parsnip, peach and red pepper. It is unusual that green pepper seems not to contain lipids whereas yellow and red pepper does. This may have been due to interference from another band. The same could also be said of parsnip and peach.

FTIR analysis of lipids within foods is normally used for the assessment of the degree of unsaturation and saturation of the lipid by comparing the ratio of sp3 methyl bands to that of sp2 carbons by comparison of bands at 1465 and 1418 cm^{-1} respectively. The amount of free fatty acids (an indicator of rancidity/breakdown of lipids) can also be determined within lipids by looking at deconvolution of bands at 1710 cm^{-1} for the carboxylic acid bands of the free acids and the carboxylic acid group at 1746 cm^{-1} for the esters [144].

The functionalities that can interfere with with germanium determination in the presence of lipids are the Ge-O band of 2946 cm^{-1} and also the C=O (1691 cm^{-1}) functionality is common to both germanium sesquioxide and lipids. Lastly, the CH_2 stretch for the lipids can be interfered with by the Ge=O band at 1413 $cm^{-1}$from germanium dioxide and germanium sesquioxide. In comparison to table 2.4, there are

only 7 out of 10 FTIR bands, for lipids described here, when taking into account potential bands due to lipids that can interfere with germanium determination.

2.4.1.5 Carbohydrates

Carbohydrates are the most abundant biomolecule in nature and are essential to life in general. Carbohydrates consist of basic carbohydrate units called monosaccharides and are "straight chain polyhydroxy alcohols"such as glucose that contain a range of functionalities including C=O, C-C and CH_3 to name but a few. Disaccharides are two monosaccharides that are linked in a glycosidic link (R-C-O-C-R). Examples of these are sucrose or table sugar that consists of fructose and glucose. Polysaccharides are polymers of monosaccharide units such as cellulose. Cellulose can possess up to 15000 d-glucose units. Polysaccharides possess a greater number of glycosidic links than disaccharide due to their polymeric nature. Amylopectin and amylose are storage polysaccharides and form the constituents of starch in plants. This makes them a good source of energy for the plant and can be found abundantly within the plant structure [140].

In short, the C-O-C bond becomes the primary means of identification for the saccharides as it is the most unique functionality for them [140]. Each saccharide type has a specific band that are indicated as follows (see Table 2.9).

Table 2.9 IR bands associated with carbohydrate functional groups [127].

Assignment	Functional Group	Ideal/cm^{-1}
Saccharides	vC-O-Cmono/disaccharide	847
		898
		477
	vC-O-Cpolysaccharide	1122
		1094
	v(C-O-C)amylose/amylopectin	941
		868
		477

2.4.1.5.1 Carbon oxygen network (C-O-C)di/monosaccharides

The carbon oxygen network can be found at bands of 847, 898 and 477 cm^{-1}. These bands are in a noisy range of the spectrum and even with enhancement can be hard to distinguish from noise. The carbon oxygen network comes from the formation of hemiacetal rings in the case of monosaccharides like glucose and fructose [137]. The carbon oxygen network can be found in the case of a number of foodstuffs like carrot, apple and potato (refer to table 2.10). This gives an indication of the presence of mono/disaccharides in these foodstuffs.

Table 2.10 Results for IR bands of Carbohydrate molecules in food (Note: N/V refers to No Visible band)

	Saccharide Functional Groups/cm^{-1}							
Functional Group	**vC-O-Cmono/disaccharide**			**vC-O-Cpolysaccharide**		**v(C-O-C)amylose/amylopectin**		
Model IR bands	**847**	**898**	**477**	**1122**	**1094**	**941**	**868**	**477**
Apple	**867**	**892**	**468**	**1073**	**1045**	**N/V**	**867**	**468**
Carrot	**829**	**900**	**466**	**N/V**	**1046**	**N/V**	**865**	**466**
Cauliflower	**N/V**	**901**	**442**	**1078**	**1038**	**N/V**	**N/V**	**498**
Cucumber	**N/V**	**916**	**442**	**1081**	**1046**	**N/V**	**866**	**N/V**
Garlic	**820**	**N/V**	**441**	**N/V**	**1044**	**N/V**	**865**	**470**
Ginger Tablet	**N/V**	**N/V**	**425**	**1080**	**N/V**	**N/V**	**857**	**466**
Ginseng Tablet	**N/V**	**N/V**	**425**	**N/V**	**1031**	**N/V**	**N/V**	**464**
Green Pepper	**N/V**	**N/V**	**436**	**N/V**	**1044**	**N/V**	**868**	**498**
Lettuce	**824**	**N/V**	**414**	**N/V**	**1045**	**N/V**	**N/V**	**498**
Mushroom	**N/V**	**930**	**454**	**N/V**	**1020**	**N/V**	**887**	**N/V**
Parsnip	**N/V**	**925**	**457**	**N/V**	**N/V**	**N/V**	**863**	**N/V**
Peach	**N/V**	**N/V**	**436**	**N/V**	**1048**	**969**	**N/V**	**436**
Pearl Barley	**N/V**	**931**	**433**	**N/V**	**1004**	**N/V**	**862**	**433**
Potato	**860**	**936**	**454**	**N/V**	**992**	**936**	**860**	**454**
Red Pepper	**853**	**N/V**	**457**	**N/V**	**976**	**N/V**	**N/V**	**457**
Scallion	**N/V**	**N/V**	**491**	**N/V**	**N/V**	**N/V**	**N/V**	**419**
Soya Flour	**N/V**	**N/V**	**421**	**1073**	**N/V**	**N/V**	**N/V**	**421**
Soya Mince	**N/V**	**N/V**	**431**	**N/V**	**993**	**945**	**886**	**431**
Turnip	**868**	**987**	**437**	**1057**	**987**	**N/V**	**N/V**	**437**
Yellow Pepper	**868**	**976**	**475**	**1061**	**976**	**N/V**	**868**	**475**

2.4.1.5.2 Carbon oxygen network (C-O-C)polysaccharides

The carbon oxygen network in polysaccharides can be found at IR bands of 1122 and 1094 cm^{-1} (see Table 2.10). Polysaccharides are structural materials making up the bulk of a food matrix using polymers of monosaccharides. Cellulose would be the

most common in plants and consists of a series of β-D-glucose units. The polysaccharide carbon oxygen network was found in the case of cauliflower and peach among others. This means these foodstuff do contain polysaccharides including cellulose.

2.4.1.5.3 Carbon oxygen network (C-O-C)amylose/amylopectin

The carbon oxygen network in amylose and amylopectin can be found in bands at 941, 868 and 477 cm^{-1}. Amylopectin and amylose is an energy storage molecule for plants. This eventually forms into the polysaccharide known as starch. Thus finding the presence of amylopectin and amylose can indicate the presence of starch in foodstuffs. The presence of amylopectin/amylose was found in potato, carrot and ginger tablet amongst others [127].

2.4.1.5.4 Foods that contain carbohydrates

As discussed previously, the main identifying functionality for carbohydrates is the C-O-C band. The band can be different for each type of saccharide from monosaccharide to polysaccharide. All the foodstuffs studied show the presence of at least 2 of these bands. This would seem to confirm that there is a presence of carbohydrates present in all foods studied. These carbohydrates seem to all consist of the previously stated saccharide types as well. Most foods have complex carbohydrate systems so this would be expected.

Foods that contain carbohydrates are quite normally found in plants due to the presence of polysaccharide supports such as cellulose and pectin used in the structural composition of fruit/vegetable and also starch for energy storage within the plant. Interferences that this can produce for the determination of germanium sesquioxide and germanium dioxide can normally be found with the Ge-O-Ge bands at 927 to1240 cm^{-1} (discussed in greater length in section 2.3.1.6) and also the Ge=O bands at 555 and 798 cm^{-1} [126].

2.4.1.6 Possible Interfering bands on germanium oxygen network band due to foodstuffs

The major interfering bands that would obscure the germanium oxygen network band were mainly due to carbohydrates and in small part to lipids. The lipid interference is broad due to the carbon-carbon band in the 1100 – 800 cm^{-1} region of the FTIR spectra. This means that it could very easily obscure the small peak range of 930 – 920 cm^{-1}. This might explain the non-visibility of the Ge-O peaks in the case of the ginseng tablet and cucumber (refer to table 2.11).

The major interfering bands would be due to the saccharides glycosidic linkages or C-O-C bands. They produce peaks in the range of 1122 – 477 cm^{-1}. The peaks are well defined and relatively sharp but they are fairly close to the Ge-O-Ge peak at 927 cm^{-1}. In the case of the C-O-C bands in amylopectin/amylose, there are two peaks that can cause significant interference at 941 and 868 cm^{-1}. This degree of proximity makes it hard to distinguish if the band seen at 920 - 930 cm^{-1} is due to Ge-O or one of the C-O-C peaks for a saccharide.

Table 2.11 IR bands comparison between Germanium Oxygen Networks (Ge-O-Ge) and Carbon Oxygen Networks (C-O-C)

	Germanium Functional Group/cm^{-1}			Cellulose Functional Group/cm^{-1}	
Functional Group	**Ge-O-Ge**			**vC-O-Cpolysaccharide**	
Model IR bands	**927**	**1047**	**1240**	**1122**	**1094**
Apple	**929**	**1052**	**N/V**	**1073**	**1045**
Carrot	**925**	**1046**	**1238**	**N/V**	**1046**
Cauliflower	**932**	**1038**	**1236**	**1078**	**1038**
Cucumber	**N/V**	**1055**	**1227**	**1081**	**1046**
Garlic	**930**	**N/V**	**N/V**	**N/V**	**1044**
Ginger Tablet	**923**	**N/V**	**N/V**	**1080**	**N/V**
Ginseng Tablet	**N/V**	**1031**	**1222**	**N/V**	**1031**
Green Pepper	**N/V**	**1044**	**1217**	**N/V**	**1044**
Lettuce	**N/V**	**N/V**	**1225**	**N/V**	**1045**
Mushroom	**930**	**1020**	**1295**	**N/V**	**1020**
Parsnip	**925**	**996**	**1319**	**N/V**	**N/V**
Peach	**N/V**	**992**	**N/V**	**N/V**	**1048**
Pearl Barley	**931**	**1012**	**1336**	**N/V**	**1004**
Potato	**936**	**992**	**1333**	**N/V**	**992**
Red Pepper	**922**	**1014**	**1232**	**N/V**	**976**
Scallion	**N/V**	**1014**	**1245**	**N/V**	**N/V**
Soya Flour	**N/V**	**1048**	**1231**	**1073**	**N/V**
Soya Mince	**N/V**	**993**	**1235**	**N/V**	**993**
Turnip	**918**	**1007**	**1234**	**1057**	**987**
Yellow Pepper	**N/V**	**N/V**	**1243**	**1061**	**976**

The interfering bands described in table 2.11 shows that the C-O-C band from cellulose is interfering with the Ge-O-Ge band for germanium sesquioxide. The Ge-O-Ge band is the primary indicator of the germanium oxygen network that is specific to germanium sesquioxide. The Ge-C band at 612 cm^{-1} could prove the presence of organic germanium i.e. germanium compound with the presence of carbon in its structure. This is not entirely specific to germanium sesquioxide as discussed in section 2.3.1.1.3. It seems to be interference free relative to the IR band values that have been collated for the other biomolecules studied and, therefore is the most likely band to be used for Ge determination using FTIR. This Ge-C band could still be interfered with, however, by some other IR band not being accounted for in this study or too weak to be deduced properly.

This interference in food analysis via FTIR has been seen in other areas of research such as the ethanolysis of soybean oil as determined by Zagonel *et al.* [145]. The groups looked at the tricglycerides and ethyl esters that were involved in the ethanolysis process with respect to soybean oil use. The 1700-800 cm^{-1} region of the spectrum was analysed for the production of the alcohol with PCA treatment done on two bands associated with the C=O functionality. The group also used size exclusion chromatography with a refractometer for more accurate determinations of triolein and ester content so as to minimise interferences from other compounds. It was found the FTIR predictions were around ± 1% of the predicted % content levels from the multivariate FTIR calibration model. The interference of saturated fats in low level trans fat determination has also been noted as a problem in FTIR by Mossoba *et al.* [146]. The group determined that there was weak band interference from the 962-956 cm^{-1} region from the saturated fats. The group reported that this could lead to false positives for trans fat bands that absorb at 966 cm^{-1}. The limit of quantitation for the trans fats was determined in the end for 1% of total fat using their method.

Taking into account that the germanium compounds are of a lower concentration than that of the other matrix interferences in the foodstuffs, an FTIR spectrum overlay (see Fig. 2.7) has been compiled based on the intensity values relative to that of the germanium content levels determined in chapter 3 for foodstuffs analysed in this chapter.

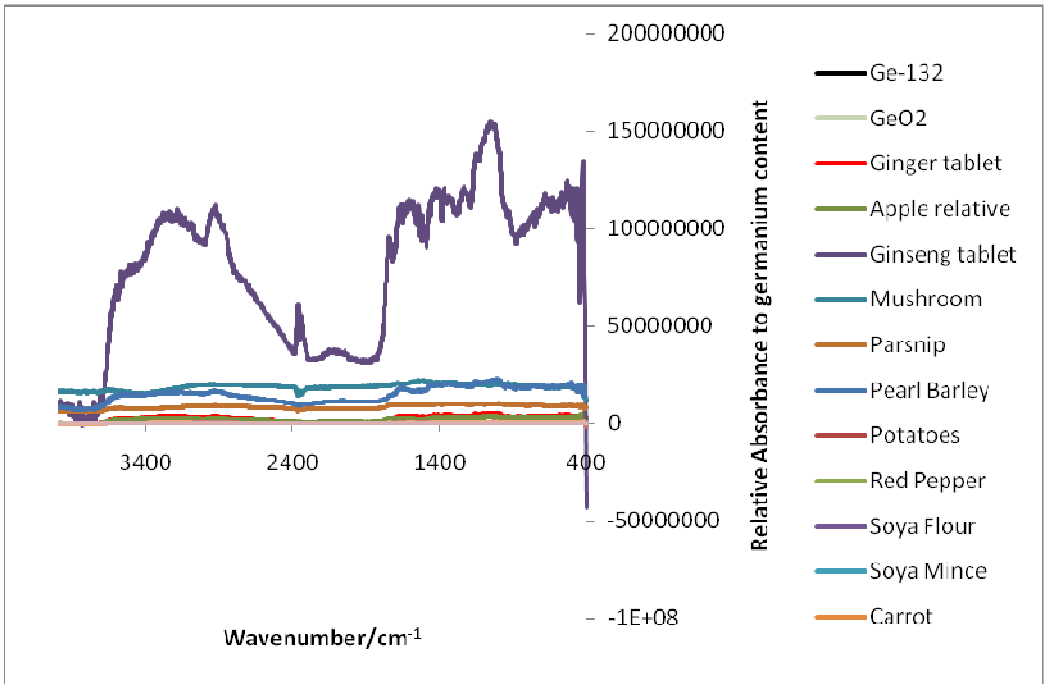

Fig. 2.7 FTIR spectra relative absorbance overlays for foodstuffs versus germanium compounds

The above figure indicates the relative FTIR absorbance values to that of Ge-132 and GeO_2. The spectra are mainly dominated by ginseng tablet and then followed by mushroom at a lower intensity. The germanium sesquioxide and germanium dioxide are of very weak intensity in grey and black and do not even show beyond the baseline with some of the weaker absorbing foodstuffs. This would indicate that germanium compounds would not have a strong absorbance relative to interferences in the foodstuff matrices. Thus, FTIR spectroscopy is not conclusive for the determination of germanium in foodstuffs.

2.4.2 FTIR analysis of soils

Soils primarily consist of mineral material, organic matter, microbes and a host of other components but it is primarily inorganic mineral matter. This is in the region of 45 % while the organic matter content can be as little as 5 % with air and water making up the subsequent 50 %. The organic portion of the soil contains animal biomass and cellulose that comes from decaying plant and animal matter. The cellulose can be broken down into glucose units by cellulolytic microbes. This provides a source of nutrition for the plants. The mineral/inorganic portion of the soil

consists of secondary silicates and iron and manganese oxides to name but a few. These minerals serve as an important source of nutrients for plants as well as an exchange matrix for cations like ammonium and calcium in a process of ion exchange [147,148].

In contrast to the foodstuffs, the soils possess a more pronounced content of inorganic minerals. This becomes even more important when the sample is dessicated. Bands of interest would be bands due to silicates that would be in the form of Si-O and Si-O-Si bands in the soil. Also the C-O-C bands from cellulose from decaying plant matter are of interest. Bands that might be relevant are the R-NH_2 and R-(C=O)-N-R for proteins. The aromatic rings in lignin are a primary constituent of plant cell walls. Bands that were also investigated were the C=C and C=O bands to assess the presence of fatty acids and carbohydrates [122,149].

2.4.2.1 Hydroxyl Group (R-OH)

In each one of the soil samples from site 1-12 there was evidence of a hydroxyl band. This was probably due to some degree of moisture remaining in the soil sample after desiccation as soil is at least 25% water and there could still be moisture traces in the samples even with dessication e.g. sorption of moisture from atmosphere by dried soil samples [147]. The spectrum could also be picking up the hydroxyl groups attributable to cellulose or other types of hydroxyl group containing organic compounds such as sugars or fats from decomposed vegetation (see Table 2.12).

Table 2.12 Functional groups commonly found in IR spectra of soils shown in the ideal row of the table. [122,127,149,150] The rest of the rows refer to results for IR bands found in Soil Samples from Sites 1-12.

	Functional groups common to soil/cm^{-1}														
Sample	Ge-O-Ge			Alcohol (R-OH)	Amine (R-NH2)	C-H bonds (symmetric)	C-H bonds (asymmetric)	C=O (carboxylic acids, aldehydes, ketones, esters)	C=C (aromatic groups conjugated with C=O and COO- groups)	Amides in proteins (R-N-H-R)	Aromatic rings in lignin	C-O-C (cellulose)	Si-O-Si	Si-O	
Ideal	927	1047	1240	3600-3000	3400	2870	2920	1740-1698	1600-1613	1653	1510	1081	780-810	900-1200	
Site 1	N/V	1031	N/V	3281	N/V	2853	N/V	N/V	1601	N/V	1438	1031	800	1031	
Site 2	N/V	1029	N/V	3324	N/V	N/V	2926	N/V	N/V	1636	1430	1104	798	1029	
Site 3	N/V	1033	N/V	3307	N/V	N/V	2922	N/V	1616	N/V	1428	1104	799	1033	
Site 4	N/V	1028	N/V	3325	N/V	N/V	2924	N/V	1610	N/V	N/V	1119	799	1028	
Site 5	N/V	1035	N/V	3292	N/V	N/V	N/V	N/V	1611	N/V	1425	1035	801	1035	
Site 6	N/V	1028	N/V	3354	N/V	N/V	2923	N/V	1616	N/V	1423	1028	801	1028	
Site 7	N/V	1018	N/V	3311	N/V	N/V	N/V	N/V	1610	N/V	N/V	1018	799	1018	
Site 8	N/V	1024	1227	3373	N/V	N/V	2920	N/V	1600	N/V	1431	1122	801	1024	
Site 9	N/V	1032	N/V	3362	N/V	N/V	2940	N/V	N/V	1651	N/V	1032	800	1032	
Site 10	N/V	1041	N/V	3386	N/V	N/V	2924	N/V	1605	N/V	N/V	1041	800	1041	
Site 11	N/V	1031	1222	3492	N/V	N/V	2930	N/V	1597	N/V	N/V	1114	797	1031	
Site 12	N/V	1032	N/V	3367	N/V	N/V	2933	N/V	1610	N/V	1413	1032	801	1032	

It is not possible to use the OH band as a definitive means of assignment as it is attributable to quite a number of biomolecules and moisture. It can, however, be used in combination with other bands as a means of cross-inference when related to other bands in the fingerprint region of the spectrum (see fig 2.6).

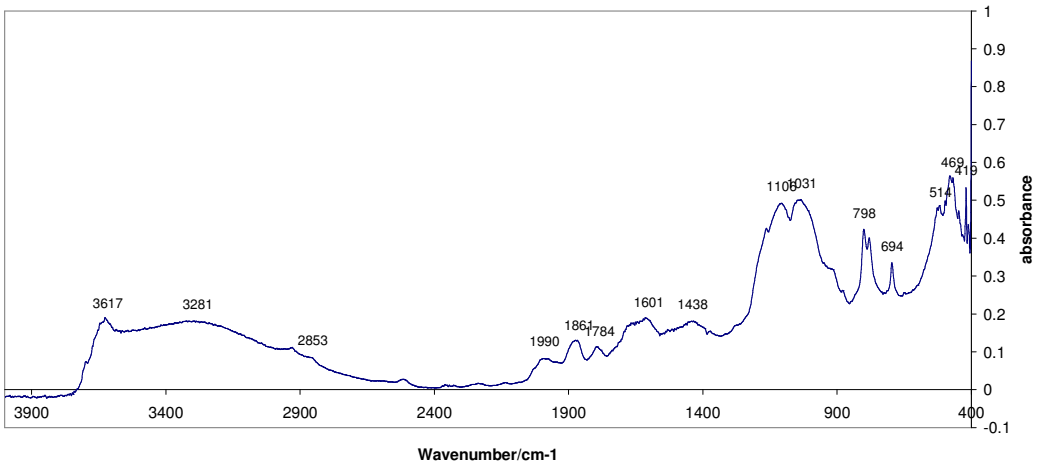

Fig 2.6 IR spectrum of Soil Sample Site 1

2.4.2.2 Amine ($R\text{-}NH_2$) and Amides (R-(C=O)-N-R)

There was no sign of an amine band in any of the soil samples. This is unusual as decomposed organic matter should have some traces of amine associated with the breakdown of proteins into their constituent amino acids. Most likely the FTIR spectra are too noisy and are overshadowing the band for $R\text{-}NH_2$.

Amides would be present in proteins typically found in soil. The wavenumber for this functionality is 1653 cm^{-1}. This band was only observed for soil sample sites 2 and 9 which are not as expected as there are proteins present in any type of soil. Again, the bands are not apparent probably because of noise and interference from other bands.

2.4.2.3 Carbon - Hydrogen bands (C-H)

The C-H bands were visible for most soil samples. They were predominantly symmetric as opposed to asymmetric. These C-H bonds may be attributable to the decomposing organic matter present in the soil, as organic matter is the main constituent of any type of soil.

2.4.2.4 Carbon – Carbon double bonds (C=C) and Carbonyl bands (C=O)

The carbon-carbon double bond occupies the region of 1600 - 1613 cm^{-1}. Most of the soil sample sites exhibit this band with the exception of site 2. This is probably because of the presence of aromatic groups in the soil due to natural compound such as unsaturated lipids, phenyl compounds and other unsaturated compounds.

The band assigned to carbonyl groups were not observed in any part of the soil samples which is surprising as soil should contain cellulose, sugars and lipids from plants and animals either from decomposition or other natural processes. This may be due to interference from other bands.

2.4.2.5 Aromatic Rings in Lignin

Band assigned to aromatic rings present in lignin is seen at 1510 cm^{-1}. It seems that it is present in most soil samples with exception of 7, 9, 10 and 11. Lignin is a constituent of wood and as such would be expected in most soil especially park areas where there is a higher abundance of trees but this is not always the case. This is the case with site 3 that was taken from a park site but the other park sites don't show any evidence of a lignin band. This may have been due to noise on the FTIR spectra or interference from a stronger absorbing band.

2.4.2.6 Cellulose (C-O-C), Si-O, and Ge-O-Ge

Cellulose is identified namely by its C-O-C band at about 1081 cm^{-1}. This should be visible in most of the soil samples. It seems to be present in all of the sample sites. This is to be expected as soil is composed of decaying plant matter and should give the strongest band on the spectrum. It is present for all soil samples investigated (see Table 2.12).

Similarly, the Si-O band absorbs around 900 – 1200 cm^{-1}. This band directly interferes with the Ge-O-Ge band at 927-1240cm^{-1} and also that of the C-O-C network at 1081cm^{-1}. This represents a significant problem with trying to attribute a band in this area to any single functionality. The reason why these bands absorb so similarly is because the elements Si, Ge and C all lie in group 4 of the periodic table giving them rather similar behaviour in terms of their vibrational activity when it comes to

the oxygen networks. This was found earlier with foodstuffs highlighting the problems trying to analyse complex biological matrices such as food and soil.

The interferences observed in Table 2.13 shows that it is difficult to assess the presence of germanium sesquioxide in any of the soil sample sites. The cellulose band is present for all of the soil sample sites investigated as well as the Si-O band. Since soils are primarily inorganic/mineral based and contain large amounts of silicon based materials, it is highly unlikely that germanium sesquioxide can be found in soil utilising FTIR spectroscopy.

Table 2.13 IR bands comparison between Germanium Oxygen Networks (Ge-O-Ge) and Carbon Oxygen Networks (C-O-C) and Silicate bands (Si-O)

Sample	Ge-O-Ge/cm^{-1}			C-O-C (cellulose) /cm^{-1}	Si-O/cm^{-1}
Ideal	927	1047	1240	1081	900-1200
Site 1	N/V	1031	N/V	1031	1031
Site 2	N/V	1029	N/V	1104	1029
Site 3	N/V	1033	N/V	1104	1033
Site 4	N/V	1028	N/V	1119	1028
Site 5	N/V	1035	N/V	1035	1035
Site 6	N/V	1028	N/V	1028	1028
Site 7	N/V	1018	N/V	1018	1018
Site 8	N/V	1024	1227	1122	1024
Site 9	N/V	1032	N/V	1032	1032
Site 10	N/V	1041	N/V	1041	1041
Site 11	N/V	1031	1222	1114	1031
Site 12	N/V	1032	N/V	1032	1032

Interferences in soil bands determinations have been reported by groups such as nitrate determinations within soil using FTIR by Linker *et al.* [151]. The group looked at nitrate absorptions at 1350 cm^{-1} but found that the primary problem with the study was the levels of carbonate content associated sample created an interference at this band. The carbonate stretches were quite intense at the 1450 cm^{-1} in the case of highly calcareous soils. They managed to correct this issue, the group implemented PCA and neural network modelling and found it worked on nitrate determinations with soils with high carbonate contents. Soil analysis in forensic analysis via FTIR involves the

use of what is known as the preparation of "synthetic soil" for interference reduction of inorganic components [125]. The group accomplished this by adding 10 % Trizma (tris(hydroxyl-methyl) aminomethane) to iron oxide and the spectrum of the synthetic soil spectrum was taken from that of subsequent soil samples.

As was previously discussed in section 2.4.1.6, the absorbance relative to the germanium content in the soil can be determined approximately. This involved looking at the germanium content in soil as determined in chapter 3 and correcting soil sample absorbance relative to that of germanium absorbance. This was compiled into a spectral overlay as seen in fig. 2.9.

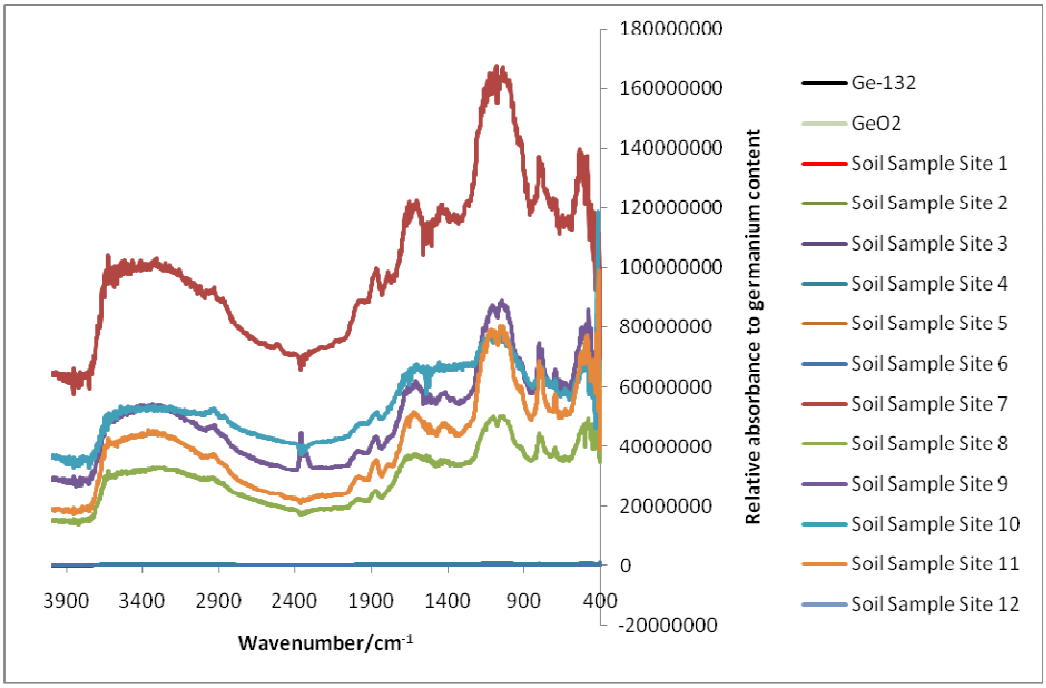

Fig. 2.9 FTIR spectra relative absorbance overlays for soils versus germanium compounds

Fig. 2.9 shows that the chances of detection of the germanium compound are quite low in the case of soil sample sites 7, 8, 9, 10 and 11. The other soil samples based on the chart look as if they have the same relative absorbance as that of germanium sesquioxide and germanium dioxide. The relative absorbances, however, of the other soil samples are in the order of 100,000 times more intense than that of the

germanium compounds absorbance. Their absorbance is overshadowed by the intensity of the other soil samples at the 20 to 200 $x10^6$ absorbance range.

2.5 Conclusion

Diffuse reflectance FTIR of foodstuffs and soils can yield detailed qualitative data as regards components in the food/soil sample matrix that would not be available with more non-specific techniques such as UV/Vis or fluorescence spectroscopy. The sample preparation for both sample types was quite simplistic with only oven desiccation being required.

The investigation of food and soils shows that germanium sesquioxide and germanium dioxide cannot be readily determined in either sample type. This was shown by the interference of the carbon oxygen network, C-O-C from cellulose with that of the germanium oxygen network, Ge-O-Ge in germanium sesquioxide using the food samples.
The primary interferents in soil for the Ge-O-Ge bands were Si-O from silicates and silica in the soil and C-O-C from cellulose in decaying plant matter.

The trace nature of germanium in soil and food makes the likeliness of determination of germanium(IV) compounds in soil using FTIR a difficult prospect. Additionally, levels are most likely well below the limit of detection of the FTIR instrument. The germanium sesquioxide and germanium dioxide signals would be extremely small in comparison to more abundant components such as proteins, lipids and carbohydrates. This decreases the possibility of identifying germanium(IV) compounds via FTIR spectroscopy.

Hence, the diffuse reflectance FTIR analysis of germanium(IV) compounds in foods and soils is not feasibly achievable without some form of radical sample pre-treatment or preconcentration technique.

Chapter 3: Atomic Absorption Spectroscopy of Ge, Cu, Pb and Fe levels in Foods and Soils

3.1 Introduction

The analysis of trace metal content has been used in foods to assess their nutritional or toxic qualities relative to the nature of the metal being analysed be it toxic lead or nutritional copper. These aspects of trace metal analysis in soils and foods gives a broader understanding of how metals are distributed in food and a better idea of the effects of certain biological sample matrix components in terms of metal accumulation. This can be found in the case of leafy vegetables or fungus species [152,153].

Trace metal content in food and soil samples can be analysed through a variety of means such as EDTA complexation in combination with capillary electrophoresis [154] and polarography [155]. The main method of analysis for trace metal determination is Atomic Absorption Spectrometry (AAS) subdivided into two subcategories of sample atomisation i.e. flame and graphite furnace. Flame analysis is normally suitable for ppm (part per million) concentrations of metals present in a sample and graphite furnace is normally regarded as being suitable for ppb (part per billion) quantities of trace metal in a sample [156].

The trace metal content of soil samples can be used to assess the nutritional or polluted status relative to flora and fauna. This can be best assessed by performing representative samples over areas of 1 hectare or more. Metals that are normally analysed are copper, iron and zinc for the nutritional status of the soil and heavy metals such as lead, arsenic, and cadmium are analysed in relation to toxic aspects of the soil. The content levels of the soil can have a knock on effect on accumulation in the herbage or vegetables growing in the soil [157].

3.1.1 Digestion

The analysis of trace metals can only begin when the sample is pretreated through techniques such as dissolution or sonication [158]. These methods may not be suitable for evaluating the total amount of trace metals that can be sequestered in components of a biological matrix such as metalloproteins [159] or complexed with polyphenolic substances [91] for example. This has to be remedied by more aggressive sample treatment from acid digestion using powerful acids such as hydrofluoric, hydrochloric and HNO_3. These acids have the capability of completely dissociating the organic components of a biological matrix and freeing the bound transition metals and converting them to more readily volatilisable substances such as metal salts like nitrates, in the case of HNO_3. The content of organic matter in the biological sample determines the composition or strength of the acid digestion solution [160].

Types of samples digestion include open vessel digestion and closed vessel digestion. Open vessel digestion involves the use of a sample dissolved in reagents heated on hotplates, typically, and vessels can be made of Teflon or glass. Closed vessel digestion is the use of closed pressure vessels made from Teflon or quartz glass. These systems normally involve the use of microwave heating for better temperature control. The processes can be compared in terms of sample weight, reagent consumption and process time as seen in table 3.1.

Table 3.1 Comparison of sample preparation parameter between open and closed vessel digestion [161]

	Open Vessel	Closed Vessel
Sample weight/g	0.5-10	0.1-1
Reagent consumption/mL	10-100	2-10
Typical process time/min	120-600	15-60

The open vessel as can be seen from table 1 is more resource consuming than that of the closed vessel setup. The open vessel is the simplest in terms of operator skill and equipment to implement. This is offset by problems such as poorer reproducibility and long decomposition times with a greater mix of reagents required. The closed vessel setup on the other hand uses less resources and has a quicker turnaround. There

is also greater temperature control with the digestion process via temperature programs, greatly enhancing overall reproducibility [161].

3.1.1.1 Soil Digestion

The digestion of soil can be accomplished by the use of well-established procedures such as aqua regia digestion (3:1 HNO_3:HCl) commonly used by the USEPA in general [162] with the development of more advanced digestion solutions such as the modified aqua regia method utilising hydrofluoric acid in combination with HCl and HNO_3 [163].

The type of digestion environment also has a major impact on the recovery of the trace metals in the soil sample. It has been established that the best digestion environment for soil samples is microwave-assisted digestion as it has the greatest degree of precision between soil digests but doesn't compare to the overall recovery of trace metals using open-vessel digestion systems [164,165].

Many publications have developed digestion methods for soil analysis based on SRM (soil reference materials) and analyse an environmentally indicative range of metals such as lead, cadmium, copper and iron. This was evaluated by C. Mico *et al.* [164] in relation to the analysis of calcareous soils (high carbonate content). Copper and lead were among the metals that were examined in relation to recovery levels from the SRM. The group found recoveries of 91 % and 96 % for lead and copper with respect to open-vessel digestion using a modified aqua regia method. This was higher than the values obtained for microwave-assisted digestion using aqua regia digestion with yields of 87 % and 93 % for lead and copper. The RSD values were lower in the case of microwave-assisted digestion as opposed to those of the open vessel digestions but Cu and Pb at values of 5 % and 7 % RSD were reported in the open-vessel digestions, well within acceptable parameters [164].

3.1.1.2 Food Digestion

Food digestions have to be treated differently than soils as they have radically different matrix components and ratios of these components. They are mainly much more organic than soil, which contains a higher mineral content and an extremely low organic content. This requires the use of digestion solutions that are more preferential to the digestion of organic biological matrices e.g. HNO_3 and $HClO_4$ [152,166].

The use of open and closed vessel methodologies for food digestion is subject to the same issues that occur with soils. The analytical sample portions are vital though, in terms of striking a balance between complete digestion of metals and using an adequate sample amount to allow detection of specified metals. It is especially important in the case of microwave digestion as the buildup of gas from too much sample can prove particularly hazardous [167].

Microwave assisted digestion was utilised by Erdogan *et al.* [168] for the analysis of Fe, Zn, Mn and Cu in legumes. This involved looking at parameters such as acid volume and temperature program modification for the microwave. They found that the establishment of adequate digestion for each legume such as chickpeas could best be achieved by tailoring the microwave program for each legume. The microwave programs were modified specifically for the chickpeas, lentils and kidney beans. The kidney beans, for example, had an optimal digestion program were 4ml HNO_3: 4ml H_2O_2 at 150 – 300 W at 7 min for Cu and 150 W for Zn for a total of 10 min. This method also included a predigestion step for the sample of 5 min at 2 ml HNO_3 and also the use of ice bath cooling of the sample in digestion vessel before and after the primary digestion step.

In terms of open-vessel setups, this can be achieved by the use of HNO_3 either solely or in combination with another acid such as $HClO_4$. This normally involves the dessicated food sample being digested by 10 ml of HNO_3 at temperatures between 70 to 130 ^{0}C until brown fumes appear due to nitrogen dioxide. In the case of the HNO_3/$HClO_4$ digestion method, this is followed by the addition of 1 ml of $HClO_4$. This is for the purpose of dissolving the organic parts of the food matrix that cause yellow colouring of the digest solution. This leaves a clear colour which is less susceptible to spectrometric interferences for analysis. **N.B. The critical step is to**

prevent this solution from evaporating to dryness as there is a risk of explosion [153,165,166].

3.1.2 AAS study of metals in biological samples

AAS or atomic absorption spectroscopy study of any metal in a sample is an effective way of determining its concentration. It is mediated by factors such as the external light source e.g. Hollow Cathode Lamp (HCL) for a given element (see fig. 3.1). The type of atomisation is also important i.e. whether it is flame or electrothermal in nature can cause atomisation of the metal elements more intensely than the other. The advantages of the electrothermal furnace design over that of the combustion flame is the lower background, sample consumption and detection limits. Drawbacks to the furnace design are sample preparation times for electrothermal analyis, the use of matrix modifiers specific to a particular element analysis and analysis runtimes tend to be longer. AAS in general also can be quite limited in comparison to atomic emission techniques where there is the capability of analysing many elements simultaneously i.e. emission spectrum is taken as a whole meaning multielement runs can be completed in faster times [169].

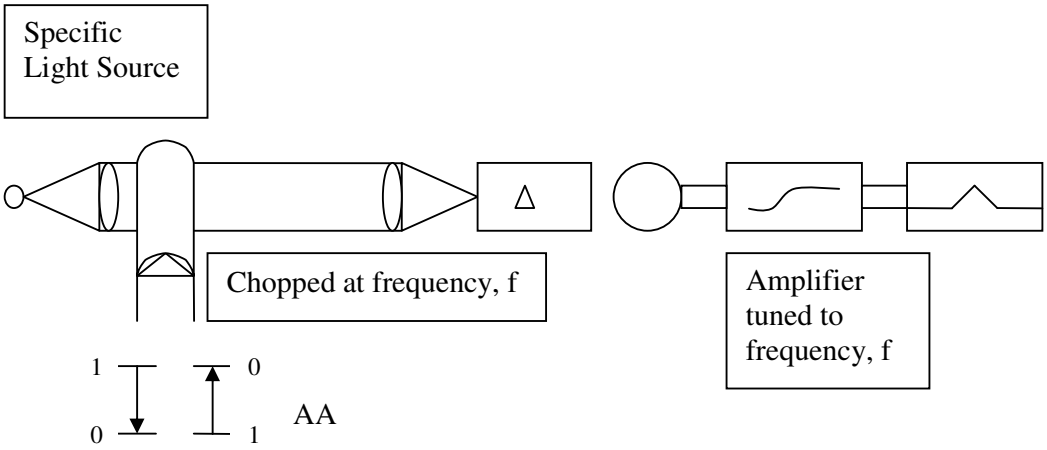

Figure 3.1 Typical layout of atomic absorption setup. The setup has a specified light source shining through a combustion flame (in this example) where sample is being atomised. The light interacts with the metal atoms and is absorbed promoting them to an excited energy state whereby the falloff in light intensity from the light source at x wavelength is measured via a photodiode, amplified and recorded via computer [169]

The AAS analysis of biological samples such as soil and vegetables can be related to the content of the metal being analysed in the foodstuff i.e. would it be suited to electrothermal analysis such as graphite furnace (GF) AAS or more flame analysis such as Flame AAS. If the content of the metal is high, say in the case of Fe in a soil sample, it can be more easily analysed via flame AAS as it is suited more to ppm levels. Low metal content can be more effectively analysed by GFAAS, as in the case of Pb in food and soil, as it is more more suited to ppb levels [157,170].

Hydride Generation (HG) AAS is also another method that could be suited to the analysis of foods and soils with the derivatisation of metals present in the sample matrix with a tetrahydroborate(III) solution generating a metal hydride species followed by the atomisation of the samples on atomisers like graphite furnace. This method improves the volatilisability of the metals for the atomisation process for atomic spectroscopy making it easier to detect the metals than conventional atomic spectroscopy techniques such as flame and graphite furnace AAS individually. Common sources of interference in these systems can be due to the type of hydride generation system, the nature of the reducing agent and acid, their mixing order and the type of atomizer utilised.

$$\begin{bmatrix} Analyte \\ e.g.Sb(III), Ge(IV), Se(IV) \end{bmatrix} \xrightarrow{NaBH_4+HCl} \begin{bmatrix} Volatile\ analyte\ hydride \\ e.g.GeH_2, SbH_3, SeH_2 \end{bmatrix} \xrightarrow{Atomization} \begin{bmatrix} Detector \\ e.g.GFAAS \end{bmatrix}$$

Fig. 3.2 Block representation of hydride generation process for atomic spectroscopy

3.1.2.1 AAS study of metals in Food

AAS analysis of food can relate to a broad range of elements but is normally centred around Cu, Pb, Zn, Mn, Fe, Ni and Co [152,171,172]. These metals are assessed in terms of their impact on the nutritional quality of the foodstuff and also the degree of contamination from heavy metals. This data is crucial to understanding the origin of ailments or health benefits associated with foods from a particular population [170].

Germanium in food samples was analysed by McMahon *et al.* [31] using GFAAS. This study was to evaluate the ideal parameters required for Germanium determination and also to ascertain the content in foods from apples to soya products.

The method showed a characteristic mass value of 3.50 µg L^{-1} and a Limit of Detection (LOD) of 3.37 µg L^{-1}. These improved values were attributable to a modification of the graphite furnace temperature program to a sample drying time of 30 sec at 85 ^{0}C.

Metal determinations of Cu, Cd and Pb among others have been performed in mushrooms by Soylak *et al.* [152] The determinations of the content of these elements was performed via Flame AAS for Fe, Cu, Mn, and Zn and via high gain antenna (HGA) graphite furnace for Pb, Cd, Co, Cr and Ni contents. The Cu, Pb and Fe levels were found to be somewhere in the region of 13.4 - 50.6 µg/g, 0.75 - 1.99 and 102 – 1580 µg/g respectively. The variation in the values was attributable to various species of mushroom that have slight variations in their biological matrix leading to differences in uptake of elements.

3.1.2.2 AAS study of metals in Soil

Mahmut *et al.* [173] performed a study of heavy metal pollution in surface soil in the Thrace region of Turkey utilising graphite furnace AAS. The reason behind this study was to see the impact of metal pollution during industrial and agricultural development activities in the Thrace region. They compared their values for heavy metal content in the thrace region soil with recommended safe level values for Dutch soil. The data is as follows: (See Table 3.2)

Table 3.2: Normal levels of heavy metal contents in Dutch soil with indicated safe levels for stated metals in the Thrace region of Turkey [173]

Element	Concentration/mg.kg^{-1}	Max levels (Dutch standard)/mg.kg^{-1}
As	1.9-51	6
Cr	20-830	250
Cu	1.8-167	100
Pb	4.8-968	100
Ni	2.6-249	150
Zn	6-165	500

The data showed that there was a tendency for pollution to occur for metals such as nickel and lead which are quite toxic to humans. The study did find however that the elemental concentrations could be due to some type of transboundary contamination and also that there has never been a study to ascertain the natural background levels of these elements due to bedrock in the soils that were sampled in this study. The study recommended that further studies be taken especially around the Istanbul city area to ascertain the impact of this soil pollution on drinking water supplies for the human population.

Rucandio *et al.* [174] were responsible for the investigation of cadmium determination in a soil, coal fly ash and sediment samples using different matrix modifiers. This was done for the purpose of determining the percentage recovery of the cadmium in the samples relative to several types of modifiers. Cadmium tends to volatize out other matrix constituents leading to loss of cadmium content in a given sample during the ashing stage of graphite furnace analysis. It was found that without modifier, the recovery for the soil samples was about 30 %, and about 20 – 30 % for coal fly ash and sediment. This figure was significantly boosted in the presence of modifiers such as tungsten with a recovery range of 70 – 110 % for all three sample matrices. The most preferable matrix modifier was found to be 2 % $NH_4H_2PO_4$ and 0.4 % $Mg(NO_3)_2$ as it gave % recoveries of 100 – 110 %, gave the least background absorbance interference of all the modifiers and exhibited the least corrosive action on the graphite tube. This method was shown to have optimal atomization at temperatures of 1900 ^{0}C and a detection limit of 26 ng.g^{-1} [174].

3.2 Aims

- To perform graphite furnace and flame AAS analysis relative to the content of germanium, lead, copper and iron metals in food and soil samples and instrument suitability for analysis
- Comparison of results with acceptable values described in literature from established sources in the field such as the EPA and FDA
- To identify a relationship between the soil and food metal contents with a focus on germanium content

3.3 Experimental

3.3.1 Instrument

Varian SpectrAA-50 Flame AAS spectrometer, Varian SpectrAA-600 with GTA-100 graphite furnace attachment and S&J Junipier Hollow Cathode Lamps for Cu, Fe, Pb and Ge.

3.3.2 Chemicals

Analytical grade concentrated HNO_3 (70 %), analytical grade $HClO_4$ 1000 ppm analytical grade stock solution of Ge, Fe, Cu, Co, Ni, Cd, Pb and Zn supplied by Reagecon and Merck, analytical grade conc. HNO_3. (70 %), analytical grade $HClO_4$, Millipore deionised water. The soil reference material was acquired from Resource Technology Corporation called RTC-CRM025-050 Soil Reference Material. All reagents were used without further purifcation

3.3.3 Method

3.3.3.1 Soil Sample collection

Soils were collected via a stainless steel trowel about 10 cm from beneath the soil [175] and filled into 250 ml plastic sample vessels. Details are given in table 2.2.

3.3.3.2 Soil Sample Preparation

0.5 g of the desiccated soil sample was weighed and quantitatively transferred to a 100 ml Erlenmeyer flask. 2.5 ml of concentrated HNO_3 and 7.5 ml of concentrated HCl were added to the soil and were allowed to digest overnight.

After this time, the solution was heated at about 95 ^{0}C until a moist salt appeared. This was followed by sonicating the remaining salt solution into 25 ml of 1 % v/v HNO_3. This was subjected to centrifugation at 6000 rpm for a period of 10 min. The supernatant fluid was gravity filtered into a 50 ml volumetric flask and made up to the mark with 1 % v/v HNO_3.

3.3.3.3 Nitric/$HClO_4$ digestion of food

0.5 g of desiccated food sample (refer to section 2.2.3.1 for preparation details) was weighed and quantitatively transferred to a 100 ml Erlenmeyer flask (see table 3.3 for food sample list). 10 ml of concentrated HNO_3 was added to the food and was allowed to digest overnight. The solution was heated at about 95 ^{0}C until all that was left in the flask was ~ 2ml of HNO_3 solution. 2 drops of $HClO_4$ was added and evaporation of the rest of the solution was allowed until a moist salt was formed. The remaining salt solution was sonicated in 25 ml of 1 % v/v HNO_3. This was followed by centrifugation of the solution at 6000 rpm for a period of 10 min. The supernatant fluid was gravity filtered into a 50 ml volumetric flask and made up to the mark with 1 % v/v HNO_3. See table 2.1 for details.

3.3.3.4 Element standard preparation

All glassware was rinsed with HNO_3 and deionised water. A 1 % v/v solution of HNO_3 was prepared in a 1000 ml volumetric flask with deionised water. The appropriate volume of 1000 ppm stock metal solution was transferred to a 50 ml volumetric flask that corresponded to the concentration of standard needed and was made up to the mark with 1 % (v/v) HNO_3. The volumetric flasks were stoppered and mixed to give homogeneous distribution of solution. Samples analysed by flame AAS were left undiluted with the exception of high content metals like iron. Graphite furnace AAS samples were diluted as needed (normally a 1 in 20 dilution). The standard curve was obtained using the external standards method. A calibration curve of a 1% (v/v) HNO_3 blank and 5 standards that were suitable for the concentration range being examined for a particular metal e.g. 0-3 mg/L for Cu.

3.3.3.5 AAS analysis

Pb, Cu, Fe levels in soils was analysed via Flame AAS according to parameters specified in table 3.5. Ge level was analysed in soils via GFAAS according to parameters specified in table 3.6 and 3.9.

Cu, Ge and Pb levels in foods were analysed via GFAAS according to parameters specified in tables 3.7 to 3.9.

Fe was analysed via Flame AAS according to parameters specified in the following table 3.5.

Table 3.5: Parameters utilised using the SpectrAA-50 for flame AAS analysis of metal contents in foods and soils.

Instrument Parameters	Cu	Fe	Pb
Wavelength/ nm	324.8	248.3	217
Slit width/ nm	0.5	0.2	1
Lamp Current/ mA	6	6	5
Fuel	acetylene	acetylene	acetylene
Support	Air	air	air
Flame Stoichiometry	oxidizing	oxidizing	oxidizing
Standard conc. range/ppm	0-5	0-10	0-5
Replicate scan	3	3	3

Table 3.6: General parameters that were utilised for GFAAS analysis of specified metals in foods and soils on the SpectrAA-600 with GTA-100 graphite furnace for specified metals in foods and soils.

Instrument Parameters	Cu	Ge	Pb
Wavelength/ nm	324.8	265.2	217
Slit width/ nm	0.5	1	0.5
Lamp Current/ mA	6	5	7
Replicate scan	3	3	3
Total injection volume/µL	15	15	15
Sample volume/µL	10	10	10
Standard conc./ppb	0-100	0-100	0-100

Table 3.7: Lead temperature program as per the cookbook method on the SpectrAA-600 software

Step	Temp/^{0}C	Time/s	Flow/(L/min)	Gas type	Read	Signal Storage
1	85	5	3	Normal	No	No
2	95	40	3	Normal	No	No
3	120	10	3	Normal	No	No
4	400	5	3	Normal	No	No
5	400	1	3	Normal	No	No
6	400	2	3	Normal	No	Yes
7	2100	1	3	Normal	Yes	Yes
8	2100	2	3	Normal	Yes	Yes
9	2100	2	3	Normal	No	Yes

Table 3.8: Copper temperature program as per the cookbook method on the SpectrAA-600 software

Step	Temp/^{0}C	Time/s	Flow/(L/min)	Gas type	Read	Signal Storage
1	85	5	3	Normal	No	No
2	95	40	3	Normal	No	No
3	120	10	3	Normal	No	No
4	800	5	3	Normal	No	No
5	800	1	3	Normal	No	No
6	800	2	3	Normal	No	Yes
7	2300	1	3	Normal	Yes	Yes
8	2300	2	3	Normal	Yes	Yes
9	2300	2	3	Normal	No	Yes

Table 3.9: Germanium temperature program as per the method described by McMahon *et al.*[31]

Step	Temp/^{0}C	Time/s	Flow/(L/min)	Gas type	Read	Signal Storage
1	85	30	3	Normal	No	No
2	95	40	3	Normal	No	No
3	120	10	3	Normal	No	No
4	700	5	3	Normal	No	No
5	700	1	3	Normal	No	No
6	700	2	3	Normal	No	Yes
7	2600	1.3	3	Normal	Yes	Yes
8	2600	2	3	Normal	Yes	Yes
9	2600	2	3	Normal	No	Yes

3.4 Results and Discussion

Metal contents of soil and food samples are mentioned for Fe, Cu, Pb and Ge. The following sections will interrelate the metal contents determined for the samples with that recommended safe metal content ranges for foods and soils from bodies such as the EPA and the FDA. The concept behind this data collation is to look at the soils from the Santry/Glasnevin locale and if any of the areas are suitable, with respect to the metals analysed, for urban farming with a special focus on germanium content having an impact on vegetable enrichment.

The results from the foodstuffs can be used to gauge the average level of germanium present for a range of commonly grown vegetables. Cu, Fe and Pb are also used as reference points for comparison of typical metals that are of biological interest in both food and soil. Knowing, the germanium content within the soil and then further differentiating it into organic and inorganic forms (if such future work is ever carried out), it would be possible to identify how beneficial it would be for vegetable growth. The novelty of the study lies in the analysis of soils from the northside Dublin area for germanium content. A study for this area for germanium levels has not been conducted in the literature to the best of the authors' knowledge.

3.4.1 Analysis of Soil samples:

Sampling of soils was performed at 12 different sites around the Santry/Glasnevin area. 4 sites were associated with soil off the DCU campus. 4 of the other sites were associated with parks in the Santry/Glasnevin area namely Santry Demesne and Albert College Park. The other 4 sites were taken from a suburban area in Santry that would be close to large volumes of traffic. Notes were taken of the general description of the area and anything that might be environmentally significant.

The Santry/Glasnevin area has a good ratio of green area to developed areas. All houses in the suburbs have a garden and there are 2 major parks in the vicinity with plenty of trees. There is also no heavy industry in the area that could be a contributory factor to pollution. The negative points about the area is that it is close to major road traffic networks such as the swords road that is a major traffic artery between the M50/M1 and north inner city Dublin meaning traffic is very heavy and could lead to excessive car exhaust emissions in the area. This could be a strong influence on pollution levels in the soil in the rhizosphere (0 – 10 cm from surface) which may take in heavy metals such as cadmium and lead making these elements more bioavailable to surrounding plantlife [176,177]. The acceptable levels for metal content in non-polluted agricultural soil is stated in table based upon EPA guidelines [178]. In the case of germanium, the levels have been taken from the work of Pendias *et al* [179].

Table 3.10 Metal content values present in non-polluted agricultural soil

Element/Metal	Content/(mg/kg)
Fe	10000-50000
Cu	2-100
Pb	2-80
Ge	0.0003 – 0.0024

3.4.1.1 Iron content in soil

Iron levels in the soil were found to be a minimum of 16062.0 ± 506.3 µg/g and a maximum of 20025.1 ± 842.3 µg/g (see fig. 3.3) with an average of 18465 ± 832.9 µg/g altogether for the 12 soil sites in the Santry/Glasnevin area (see table 3.11). The average iron content in most non-polluted Irish soiltypes is 10000-50000 µg/g according to the EPA [178]. The data from the soil samples suggest that the iron

content is well within acceptable parameters with the exception of soil sample site 1. This might be attributable to the fact that the soil was freshly overturned at the time of sampling when there was construction works in progress. The soil may not even be indigenous to that particular area. The RSD values for the soil samples are generally good with the only exceptions being 1, 8 and 10 but this is only due to the presence of obvious outliers in the replicates. The % recovery is the best so far, with this particular SRM, with an average of 88.7±7.8 %. This is well within the 81 – 121 % [163] allowable range and gives more confidence to the reliability of the results.

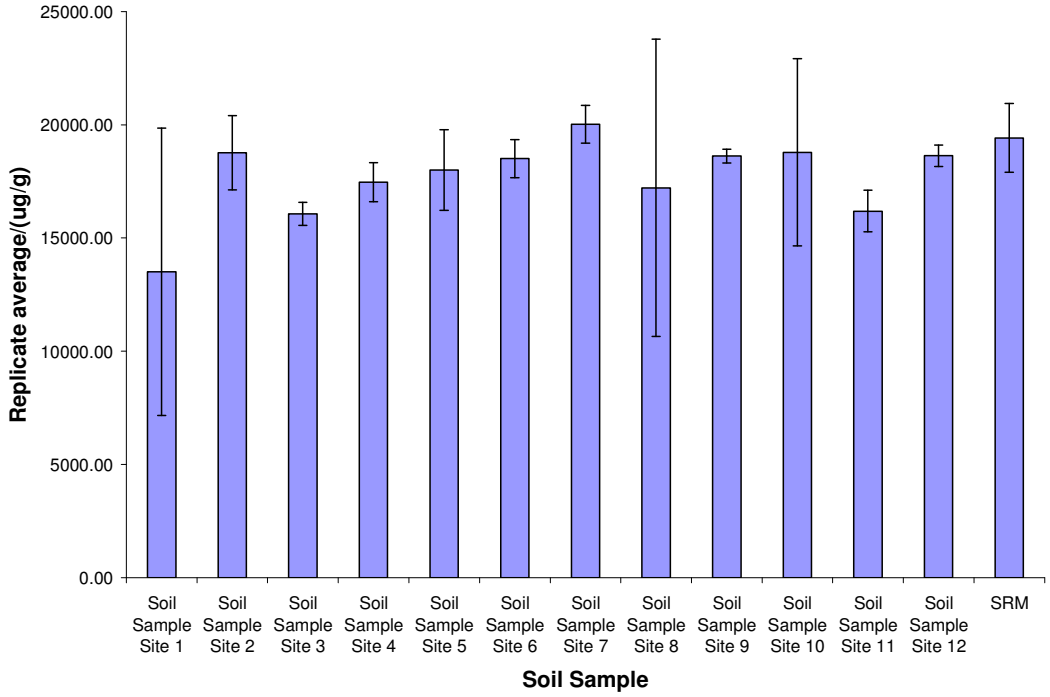

Fig. 3.3: Average Fe content in soil from sample sites 1-12. Data based on triplicate results.

Table 3.11: Table of Fe content values for soil sample sites 1-12 and SRM (n=3).

Sample	Replicate1/(µg/g)	Replicate2/(µg/g)	Replicate3/(µg/g)	Replicate average/(µg/g)	STDEV	%RSD
Soil Sample Site 1	6190.6	16899.5	17440.2	13510.1	6344.7	47.0
Soil Sample Site 2	17215.6	20484.6	18612.4	18770.9	1640.3	8.7
Soil Sample Site 3	16644.6	15812.4	15729.1	16062.0	506.3	3.2
Soil Sample Site 4	16875.1	18448.4	17078.8	17467.5	855.6	4.9
Soil Sample Site 5	16229.1	19801.4	17983.1	18004.6	1786.3	9.9
Soil Sample Site 6	19261.1	18655.7	17592.1	18503.0	844.9	4.6
Soil Sample Site 7	19656.5	20988.9	19430.0	20025.1	842.2	4.2
Soil Sample Site 8	9652.9	20480.0	21516.2	17216.4	6570.6	38.2
Soil Sample Site 9	18423.3	18976.8	18461.0	18620.4	309.3	1.7
Soil Sample Site 10	14038.9	21648.0	20654.7	18780.5	4136.3	22.0
Soil Sample Site 11	15967.0	15396.9	17196.4	16186.8	919.6	5.7
Soil Sample Site 12	18381.9	18330.7	19174.8	18629.1	473.3	2.5
SRM	17688.7	20508.3	20070.5	19422.5	1517.4	7.8
% Recoveryof SRM	80.7	93.6	91.6	88.7	6.9	7.8
SRM Fe cert value/(ug/g)	21906.0					

Iron is one of the major constituents in the earth's crust and has a relative abundance of 45 % in nature. Iron deficiency is quite a widespread problem associated with crop growth but isn't related entirely to overall soil content but relates instead to how plants take up iron from the soil based on factors such as pH or presence of iron soil strata such as the rhizosphere. Iron content in soil has also been mediated by artificial factors such as fertilisers. This partially accounts for why it has levels in the high 1000 µg/g's in most soils [179,180].

Iron is an important constituent in soils as it helps regulate biochemical functions in plants and it is the primary element in energy processes such as the production of chlorophyll and forms organic iron complexes that can mediate photosynthetic electron transfer [179]. Soils with too high an iron content can lead to conditions such as chlorophyll reduction, plant growth inhibition and compromised photosynthesis [181].

3.4.1.2 Lead content in soil

Lead levels in the soil were found to be a minimum of 32.1 ± 0.7 µg/g and a maximum of 266.2 ± 34.1 µg/g for soils in the Santry/Glasnevin area (see fig. 3.4). The average value for the soil sites was 113.0 ± 6.2 µg/g (see Table 3.12). The average figure for lead content in Irish soils according to the EPA is 2-80 µg/g [178]. The data found in this study would seem to suggest that the lead content is higher than the national average indicating that the soil is polluted. This might be in part due to the fact that the main source of lead would be from exhaust emissions from excessive car traffic in the Santry/Glasnevin area. Another more plausible explanation is that the lead content is being overestimated as indicted by the SRM recovery of 151.2 ± 12.8%. This falls about 30 % outside the optimal 81 – 121 % recovery zone for digestions. It is probable that Pb levels may be within the average range quoted by the EPA. According to Dutch EEA figures, the maximum allowable quantity for lead in soil is 150 µg/g so it seems that the soil is not posing a critical threat to the environment except in the case of sites 9 and 10, which are taken from park sites making them particularly polluted [173].

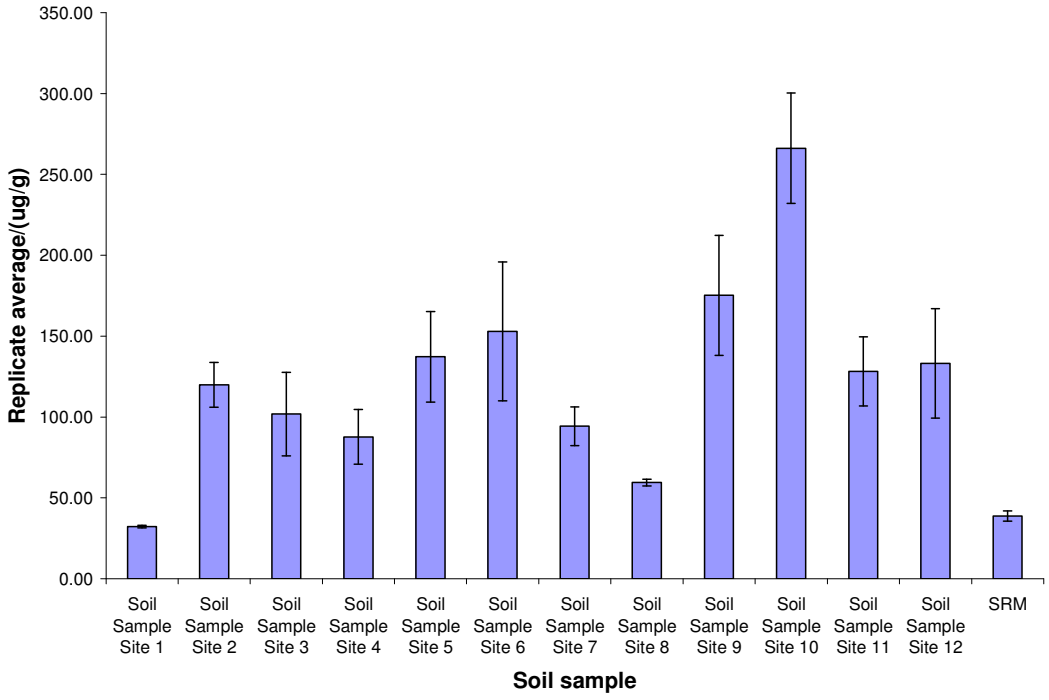

Fig. 3.4: Average Pb content in soil from sample sites 1-12 (n=3)

Table 3.12: Table of Pb content values for soil sample sites 1-12 and SRM (n=3).

Sample	Replicate1/(µg/g)	Replicate2/(µg/g)	Replicate3/(µg/g)	Replicate average/(µg/g)	STDEV	%RSD
Soil Sample Site 1	32.3	31.3	32.8	32.1	0.7	2.3
Soil Sample Site 2	133.9	119.7	106.1	119.9	13.9	11.6
Soil Sample Site 3	131.7	86.8	86.9	101.8	25.9	25.5
Soil Sample Site 4	107.1	76.1	79.8	87.6	16.9	19.3
Soil Sample Site 5	169.4	119.4	122.7	137.2	27.9	20.4
Soil Sample Site 6	202.3	124.6	132.0	152.9	42.9	28.0
Soil Sample Site 7	108.0	85.4	89.4	94.3	12.0	12.8
Soil Sample Site 8	61.7	58.3	58.1	59.4	2.0	3.4
Soil Sample Site 9	218.1	152.2	155.2	175.2	37.2	21.3
Soil Sample Site 10	304.3	255.8	238.4	266.2	34.1	12.8
Soil Sample Site 11	152.7	113.7	118.0	128.1	21.4	16.7
Soil Sample Site 12	171.4	107.5	120.5	133.1	33.8	25.4
SRM	35.5	38.6	42.0	38.7	3.3	8.5
% Recovery of SRM	138.6	150.8	164.2	151.2	12.8	8.5
SRM Pb cert value/(ug/g)	25.6					

Lead is regarded as having no biological function in nature but can be accumulated in plants through root sorption. Toxic levels of lead can lead to ailments such as root elongation, plant growth inhibition and decreases in seed germination [182].

The main source of lead is attributable to car exhaust emissions and has a major impact on the environment when car traffic is high. This was found by Bacon *et al.* [175] when he performed studies of Scottish soils in three distinct area categories moor, wood and roadside. He found that there were lead levels in the region of 20-84 µg/g from soil samples taken 0-30 cm in the soil collectively. This was similar to the levels that were found in this study. The Pb levels were actually much higher in the case of wood and moorland soils with ranges of 17-260 and 26-350 µg/g recorded respectively. The lower result for the roadside was attributed to disturbance of the soil due to road development and maintenance.

The relationship of lead content in soil relative to car exhaust was further explored by Motto *et al.* [183]. This study established that there was a relationship between lead content in soil with proximity to heavy traffic associated with highways. Pb content was found to decrease with increasing distance from the highways. This doesn't seem

to be entirely the case in relation to the Pb content figures in this study where sites 3 and 4 taken from park sites match up more or less those taken from roadside soil samples.

3.4.1.3 Copper content in soil

Copper levels in the soil sampled were found to be a minimum of 27.3 ± 3.6 µg/g and a maximum of 93.2 ± 7.6 µg/g (see fig. 3.5) with an average value of 52.6 ± 3.1 µg/g (see Table 3.13). The national average for copper content is 2-100 µg/g for non-polluted Irish soils according to the EPA [178]. This would suggest that soils from the Santry/Glasnevin area are not polluted for copper. The RSD values for the copper analysis are good with the highest being 13.2 % in the aqua regia studies and gives extra confidence in the reliability of the analysis. Also, the SRM shows a % recovery of 124.1 % in relation to soil. This is only marginally outside the ideal 81-121% recovery range.

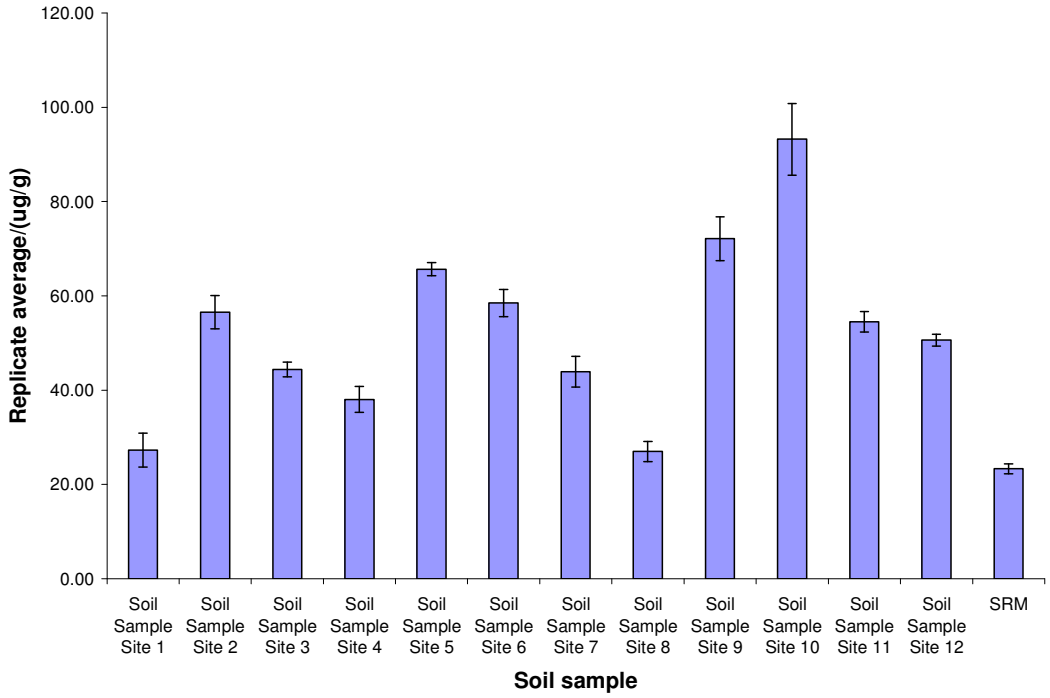

Fig. 3.5: Average Cu content in soil from sample sites 1-12 (n=3).

Table 3.13: Table of Cu content values for soil sample sites 1-12 and SRM (n=3).

Sample	Replicate1/ (µg/g)	Replicate2/ (µg/g)	Replicate3/ (µg/g)	Replicate average/(µg/g)	STDEV	%RSD
Soil Sample Site 1	23.5	30.7	27.6	27.3	3.6	13.2
Soil Sample Site 2	59.8	57.0	52.8	56.5	3.5	6.3
Soil Sample Site 3	44.0	46.1	43.1	44.4	1.5	3.5
Soil Sample Site 4	36.6	41.2	36.2	38.0	2.8	7.3
Soil Sample Site 5	67.3	65.0	64.7	65.7	1.4	2.1
Soil Sample Site 6	61.1	58.9	55.4	58.5	2.9	4.9
Soil Sample Site 7	40.8	47.3	43.7	43.9	3.2	7.4
Soil Sample Site 8	24.5	28.3	28.1	27.0	2.1	7.9
Soil Sample Site 9	77.4	68.7	70.3	72.1	4.6	6.4
Soil Sample Site 10	85.6	100.7	93.3	93.2	7.6	8.1
Soil Sample Site 11	52.0	55.4	56.1	54.5	2.2	4.0
Soil Sample Site 12	49.3	51.8	50.7	50.6	1.2	2.4
SRM	22.1	23.8	24.0	23.3	1.1	4.5
% Recovery of SRM	117.6	126.6	127.9	124.0	5.6	4.5
SRM Cu cert value/(ug/g)	18.8					

Copper contamination of soil can be sourced relative to copper materials used in construction or electrical goods as well as fertilisers and sludge [179]. Unusual incidences of contamination can be found in French vineyard soils from application of fertilisers rich in $CuSO_4$. This led to contents of 200-500 µg/g for French vineyard soil as opposed to 4-30 µg/g in normal French soil [184]. Soils sample site 2 was taken from an area with a lot of waste including electrical appliances but didn't show any elevated copper levels. Soil sample site 10 had the highest copper content but was taken from Albert College Pk. This may have been due to copper contamination from fertiliser rather than domestic waste.

Copper toxicity results in features such as growth inhibition, chlorophyll content reduction and negative changes in the metabolic activity of the plant. This can be offset by inherent benefits. Copper from the soil does play a vital role in plants such as controlling water permeability of plant structure, production of DNA and RNA in the plant and acts as a defence against disease at controlled amounts [179,185].

3.4.1.4 Germanium content in soil

The germanium levels in soil were found to be a minimum of 64.2 ± 31.2 µg/g and a maximum of 122.4 ± 52.6 µg/g (see fig. 3.6) with an average value of 79.9 ± 21.8 µg/g (see Table 3.14). The only comparative data comes from Pendias *et al.* [179] stating that the ideal value for germanium content in soil is 0.3 to 2.4 µg/g. The levels seen in this study seem to be 50 times higher. This represents either that there is major contamination of germanium from an unknown source or more likely that the GFAAS determination of germanium in soils method used in this study is unreliable. There is no SRM available for germanium levels and as such it is difficult to ascertain the recovery levels of the method. Another factor that contributes to the uncertainty of the germanium results is the high RSD values that indicate that the digestions were inconsistent or the GFAAS determinations were fluctuating from run to run.

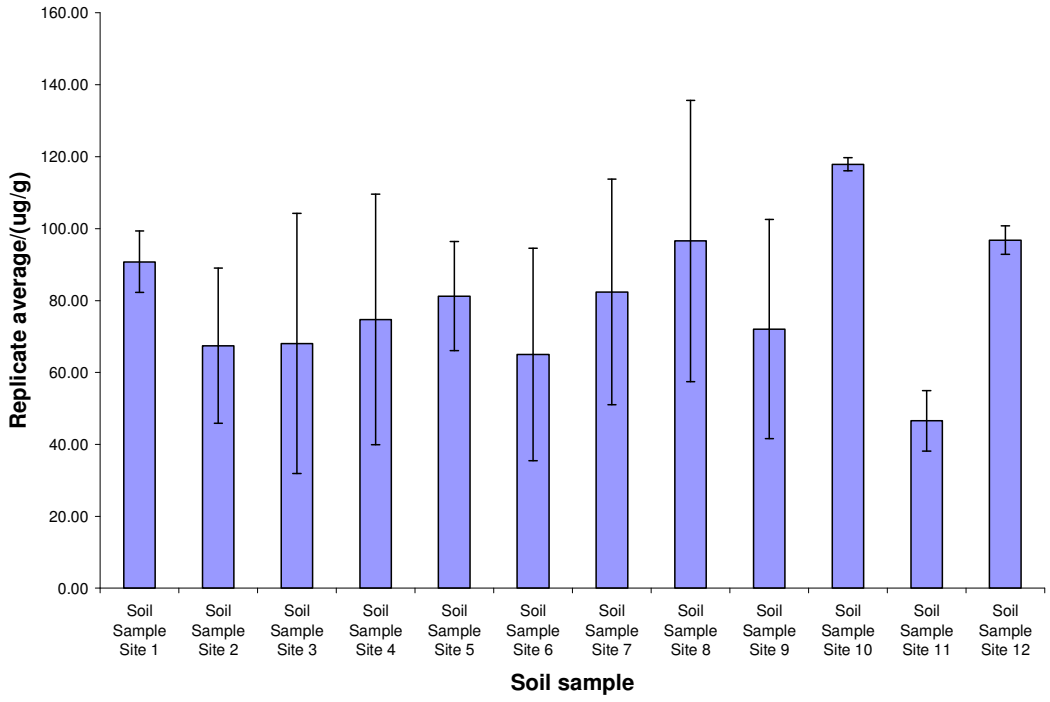

Fig. 3.6: Average Ge content in soil from sample sites 1-12 (n=3).

Table 3.14: Table of Ge content values for soil sample sites 1-12 and SRM (n=3)

Sample	Replicate1/(µg/g)	Replicate2/(µg/g)	Replicate3/(µg/g)	Replicate average/(µg/g)	STDEV	%RSD
Soil Sample Site 1	96.8	40.5	84.7	74.0	29.6	40.1
Soil Sample Site 2	176.1	52.1	82.7	103.7	64.6	62.3
Soil Sample Site 3	150.7	42.5	93.6	95.6	54.1	56.6
Soil Sample Site 4	137.7	50.1	99.3	95.7	43.9	45.9
Soil Sample Site 5	149.2	70.5	91.9	103.9	40.7	39.2
Soil Sample Site 6	144.5	44.1	85.9	91.5	50.4	55.1
Soil Sample Site 7	137.9	60.2	104.6	100.9	39.0	38.6
Soil Sample Site 8	174.0	68.9	124.2	122.4	52.6	43.0
Soil Sample Site 9	146.3	50.5	93.6	96.8	48.0	49.6
Soil Sample Site 10	116.6	59.4	119.1	98.4	33.8	34.3
Soil Sample Site 11	52.5	40.6	99.6	64.2	31.2	48.6
Soil Sample Site 12	93.9	57.8	99.5	83.7	22.7	27.1

Germanium is normally absorbed into plants quite efficiently in the form of GeO_2 but has been known to inhibit plant growth at quantities exceeding 1ppm on average and can lead to effects such as plant growth and germination inhibition [179]. The levels found in this study are unrealistic, otherwise there would be an increase in plant myopathy (plant death/sickness) in the general Santry/Glasnevin area.

Asai *et al.* [13] speculated that the Germanium content in soil was linked strongly to plant absorption of the element. In studies of coal, he found that there were higher contents of germanium in wood sections of coal nuggets. He theorized that the germanium content was namely coming from plant matter as opposed to from the soil. He also said that the germanium content of the soil had an influence on the plant's defences.

3.4.2 Foodstuff Sample Results

As discussed in section 3.3.2.2, the soil samples analysed may give some indication of the content of the metals in foods. It is possible that not all the metals will be absorbed in the foodstuffs due to issues of bioavailability, influenced by the form of the metal in the soil. All foodstuffs analysed in the following sections will be compared to the previously obtained soil sample average values and see if the determined metal levels give any correlation with the vegetables studied.

The FDA guidelines (refer to table 3.15) are only applicable to copper and iron content for dietary consumption. They do not have lead toxicity levels but are generally regarded as not to be ingested and germanium is so trace that it is not even mentioned in the dietary tables. The recommended plant levels are thus indicated at relevant points in the following sections in this body of work from other reference sources.

Table 3.15 RDA of elements in this study for an average adult [186]

Element	**RDA for average adult/(mg/day)**
Copper	0.9
Iron	0.008
Germanium	Not mentioned
Lead	Not mentioned

3.4.2.1 Germanium content of food

Germanium levels in food were very high with a range of 5.7 to 604.1 µg/g (see Table 3.16) using the method developed by McMahon *et al.* [31] The only exceptions were when 1 % v/v analytical grade HNO_3 was used as the makeup solution as opposed to deionised water. Additionally, a $HNO_3/HClO_4$ digestion method was applied to all foodstuffs to ensure greater result comparibility instead of using tailored extraction solutions for each foodstuff group i.e. dissolution of soya products to obtain dissolvable germanium [104]. The samples and standards were matrix matched along with the digestion which was shown to be fairly reproducible across the other element analyses (refer to fig. 3.7). In this determination, the % RSD was 122 % as in the case of yellow pepper.

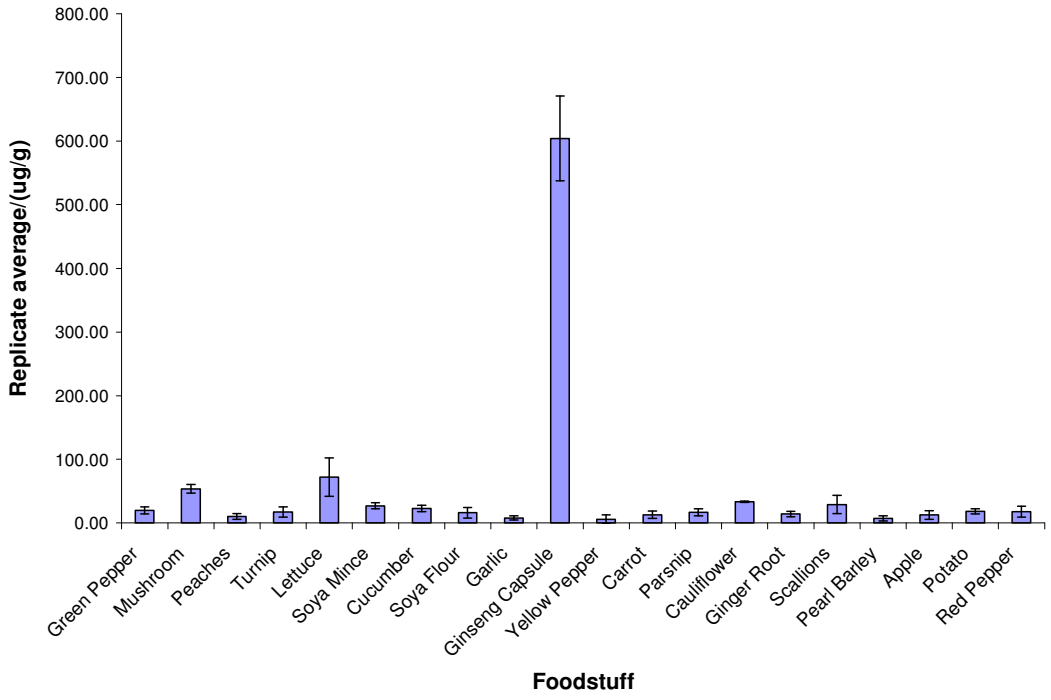

Fig. 3.7: Average Ge content in foodstuffs studied (n=3).

Table 3.16: Table of Ge content values for food samples (n=3).

Sample	Replicate1/(µg/g)	Replicate2/(µg/g)	Replicate3/(µg/g)	Replicate average/(µg/g)	STDEV	%RSD
Green Pepper	17.8	25.8	15.1	19.6	5.5	28.4
Mushroom	46.9	53.4	60.3	53.5	6.7	12.5
Peaches	11.6	13.8	5.1	10.2	4.5	44.5
Turnip	14.3	26.2	11.2	17.3	7.9	45.8
Lettuce	103.7	43.7	68.2	71.9	30.1	42.0
Soya Mince	24.1	32.3	24.1	26.8	4.7	17.6
Cucumber	28.3	21.1	18.8	22.7	4.9	21.7
Soya Flour	17.6	23.7	7.2	16.2	8.3	51.6
Garlic	8.7	10.5	4.5	7.9	3.1	38.7
Ginseng Capsule	526.9	642.7	642.5	604.0	66.8	11.1
Yellow Pepper	1.1	2.2	13.7	5.7	6.9	123.0
Carrot	6.2	16.5	15.5	12.7	5.7	44.8
Parsnip	15.1	22.8	12.3	16.7	5.4	32.5
Cauliflower	33.7	34.1	32.1	33.3	1.1	3.2
Ginger Root	9.1	17.2	15.4	13.9	4.3	30.6
Scallions	26.4	44.3	16.2	29.0	14.2	49.1
Pearl Barley	6.8	11.4	3.7	7.3	3.9	53.4
Apple	13.6	19.0	5.3	12.6	6.9	54.4
Potato	19.4	14.0	21.2	18.2	3.7	20.6
Red Pepper	17.9	26.2	8.7	17.6	8.7	49.5

McMahon *et al.* [31] clearly showed that the germanium content should be trace with most foodstuffs giving values of less than 1 µg/g. The figures found in this study seem to disagree with this data by at least a factor of 10. A certified material has not been used to verify the accuracy of the method, as a suitable sample of known Ge content is not available. In this study, the blank, even when matrix matched (in 1% v/v HNO_3), had an absorbance of 0.0150. The blank was referenced to 0 absorbance but the range of the absorbance was 0 – 0.0350 for a 0-100 ppb Ge standard curve. The magnitude of the makeup solution interference as seen in the blank compared to the calibration curve, in part explains, the problems that occurred with Ge determination.

There are few sources in the literature that can confirm some of the results seen in this study. Yang *et al.* [187] analysed white mushroom with other botanical extracts getting a value of 0.0884 ± 0.00019 µg/g. Our mushroom sample was determined to be 53.5 ± 6.7 µg/g which is about 50 times higher than that found by Yang *et al.* The highest content of Germanium was found to be in Ginseng capsules at 642.6 ± 0.19 µg/g but this figure may be overestimated from absorption interferences from excipients in the capsule powder. The next highest is Lettuce with a value of 56.0 ± 17.3 µg/g. The lettuce values corroborates with average Ge soil content values of 79.9 µg/g. The reason why lettuce has a high content of Germanium maybe due to the fact it is a leafy vegetable and capable of bioaccumulating a number of metal species in its' leaves. It is not possible to compare the Ginseng capsule as it is a concentrated extract from Panax Ginseng and also it is not indigenous to Ireland.

Germanium can have beneficial effects or toxic effects depending on the form it is present in. The inorganic form of germanium or germanium dioxide is normally associated with toxicity and can lead to conditions such as renal failure or kidney dysfunction as well as other symptoms like nausea and gastrointestinal disorder [188,189].

The organic forms such as germanium sesquioxide and spirogermanium have been shown to have antioxidant properties and anticancer effects among other therapeutic qualities. Organic germanium has been shown to be effective on spindle cell carcinoma via oral administration [111,190].

3.4.2.2 Iron content of food

Iron levels in food were found to be high in all instances with a range of 11.9 to 841.8 µg/g (see Table 3.17). The RSD values were very high also in some instances, compromising the dependability of the results obtained in this study. These exceptionally high iron levels are attributable to iron enrichment practice of the soil from overzealous use of fertilizers. The soil results giving an Fe soil average content at 18465.7 µg/g confirms this observation. It also means that a small fraction of the Fe in soil is taken in by vegetables and fruit. This shows that high iron content in soil can give high content in food. According to Zhenli *et al.* [180] the opposite can often be the case where certain plant types have trouble getting iron as they normally take it from the rhizosphere or may have metabolism issues with some forms of iron etc. The acceptable content levels for iron can be in a range of 24-73 µg/g for leafy vegetables and 18-65 µg/g for root vegetables (see fig. 3.10) [166]. This seems to tie in with the figures observed for some of the foodstuffs such as turnip, parsnip and carrot that were sourced from this country.

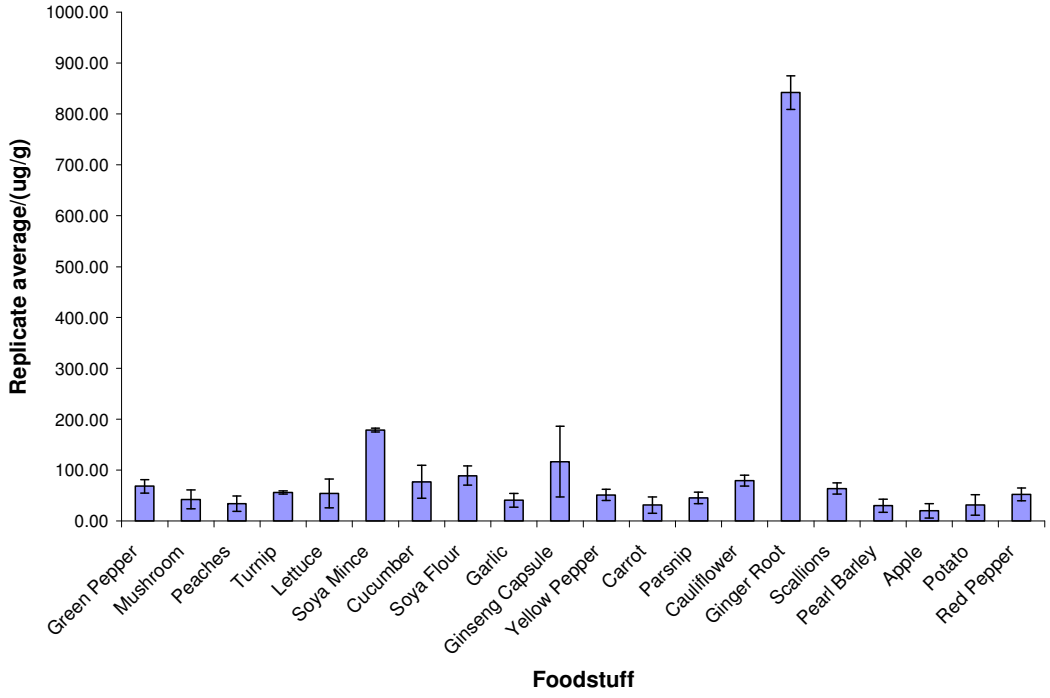

Fig. 3.10: Average Fe content in foodstuffs studied (n=3).

Table 3.17: Table of Fe content values for food samples (n=3).

Sample	Replicate1/(µg/g)	Replicate2/(µg/g)	Replicate3/(µg/g)	Replicate average/(µg/g)	STDEV	%RSD
Green Pepper	83.3	57.5	64.7	68.5	13.3	19.4
Mushroom	60.0	44.8	23.3	42.7	18.4	43.1
Peaches	48.4	18.4	36.2	34.3	15.1	44.0
Turnip	53.7	59.6	55.8	56.3	3.0	5.3
Lettuce	46.0	86.1	31.3	54.5	28.4	52.1
Soya Mince	183.0	177.5	176.1	178.9	3.6	2.0
Cucumber	114.5	55.4	61.8	77.3	32.4	42.0
Soya Flour	95.9	104.1	68.0	89.3	18.9	21.2
Garlic	56.5	34.2	32.5	41.0	13.4	32.7
Ginseng Capsule	105.9	190.9	53.2	116.7	69.5	59.6
Yellow Pepper	63.0	41.6	50.0	51.5	10.8	21.0
Carrot	50.1	20.8	24.5	31.8	16.0	50.3
Parsnip	53.8	50.6	32.5	45.6	11.5	25.2
Cauliflower	89.8	68.3	79.7	79.3	10.8	13.6
Ginger Root	878.1	814.1	833.1	841.7	32.9	3.9
Scallions	76.7	56.8	58.3	63.9	11.1	17.3
Pearl Barley	44.8	26.3	19.6	30.2	13.0	43.1
Apple	36.5	10.4	13.4	20.1	14.3	71.1
Potato	54.9	19.5	20.8	31.8	20.0	63.1
Red Pepper	66.6	46.0	44.3	52.3	12.4	23.7

The highest levels for iron is seen in ginger root, soya mince and ginseng capsule. Ginger root has the most iron content at 841.8 µg/g. This is partially explained by the fact that the ginger root is a root vegetable and these have a greater tendency to accumulate micronutrients/elements than other vegetation. This was corroborated by a study performed by Tarwadi *et al.* [191] comparing root and leafy vegetables among which were ginger. On average, the root vegetables showed a higher uptake of iron than the other vegetable classes.

Iron is essential to the human body for growth and mental development and is an integral part of the human body with up to 4.5 g being present in an average male human and 65% of this is bound to haemoglobin. Iron deficiency can lead to problems such as anemia and mental retardation [192].

3.4.2.3 Lead content of food

Lead levels in food are found to be quite high in this particular study with levels in a range of 1.0 -15.5 µg/g (see Table 3.17). The content figures seem to agree with observations made by Demirezen *et al.* who looked at heavy metals in Turkey. They recorded values of 3-8 µg/g for agricultural vegetables [153]. The data in this study gives overall quite low values for lead content for most foodstuffs if we exclude lettuce and ginseng capsule averaging 1.1-3.5 µg/g.

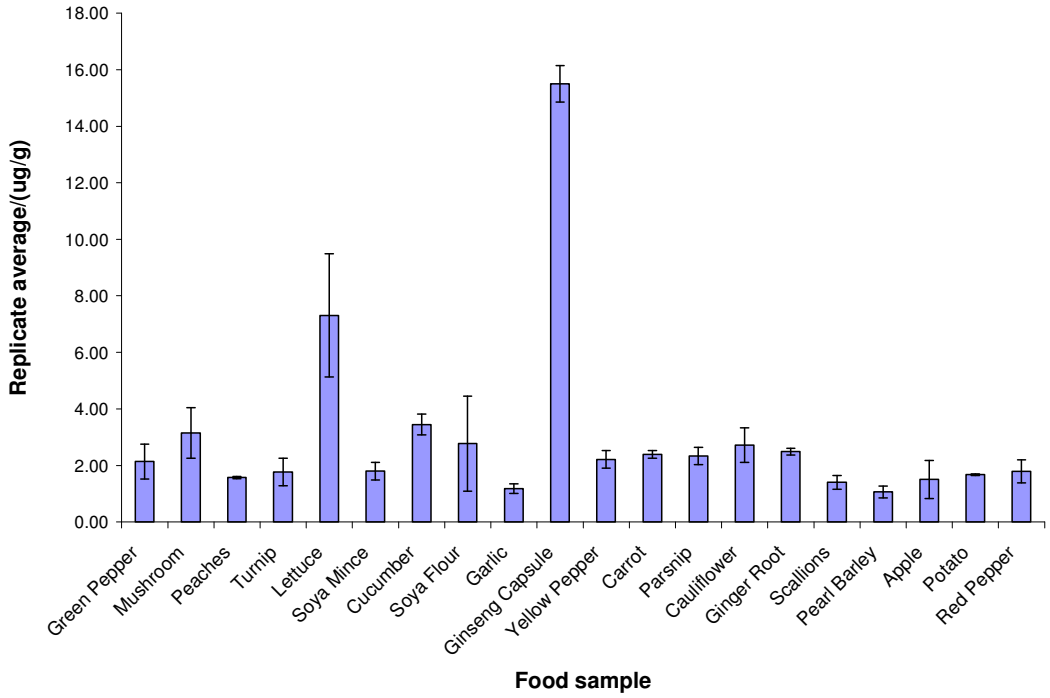

Fig. 3.10: Average Pb content in foodstuffs studied (n=3).

Table 3.17: Table of Pb content values for food samples (n=3).

Sample	Replicate1/(µg/g)	Replicate2/(µg/g)	Replicate3/(µg/g)	Replicate average/(µg/g)	STDEV	%RSD
Green Pepper	2.1	2.8	1.5	2.1	0.6	28.6
Mushroom	3.8	3.5	2.1	3.2	0.9	28.3
Peaches	1.6	1.6	1.6	1.6	0.0	2.3
Turnip	2.1	2.0	1.2	1.8	0.5	27.5
Lettuce	5.9	9.8	6.2	7.3	2.2	29.8
Soya Mince	1.8	2.1	1.5	1.8	0.3	17.3
Cucumber	3.6	3.8	3.0	3.5	0.4	10.7
Soya Flour	4.7	1.8	1.8	2.8	1.7	60.8
Garlic	1.4	1.0	1.2	1.2	0.2	14.7
Ginseng Capsule	15.7	16.0	14.8	15.5	0.6	4.1
Yellow Pepper	2.1	2.6	2.0	2.2	0.3	14.0
Carrot	2.4	2.5	2.3	2.4	0.1	5.6
Parsnip	2.6	2.4	2.0	2.3	0.3	12.8
Cauliflower	2.8	3.3	2.1	2.7	0.6	22.4
Ginger Root	2.4	2.5	2.6	2.5	0.1	4.9
Scallions	1.6	1.4	1.2	1.4	0.2	17.5
Pearl Barley	1.3	0.9	1.0	1.1	0.2	19.3
Apple	1.2	1.1	2.3	1.5	0.7	44.6
Potato	1.7	1.7	1.6	1.7	0.0	1.8
Red Pepper	2.0	2.0	1.3	1.8	0.4	22.7

These figures are at relatively safe levels as they are half that quoted in the Turkish study. Normally, a plant uses only 2-6 ppb of lead in its biological processes. Content levels as low as 1 ppm can interfere negatively with plants such as corn leading to inhibition and photosynthesis causing variable physical effects like lesions or discolouring [179]. Ginseng capsule has a high lead content. This is quite unusual since it is normally selective towards more nutritional elements like copper and iron.

Lettuce is more explainable because of the fact it is a leafy vegetable, it is more prone to accumulate heavy metals than other vegetation. Demirezen *et al.* [153] also observed this with their lettuce sample with levels as high as 9.7 µg/g found for urban lettuce samples and 4.4 µg/g for agricultural samples. The highest content was observed in Ginseng capsule at 15.5 µg/g. This high value could be attributed to matrix interferences from the capsule excipients. The lead levels observed in foods only form a small fraction of those observed in the average Pb content value in soil of 113.0 µg/g. This might be due to the lack of a biological role for Pb in plant development as discussed previously. The vegetables would therefore not be selective to accumulation of Pb as a result. Excessive lead levels in the human body, ≥ 10

µg/dL blood level, can lead to oxidative stress induced disorders such as hypertension, kidney disease and neurodegenerative disease [193,194].

3.4.2.4 Copper content of food

Copper levels in food tend to vary across the board with vegetables showing relatively low levels of copper in a range of 2.7-18.8 µg/g (see fig. 3.11). The RSD values for the copper analysis using HNO_3/ $HClO_4$ digestion are 1.7-35.3 % RSD being observed (see table 3.18). The eastern herbs and foods show more elevated contents. Ginseng capsule had the highest copper levels by far with 18.8 µg/g (see fig. 3.11) making it the most nutritious in terms of its' copper content. Mohammad *et al.* [195] in a study of copper uptake by panax ginseng roots found that it is capable of taking up a rather large amount of copper with concentrations of 0-50 µM. The level of accumulation is dependent on time duration and element concentration in the soil. Most Asian soils have abundant elements so this accounts for the high elemental contents observed.

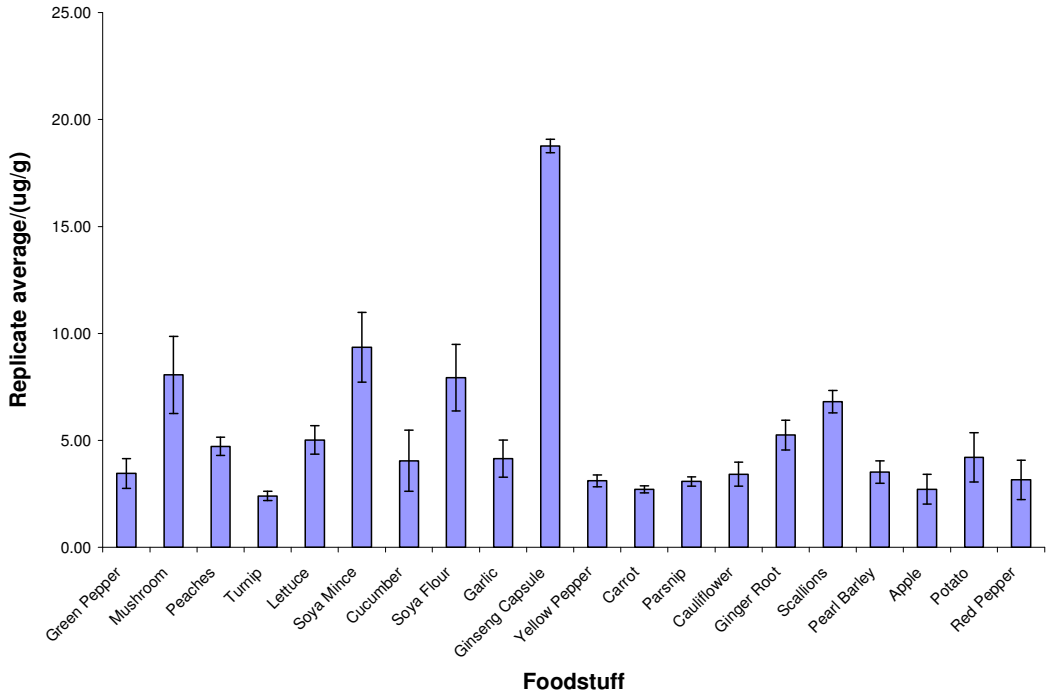

Fig. 3.11: Average Cu content in foodstuffs studied (n=3).

Table 3.18: Table of Cu content values for food samples (n=3).

Sample	Replicate1/(μg/g)	Replicate2/(μg/g)	Replicate3/(μg/g)	Replicate average/(μg/g)	STDEV	%RSD
Green Pepper	2.9	3.3	4.2	3.5	0.7	20.2
Mushroom	7.1	10.1	7.0	8.1	1.8	22.4
Peaches	5.0	4.9	4.2	4.7	0.4	8.9
Turnip	2.4	2.2	2.6	2.4	0.2	9.1
Lettuce	4.3	5.4	5.4	5.0	0.7	13.4
Soya Mince	7.5	10.1	10.5	9.4	1.6	17.4
Cucumber	5.6	3.6	2.9	4.0	1.4	35.3
Soya Flour	8.4	9.2	6.2	7.9	1.5	19.5
Garlic	4.9	4.4	3.2	4.2	0.9	21.0
Ginseng Capsule	18.9	18.4	18.9	18.8	0.3	1.7
Yellow Pepper	3.0	2.9	3.4	3.1	0.3	8.8
Carrot	2.6	2.7	2.9	2.7	0.2	6.1
Parsnip	3.3	2.9	3.0	3.1	0.2	7.2
Cauliflower	2.8	3.5	3.9	3.4	0.6	16.4
Ginger Root	4.7	5.1	6.0	5.2	0.7	13.3
Scallions	7.2	7.0	6.2	6.8	0.5	7.8
Pearl Barley	3.1	4.1	3.3	3.5	0.5	14.8
Apple	1.9	3.2	3.0	2.7	0.7	25.6
Potato	5.3	3.0	4.3	4.2	1.2	27.5
Red Pepper	3.4	2.1	3.9	3.2	0.9	29.3

It has also been found by groups such as Neelam *et al.* [58] that soya mince has 9.36 μg/g and soya flour has 7.93 μg/g of Cu. The reason for the variation between the two is attributed to different forms of processing such as defatting or solvent extraction leading to variances in nutrient loss. Mushrooms copper levels are the third highest at 8.06 μg/g. This corresponds to observations from Mustafa *et al.* [196] who looked at a variety of different mushroom species with 18.9 – 64.8 μg/g Cu levels and a precedence for mushroom to accumulate more nutritionally beneficial elements such as iron and copper than heavy elements like lead and cadmium. This makes it potentially more nutritional than other types of foodstuff. The observed Cu levels in food tie in quite well with the Cu soil content average of 52.6 μg/g. This would suggest that a high fraction of available copper in soil is used by vegetables in their development. This is to be expected as copper is an essential element in plants.

Copper deficiency can lead to ailments such as cardiovascular problems, energy loss/fatigue and metabolisation issues in humans. Copper overdose or overload can lead to more severe conditions like Wilson's disease where copper is retained strongly

in the liver. Copper is also essential for proteins where it can induce certain biological effects like metallothionein production [197].

3.4.3 Areas of improvement for metal content analysis of foods and soils

The study represented in this chapter is in general not suitable for publication in an analytical journal with the RSD values that have been found for the food and soil samples analysed. It also is marred by problems with germanium detection with rather strong interferences being found in comparison to the germanium levels indicated by McMahon *et al.* [31] in their method. These interferences could also be found in the other metal studies to some extent performed in this chapter. This could be to do with factors such as the atomisation process, the presence of interferents in the samples (nitrates and carbonates) and the choice of digestion process all have contributed to the unsatisfactory nature of the results presented here. The use of standard additions method for example could have overcome some of the matrix interferences within the sample as external standardisation cannot.

The atomisation process utilised here was graphite furnace and flame using atomic absorption spectroscopy. These methods can reach atomisation temperatures of 2500 and 1100 ^{0}C respectively. Improvement in atomisation can only be achieved by increasing the temperature to Inductively Coupled Plasma (ICP) atomisation. The plasma itself burns between 6000 to 10000 ^{0}C. This increase in temperature allows the user to reduce interferences substantially and allows the use of Optical Emission Spectroscopy (OES) sensing as opposed to absorption to quantitate the elements further reducing interference as atomic emission spectra are generated in discrete narrow wavelengths for an element [198].

The selection of open vessel digestion using a hotplate setup was also a problem with the work used in this body of work. The open vessel digestion setup has recovery issues with metal nitrates being potentially lost due to evaporation or not being fully digested due to insufficient heating time upon reaching a nearly dry state. The use of closed vessel digestion with microwave assistance is the preferred method of digestion for most preparation of samples. The % recovery are improved with a number of high temperature programs. The system has more configurability with

temperature programming and henceforth, greater reproducibility in the digestion process [164,165].

The application of all these refinements to the analysis of Cu, Fe, Pb and Ge in foods and soils would have given lower interferences, better reproducibility and greater confidence in the results obtained

3.5 Conclusion

The analysis of metal content in soils was found to be generally reasonable with most soil samples not being excessively contaminated in relation to the elements that were analysed. The Pb levels in soils were high in most instances (maximum soil levels 80 mg/kg) but were not critically contaminated with the exception of sites 9 and 10. The Cu and Fe levels in soil were within acceptable content levels (Cu and Fe max soil levels being 50000 and 100 mg/kg respectively) indicating healthy levels for plant growth. The Ge content values were found to be excessively high (maximum Ge soil levels 0.0024 mg/kg) and they do not comply with known acceptable Ge levels in soil. It is possible there was a problem in determination of this element with relation to soils possibly caused by common interferences such as carbonates, nitrates, sulphates etc. present in the soil [179].

The analysis of the metal content in foodstuffs were in general acceptable with most of the samples analysed showing optimal metal content levels indicating good nutritional quality and little toxicity relative to the metals determined. The Ginseng capsule showed high contents of all studied metals but this may have been due to interferents from excipients present in the capsule. The Fe and Cu levels were present in healthy amounts and prove nutritionally beneficial and promote good general health. The Ge content in foods are quite high and seem to contradict previous observations of this group by a factor of 10. The Pb levels in foods were found to be generally acceptable except in the case of the Ginseng capsule but the interferences are probably related to excipient interference.

The digestion that gave the best overall precision was the aqua regia digestion for soil. The SRM only showed precisions in the region of 4 - 8 % but less adequate recoveries ranging from 88 – 151 % for Pb, Cu and Fe. Germanium, however, could not be evaluated due to the lack of an SRM for germanium content. The $HNO_3/HClO_4$ digestion for food did not utilise a certified reference material as the sample matrices were very diverse. One particular certified reference material could not account for the recoveries in each and every sample. The precision wasn't as good as that in the aqua regia digestions with fluctuations of 1.79 % to 71.11 %. This lack of precision could be attributed to natural variance or complications in the open vessel digestion.

The metals present in soils and foods are present can be chelated/sequestered by biological molecules like proteins or polyphenols but these results will help ascertain the percentage of the metal present in a particular form/complex. This could be of use for the next chapter, which tries to establish the chelation of a particular group of polyphenols called isoflavones for the metals studied in this chapter. Based on the results of this chapter for germanium content determination, an alternate method is required combined with an interlaboratory study.

Chapter 4: UV/Vis determinations of the stoichiometry of isoflavone metal chelates with Cu(II), Fe(III) and Ge(IV) compounds

4.1 Introduction

Flavonoids have the ability to complex with reduced forms of transition metals such as Fe(II), Fe(III), Cu(II) and Al(III) [199]. This is an important property that allows them to, for example, mediate copper and iron overload oxidative stress conditions such as artherosclerosis and lipid peroxidation from iron promotion of the Fenton reaction [9].

The common stoichiometries for metal:flavonoid complexes are 1:1 and 1:2 but there are exceptions to the rule such as 2:3 stoichiometries like in the case of naringenin complexing with Cu(II) [80]. pH plays a major role in flavonoids behaving as either a unidentate or bidentate ligand with a metal ion i.e. the number of chelation sites available for binding with metals. This is caused by protonation/deprotonation of hydroxyl groups on the flavonoid which in turn is dependant on the pKa of the molecule and the activation/deactivation of the chelation sites [80].

Flavonoids by nature are weak polybasic acids that have a tendency to be protonated. Complexes are normally formed in slightly acidic or neutral conditions because of this. The optimal pH for flavonoid complexation has been found on average to be 6.0 according to Malesev *et al.* [10] He also commented that the pH range for successful flavonoid metal chelation is 3-10 pH units. Anything outside of this range would cause destabilisation of the chelate.

Isoflavone metal chelates have been synthesised in the past by Chen *et al.* [200] who studied biochanin A chelated to metals such as Cu(II), Cd(II) and Zn(II). The only other literature citing a chelation study of isoflavone metal chelates was M. Lurdes Mira *et al.* in 2002 [9]. They used the isoflavones, genistein and daidzein. The study dismissed the chelation of isoflavones with Cu(II) and Fe(III) after seeing no bathochromic shift/change in the UV/Vis spectra of the aforementioned isoflavones. This chapter investigates if isoflavones (namely genistein and daidzein) can chelate with Cu(II) and Fe(III) and in which stoichiometry the isoflavone metal chelates exist and represents one of the first bodies of work to be undertaken in categorising isoflavone chelates with transition metals[9,200].

4.1.1 Mole ratio studies of flavonoid metal chelates

Stoichiometry is defined "as the mass relationship among reacting chemical species" [139]. This mass relationship is related by the number of moles that the reacting species have. In relation to the stoichiometry of a complex, it is determined using a series of UV/Vis determination methods known as the method of continuous variations (Job plot), the mole-ratio method and the slope-ratio method. The one used primarily in this research project is the mole-ratio method.

The mole ratio method requires that the molar concentration of one of the analytes is kept static while the other analyte has its molar concentration modified to give varying degrees of mole ratio between the two analytes from, for example, 0-3 as indicated in figure 4.1. A plot of absorbance vs. mole ratio of the analytes is then called a mole ratio plot.

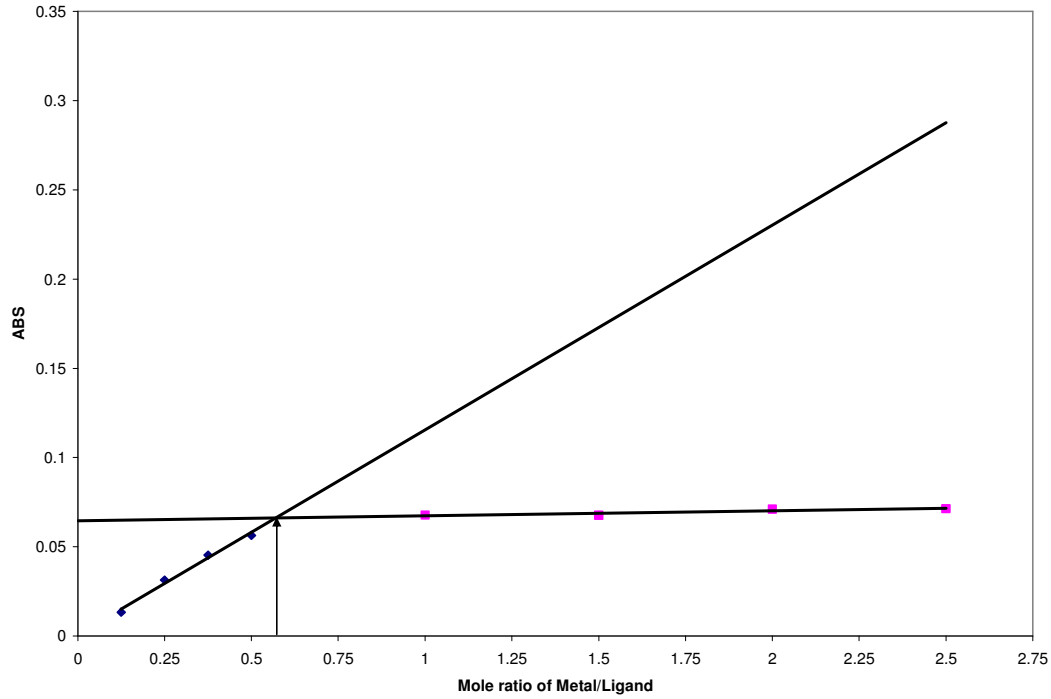

Fig 4.1. Typical mole ratio plot of Absorbance vs. Metal/Ligand (M/L) ratio

In fig. 4.1, it is shown that the stoichiometry is near 0.5. This would represent that 1 mole of metal cation is being complexed by 2 moles of ligand. This is referred to as a 1:2 stoichiometry or a 1:2 complex. [139]

Flavonoid metal chelate studies have been performed as far back as 1956 using UV/Vis spectrophotometry. This study was performed by Jurd *et al.* [199] working with UV/Vis spectroscopy to determine the stoichiometries of aluminium flavonoid metal complexes. Fig 4.2 shows the chelation sites he deduced in flavonoids that are most likely to have metals bind to them.

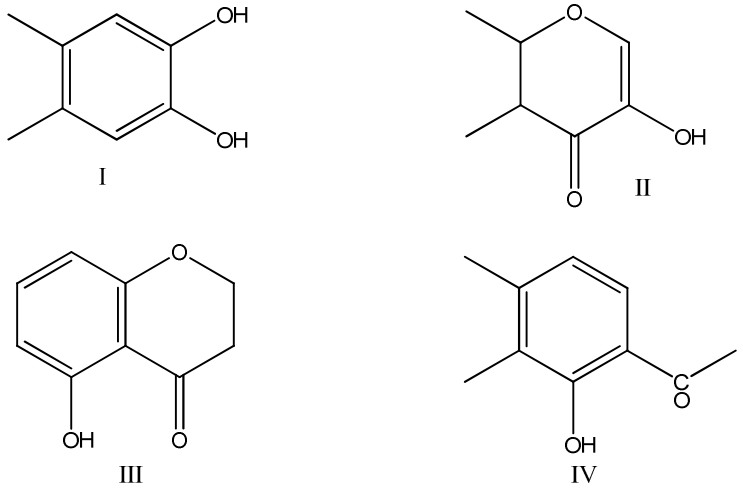

Fig. 4.2 (I) o-dihydroxy phenols, (II) 3-hydroxychromes, (III) 5-hydroxychromes and (IV) o-hydroxycarbonyl derivatives [199].

Having at least one of these structural components was speculated to allow chelation with metal species such as Al(III), Cu(II) and Fe(III). After studies with 5 flavonoids, among which were kaempferol and quercetin, a 1:2 stoichiometry was normally found for aluminium flavonoid chelates and a very interesting 1:1 ratio resulted in a polymeric metal flavonoid complex forming a sequence such as [-M-F-M-F-M-F-M-] [199].

UV/Vis spectroscopy is not the only technique that can be used for inference of stoichiometry of flavonoid metal complexes. Molecular modelling packages using sophisticated quantum mechanics simulation technology can also be used to predict stoichiometries of suggested metal flavonoid chelates. This was done by Leopoldini *et al.* [95] with Fe(II)quercetin complexes. The molecular modelling studies came up with optimized geometries of several probable iron quercetin complexes at different stoichiometries, taking into account other factors such as hydration of the iron metal cation to form new stoichiometries. It was predicted that the Fe(II) metal cation has the most probability of forming a high spin octahedral complex.

This results in an 1:2 complex with the quercetin ligands being formed but with the additional need to interact with 2 water molecules as indicated in fig. 4.3. This complex formation allows the stabilisation of the complex by forming a coordinate bond with the C3 and C4 3-OH groups in quercetin and then bonding with the water molecules. This is described as the most energetically favourable arrangement and satisfies the octahedral conformation of Fe(II).

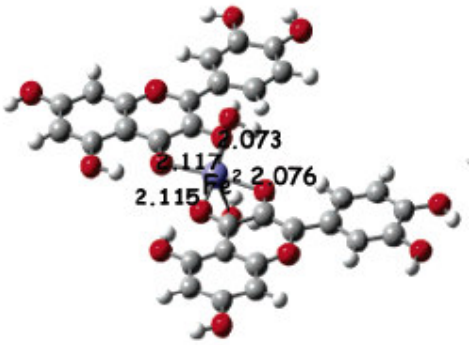

Fig. 4.3 A hydrated iron quercetin complex with an M/L ratio of 1:2. [95]

4.1.2 Job plots of flavonoid metal chelates

Job plots are used as an alternative method of stoichiometric identification where it involves the use of mole fractions as opposed to mole ratios. It relies upon the mixing of an equimolar solution of ligand and metal and then use of the mole fraction curve maximum to identify the stoichiometry.

The job plot was the method used to determine the stoichiometry of the Cu(II)-morin complex as carried out by Panwhar *et al.* The group found the mole fraction was 0.5 meaning the complex had a stoichiometry of 1:1 M/L (see fig. 4.4). The curve absorbance data was collected at a value of 424 nm, the group referred to this as band III for the Cu(II)-morin complex spectrum and was a key indicator of chelation [201]

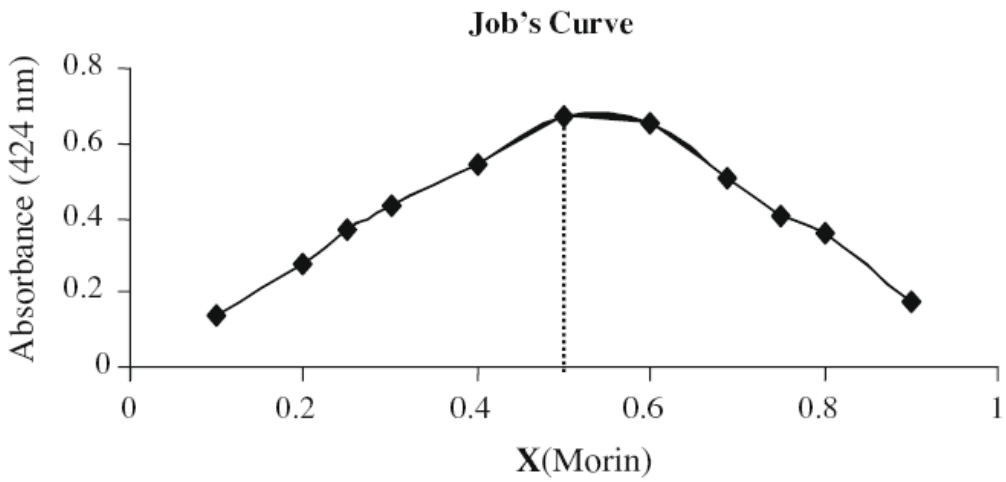

Fig. 4.4 A typical job plot that was determined for a Cu(II) morin complex collected at 424 nm characteristic complex band [201]. Note the mole fraction at 0.5 is indicative of a 1:1 stoichiometry.

Bukhari *et al.* used the job plot for stoichimetry determination of cobalt-quercetin complex. They found the stoichiometry was 2:1 M/L or 0.33 mole fraction of quercetin. The data points were collated at the characteristic band of the complex at 427 nm [202].

4.1.3 Isoflavone metal chelates

The known chelation sites on the isoflavone that can possibly interact with metals are the 4-carbonyl group on the C ring and 5-OH groups located on the A ring part of the isoflavone [90,203]. This is based on literature for other flavonoid species and has been verified by Chen *et al.* who found this to be the case in their isoflavone metal chelates in general [200]. It is possible with variations in pH and solvent conditions that different copper and iron isoflavone chelates will form. Bearing this in mind, it might be possible for other hydroxyl functionalities to interact such as the 7-OH group present in all of the isoflavones [9].

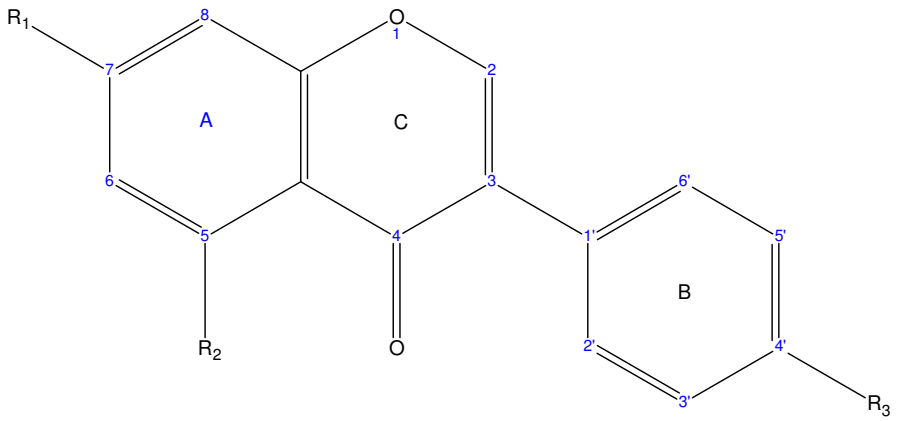

Fig. 4.5 Base Structure of isoflavones daidzein(R1=H, R2=OH, R3=OH) genistein(R1=OH, R2=OH, R3=OH) and biochanin A (R1=OH, R2=OH, R3=OCH_3)

The isoflavones concentrated on in this study are biochanin A, genistein and daidzein. In the above figure, it is apparent that the 4-keto and 5-OH functionality is common to biochanin A and genistein but not daidzein. The effect of the lack of these functionalities on complex formation is investigated here.

Daidzein, genistein and biochanin A are part of the isoflavone family. The isoflavones are uncommon among plants due to the specific nature of their reaction i.e. chiefly mediated by isoflavone synthase. Genistein, for example, is capable of antimicrobial and anti-cancer properties and is remarked as the most biologically active of the isoflavones [98]. Biochanin A and daidzein also have cardioprotective, antioxidant and anti-cancer properties making the isoflavones in general, a beneficial phytoestrogen supplement [99]. Isoflavones normally occur in nature in leguminous species such as soya products and walnuts in a very high degree but can be found in extremely trace quantities in non-leguminous foods like cranberries and currants [88,204].

Isoflavones have been found to have a pro-oxidant effect in the presence of Cu^{2+} according to Cao *et al.* [205] This study was assessed by assays of peroxyl radical mediation by flavonoids in non-copper and copper enriched systems. It was also found that the degree of hydroxylation of the flavonoid structure plays a critical role

in its pro-oxidant/antioxidant properties. Although copper is regarded traditionally as a prooxidant, some complexes of Cu(II) and rutin and dihydro-quercetin show greater antioxidant ability against free radicals than their uncomplexed flavonoid counterparts [10].

Isoflavones were also found to mediate non-heme iron concentration in the blood that can lead to oxidative stress at overload levels due to haber-weiss lipid peroxidation as investigated by Swain *et al* [101]. The study focused upon the relationship of the iron index of peri-menopausal women and the intake of soy protein containing foods that would have large quantities of isoflavones. The study found that the iron index was significantly reduced by week 12 of the study and increased the total antioxidant activity of the women. It was found by week 24 that the low concentrations of iron had a beneficial antioxidant effect contributing greatly to the overall anitioxidant activity. Fe (III) and Fe(II) complexes of flavonoids were studied by Moridani *et al* [102]. In the iron flavonoid complexes, it was proposed that the 2:1 flavonoid:iron arrangement gave the best result for mediation of oxidative stress due to hypoxia-reoxygenation injury in rat hepatocytes. The free flavonoid forms including quercetin and rutin showed less free radical scavenging capability or cytoprotective ability.

The main method of identification of flavonoid metal chelates is UV/Vis spectroscopic identification through a bathochromic shift in the absorption spectra of the flavonoids when complexed with a metal. The bathochromic shift is related to the pH of the medium with more acidic conditions leading to less of a bathochromic shift as the chelation characterisitcs of the flavonoid with metals increases protonation of the hydroxyl groups. Flavonoids have two distinct absorption bands, band I and II. Band I is found between 300-550 nm and is related to the $\pi \rightarrow \pi^*$ transitions for the B ring. Band II is found between 240-285 nm and results from the $\pi \rightarrow \pi^*$ transition from the A ring. The absorption maxima are determined by the degree of hydroxylation/conjugation of these ring systems and thus are different for each species of flavonoid. [9,10]

4.2 Aims

- The study of different types of Fe(III), Cu(II), Cd(II), Co(II), Ni(II), Pb(II), Zn(II) and Ge(IV) metals with daidzein, genistein and biochanin A
- The stocihiometric evaluation of successful chelates in methanol using the job and mole ratio plot methods
- The examination of stoichiometry changes within successfully formed chelates at different pH's

4.3 Experimental

4.3.1 Instrument

Varian Cary 50 Scan Dual Beam UV/Vis spectrophotometer,
WTW pH 526 pH meter, Hellmer Quartz UV/Vis low volume cuvettes.

The UV/Vis scan parameters were set to 200-700 nm with a medium scan speed (or a scan rate of 600 nm/min) with baseline correction using makeup solution for sample sets. All files were saved in ASCII format to aid data collation and interpretation.

4.3.2 Chemicals

Daidzein was supplied by Sigma-Aldrich, Ireland, genistein and biochanin A were supplied by Fluka Chemicals through Sigma-Aldrich, Ireland. Metal nitrate salts of Fe(III)nitrate.$9H_2O$, Cu(II)nitrate.$3H_2O$, Cd(II)nitrate.$4H_2O$, Co(II) nitrate.$6H_2O$, Pb(II)nitrate, Ni(II)nitrate.$6H_2O$ and Zn(II)nitrate.$6H_2O$ were supplied by Merck Chemicals. All metal nitrate salts were of analytical grade and used without further purification.
Germanium sesquioixde and germanium dioxide were supplied by Sigma-Aldrich, Ireland. HPLC grade methanol was used for sample preparation with 0.1 % w/v HCl and NaOH solutions used for pH adjustment purposes. pH buffer calibrants were pH 4.0 and 7.0 from Riedel de Haen.

4.3.3 Method

4.3.3.1 Isoflavone stock solutions

5 mmol quantities of daidzein, genistein and biochanin A were weighed out and transferred to 10 ml volumetric flasks and made up with 100 % MeOH to give a 5 mM solution.

4.3.3.2 Metal solution

A 25 mM solution of the appropriate metal salt was made up in a 20 ml volumetric flask with methanol. This was followed by the dilution of the solutions to a 2.5 mM working solution in 10ml volumetric flasks.

4.3.3.3 Germanium solutions

A 25 mM solution of the germanium compound was made up in 20 ml of deionised water. This was followed by diluting the germanium solutions to 2.5 mM using the appropriate volume of stock solution.

4.3.3.4 Chelation study

50 µM concentrations of the isoflavone was prepared in methanol using 10 ml volumetric flasks. This was followed by the addition of 200 µL amounts of the 2.5 mM metal working solution. The volumetric flask was then made to the mark with methanol. This gave a sample solution of 50 µM metal versus 50 µM isoflavone.

4.3.3.5 Mole Ratio study

A 2.5 mM solution of Cu(II) and Fe(III) were made up to the mark with Methanol. The 50 µM amounts of the isoflavones were made up in the same manner as stated for the chelation study with varying amounts of the 2.5 mM solutions of Cu(II) and Fe(III) for each sample to give varying molar concentrations of the metals versus the static concentration of the isoflavone.

4.3.3.6 Job plot study

100 µM solutions of the isoflavones and metals were prepared from stock solutions in methanol in 10 mL volumetric flasks. The volume ratios were adjusted from 0 metal: 10 isoflavone to 9 metal: 1 isoflavone.

4.4 Results and Discussion

4.4.1 Chelation study of metals

The chelation study consisted of scanning 50 µM quantities of isoflavone against 50 µM quantities of metal. These metals were studied by AAS as detailed in chapter 3. Chelations were also noticed for some previously studied metals, particularly ones that were in the UV end of the spectrum e.g. the primary atomic absorption wavelength of Pb was 217.0 nm. To successfully identify a metal isoflavone chelate via UV/Vis spectroscopy, the metal chelates with the isoflavone must generate a bathochromic shift for subsequent mole ratio studies. Another indicator of successful isoflavone metal chelation is the presence of a coloured metal isoflavone sample solution. This is not a definitive inference but acts as a good "rule of thumb" that chelation has worked [203] and has been proven in the past by Chen *et al.* Chelation can be seen for isoflavone samples where no UV activity is present whatsoever [200].

There are bathochromic shifts observed in the case of Fe(III) and Cu(II) genistein chelates as indicated in fig. 4.6 and table 4.2. The bathochromic shifts for genistein upon addition of Fe(III) and Cu(II) were 46 ± 0 and 56 ± 0 nm respectively. There was no wavelength variation seen between replicates of the samples indicating that any wavelength shifts were due to interactions between the metals and isoflavones alone. This also applies to the chelation studies of biochanin A and daidzein, discussed further in this chapter.

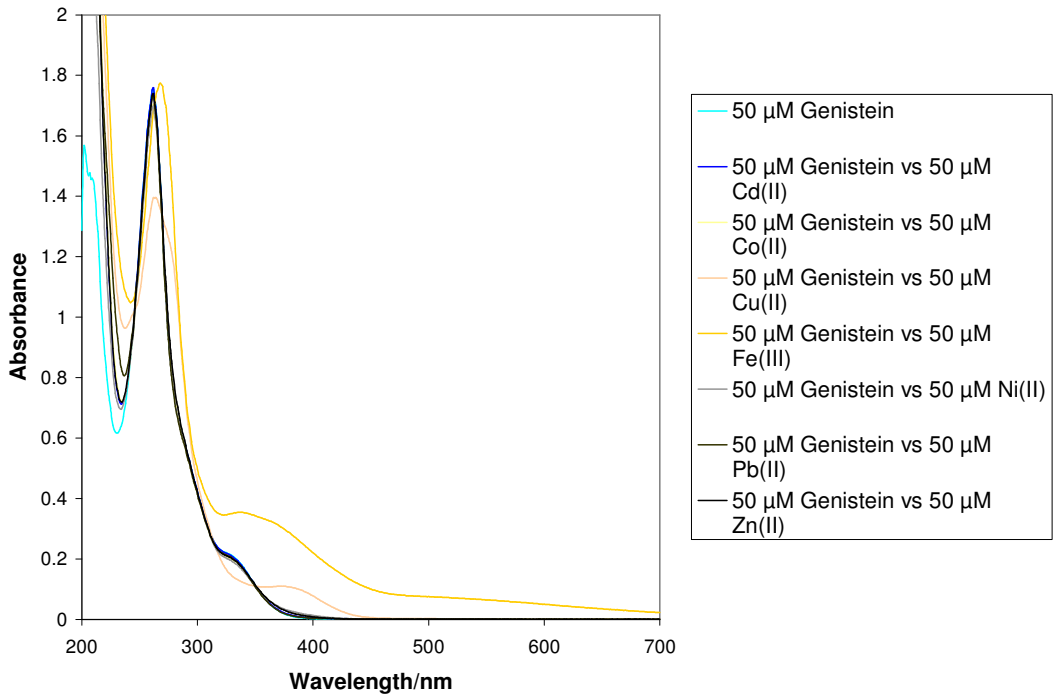

Fig. 4.6 Chelation plot of 50 µM genistein chelated with 50 µM quantities of specified metals in methanol n=3

Table 4.2 Bathochromic and hypsochromic shifts for genistein metal complex chelation studies performed in triplicate

Chelating metal	Band I/nm	ABS I	Band I shift/nm	Band II/nm	ABSII	Band II shift/nm
Genistein	318±0	0.2371±0.0068	0±0	262±0	1.7556±0.0425	0±0
Cd(II)	318±0	0.2369±0.0095	0±0	262±0	1.7587±0.0548	0±0
Co(II)	318±0	0.2264±0.0038	0±0	262±0	1.7028±0.0245	0±0
Cu(II)	374±0	0.1093±0.0025	56±0	262±0	1.3957±0.0428	0±0
Fe(III)	364±0	0.3241±0.0204	46±0	268±0	1.7735±0.0661	6±0
Ni(II)	318±0	0.2235±0.0023	0±0	262±0	1.6980±0.0188	0±0
Pb(II)	318±0	0.2305±0.0061	0±0	262±0	1.7328±0.0370	0±0
Zn(II)	318±0	0.2295±0.0109	0±0	262±0	1.7391±0.0627	0±0

Both chelates showed a distinct colour change when the metal and genistein solutions were mixed indicating possible metal chelation. Cu(II)genistein showed a pale yellow colour upon mixing and Fe(III)genistein showed a purple/turquoise colour. The major bathochromic shift of Fe(III) is the same as the one seen in daidzein but the observed

colour change at sample preparation indicates chelation did occur with genistein. The other metals showed no bathochromatic shifting whatsoever indicating no chelation has occurred that can be detailed by UV/Vis observations. A more definitive interpretation of isoflavone metal chelation could be obtained by using ESI-MS but this is outside the scope of this chapter. This is also indicated by stoichiometric studies involving genistein where no colour change was observed (again this does not mean chelation did not take place, just spectral shifts in the band did not occur).

The colours observed for the copper isoflavone chelates are in keeping with metal complex reaction observations of Jungbluth *et al.* [90] where a yellow colouration resulted upon the formation of the Cu^{2+} flavonoid metal complex in alcohol solvents. The purple colour of the iron isoflavone metal chelates was also observed in the formation of the iron flavonoid complex during oxidation of quercetin. The colour of the complexes is strongly linked to water content i.e. more water content equals a less stable coloured complex in the case of flavonols.

The biochanin A metal complex chelation plot in fig. 4.7 shows the presence of a metal biochanin A chelate for Fe(III) and Cu(II). Yet again, the same colours were observed for the biochanin A metal chelates with Fe(III) chelates yielding a purple/turquoise colour and Cu(II) giving a pale yellow colour. This result was expected as biochanin A is a derivative of genistein. It may indicate that the two of them have very similar chelation characteristics. Since the two of them have similar pKa values, [206] they would be protonated and deprotonated similarly for the 7-OH and 5-OH groups. The other metals show no indication of chelation with biochanin A as indicated by the 0 nm shifts in bands I and II. Chen *et al.* [200] however observed that chelation can take place between Ni(II), Co(II), Cu(II), Mn(II) and Zn(II). These chelates were synthesized without any formal chelation study or stoichiometric evaluation. The synthesized chelates were also evaluated in a more indepth fashion (mass spectrometry, IR spectroscopy etc.) than this precursory study. Chen *et al.* did not investigate the effects of chelation of biochanin A with Fe(III) so this is the first indication of biochanin A chelation with Fe(III). Malesev *et al.* [10] stated that flavonoids primarily chelate with Fe(II), Fe(III) and Cu(II). They have been known to chelate with Al(III) but nothing is known about how this metal would interact with isoflavones.

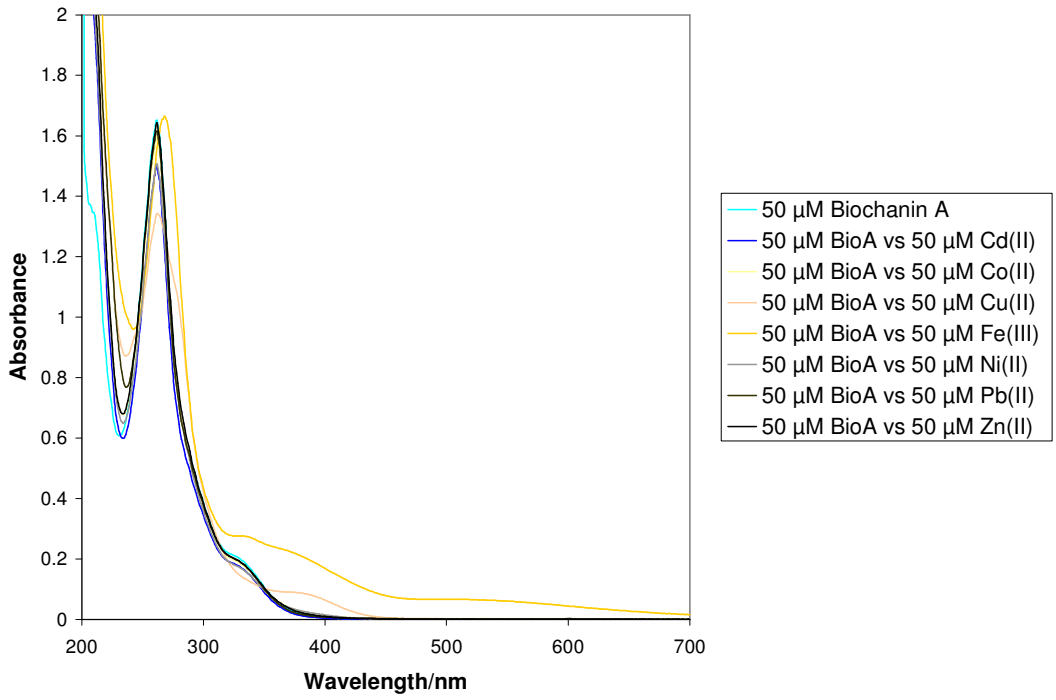

Fig. 4.7 Chelation plot of 50 µM biochanin A chelated with 50 µM quantities of specified metals in methanol performed in triplicate

Table 4.3 Bathochromic shifts for biochanin A metal complex chelation studies performed in triplicate

Chelating metal	Band I/nm	ABS I	Band I shift/nm	Band II/nm	ABSII	Band II shift/nm
Biochanin A	318±0	0.2270±0.0041	0±0	262±0	1.6510±0.0270	0±0
Cd(II)	318±0	0.2085±0.0204	0±0	262±0	1.6878±0.1670	0±0
Co(II)	318±0	0.2161±0.0075	0±0	262±0	1.5969±0.0430	0±0
Cu(II)	376±0	0.0891±0.0031	58±0	262±0	1.3436±0.0230	0±0
Fe(III)	364±0	0.2340±0.0085	46±0	268±0	1.6642±0.0514	6±0
Ni(II)	318±0	0.2006±0.0113	0±0	262±0	1.5066±0.0753	0±0
Pb(II)	318±0	0.2185±0.0052	0±0	262±0	1.6154±0.0308	0±0
Zn(II)	318±0	0.2196±0.0170	0±0	262±0	1.6428±0.1111	0±0

The daidzein metal chelate plot in fig. 4.8 reveals a rather large bathochromic shift for the Fe(III) daidzein chelate giving the impression that chelation has been successful. This can also be seen in table 4.4 where Fe(III) causes a significant bathochromic shift of 62±0 nm in Band I of daidzein. No change in colour for the metal chelate

solution was observed. The other metals showed little impact on the spectrum of daidzein with shifts never exceeding 1 nm for Bands I and II suggesting these metals are not complexing with daidzein, according to this method.

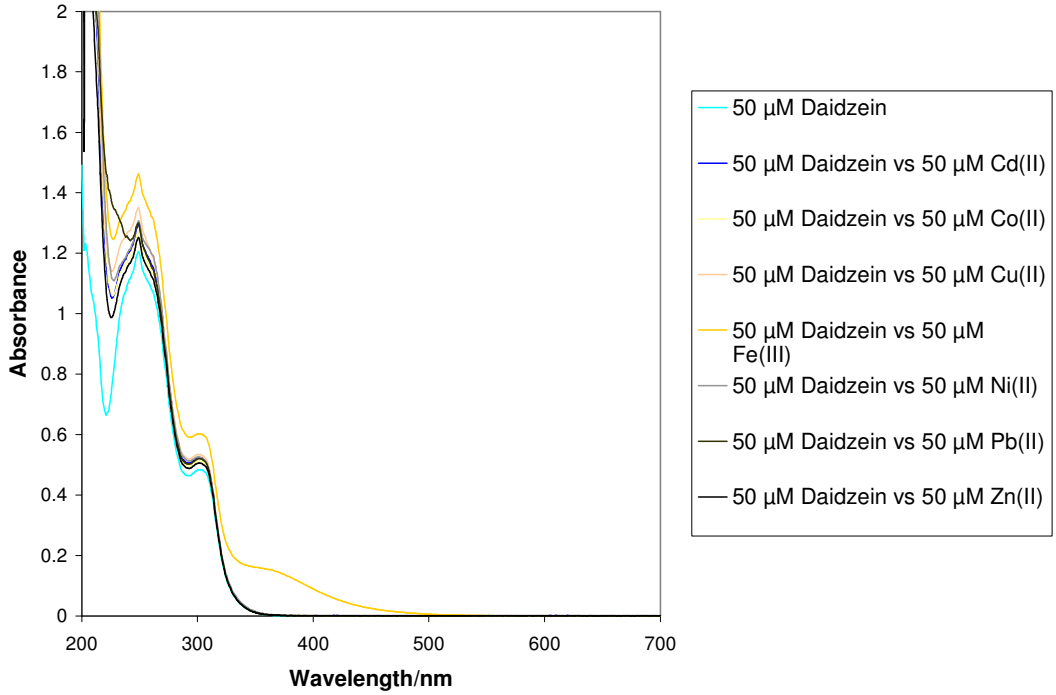

Fig. 4.8 Chelation plot of 50 µM daidzein chelated with 50 µM quantities of specified metals in methanol n=3.

Table 4.4 Bathochromic shifts for daidzein metal complex chelation studies performed in methanol performed in triplicate.

Chelating metal	Band I/nm	ABS I	Band I shift/nm	Band II/nm	ABSII	Band II shift/nm
Daidzein	302±0	0.4841±0.0141	0±0	249±0	1.2054±0.0355	0±0
Cd(II)	301±0	0.5239±0.0155	0±0	249±0	1.2947±0.0365	0±0
Co(II)	301±0	0.5125±0.0143	0±0	249±0	1.2699±0.0345	0±0
Cu(II)	301±0	0.5348±0.0048	0±0	249±0	1.3510±0.0116	0±0
Fe(III)	364±0	0.1518±0.0097	62±0	249±0	1.4625±0.0469	0±0
Ni(II)	301±0	0.5262±0.0198	0±0	249±0	1.3078±0.0539	0±0
Pb(II)	301±0	0.5204±0.0059	0±0	249±0	1.3002±0.0145	0±0
Zn(II)	301±0	0.5061±0.0137	0±0	249±0	1.2518±0.0338	0±0

The reason why band I is of a much lower intensity than might be associated with some other flavonoid like flavanones and flavonols was explained by Deng *et al.* [79] when they commented on the spectrum of biochanin A in methanol. The lack of conjugation between the B ring and the pyrone carbonyl group (C ring) is not apparent and thus band I is of significantly reduced intensity. This is a useful parameter for distinguishing between isoflavones and other flavonoid species with 4 keto groups were resulting in a much higher absorption band than the B-phenyl ring is connected to the 2-C position. (Refer to fig. 4.4)

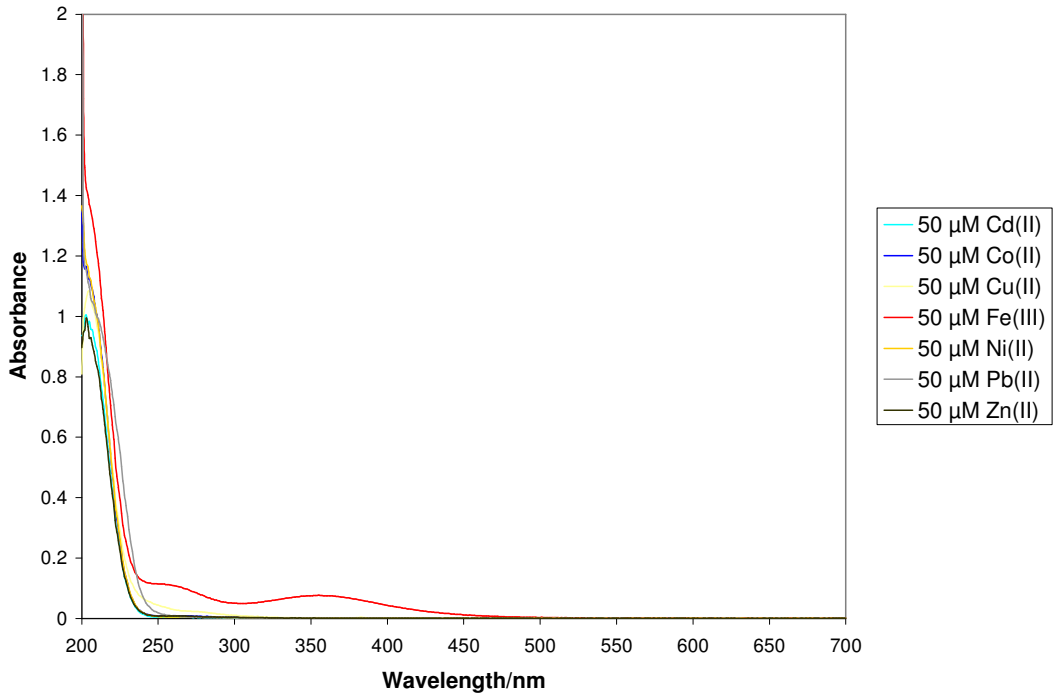

Fig. 4.9 Chelation plot of 50 µM quantities of metal in methanol performed in triplicate.

The isoflavone versus germanium chelation studies (see fig. 4.10) did not indicate chelation for the germanium species. Germanium dioxide and germanium sesquioxide don't tend to be have a UV/Vis spectrum as they have a very high $\pi \rightarrow \pi^*$ transition due to the high energy gaps associated with germanium oxygen networks i.e. the electrons are held tightly by the large electronegative potential of germanium. The UV/Vis range of the electromagnetic spectrum has insufficient energy to overcome this energy gap so no UV/Vis spectrum can be seen for germanium (IV) compounds (see Fig. 4.10) [104]. No bathochromic shift was observed in the above spectra for

biochanin A, daidzein and genistein. The germanium in the compounds is not in a dissociated form so it may prove an inhibitory factor to successful metal chelation. Germanium dioxide has been shown to chelate with quercetin in a 1:1 ratio when used in the presence of the surfactant, Brij-35 as found by Garcia-Campana *et al.* [207] This was discovered under fluorescence analysis, however, and not via UV/Vis spectroscopy. Additional work using fluorescence spectroscopy may prove useful in determining whether complexation occurs.

No colour change could be observed when the germanium compound solutions and the isoflavone solutions were mixed. Previous work in this group indicated that germanium sesquioxide did bind successfully to the flavonoid quercetin[104]. Fluorescence spectroscopy, however, was used to indicate the presence of a isoflavone metal chelate. No previous literature has been found investigating the complexation of the isoflavones genistein, biochanin A and daidzein with germanium sesquioxide and germanium dioxide and this represents the first attempt at investigating this chelation [104].

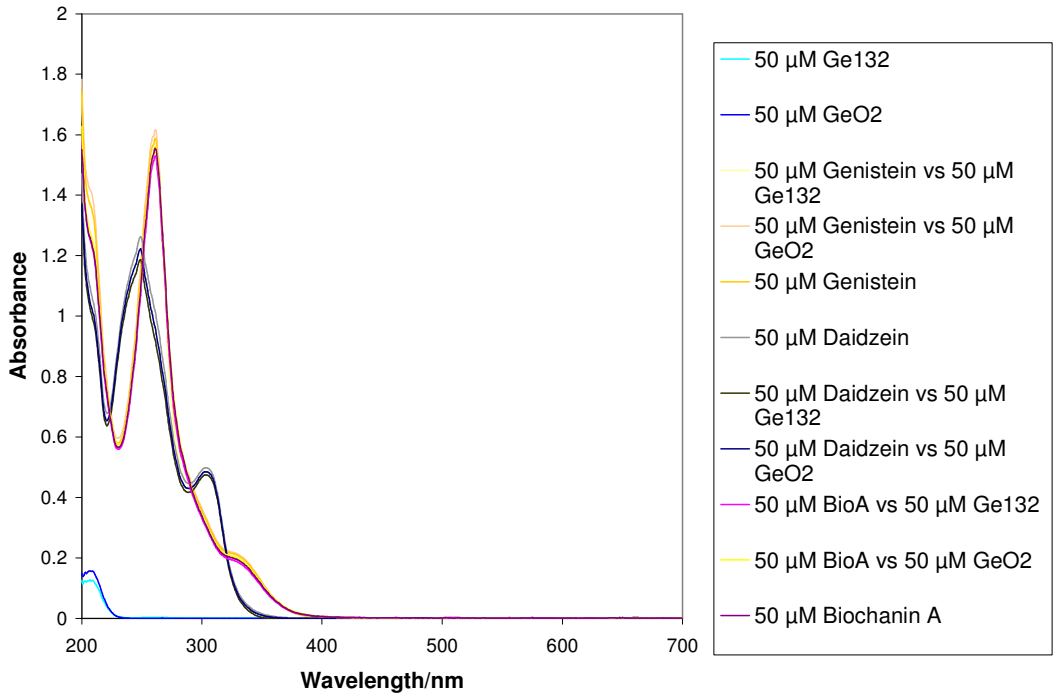

Fig. 4.10 Chelation plot of 50 µM isoflavones, in methanol, chelated with 50 µM quantities of germanium(IV) compounds, in water performed in triplicate.

Table 4.5 Bathochromic and hypsochromic shifts for isoflavone germanium complexes chelation studies.

Chelating metal	Band I/nm	ABS I	Band I shift/nm	Band II/nm	ABSII	Band II shift/nm
Daidzein	304±0	0.4982±0.0211	0±0	248±0	1.2631±0.0540	0±0
Daidzein vs. GeO_2	304±0	0.4854±0.0047	0±0	248±0	1.2223±0.0163	0±0
Daidzein vs. Ge132	304±0	0.4746±0.0278	0±0	248±0	1.1866±0.0674	0±0
Biochanin A	318±0	0.2119±0.0064	0±0	261±0	1.5551±0.0297	0±0
Biochanin A vs. GeO_2	318±0	0.2160±0.0035	0±0	261±0	1.5612±0.0247	0±0
Biochanin A vs. Ge132	318±0	0.2050±0.0044	0±0	261±0	1.5293±0.0239	0±0
Genistein	318±0	0.2255±0.0095	0±0	261±0	1.5881±0.0661	0±0
Genistein vs. GeO_2	318±0	0.2304±0.0053	0±0	261±0	1.6152±0.0385	0±0
Genistein vs. Ge132	318±0	0.2190±0.0061	0±0	261±0	1.5416±0.0401	0±0

4.4.2 Stoichiometry studies of isoflavone metal chelates at varying pH levels

The mole ratio studies involved looking at the isoflavone metal chelates at an unadjusted pH of 7.3 and then exploring more extremes of pH from 4-9. This would give a better understanding of the deprotonation/protonation behaviour of the chelation sites and furthermore assess the variations in complex stoichiometries associated with pH change. The respective pKa's for stated isoflavones are 7.54, 7.2 and 7.2 [77,206,208]. Additionally, flavonoids are in general weak polybasic acids that are very susceptible to protonation. According to literature, the ideal pH for forming a flavonoid metal complex is between pH 5.5-6.0. [9,10]

The establishment of the mole ratio values for the following studies was done using a modified version of the mole ratio equation. The balanced equation below applies to

the reaction between any metal ion, M, with a ligand, L and ML, the subsequent complex that they produce

$$nM + nL \leftrightarrow M_nL_n \qquad \textit{Eq 4.1}$$

This can later be derived as the equation:

$$A = \varepsilon_{M_n}[M_n] + \varepsilon_{Ln}[L] + \varepsilon_{M_nL_n}[M_nL_n] \qquad \textit{Eq 4.2}$$

It is assumed in the mole-ratio plot that $\varepsilon_m = 0$ whereas the other two quantities ε_L and ε_{ML} are attributed to the two lines of the mole ratio plot. [139] This can then be further derived into an equation for the point of inflexion between 2 curves and additionally takes into account the variables of the mole ratio plot.

$$Mole\,Ratio = \frac{c_{MnLn} - c_{Ln}}{m_{Ln} - m_{MnLn}} \qquad \text{where, c = intercept of line, m = slope of line} \qquad \textit{Eq 4.3}$$

The lower mole ratio plot line therefore belongs to Ln, and MnLn belongs to the higher mole ratio plot line. Thus the mole ratio can be successfully derived.

In the case of the Job plots, the stoichiometry will be determined relative to the mole fraction of the isoflavone or $X_{isoflavone}$. The Job plots were only used for confirmation of values at pH 7.3 (or the unadjusted methanol) so as to better ensure the stoichiometries were accurate before synthesis began as methanol would be used in the synthesis. These mole fraction values are derived from the molarity of metal versus the molarity of isoflavone or simply put in the following relationship:

$$X_{isoflavone} = \frac{moles_{metal}}{moles_{isoflavone}} \qquad \text{Eq. 4.4}$$

4.4.2.1 Biochanin A/genistein metal chelates

The first set of mole ratio studies were performed for biochanin A/genistein versus Cu(II). They were first performed at a pH of 7.3 (i.e. the unadjusted pH of methanol). The results are shown in fig. 4.11 and fig. 4.12

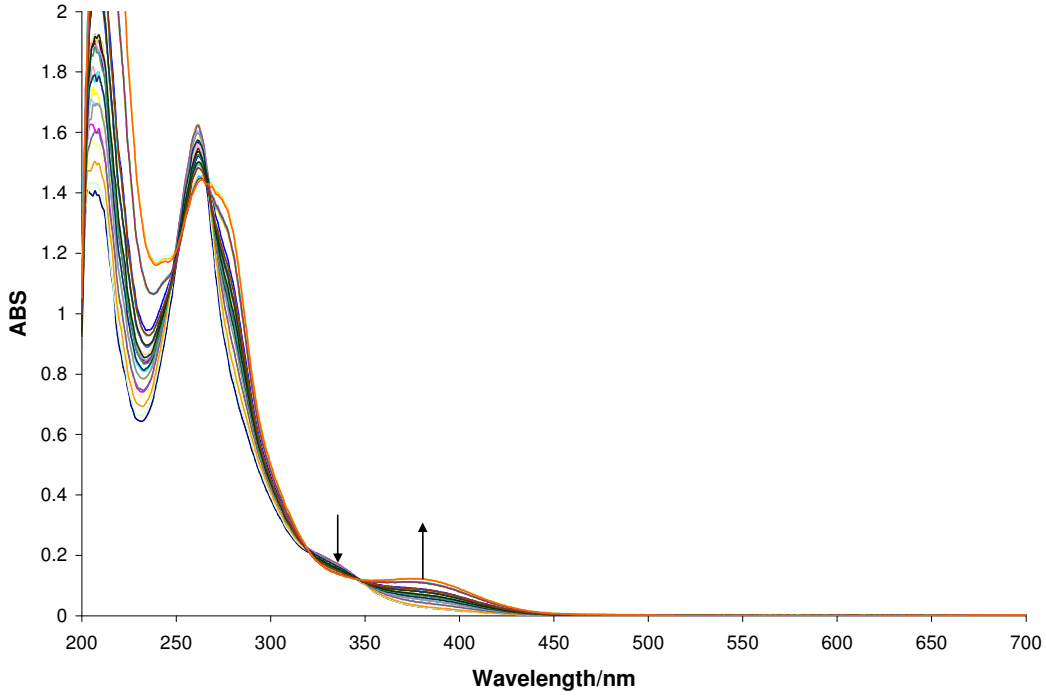

Fig. 4.11 UV/Vis overlay plots of 50 µM biochanin A versus 5 to 300 µM Cu(II) in methanol

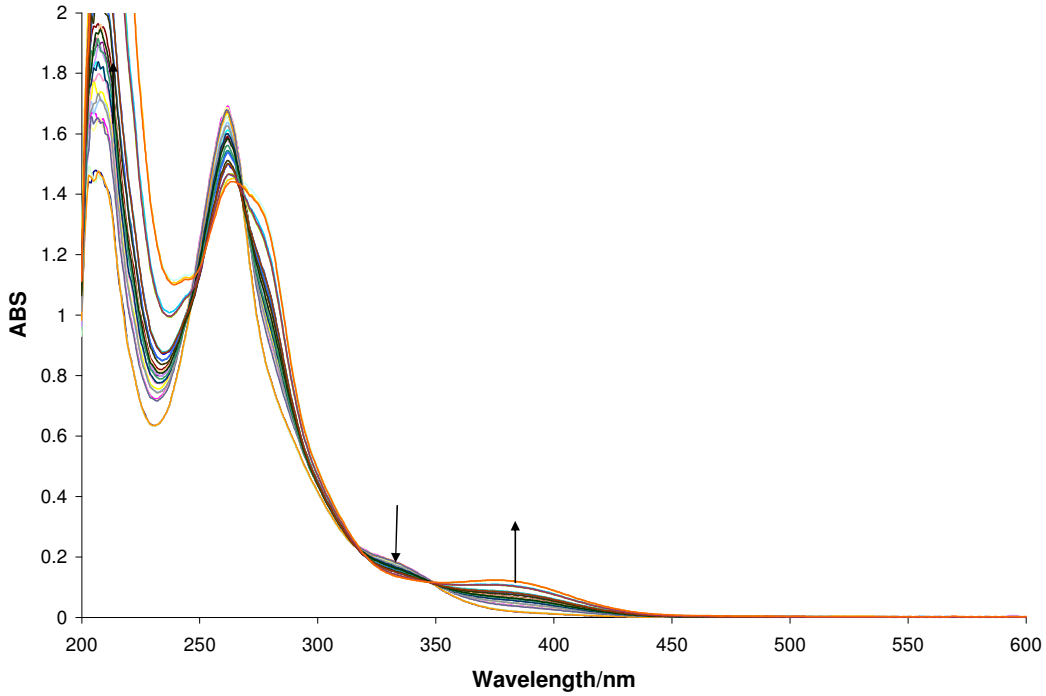

Fig. 4.12 UV/Vis overlay plots of 50 µM genistein versus 5 to 300 µM Cu(II) in methanol.

The biochanin A Cu(II) metal chelate forms a distinct band at 376 nm as seen in fig. 4.11. This is corroborated by the chelation plots shown earlier in section 4.3.1. This band will be subsequently used for all quantitative determinations of mole ratio of Cu(II) biochanin A/genistein chelates.

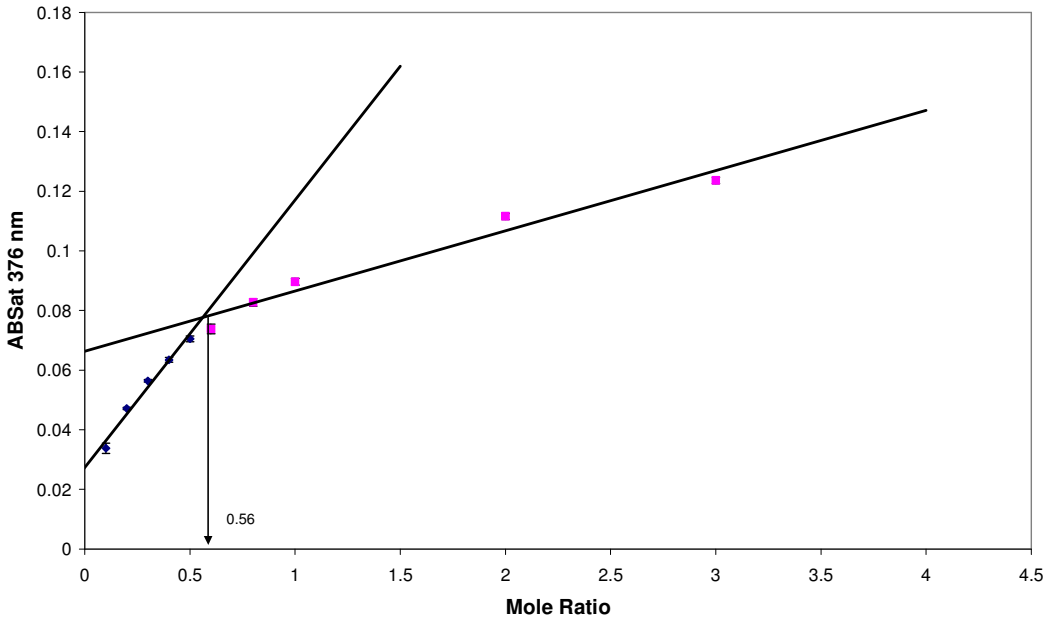

Fig. 4.13 Mole ratio plots of 50 µM biochanin A versus 5 to 300 µM Cu(II) in methanol.

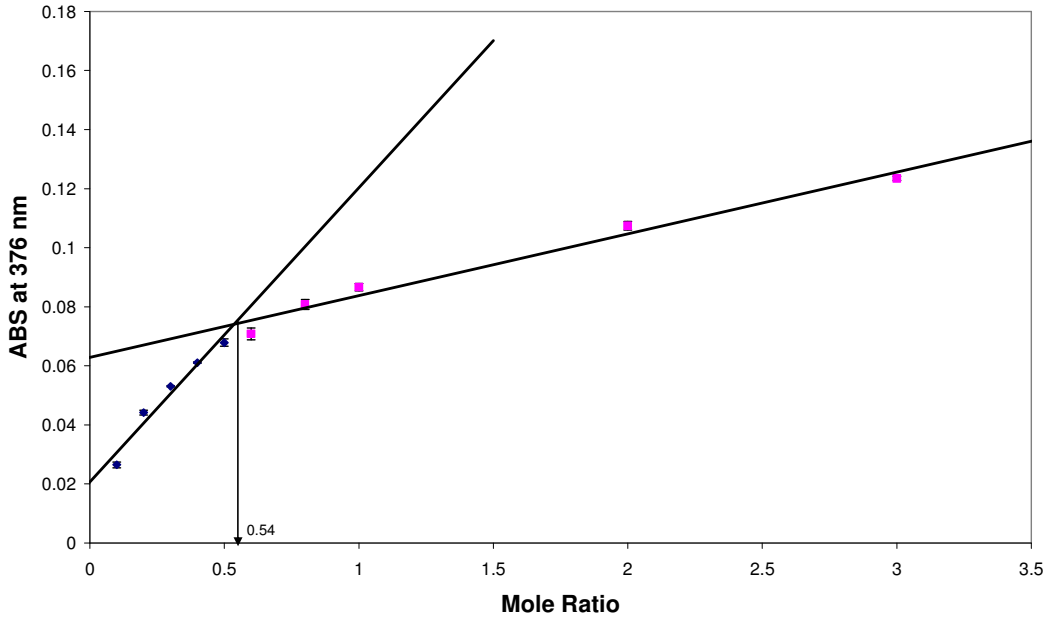

Fig. 4.14 Mole ratio plots of 50 µM genistein vs. 5 to 300 µM Cu(II) in methanol.

The mole ratio plot of Cu(II) biochanin A metal chelate revealed an average of 0.56 ± 0.01 while the mole ratio plot of Cu(II)genistein was closer to 0.54 ± 0.01 (see fig. 4.12). These values indicate a stoichiometry of 1 mole Cu(II) to 2 moles of biochanin

A/genistein. In the case of Cu(II) quercetin complexes, a stoichiometry of 1:2 M/L has been observed [82]. Chen *et al.* confirmed that their Cu(II)biochanin A chelate had the same stoichiometry of 1:2 M/L [200].

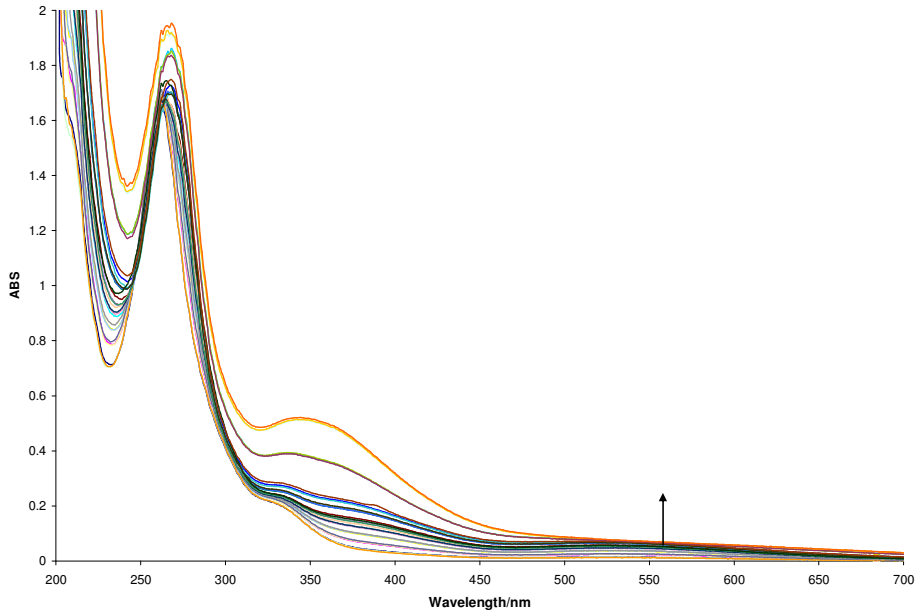

Fig. 4.15 UV/Vis overlay plots of 50 µM biochanin A versus 5 to 300 µM Fe(III) in methanol.

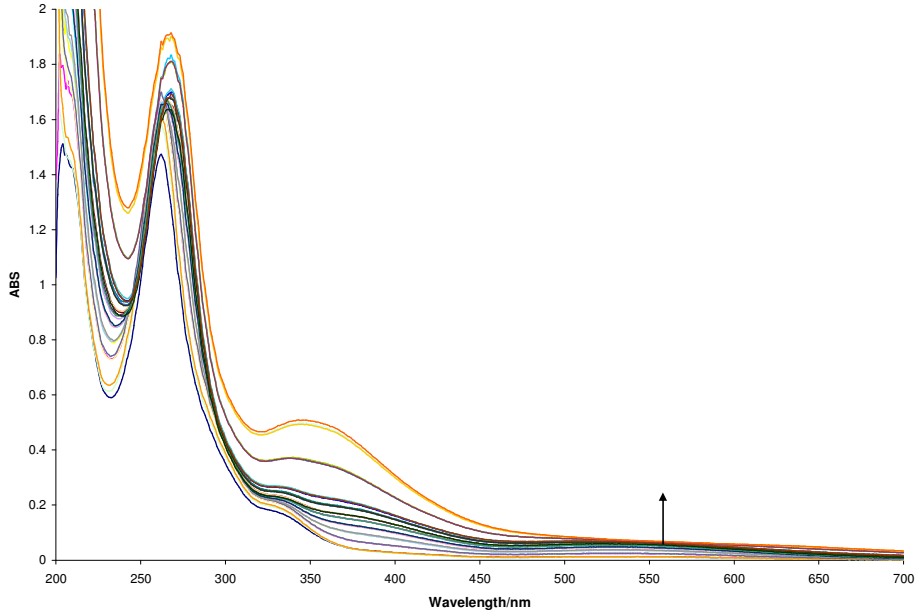

Fig. 4.16 UV/Vis overlay plots of 50 µM genistein and 5 to 300 µM Fe(III) in methanol.

In the mole ratio study of Fe(III) biochanin A/genistein metal chelates, it was found that at pH 7.3, the most characteristic band was present at 550 nm as seen in figures 4.15 and 4.16. This can lead to absorptions in the near UV or visible region and shifts the electron density from the ligand to the metal ion [209]. This is confirmed by literature that states that Fe^{3+} is reduced to Fe^{2+} in the presence of the flavonoid ligand [90].

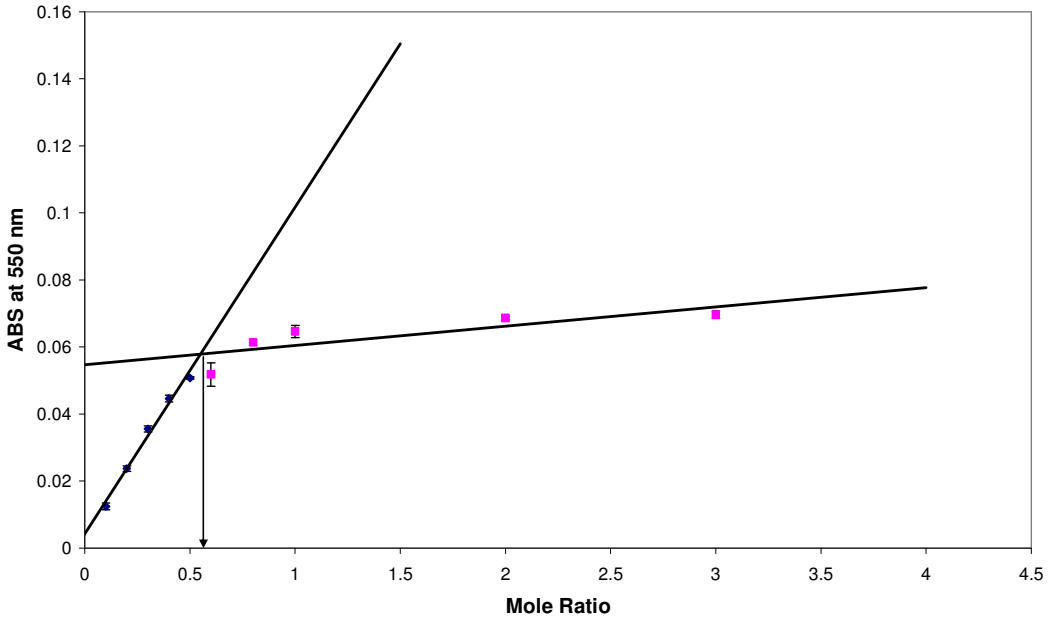

Fig. 4.17 Mole Ratio plots of 50 µM biochanin A versus 5 to 300 µM Fe(III) in methanol.

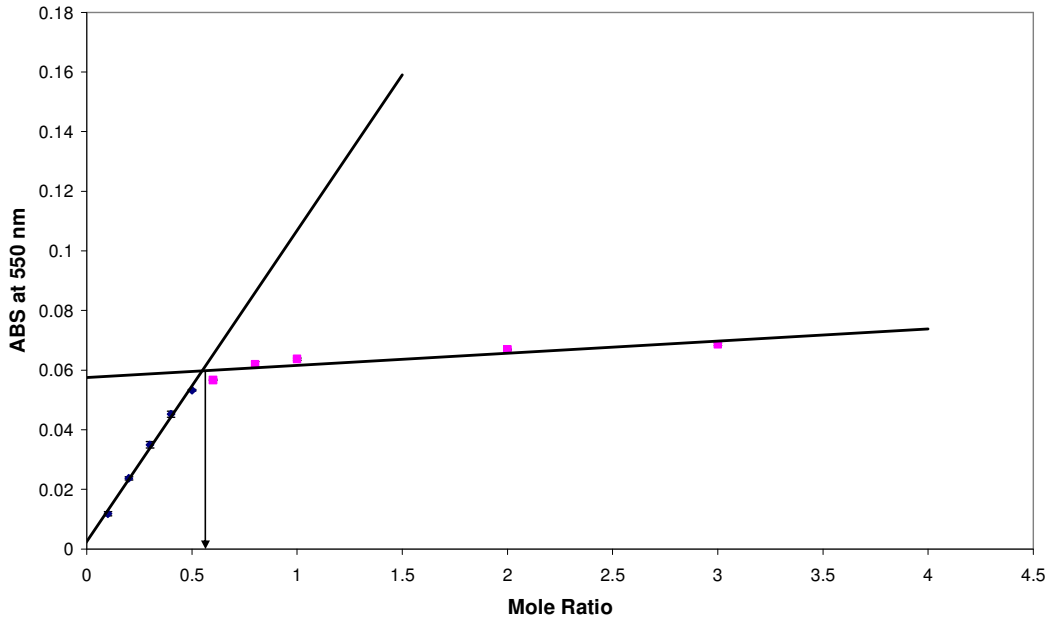

Fig. 4.18 Mole Ratio plots of 50 µM genistein vs. 5 to 300 µM Fe(III) in methanol.

The mole ratio plot of Fe(III) biochanin A gives a value of 0.55 ± 0.02 meaning that there is a stoichiometry of 1 mole of Fe(III) to 2 moles of biochanin A. The Fe(III) genistein mole ratio plot is in agreement with this result giving a mole ratio of 0.55 ± 0. This result agrees very well with the literature on Fe(III) flavonoid complexes [95], confirmed by 1:1 and 1:2 M/L stoichiometries reported for Fe(III) quercetin complexes. The main chelation sites for quercetin that have been identified are at the 3-hydroxy/5-hydroxy and 4-oxo groups and the catechol moiety [95]. The stoichiometry of the Fe(III) biochanin A/genistein complex at 1:2 M/L may be indicative that the complexes are chelating at the 4-keto(oxo) and the 5-OH site.

The Job plots below were used to confirm the stoichiometry of the copper and iron chelates of biochanin A and genistein. Their peaks were recorded respectively at 376 nm for the copper chelates and 550 nm for the iron chelates. The mole fraction maximum relative to the isoflavones in all cases was 0.6 indicating a stoichiometry of 1:2 M/L. This concurs with the observations that were made in the mole ratio studies previously and therefore, this is the stoichiometric mix that will be used in further synthesis of the chelates in methanol.

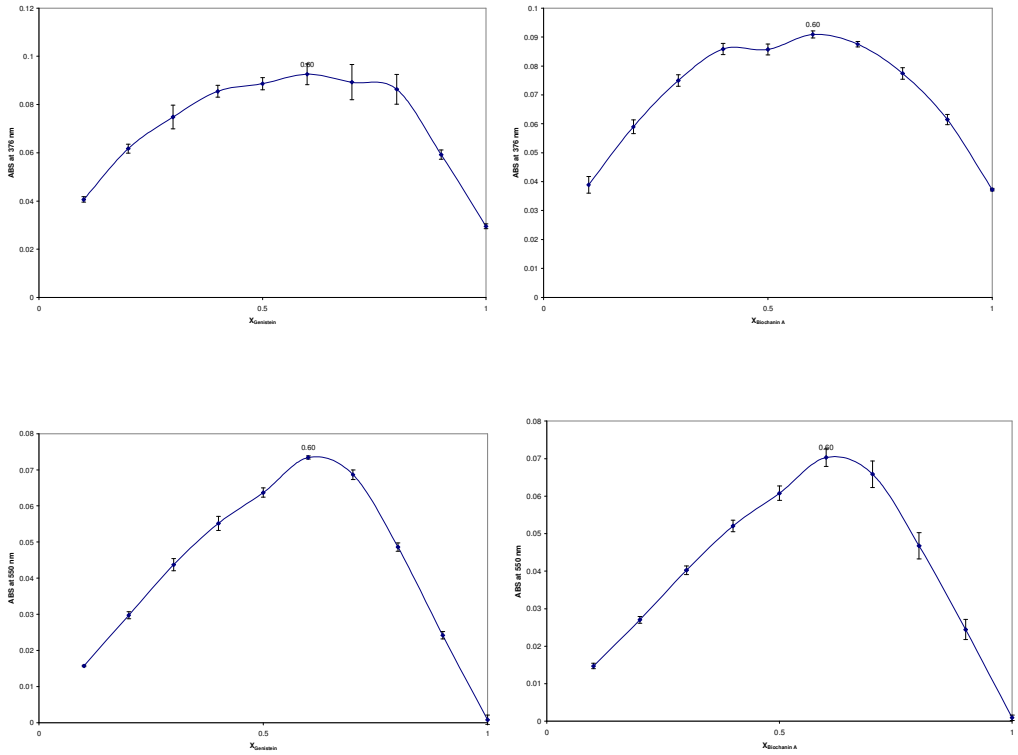

Fig. 4.19 Job plots of Cu(II)genistein (top right), Cu(II)biochanin A (top left), Fe(III)genistein (bottom right), Fe(III)biochanin A (bottom left)

The job plot method has already been used for investigation of metal flavonoid stoichiometries such as by de Souza *et al.* when looking at 3-hydroxyflavone with copper [84]. They hypothesized from a mole fraction value (relative to the flavonoid) of 0.5 that the stoichiometry was 1:1. These results were obtained in pure methanol but the 3-hydroxyflavone differs from genistein and biochanin A by having an OH group solely on the 3-Carbon position and nowhere else. This may account for the varying stoichiometry.

The mole ratio data was mapped out at pH's of 4, 6 and 9 with 6 being the suggested optimal pH for most flavonoid metal chelate species and pH 4 and 9 being near the limits of stability of most metal flavonoid chelates. Anything outside the range of pH 3-10, normally results in destabilization of the flavonoid metal chelates (See Table 4.6) [10].

Table 4.6 Mole ratio values (M/L) of metal chelates of biochanin A and genistein measured at different pH's. n =3 replicates. (Refer to table 4.7 for more detailed breakdown of replicates)

Name	*pH 4*	*pH 6*	*pH 7.3*	*pH 9*
Cu(II) biochanin A	1.11±0.02	1.19±0.03	0.56±0.01	0.60±0.01
Fe(III) biochanin A	0.59±0.02	0.58±0.01	0.55±0.02	1.10±0.06
Cu(II) genistein	1.25±0.06	1.08±0.06	0.54±0.01	0.66±0.02
Fe(III) genistein	0.6±0.03	0.59±0.01	0.55±0	0.95±0.01

The biggest fluctuations in mole ratio value can be seen for Cu(II) chelates ranging from 1 to 0.5 in the pH range of 4-9. The Fe(III) biochanin A metal chelate stays relatively constant until it reaches more basic pH's such as pH 9.0 where it undergoes a complete inversion of stoichiometry from 1:2 to 1:1 M/L. This kind of M/L ratio variation has been observed by groups like Torreggiani *et al.* [87] who claimed that the chelation of Zn(II) with catechin was influenced by pH which dictated the M/L ratio. The group also found that at pH's close to the pKa of catechin, no chelation of Zn(II) would take place whatsoever with noted increasing chelation power with increasing pH past a pKa of 8.5. The only other hydroxy group that is susceptible to deprotonation is the 7-OH group when the pH is between 7.2-10 [203] but this would not agree with previously established information on chelation sites in flavonoids [82,93]. It would, however give some explanation as to why the M/L ratio for Cu(II) biochanin A is 1:1 at pH's 4 and 6.

The unusual thing about the Fe(III) biochanin A metal chelate at pH 9.0 is that it forms a red precipitate. This has not been observed with most of the other biochanin A metal chelates. This is possibly attributable to the formation of iron hydroxide ($Fe(OH)_3$)in solution with the heightened OH^- concentration, from NaOH, as iron hydroxide forms a red precipitate [210]. This makes UV/Vis spectroscopic determination more difficult at the higher concentrations of Fe(III) and decreases the signal to noise ratio. This could prove problematic for accurate determinations of mole ratio for future studies at extremely basic pH's for isoflavone iron chelates. The

reason for the 1:1 M/L stoichiometry of Fe(III) may be due to biochanin A having the same pKa as genistein [206] and would deprotonate in the same fashion. Genistein tends to lose a 7-OH group when the pH exceeds it's pKa of 7.2 but is less than 10. This could be the same with biochanin A and would mean that there is a possibility of the Fe(III) metal ion complexing at this site [208]. This would at least partially explain what is being observed.

Table 4.7 Mole ratio values (M/L) metal chelates of Biochanin A and Genistein measured at different pH's

Name	pH	Mole Ratio R1	Mole Ratio R2	Mole Ratio R3	Mole Ratio average	STDEV	%RSD
Cu(II) biochanin A	4.00	1.09	1.11	1.14	1.11	0.02	2.22
Fe(III) biochanin A	4.00	0.60	0.58	0.61	0.59	0.02	2.76
Cu(II) genistein	4.00	1.26	1.30	1.19	1.25	0.06	4.67
Fe(III) genistein	4.00	0.57	0.63	0.59	0.60	0.03	4.60
Cu(II) biochanin A	6.00	1.20	1.16	1.21	1.19	0.03	2.16
Fe(III) biochanin A	6.00	0.60	0.58	0.58	0.58	0.01	1.83
Cu(II) genistein	6.00	1.15	1.03	1.05	1.08	0.06	5.86
Fe(III) genistein	6.00	0.60	0.59	0.58	0.59	0.01	2.09
Cu(II) biochanin A	7.30	0.56	0.55	0.57	0.56	0.01	1.82
Fe(III) biochanin A	7.30	0.57	0.53	0.55	0.55	0.02	3.09
Cu(II) genistein	7.30	0.54	0.55	0.52	0.54	0.01	2.02
Fe(III) genistein	7.30	0.55	0.55	0.54	0.55	0.00	0.78
Cu(II) biochanin A	9.00	0.62	0.60	0.59	0.60	0.01	2.37
Fe(III) biochanin A	9.00	1.17	1.05	1.08	1.10	0.06	5.70
Cu(II) genistein	9.00	0.64	0.66	0.68	0.66	0.02	3.23
Fe(III) genistein	9.00	0.96	0.94	0.96	0.95	0.01	0.94

A triplicate study was performed to establish the validity of the stoichiometry values taken from UV/Vis studies of biochanin A/genistein chelates at pH 6.0 (ideal pH for formation of flavonoid metal chelates) and 7.3 (unadjusted pH of methanol). As can be seen from the above table, most of the values are within acceptable parameters with the RSD range being 0.78-5.86% indicating good precision.

4.3.2.2 Daidzein metal chelates

Mole ratio studies were also performed for daidzein metal complexes at pH's of 4 and 9 for both Fe(III) and Cu(II). This was done using the same parameters that were utilised for biochanin A and genistein.

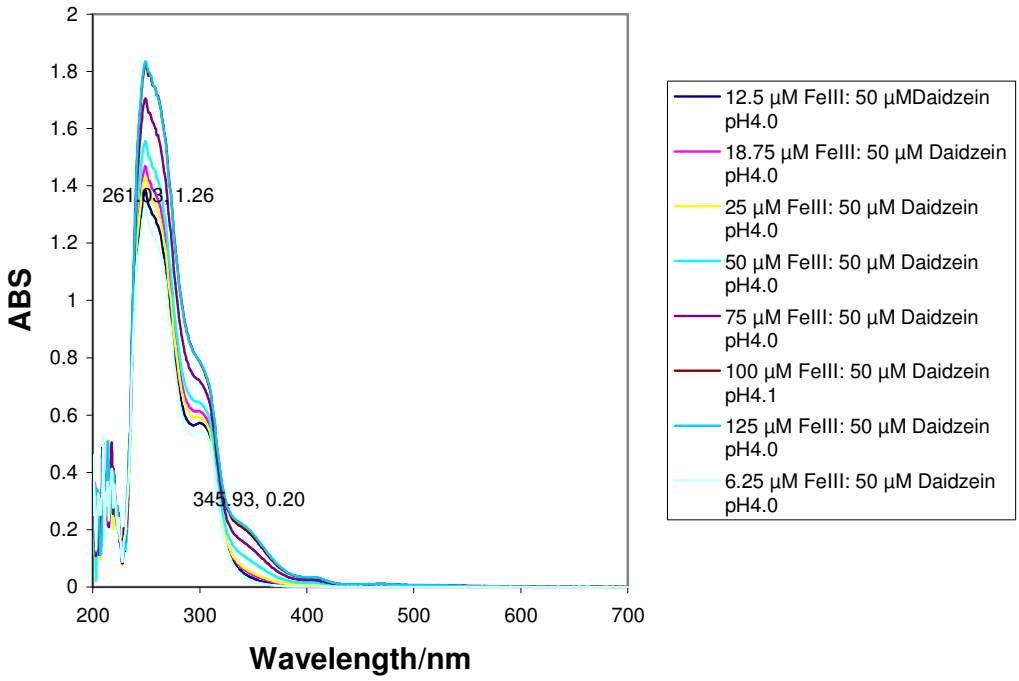

Fig. 4.20 UV/Vis spectroscopy overlay plots of 50 µ M daidzein versus 6.25 µM to 250 µM Fe(III) at pH 4.0 in methanol.

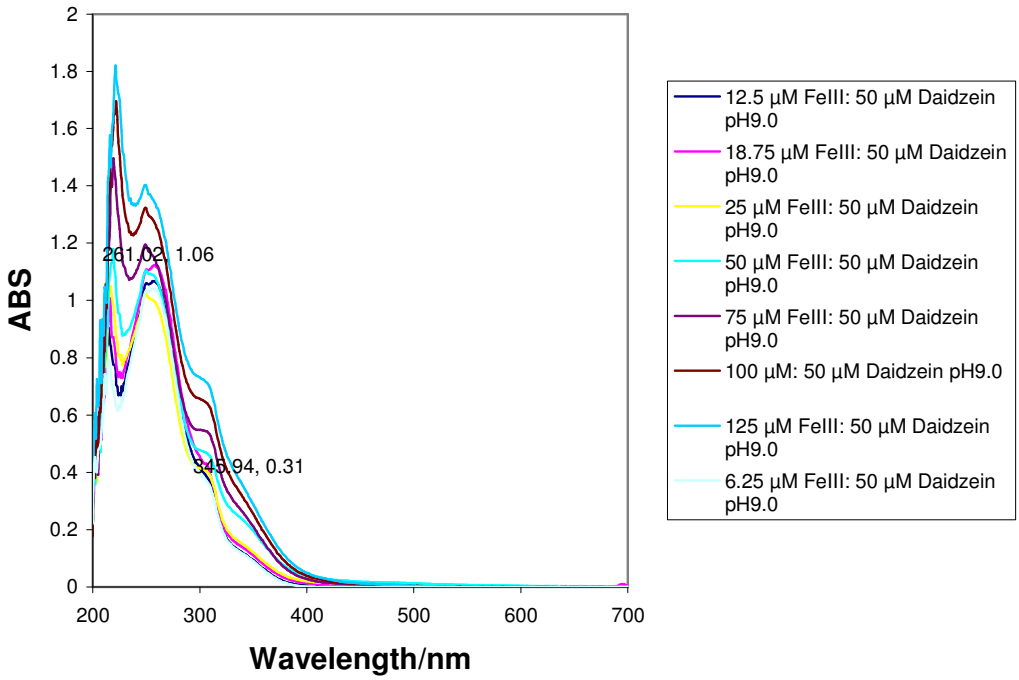

Fig. 4.21 UV/Vis spectroscopy, overlay plots of 50 µ M daidzein versus 6.25 µM to 250 µ M Fe(III) at pH 9.0 in methanol.

There is no band evident at 550nm for daidzein Fe(III) which would result from a bathochromic shift associated with successful isoflavone metal chelation (see fig. 4.20). This is also reflected by the lack of any colour change during sample preparation of the complex at both pH's.

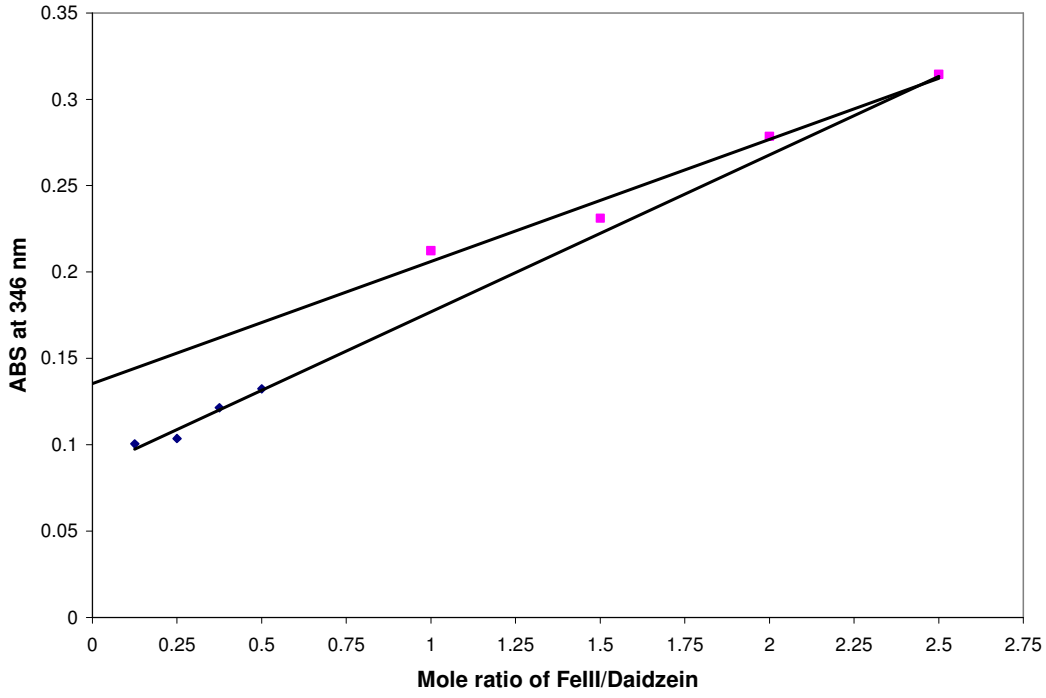

Fig. 4.22 Mole ratio plots of 50 µM daidzein versus 6.25 µM to 125 µ M Fe(III) at pH 9.0 in methanol

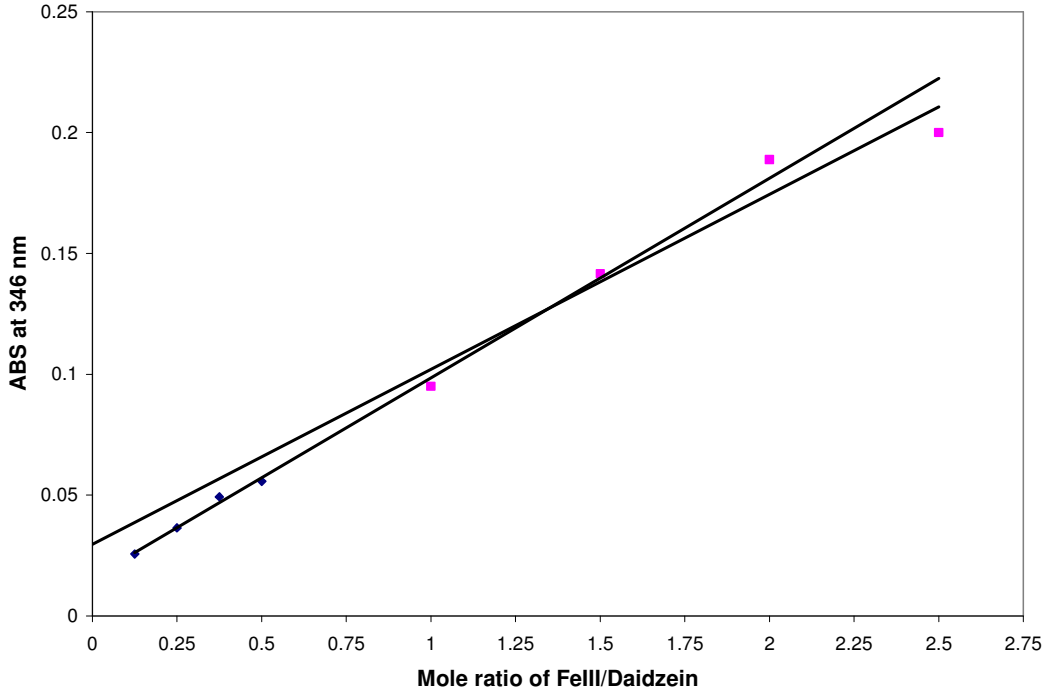

Fig. 4.23 Mole ratio plots of 50 µ M daidzein vs. 6.25 µ M to 125 µ M Fe(III) at pH 4.0 in methanol

The lack of a point of inflexion and no distinctive tangent for the daidzein:Fe(III) mole ratio plots at pH 4.0 and 9.0 further verifies that there is no metal-ligand interaction (see fig. 4.22 and 4.23). This reflects a poor chelating ability for daidzein with Fe(III). This would suggest that deprotonation of daidzein occurs beyond a pH of 7.54, the pKa of the 7-OH group on daidzein.[211] This would imply that there is a need for the metal to chelate with the 4-keto, 5-OH site on an isoflavone before it can allow chelation with metals on the 7-OH group.

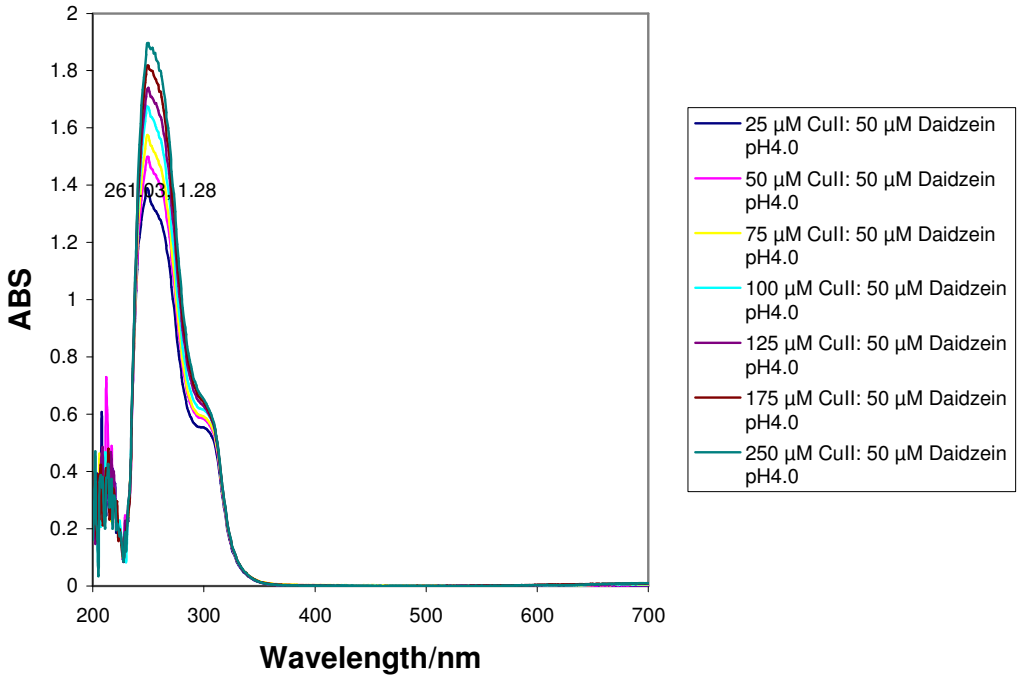

Fig. 4.24 Mole ratio plots of 50 µM daidzein versus 25 µM to 250 µM Cu(II) at pH of 4.0 in methanol

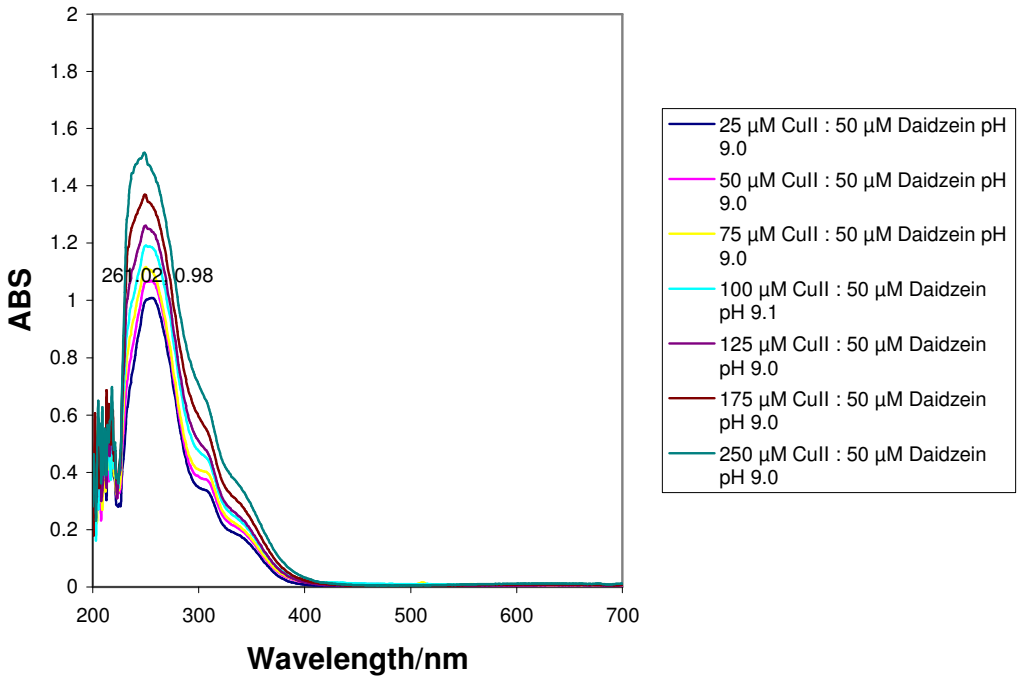

Fig. 4.25 Mole ratio plots of 50 µM daidzein versus 25 µM to 250 µM Cu(II) at pH 9.0 in methanol.

There was also no sign of a distinct band at 376nm for Cu(II) daidzein as was the case for biochanin A and genistein at pH 4.0 and 9.0 (see fig. 4.17). Additionally, there was no colour change observed for the Cu(II) daidzein complex solution at either of these pH's further confirming this observation.

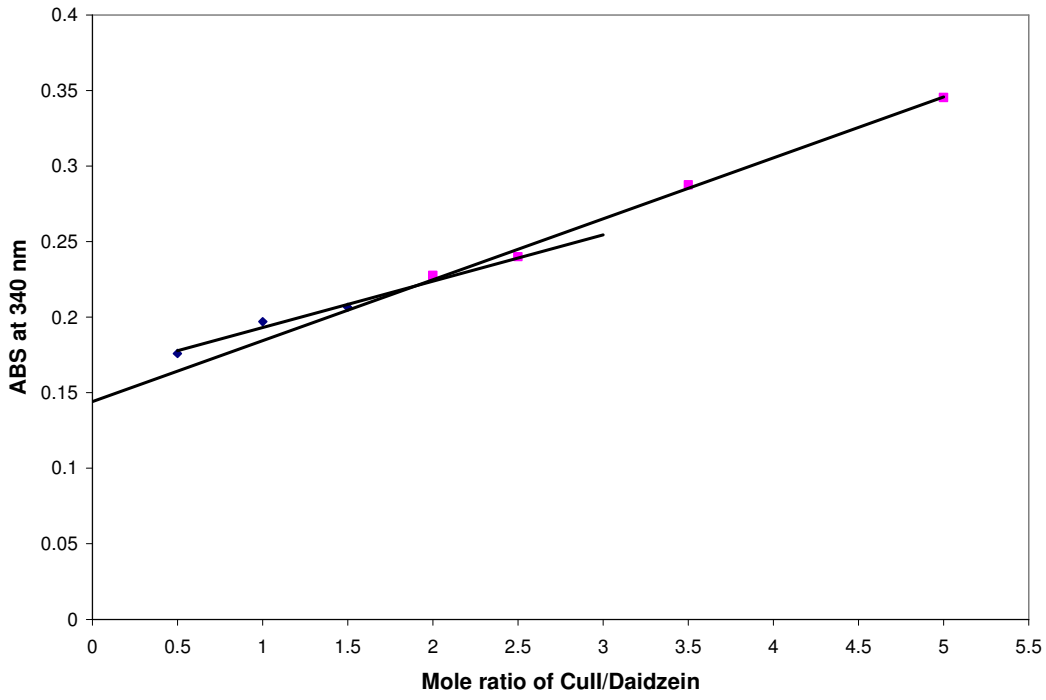

Fig. 4.26 Mole ratio plots of 50 µ M daidzein versus 25 µ M to 250 µM Cu(II) at pH 9.0 in methanol.

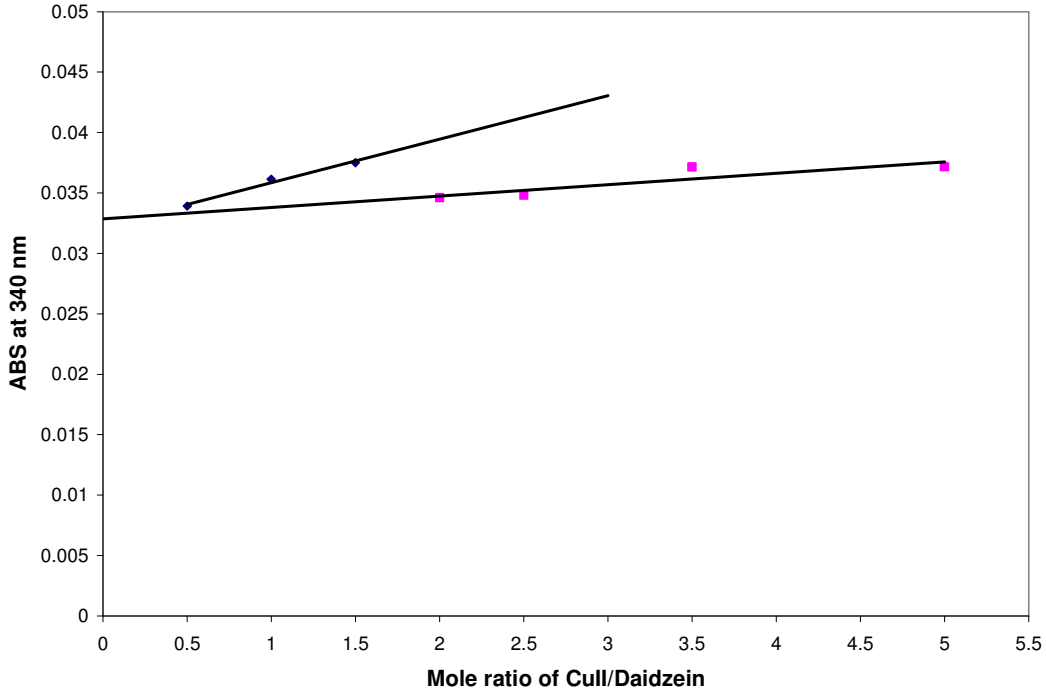

Fig. 4.27 Mole ratio plots of 50 µM daidzein versus 25 µ M to 250 µM Cu(II) at pH 4.0 in methanol.

There were also no isoflavone metal chelation for Cu(II) daidzein at pH 4.0 and 9.0 (see fig. 4.26 and 4.27). This reflects a poor chelating ability for daidzein with Cu(II). This has been observed before by Kuo *et al.* [212] who stated that genistein and daidzein did not chelate with Cu(II) and Fe(III). Kuo did find that flavonols such as quercetin and kaempferol did have the ability to chelate. These flavonols possess 4-keto, 5-OH groups as well as the 7-OH functionality. This chelation site is not present in daidzein and is proving an inhibitory factor to it being chelated by the metals Cu(II) and Fe(III).

4.5 Conclusion

The analysis of isoflavone metal chelates indicated that the isoflavones gensitein and biochanin A, a genistein derivative, chelate to Cu(II) and Fe(III) at a pH range of 4.0-9.0. Chelation was not observed for daidzein with the metals studied over this pH range.

Genistein and biochanin A form 1:2 and 1:1 M/L stoichiometries with Fe(III) across a pH range of 4.0-9.0. They also form stochiometries of 1:2 and 1:1 M/L with Cu(II) in this pH range. The Job plot confirmed that the stoichiometries of the chelates are 1:2 for all isoflavone metal chelates in methanol at pH of 7.3.

The Ge(IV) compounds, germanium sesquioxide and germanium dioxide were shown not to chelate with the isoflavones in this study using UV/Vis spectroscopy. This represents a novel result as germanium(IV) compounds have not been chelated with isoflavones before in the current literature.

This body of work also reflects the first stoichiometric study of genistein with Cu(II) and Fe(III) and also biochanin A with Fe(III). The work done here may give others the basis to start successful categorization of stoichiometries of glycosylated or malonyl forms of genistein.

The stoichiometries at a physiological pH value of 7.3 [10] is of particular interest as it gives an *in vitro* appraisal of the M/L ratio of genistein and biochanin A. This information could be of benefit for other researchers trying to carry out in vivo studies of isoflavones with Cu(II) and Fe(III).

Chapter 5: Synthesis and characterisation of isoflavone metal chelates

5.1 Introduction

The synthesis of flavonoid metal chelates has previously been performed with flavonoids such as quercetin, kaempferol and genistein complexed to transition metal species such as Cu(II), Fe(III) and Al(III). Given that there is up to 4000 types of flavonoids and a large number of viable transition metal species capable of binding with these flavonoids, this brings the number of possible flavonoid metal chelates to tens of thousands [10]. This gives a lot of scope for synthesising potential biologically active agents.

Isoflavone chelates of biochanin A (4'-methoxy-5,7-dihydroxyisoflavone) have been synthesised before by Chen *et al.* for Zn, Mn, Cu, Co and Ni [200]. The group did not try other isoflavones such as Genistein or look at Fe, a common metal involved with chelation of all isoflavones. No thermal analysis of their samples was carried out for isoflavone chelate characterisation.

Characterisation of previously synthesised flavonoid metal chelates has involved physical characterisation, elemental analysis, mass spectrometry, UV/Vis, FTIR, ESI-MS, NMR and TGA analysis [78,86,213,214]. These techniques give an appraisal of the structural moieties, molecular weight and the thermal nature of the sample. This data is invaluable in understanding other effects such as identifying therapeutic factors of the sample, e.g. more hydroxyl groups on the flavonoid nucleus means greater antioxidant activity.

The aim of this chapter was to synthesise the isoflavone metal chelates that were identified in the previous chapter and carry out an investigation of their stoichiometries using mole ratio and Job plot methods in methanol. This involved the development of an appropriate synthesis method that will compensate for the thermosensitive nature of the isoflavones [215] and also a purification method that did not compromise the coordinate bond between the isoflavones and the metals. Then the samples were characterised using physical, spectroscopic and thermal analysis techniques.

5.1.1 Synthesis of flavonoid metal chelates

The synthesis of flavonoid metal chelates depends on the flavonoid ligand and the type of metal salt being used to generate the metal chelate. A range of different synthesis techniques can be employed such as mixing or refluxing for a set period of time. The use of rotary evaporation or air drying depends on the nature of the sample and solvent used. Purification can be achieved using water; alcohol mixtures or organic solvents. Vacuum or air drying can be employed after a time [84,214,216].

The synthesis of isoflavone metal chelates is complicated by the thermosensitivity of the ligands as they breakdown in solution meaning that they are unsuitable for refluxing with metal salts. Instead, preparation of the chelates is done by long periods of stirring at room temperature. This method for flavonoid metal chelate synthesis was suggested by Bukhari *et al.* in the preparation of Cu(II)quercetin complexes. They added quercetin for 15 min to methanol and mixed in a stoichiometric amount of copper salt with more methanol for an additional 90 min. This was followed by filtering and room temperature drying of the product followed by washing with t-butanol and vacuum dessication. This synthesis gave good purity levels for the chelates as shown by elemental analysis with variances in the region of 0.2 % [214].

This type of room temperature reaction was also used by Chen *et al.* to synthesise isoflavone metal chelates. They made up the solutions in ethanol using equimolar amounts of isoflavone and metal salt with adjustment to pH 7-8 with triethylamine followed by stirring for 1 h at 40 ^{0}C with addition of the metal salt and then stirring at 60 ^{0}C for 12 h at room temperature and left standing for 2 days. Solids were filtered, rinsed with ethanol and dried under vacuum. The elemental analysis results were good overall with 0.2 to 0.5 % variances seen in the chelates between theoretical and actual values [200].

5.1.2 UV/Vis analysis

The UV/Vis analysis of flavonoid metal chelates is normally done to confirm where the flavonoid is binding within the structure specifically looking at the π-π* transition bands for the flavonoids specifically Band II (240-285 nm) for the A ring and Band I (300-400 nm) for the B ring. These flavonoid metal chelates can be identified by looking at UV band shifts. It is possible to ascertain which ring is responsible for where binding is occurring within the molecule. [10]

UV/Vis analysis was used by Nowak *et al.* for characterisation of Fe(II) and Fe(III) complexes of rutin. They saw bathochromic shifts of up to 45 nm for the iron rutin complexes for band I and up to 258 nm for Band II. They used these shifts as evidence to conclude that the iron was coordinated with the 4-C=O and the C5-OH position on the A-ring and complexes with a 2:1 M/L stoichiometry were most likely binding with the catechol moiety in the C3'-OH and C4'-OH groups on ring B [217].

Cu(II)quercetin complexes have also been characterised in this fashion as carried out by Bukhari *et al.* They noted bathochromic shifting in the case of Band I and Band II at 372 and 256 nm to an isobestic point at 441 nm, a band associated with the formation of the Cu(II)quercetin complex (refer to Fig. 5.1). It was hypothesised that these shifts were due to the Cu(II) ions binding in a 2:1 M/L stoichiometry with the 3-OH and 4-oxo groups on the A ring and binding between the 3',4'-dihydroxy groups on the B ring [214].

5.1.3 ESI-MS analysis

Mass spectrometry of isoflavone metal chelates indicates the stoichiometry of the chelates by looking at the mass to charge ratio (M/Z) and identifying the most abundant molecular ion. The fragmentation data can give information on the presence of any additional groups such as adducts that maybe present around the flavonoid metal chelate itself. [79,80,218]

ESI-MS characterisation was used by Deng *et al.* to look at the formation of Al(III)-flavonoid complexes in solution. Their study looked at Al(III) interacting with flavonoids biochanin A, kaempeferol and quercetin. It was found that the preferred stoichiometry for the majority of the aluminium complexes was 1:2 in a methanol

solvent system. They also deduced that chelation was taking place in the 5-OH and the 4-keto groups in the case of biochanin A. The molecular ion for this complex corresponded to 593 for [AlL_2] [79].

Metal complexation of flavonoids has also been used to improve their detection as documented by Satterfield *et al.* The group reported a one order of magnitude improvement using Cu(II) metal ions in conjunction with flavonoids. They further improved detectability by the introduction of an auxiliary ligand namely 2,2-bipyridine. They used other transition metal species such as Co(II) and Mn (II) but it was found that Cu(II) gave the best results overall [218].

ESI-MS has also been used to evaluate trends in iron and copper chelation as discussed by Fernandez *et al.* They found that a range of stoichiometries were available from 1:1 to 2:3 metal to ligand ratios. It was found more commonly that 1:2 was the preferred stoichiometry for Cu(II) and Fe(III) as these molecular ions showed the greatest relative abundances over the other stoichiometries [80].

5.1.4 TGA analysis

TGA analysis of flavonoid metal chelates is used to ascertain what components of the molecule are being decomposed with respect to time in comparison with a free ligand of the flavonoid. Indicators that the chelate is formed is reflected in increased thermal stability i.e. a higher temperature shift in the TGA profile and the presence of additional decomposition features such as loss of volatile species such as water. [82,214]

Comparison of TGA profiles of flavonoid metal chelates has been utilised by Torregiani *et al.* when her group was comparing thermograms of quercetin, partially neutralised quercetin (Q-Na_2), Cu(II) quercetin complexes of stoichiometries 0.5 and 2 M/L and the copper chloride salt. The group observed that the thermograms were different between the quercetin and its complexes (refer to Fig. 5.1).

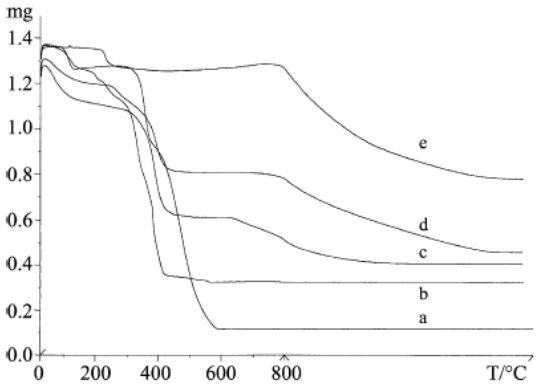

Fig. 5.1 Thermograms of (a.) quercetin (b.) quercetin-Na_2 (c.) Cu(II)-quercetin 0.5 M/L (d.) Cu(II)-quercetin 2.0 M/L and (e.) $CuCl_2.2H_2O$ [82]

The copper complexes stabilised the quercetin ligand as seen by the enhanced decomposition temperatures for their thermograms. The copper chloride salt decomposes at a far higher temperature as most chloride salts are stable at extremely high temperatures. All thermograms show signs of residual mass at the end of the TGA cycle. This was attributed to chlorides or metal oxides [82].

If elemental analysis had been performed upon the flavonoid chelate sample, it would have been possible to identify what parts of the molecule are decomposing at certain steps. Bukhari *et al.* performed TGA analysis on copper quercetin complexes. They found that decompositions from 40 to 200 ^{0}C were due to dehydration of the chelate. Decompositions at further temperatures were attributed to loss of hydrocarbon species. The residue at the end of the TGA cycle was attributed to copper oxide.[214]

5.1.5 FTIR analysis

FTIR analysis of flavonoid metal chelates involves the comparison of a free flavonoid FTIR spectrum with that of a flavonoid metal complex. The spectra are then examined for shifts in functional band assignments such as with the carbonyl and hydroxyl groups. Shifts in these bands can give information in relation to where the metal is binding e.g. carbonyl band shifting would be indicative of binding at a carbonyl group. The formation of new bands such as metal oxide bands can give confirmation that successful chelation has taken place [86,200].

FTIR analysis of Al(III) and Zn(II) complexes of quercetin, rutin and galangin were performed by de Souza *et al.* They characterised the complexes in terms of their C=O, C=C , C-O-C, OH groups and M-O groups. Using these, it was possible to elucidate where chelation of the metals was occurring within the flavonoids. By looking at shifts in the functional bands such as carbonyl band shifting between the free flavonoid and the flavonoid metal complex binding to one of the carbonyl positions is indicated. The appearance of a M-O band around the 630-600 cm^{-1} region would also be indicative of successful complex formation between the flavonoid and the metal in question [86].

The use of FTIR spectra for functional band shifting was also conducted by Chen *et al.* for isoflavone metal complexes of biochanin A whereby they also examined functional bands such as C=O, O-H, and C-OH groups. They noted that the comparison of the spectrum of biochanin A and biochanin A metal complexes exhibited carbonyl band shifting downfield by 8-22 cm^{-1}. The other functional groups showed marginal shifts in all other investigated functional bands. They also noted the appearance of weak M-O bands in the 630-600 cm^{-1} range (Refer to Fig. 5.2) [200].

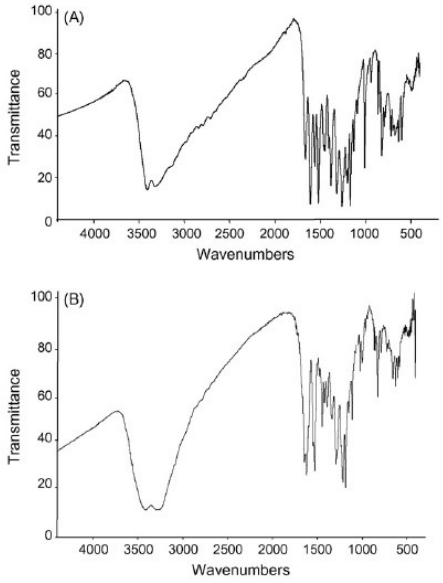

Fig. 5.2 FTIR spectra of A) quercetin and B) Cu(II) quercetin. Note how in Cu(II) quercetin spectrum that the carbonyl group is of greater intensity than that of quercetin [214].

5.1.6 H^1 NMR analysis

H^1NMR analysis of flavonoid metal chelates involves looking at markers such as the disappearance or shifting of proton peaks due to hydroxyl groups. H^1NMR is able to determine what particular hydroxyl group i.e. 3-OH, 5-OH etc bind with these metals. These shifts are normally in the order of >0.5 ppm with shifts below this value generally due to sample variance [78,214]

Copper(II) quercetin complexes were examined by Bukhari *et al.* The quercetin molecule had 5 potential hydroxyl sites where the copper could interact. It was found in their study that the 5-OH group was shifted upfield from δ 12.50 to 11.35 ppm indicating some degree of interaction of the copper ion with the hydroxyl group. The 3-OH group proton signal, however, completely disappeared in the copper quercetin NMR spectrum. This implied the formation of a Cu-O bond between the 3-OH and the copper causing a loss of the H atom, leading to the disappearance of the signal [214].

Other investigations undertaken into flavonoid metal chelates have been conducted by Pereira *et al.* who looked at the H^1NMR spectra of Cu(II) naringin metal complexes. Naringin and the Cu(II) complex have very pronounced differences as the δ values are shifted downfield quite heavily for most cases of the hydrogens when bonded to the metal (Refer to table 5.1). Another key bit of analytical information is the absence of an NMR peak for the 5-OH group indicating that the hydrogen has been lost from this group. This is normally associated with the formation of a coordinate bond between the metal and a hydroxyl group creating an M-O group. The group recommended the use of DMSO as a solvent as opposed to methanol when conducting NMR analysis [78].

Table 5.1 The NMR tables of free naringin and the Cu(II) naringin complex (Complex 1) [78]

Group	Naringin (δ, J)	Complex 1 (δ, J)
OH	11.88(s, 4'-OH s,); 9.51(s, 5-OH)	12.05 (s, 5-OH)
$H_{2'}$,$H_{6'}$	7.17 (d, J = 8.0 Hz)	7.02 (brd, J = 6.6 Hz)
$H_{3'}$,$H_{5'}$	6.64 (d, J = 8.0 Hz)	6.52 (d, J = 7.0 Hz)
H_8	5.94 (d, $J_{H6/H8}$ = 7.0 Hz)	5.78 (d, $J_{H6/H8}$ = 5.5 Hz)
H_6	4.97 (d, $J_{H6/H8}$ = 7.0 Hz)	4.79 (br s)
H_2	5.13 (dd, $J_{H2\text{-}H3A}$ = 4.5 Hz)	5.13 (m)
H_{3A}	4.70 (dd, $J_{H3A\text{-}H3B}$ = 12.0 Hz; $J_{H2\text{-}H3A}$ = 4.5 Hz)	4.70 (brdd, $J_{H3A\text{-}H3B}$ = 12.0 Hz; $J_{H2\text{-}H3A}$ = 4.5 Hz)
H_{3B}	4.8 (dd, $J_{H3A\text{-}H3B}$ = 12.0 Hz; $J_{H2\text{-}H3A}$ = 3.0 Hz)	4.8 (ddbr, $J_{H3A\text{-}H3B}$ = 12.0 Hz; $J_{H2\text{-}H3A}$ = 3.0 Hz)

5.2 Aims

- To synthesise isoflavone metal chelates of biochanin A and genistein using the metals Cu(II) and Fe(III)
- To characterise the chelates using UV/Vis, FTIR, melting point, elemental analysis, TGA, H^1 NMR and ESI-MS analysis
- To postulate the structure of the chelates and the binding sites of the metals on the isoflavone ligands

5.3 Materials and Methods

5.3.1 Chemical and reagents

Genistein (4',5,7-trihydroxyisoflavone) was obtained from LC LABS (Woburn, MA, USA). Biochanin A (4'-methoxy-5,7-dihydroxy-isoflavone) was from Sigma-Aldrich Ireland (Dublin, Ireland). $Fe(III)(NO_3)_3.9H_2O$, and $Cu(II)(NO_3)_2.3H_2O$ metal salts were all analytical grade and were purchased from Lennox Laboratory Supplies Ltd. (Dublin, Ireland). Methanol was of analytical grade and also obtained from Lennox Laboratory Supplies (Dublin, Ireland). All chemicals were used without further purification.

5.3.2 Synthesis of isoflavone metal chelates

Synthesis of the isoflavone metal chelates is based on a method modified from Bukhari *et al.* [214]. Stoichiometric amounts of isoflavone and metal nitrate salt were mixed together i.e. 1:2 M/L for the Fe(III) isoflavone complex and 1:2 M/L for the Cu(II) isoflavone complex. The isoflavone was dissolved in 10 mL of methanol and stirred for 15 min, followed by addition of the metal salt dissolved in another 10 mL of methanol. Additional stirring of the complex solution was done for 90 min. The sample was rotary evaporated to dryness, vacuum filtered on Millipore 47 mm media pads and washed three times with t-BuOH. The samples were vacuum dessicated for 6 h, foil wrapped and stored at -20 ^{0}C until needed.

5.3.3 UV/Vis analysis

2 mg of sample was made up in 10 ml of methanol followed by a 1 in 20 dilution to 10 ppm. Both 200 and 10 ppm solutions were scanned from 200-700 nm at a scan speed of 600 nm/min using quartz cuvettes on a Varian Cary 50 UV/Vis spectrophotometer. A background scan was performed with methanol.

5.3.4 FTIR analysis

The samples were ground in a 1:20 mix with KBr. The sample/KBr mix was compressed at a pressure of 5 tonnes for 4 min on a KBr press using 13 mm die. FTIR spectra were collected in the range of 4000 to 400 cm^{-1}, a resolution of 2 cm^{-1} and 40 scans per spectrum. Background correction was carried out. The FTIR was a Varian 660-IR Mid-IR with a DGTS detector.

5.3.5 TGA analysis

An aluminium pan was tare weighed on the TGA platinum pan. Approximately 5 mg of sample was then measured out onto aluminium pan. The platinum pan was flame heated with a Bunsen to red hotness for 10 s. The parameters were set to a temperature range of 30-600 ^{0}C and a temperature ramp of 5 ^{0}C/min. The analysis was carried out on a TA instruments Q50-0650 TGA system. The data was then exported into ASCII format for excel plotting purposes.

5.3.6 ESI-MS analysis

ESI-MS characterisation was carried out on a Bruker Daltonics electrospray mass spectrometer in positive ion mode for all samples. A 400-800 M/Z range was used for the copper chelates, 400-900 M/Z for the iron chelates and 200-500 M/Z range for the isoflavones. Samples were dissolved in MS grade methanol. Samples were analysed in Dublin City University, Dublin, Ireland.

5.3.7 ^{1}H NMR Analysis

10 mg of sample was measured out for ^{1}H NMR. The sample was then dissolved in 1 mL of d^{6}-DMSO with 0.3 %v/v TMS. The NMR sample tube was analysed on a JEOL ECX-400 NMR system. The NMR system was set to the single pulse analysis profile. The parameters were as follows for the scans:

X frequency: 400 MHz

X offset: 5 ppm

X resolution: 0.7629 Hz or 0.019 ppm

Scans: 8

Range: 25 ppm

5.3.8 Elemental Analysis

Conducted at UCD Microanalytical laboratories, Belfield Campus, D4, Dublin, Ireland.

5.4 Results and Discussion

5.4.1 UV/Vis analysis

The UV/Vis analysis of the isoflavone and the synthesized chelates showed the same bands as seen in the UV/Vis stoichiometric studies of copper and iron with biochanin A and genistein (refer to chapter 4). These studies were performed on the chelates after synthesis to confirm the observations made in the stoichiometry studies in the previous chapter.

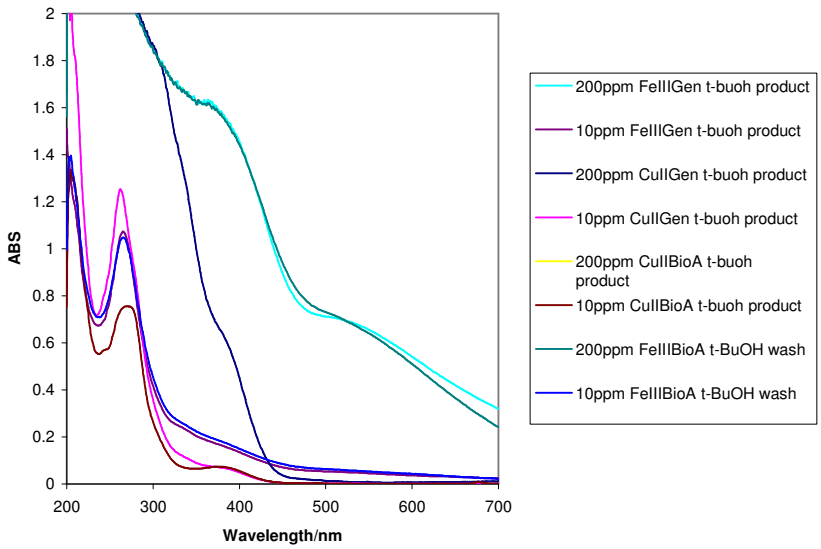

Fig. 5.3 UV/Vis analysis of isoflavone metal chelates at concentrations of 10 and 200 ppm after washing with t-BuOH in methanol.

Presence of the chelates is indicated by the presence of CT bands from 450 to 700nm for the iron chelates and a band at ~ 376nm for the copper chelates (refer to fig. 5.3). The band observed at 376 nm for Cu(II) chelation with biochanin A and genistein could potentially be due to the formation of a new ring system between the metal and oxygen atoms from the 4-keto and 5-OH positions. This is further reinforced by the reduction in intensity of Band I. This trend is also exhibited in Cu(II) quercetin complexes where band I intensity also decreases as was seen by Y. Ni *et al.* The group found that red shifts in Band I for Ring B going from 376 nm to 418 nm coincided with the intensity of the band at 376 nm decreasing in intensity with increasing concentrations of Cu(II) relative to quercetin [219].

The ligand metal charge transfer (LMCT) band at 450 to 700 nm is normally seen in instances where iron flavonoid complexes are successfully formed as observed by Leopoldini *et al.* (refer to fig. 5.4). It was noted that the LMCT band decreased in intensity that was attributable to the modification of d-d transition band, Band I associated again with ring B. The group used this as evidence that the binding primarily occurred at the 4 and 5 carbons and the 3 and 4 oxygens on the B ring or simply the 4 –keto and the 5-OH groups on the B ring [93].

5.4.2 Physical properties of chelates

The iron and copper chelates are coloured black and green respectively, which could infer the presence of metal oxide bonds in the chelates. The colour of the copper complexes was also observed by Pereira *et al.* where they noted the colour of the Cu(II) naringin complex was green for the pure product [78]. Bodini *et al.* noted the appearance of a black precipitate upon the addition of a Fe(III) salt with quercetin in the aprotic solvent, DMSO. This concurs with the black colour of the iron chelates found in these studies although the solid did not precipitate out of solution[220]. All of the copper and iron chelates show melting points in excess of 350 ^{0}C, compared to biochanin A which has a melting point of 210-213 ^{0}C and genistein which has a melting point at 297-298 ^{0}C. The copper and iron salts melt at 114 ^{0}C and 48 ^{0}C. The melting point data concurs well with other literature about flavonoid metal chelates. The melting points of transition metal isoflavone chelates found by Chen *et al.* were in the region of >300 ^{0}C. This contrasts with the M.P. of 213-215 ^{0}C they obtained for the synthesized biochanin A (4'-methoxy-5,7-dihydroxy-isoflavone) [200]. Other observations include those made by Bukhari *et al.* in relation to Cu(II)quercetin complexes where DSC analysis revealed melting points or complete thermal decomposition being in excess of 300 ^{0}C [214]. These results are further confirmed in the TGA section where TGA profiles show thermal decomposition as far as 600 ^{0}C for all investigated chelates (refer to section 5.3.6).

The elemental analysis results were calculated with respect to chelated water being present in the structure of the chelates as the copper and iron nitrate salts are hydrated (refer to table 5.2). The 1:2 M/L stoichiometries agree with %C values in the 50-52 % range for copper chelates and 43 to 45 % range for the iron chelates. The %N levels are resultant from the nitrate ions and are around 1-2 % as only one N atom exists in the structure. The elemental analysis results in general are reflective of the best purities available for the synthesized chelates after repetitive syntheses but are still not of acceptable purity in relation to accepted elemental analysis values being generally ± 0.4% between the actual and the calculated values. The Cu(II) biochanin A elemental analysis results corresponded to a %C of 62.46 and a %H of 3.38 for Chen *et al.* They too had impurity issues with their samples predicted %C level differing by 1.51 % [200]. This was not as varied as the %C gap in our study for Cu(II) biochanin

A, showing a 4.56 % gap between theorized and actual %C values, indicating a certain level of impurity.

Table 5.2: Elemental analysis and melting point results of Copper and Iron chelates of genistein and biochanin A. Theoretical values in brackets.

					Elemental Analysis		
Complex	Colour	M.P./^{0}C	Molecular Formula	Molecular Weight	%C	%H	%N
Cu(II)biochanin A	Brown Green	>350	$C_{32}H_{30}NO_{16}Cu$	748.12	55.94(51.38)	3.75(4.04)	1.85(1.87)
Cu(II)genistein	Green	>350	$C_{30}H_{26}NO_{16}Cu$	720.07	50.52(50.05)	3.23(3.64)	2.57(1.95)
Fe(III)biochanin A	Black	>350	$C_{32}H_{42}NO_{22}Fe$	848.51	47.90(45.30)	3.08(4.99)	3.40(1.65)
Fe(III)genistein	Black	>350	$C_{30}H_{38}NO_{22}Fe$	820.46	45.57(43.92)	3.04(4.67)	3.07(1.71)

The number of water molecules present as adducts for the copper isoflavone chelates based upon the elemental analysis data are 3 water adducts if you take into account that 10 oxygens are due to the 2 biochanin A/genistein ligands and 3 oxygen atoms are due to a nitrate adduct. The iron isoflavone chelates possess 2 waters that are bound to the iron centre of the complex, satisfying Fe(III) octahedral coordination bonding (refer to fig.) and 7 waters exist as adducts to the chelate.

5.4.3 Mid-FTIR spectra

The Mid-FTIR spectra were found to show evidence of chelation of the isoflavones with iron and copper. The -OH groups shows shifts of approximately 200 cm^{-1} for Fe(III) isoflavone chelates and Cu(II) biochanin A with respect to the free isoflavones with the exception of Cu(II) genistein that did not shift at all (refer to table 5.3). Tan *et al.* noted shifting of hydroxyl groups when looking at the flavonoids hesperitin, naringenin and apigenin with Cu(II) which also contained 5-OH groups around their flavonoid nuclei. In the case of the υ(OH) band, there was a wavenumber shift from 3291 cm^{-1} for apigenin to 3413 cm^{-1} indicating binding of the hydroxyl groups [216].

The carbonyl groups show a shift of 8 cm^{-1} for Cu(II) biochanin A, 37 cm^{-1} for Fe(III) biochanin A, 37 cm^{-1} for Fe(III) genistein and no shift for Cu(II) genistein. Why there is no shifting for Cu(II) genistein is not known. There is only one carbonyl group in genistein/biochanin A and this is located in the C ring of the isoflavone. The C-O-C band shows a shift of 6-10 cm^{-1} for Cu(II) and Fe(III) chelates of biochanin A and genisten indicating that binding is occurring on the C ring, at the site of the carbonyl group.

Shifting of the C=O was reported upon metal chelation by Toreggiani *et al.* in the FTIR characterisation of Cu(II)quercetin complexes with binding found at the 4-keto position as indicated by shifting of the υ(C=O) band from 1649 cm^{-1} (quercetin) to 1622 cm^{-1} (Cu(II)quercetin M/L 2). C-O-C bands shifting was also reported by Toreggiani *et al.* in a study of catechin where they saw the υ(O-C) groups shift from 1115 cm^{-1} (free catechin) to 1120 cm^{-1} (Cu(II) catechin) [82,87]. The observed increase in the intensity of the band at 1384 cm^{-1} is due to the nitrate band ions in the chelates resultant from the metal nitrate salts. This is due to asymmetric stretching by the nitrate ion and is normally found to be quite strong [221].

The C-O-H bands show 8 cm^{-1} shifts in the iron and copper chelates of biochanin A while no shifting is seen for the chelates of genistein. This was observed by Ferrer *et al.* in the case of vanadyl quercetin complexes. The bands are seen to shift from 1381 cm^{-1}(quercetin) to 1362 cm^{-1} (VO(quercetin)) and suggested binding with a hydroxyl group and the metal in question [213].

Metal oxide bands of iron and copper are also visible for all chelates involved indicating chelation has occurred. Similar metal oxide bands were observed by Chen *et al.* in their FTIR studies of isoflavone metal complexes. In particular for the Cu(II) biochanin A complex in their study, they recorded a metal oxide band at 582 cm^{-1} [200]. Cu(II) genistein does not show as much shifting in functional bands as the other chelates but does have the presence of M-O/Cu-O band at 567 cm^{-1} and also shifts for the C-O-C band and one OH band would be positive indicators that chelation has taken place.

Table 5.3: Mid-FTIR spectra peak values for biochanin A, genistein and their metal chelates

Biochanin A/cm^{-1}	*Cu(II)biochanin A/cm^{-1}*	*Fe(III)biochanin A/cm^{-1}*	*Genistein /cm^{-1}*	*Cu(II)genistein /cm^{-1}*	*Fe(III)genistein /cm^{-1}*	*Functional group assignment*
3255	3387	3079	3411	3411	3199	vOH
			3102	3178	3210	
1661	1653	1624	1654	1654	1623	vC=O
1625	1623		1616	1616		v ring (A and B)
1584	1568	1559	1570	1570	1513	v(C=C)
	1384	1384		1384	1384	v(NO_3)
1256	1248	1247	1258	1258	1257	v(C-O-H)
1174	1184	1179	1173	1179	1175	v(C-O-C)
	565	539		567	540	vM-O

5.4.4 ESI-MS analysis

The ESI-MS results indicate a 1:2 complex for Cu(II) biochanin A and Cu(II) genistein. The ESI-MS results for the Fe(III) chelates and the M/Z values correspond to chelation between the Fe(III) and the isoflavone ligands. The Cu(II) chelates also display evidence of having a 1:2 M/L stoichiometry as they have M/Z values that correspond to a molecular weight of 2 isoflavone ligands to 1 copper (refer to table 5.4). There is a discrepancy of 2 M/Z units in all M/Z values that could be attributable to loss of 2 hydrogens from the hydroxyl groups of 2 isoflavone ligands deprotonated during chelation. This may possibly be the 5-OH group in the isoflavone structure and would suggest that the site becomes deprotonated during chelation. This was observed by Satterfield *et al.* who noted that deprotonation of the quercetin ligands was noted upon chelation with Al(III), the difference was indicated by 2 M/Z units in a 1:2 M/L Al(III) quercetin complex [218].

The molecular ions for Cu(II) biochanin A agrees with those reported by Chen *et al.* who noted a value of 628.1 M/Z for Cu(II) biochanin A [200]. The fragment ions for the chelates correspond to losses from ions due to CH fragment ions from ionisation of the isoflavone ligands e.g. 602.1 to 507.8 M/Z in the case of Cu(II) genistein and the loss of methoxy (OCH_3) functionalities in the case of biochanin A chelates e.g.

loss of 31 between 599.7 and 568.7 in Fe(III) biochanin A and loss of OH units e.g. loss of 17 betweeen 568 to 551 in Fe(III) biochanin A.

Table 5.4: M/Z ESI-MS molecular ion peaks for the isoflavone metal complexes

Sample	*Molecular ions/M/Z*	*Fragment ions/M/Z*
Cu(II)Genistein	602.1	507.8, 485.7, 468.9, 437.7, 412.6
Cu(II)Biochanin A	630.3	593.5, 412.6
Fe(III)Genistein	594.4	562.9, 485.7, 437.7
Fe(III)Biochanin A	622.5	599.7, 568.7, 551.9

Based upon the previous experimental data and work the literature, Cu(II) and Fe(III) isoflavone metal chelates have a 1:2 M/L stoichiometry. It is probable that the Fe(III) chelates are of an octahedral configuration (refer to fig. 5.4 right), as the electronic configuration of Fe(III) is [Ar] $4s^0$ $3d^5$ in the low spin state, with 2 water molecules (from the hydrated metal salts) bound to the Fe atom. The copper chelates are of a probable square planar conformation (refer to fig. 5.4 left), due to the Cu(II) atom having an electronic configuration of [Ar] $4s^0$ $3d^9$ with no water molecules bound to the Cu atom [80,222]. Binding of the isoflavone ligands to the metal atoms is suspected to take place at the 5-OH and 4-keto sites. This hypothesis is supported by Chen *et al.* where they found a molecular ion of 628.1 for Cu(II) biochanin A in their studies although they did predict 630 M/Z [200].

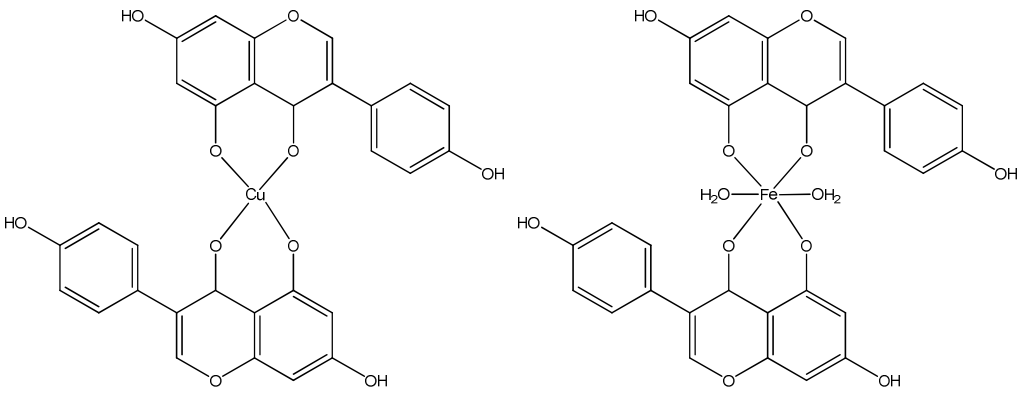

Fig. 5.4 Suggested structural configuration of Cu(II) (left) and Fe(III) (right) chelate of genistein

5.4.5 H^1 NMR analysis

In general, there is chemical shifting within the resolution of 0.019 ppm for any of the H^1 NMR signals of Cu(II) biochanin A/genistein of Fe(III) biochanin A/genistein relative to the free isoflavones. This can largely be held attributable to steadily weakening signals for the metal chelates such as the copper chelates as seen in fig. 5.5 compared to that for genistein proton NMR signal. The signal becomes extremely noisy where the proton peaks are barely distinguishable from baseline noise.

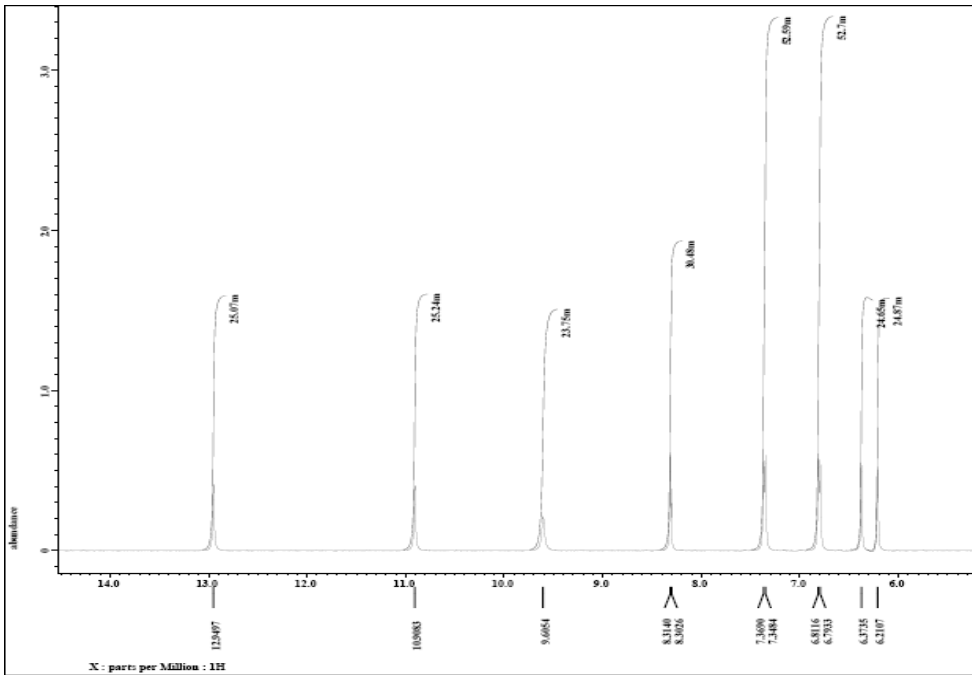

Fig. 5.5 Sample Proton NMR spectra of Cu(II) genistein.

Chen *et al.* showed similar trends in their own H^1 NMR studies of Cu(II) biochanin A versus biochanin A. In particular, they found there was very little peak shifting with the exception of the 6-H proton peak showing an appreciable shift of 0.40 ppm (refer to table 5.5). The reason why they have seen bigger proton peak shifts may be due to the fact that they used a 600 MHz NMR as opposed to the 400 MHz NMR in WIT, affording better resolution of NMR peaks [200].

Table 5.5 Table of values reported by Chen *et al.* for Biochanin A and Cu(II) biochanin A

Proton label	0CH3	6-H	8-H	3',5'-H	2',6'-H	2-H	7-OH
δ Biochanin A chemical shifts/ppm	3.77	6.21	6.37	6.98	7.47	8.35	12.92
δ Cu(II)Biochanin A shifts/ppm	3.71	5.81	6.38	6.98	7.48	8.45	12.89
δ Biochanin A shift difference/ppm	**0.06**	**0.4**	**0.01**	**0**	**0.01**	**0.1**	**0.03**

The proton NMR data for genistein and its metal chelates (refer to table 5.6) in general shows appreciable shifts for the 6-H, 8-H, 2',6'-H and 5-OH groups in the region of 0.03 ppm. The proton peak shift difference is greater than the 0.019 ppm for Cu(II) genistein so the values can be accepted as valid. The biggest shifts are in the 7-OH and the 4'-OH groups. This seems to suggest that there is some degree of binding going on near the 7-OH sites, 4'-OH sites even to some extent with the protons around rings A and B of genistein. The signal for Fe(III) genistein is substantially weakened due to paramagnetic interferences from the unpaired electron in the Fe(III) oxidation state making it hard to apply an RF magnetic field with respect to the iron centre of the complex. Thus, a weak proton NMR signal is obtained.

Table 5.6 Table of proton NMR values for genistein, Cu(II) genistein and Fe(III) genistein

Proton label	6-H	8-H	3',5'-H	2',6'-H	2-H	4'-OH	7-OH	5-OH
Δ Genistein chemical shifts/ppm	6.18	6.34	6.77	7.32	8.29	9.56	10.86	12.92
Δ Cu(II)Genistein shifts/ppm	6.21	6.37	6.79	7.35	8.3	9.61	10.91	12.95
δ shift difference Genistein/ppm	**0.03**	**0.03**	**0.02**	**0.03**	**0.01**	**0.05**	**0.05**	**0.03**
Δ Fe(III)Genistein shifts/ppm	6.21	6.37	6.8	7.36	8.31	9.59	10.88	12.95
δ shift difference Genistein/ppm	**0.03**	**0.03**	**0.03**	**0.04**	**0.02**	**0.03**	**0.02**	**0.03**

The proton NMR data for biochanin A and its metal chelates (refer to table 5.7) in general shows appreciable shifts for the 6-H, 8-H, 2-H and 7-OH groups in the region of 0.03 ppm for Cu(II) biochanin A. The binding does not seem to be localised in the A ring area contrary to the observations of Chen *et al.* [200] who noted shifts for protons associated the A ring. The signal for Fe(III) biochanin A is, again, substantially weakened due to paramagnetic interferences but can be shown to have the greatest shift at the 2-H functionality. This does not give any substantive data to make a determination as regards where binding may occur in Fe(III) genistein.

Table 5.7 Table of proton NMR values for biochanin A, Cu(II) biochanin A and Fe(III) biochanin A

Proton label	0CH3	6-H	8-H	3',5'-H	2',6'-H	2-H	7-OH	5-OH
δ Biochanin A chemical shifts/ppm	3.75	6.19	6.36	6.96	7.47	8.33	10.9	12.9
Δ Cu(II)Biochanin A shifts/ppm	3.77	6.22	6.39	6.98	7.48	8.36	10.93	12.92
δ Biochanin A shift difference/ppm	**0.02**	**0.03**	**0.03**	**0.02**	**0.01**	**0.03**	**0.03**	**0.02**
δ Fe(III)Biochanin A shifts/ppm	3.76	6.21	6.38	6.97	7.47	8.36	10.9	12.91
δ Biochanin A shift difference/ppm	**0.01**	**0.02**	**0.02**	**0.01**	**0**	**0.03**	**0**	**0.01**

Other NMR studies of flavonoids with metals have shown greater shifting of the proton peaks associated with functional groups involved with metal chelation. Le Nest *et al.* studied Zn(II) complexes with quercetin, catechin and other flavonoid derivatives. Their H^1 NMR data revealed shifts for groups such as H6' and H2' indicating binding with CO-4 and OH-3 in relation to kaempferol and tamarixetin. Quercetin was found to display shifting of the protons related to ring C affecting the CO-4/OH-3 groups with further binding found to take place in the OH-3' group on ring B [223].

5.4.6 TGA analysis of samples

TGA analysis of the complexes found that the TGA profiles are radically different between the isoflavone ligands and the complexes (refer to fig. 5.6). Biochanin A and genistein show a loss of carbon between 170-340 ^{0}C. The Cu(II) chelates themselves show loss of moisture around 30-100 ^{0}C This dip corresponds to 8.54 % mass loss for Cu(II) biochanin A and 14.13 % for Cu(II) genistein. The % water based upon table 5.2 values would be 7.23 % for Cu(II) biochanin A and 7.51 % for Cu(II) genistein. This would indicate that there are 3 waters being lost by Cu(II) biochanin A with a small fraction other volatile impurities in this range and Cu(II) genistein it seems there are more volatile impurities than the 3 waters predicted via CHN elemental analysis. This may be due to residual solvent present in the sample or some other solvent contaminant. This could account for the disparity in the theoretical and actual values of the CHN analysis. There are signs of carbon loss from 200-400 ^{0}C. Their % weight keeps dropping right to the end of the run at 600 ^{0}C indicating that more decomposition would take place after this temperature. Cu(II) flavonoid complexes also exhibit this trend as noted by Bukhari *et al.* with Cu(II) quercetin complexes. They noted that most of the decomposition for their copper chelates was present in the range of 59-480 ^{0}C, similar to the copper isoflavone chelates in this study. Also, they saw signs of water loss in their TGA profiles for the complexes [214].

The Fe(III) chelates show very steady thermal decomposition profiles with loss of water in the 30 to 100 ^{0}C range. The dips are 11.07 % for Fe(III) biochanin A and 12.53 % for Fe(III) genistein. The % water based upon table 5.2 values would be 14.87% for Fe(III) biochanin A and 15.37 % for Fe(III) genistein. This % water figure is based on the 7 water adducts on the iron chelates. The loss of the 2 waters on the iron centre itself would happen at a higher temperature due to the stronger coordinate bonding. The difference of 2 -3 % between the mass loss percentage and % water could be attributable to volatile impurities interfering with the determination at later stages of the TGA decomposition profile.

There is a gradual loss of carbon with a pronounced dip in % weight in the iron chelates at 575 ^{0}C. This would indicate more thermal decomposition could take place at a higher temperature range. These findings concur with the observations that Nowak *et al.* made in relation to their iron rutin complexes. In their studies, they

found loss of crystallisation water of the complexes initially in the 20-190 ^{0}C range with a breakdown of the metal oxide bonds in the complexes with functional group loss in the ligands themselves [217].

The copper and iron nitrate salts show pronounced loss of water initially from 30-100 ^{0}C with further decomposition from 130-230 ^{0}C attributable to nitrate loss. This would indicate the presence of chelated water in the complexes. The presence of water loss on the curves and the noticeably shifted carbon decomposition is in keeping with the findings of de Souza *et al.* with their thermal analysis of flavonoid metal complexes [86]. The thermogravimetric profiles suggest that the complexes are different to that of the metal salts or the ligands alone in terms of their thermal properties. The trend is that the chelates are more thermally stable than the ligands as they decompose at higher temperatures. The copper chelates subsequently decompose at lower temperatures than the iron chelates meaning the iron chelates are more thermally stable. Thus the order of thermal stability is isoflavone ligands < Cu(II) isoflavones < Fe(III) isoflavones. This ties in with the observations of de Souza *et al.* where he notes that free flavonoid ligands such as rutin showed lower thermal decomposition temperatures than that of its copper complexes. In turn, the copper complexes were lower still than that of the iron complexes i.e. 398 ^{0}C (free rutin)<412 ^{0}C (Cu(II) rutin) <420 ^{0}C (Fe(III) rutin) [84].

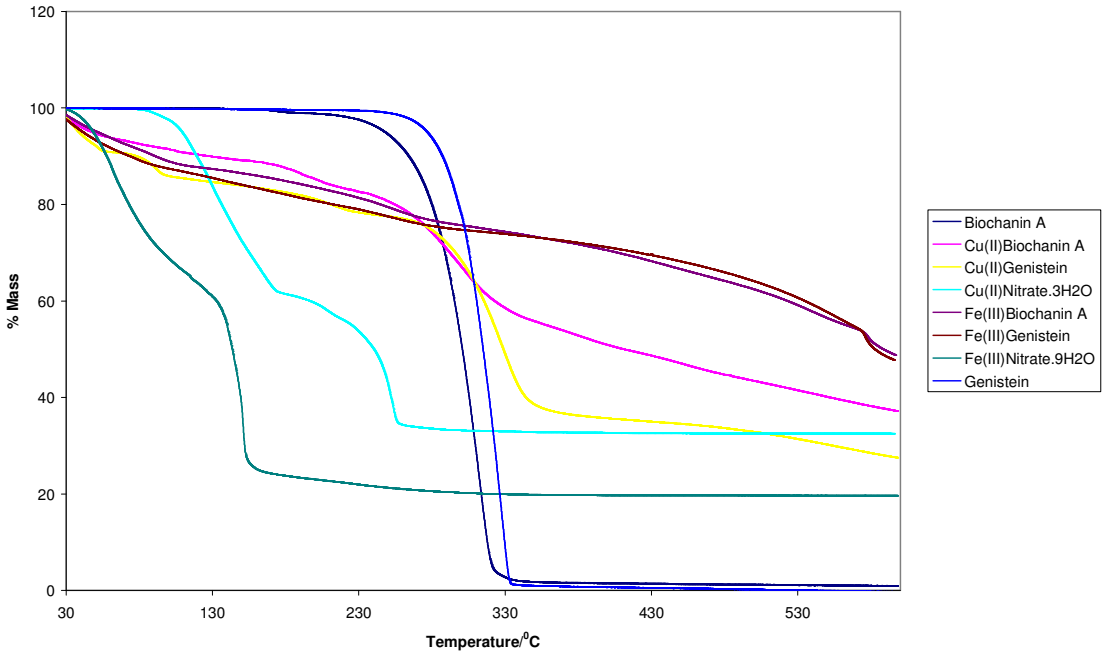

Fig. 5.6 TGA analysis profile from 30 to 600 ^{0}C for isoflavone ligands, metal salts and isoflavone metal complexes.

5.5 Conclusion

The isoflavone chelates synthesized in this chapter represent some of the first isoflavone metal chelates ever synthesized with the exception of Cu(II) biochanin A based upon current literature. Solid samples of the Cu(II) and Fe(III) chelates of the isoflavones can be synthesized using the stirring method. The purity, however, needs improvement for future work with most complexes having under 95% purity levels (based upon the elemental analysis results), the preferable level for most solids synthesized for research. This is compensated by the fact that chelation has taken place and the expected binding sites of the 4-keto and 5- OH group are supported with FTIR and UV/Vis analytical data.

The elemental analysis and ESI-MS shows that the stoichiometry of the chelates is in the region of 1:2 M/L, a point that was explored in chapter 4. The FTIR and UV/Vis analysis in this work clearly indicate that chelation has taken place and the chelation or binding sites are the 4-keto and 5-OH sites.

The melting point and thermal analysis show that metal isoflavone chelates are more thermally stable than the free isoflavone ligands. The H^1NMR data is inconclusive overall with no major proton peak shifts that would give an impression of any binding taking place within the samples. This is attributable to paramagnetic interference i.e. unpaired electrons in the metal atoms are causing signal noise as they do not align well within the magnetic field during scans.

Isoflavone metal chelates represent an area that has plenty of scope for research considering the number of biological properties that can be modulated using metals. This is an area that can be of great interest for enhancing the biological propeties of soya based products (abundant in isoflavones) and the development of novel metal based phytoestrogen compounds for therapeutic applications.

Chapter 6: Characterisation of Antioxidant Properties of Flavonoid Metal Chelates using the DPPH inhibition assay

6.1 Introduction

Flavonoids are polyphenolic in nature and like most polyphenols have inherent antioxidant properties. This can be seen especially for quercetin and kaempferol as they have quite a number of hydroxyl groups present on their flavonoid nucleus compared to some other flavonoid species. Other structural elements in flavonoids can modify its antioxidant activity such as lipophilicity or glycosylation of the flavonoid molecule in a foodstuff matrix. [205,224]

The interaction of flavonoids with transition metals is even more interesting with interactions/chelation with transition metals causing increases or reduction in antioxidant activity via the redox process. The effect of the transition metal on the flavonoid depends on the type of metal interacting with it, the oxidation state, the ratio of metal to the flavonoid and also the site that the metal binds to on the flavonoid [8,84,225].

Characterisation of antioxidant properties of flavonoids can be done by a variety of antioxidant assays and electroanalytical methods. Some of these antioxidant assays include the 2,2-diphenyl-1-picrylhydrazyl ($DPPH^{\cdot}$) inhibition assay and the superoxide dismutase (SOD) assay. Electroanalytical methods are used to characterise the oxidation potentials including cyclic voltammetry.

6.1.1 Antioxidant characterisation of flavonoid metal chelates

Antioxidant characterisation is performed on chemicals that are suspected to have antioxidant properties by assessing their antioxidant activity via *in vitro* assays such as the hydroxyl scavenging assay and the lipid peroxidation assays. Different assays give information on the variety of mechanisms an antioxidant can carry out *in vivo* such as reaction with hydroxyl radicals or stopping the formation of peroxide radicals from iron induced lipid peroxidation [226].

Antioxidant characterisation of isoflavones and their metabolites was performed by Arora *et al.* The study was performed in relation to iron (Fe(II) and Fe(III)) induced lipid peroxidation and also AAPH (2,2'-Azobis(2-amidopropane) dihydrochloride) induced peroxidation in Large Unilamellar Vesicles (LUVs) in a liposomal

environment. It was found with all these studies, that daidzein was a weaker antioxidant than genistein as it lacked the OH group at the 5-C position. The metabolites interestingly were found to have enhanced antioxidant activity compared to the unmetabolised isoflavones. This was found to be due to hydroxyl substitution in the metabolites and gave a better appraisal overall of how isoflavones may behave *in vivo* [227].

Antioxidant activity of flavonoids with iron chelation was assessed by Saskia *et al.* [228] where they used assays such as ABAP (azobisamidinopropane) induced LPO (lipid peroxidation) assays with iron dependent (Fe^{2+}/ascorbate) LPO. All of these assays were performed in microsomal systems. These assays, in general, found minor difference in the antioxidant activity of flavonoids between the iron dependent and independent assays for microsomal lipid peroxidation.

Quercetin has been examined by Chen *et al.* with less common transition metal species such as Cr(III) using the DPPH inhibition assay [229]. Quercetin and quercetin-Cr(III) complexes were compared at equimolar concentrations at various times during the DPPH inhibition incubation. It was found that the Cr(III)-quercetin complex was by far the stronger antioxidant. This can be seen as follows:

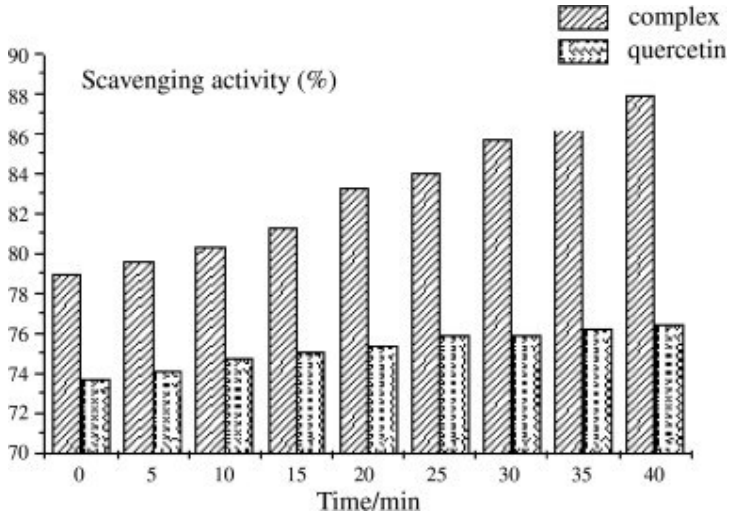

Fig. 6.1 DPPH inhibition study of quercetin versus the quercetin-Cr(III) complex [229]

6.1.2 DPPH inhibition assay

The 2,2-diphenyl-1-picrylhydrazyl ($DPPH^{\cdot}$) inhibition assay was developed by Brand-Williams *et al.* in 1995 as an alternative electron transfer antioxidant capacity study. The antioxidant or extract of interest is prepared in methanol against a volume of $6.0x10^{-5}$ M DPPH solution and the subsequent reduction in absorbance at 515 nm due to the radical in DPPH is monitored. This physically manifests itself as a change from a purple coloured solution to a yellow coloured solution upon complete reduction of the $DPPH^{\cdot}$ by the antioxidant species (AH). [230]

$$DPPH^{\cdot} + AH \rightarrow DPPH\text{-}H + A \qquad \textit{Eqn 6.1}$$

(Purple colour) (Yelow colour)

The measurement of the reduction of the band at 515 nm can be done in real time or after a period of time where the DPPH compound is reduced by the antioxidant where a steady state situation is observed. Thus, there are two variables, the concentration of the DPPH remaining, $[DPPH]_{rem}$ and the concentration of the DPPH prior to the addition of the antioxidant, $[DPPH]_{T=0}$ [8,230,231]. It can be represented as follows:

$$\%DPPH_{rem} = 100 \times \frac{[DPPH]_{rem}}{[DPPH]_{T=0}} \ldots . Eqn.\ 6.2$$

The measurement can also be quoted in terms of %DPPH inhibition by simply subtracting the $\%DPPH_{rem}$ from 100%:

$$\%DPPH_{inhibition} = 100 - \left(100 \times \frac{[DPPH]_{rem}}{[DPPH]_{T=0}} \right) \ldots . Eqn.\ 6.3$$

The DPPH inhibition assay can be applied to an antioxidant solution and analysed via UV/Vis spectrophotometry or, in the case where there are interferences from the antioxidant solution or extract around 515 nm, reversed phase-HPLC-UV/Vis can be utilised additionally as described by T. Yamaguchi *et al.* The HPLC method used an octyl column and a UV/Vis single channel detector at 515nm. The resulting peak from the DPPH (refer to fig. 6.2) was thus well-separated from the food extract overcoming interferences from food matrix components that absorbed around 515 nm. [232]

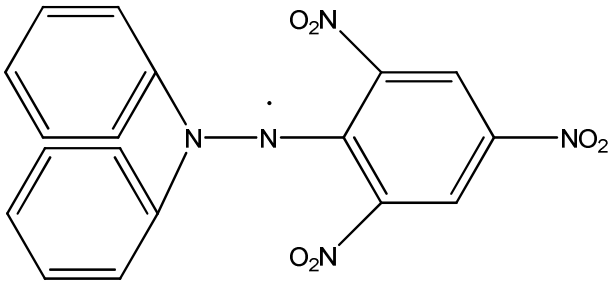

Fig. 6.2 Structure of 2,2-diphenyl-1-picrylhydrazyl (DPPH) [231]

The only disadvantage to the DPPH assay is that not all antioxidants will react in the same manner as they will to peroxyl radicals, as it is a nitrogen radical. This alters the kinetics of a reaction making some antioxidants react slower or become inert in the presence of DPPH where they would previously have reacted with peroxyl radicals. Thus it is important to have another means of assessing antioxidant activity/capacity to cross-reference these findings.[231]

The DPPH inhibition assay has been carried out for flavonoid metal complexes such as VO(IV) hesperidin complexes as investigated by Etcheverry *et al.* They looked at a range of different concentrations of free Hesperidin and Vanado Hesperidin complexes using the DPPH inhibition assay and found that there was no modulation in antioxidant activity from 0 to 100 µM quantities of the molecules. This meant that the therapeutic ability of the complex did not rest with an increase in antioxidant activity. It was found in more extensive biological tests such as cancer cell growth inhibition that the complex did have an effect on cell growth inhibition compared to the free hesperidin, meaning it was more osteogenic than antioxidant [233].

The DPPH assay has also been applied to the antioxidant measurement of germanium enrichment of yeast as researched by Lee *et al.* The yeast was enriched with 6 ppm of germanium dioxide and the germanium yeast complex was measured at concentrations of 10 to 100 $\mu g.L^{-1}$ as well as measuring the controls of germanium dioxide and Yeast. The group found there was no modulation in antioxidant capacity of the yeast as well as no signs of DPPH inhibition by GeO_2 itself [34].

6.1.3 Antioxidant synergism with flavonoid metal chelates

Antioxidant synergism by definition is when the combined antioxidant activity of two or more antioxidants is greater than the sum of the activities achievable by the antioxidants by themselves [234]. This means that the antioxidant properties of a flavonoid can be enhanced by antioxidants outside the flavonoid family such as ascorbic acid to boost the overall antioxidant acitivty of the two antioxidants [235,236]. The application of antioxidant synergism for the body of work in this chapter can see how it would interact with one of the most common antioxidants say if it was ever used in a vitamin C formulation or complemented vitamin C supplementation.

Evidence of synergistic inhibition of isoflavones with ascorbic acid on LDL (low-density lipoproteins) oxidation has been discussed by Hwang et al. The groups used the lag time or the time it took before LDL oxidation reactions proceeded as a comparison of LDL oxidation. Their research saw that the inhibition of LDL oxidation was enhanced with isoflavones and ascorbic acid with distinct increases seen with equol. Genistein saw more significant increases than daidzein [236].

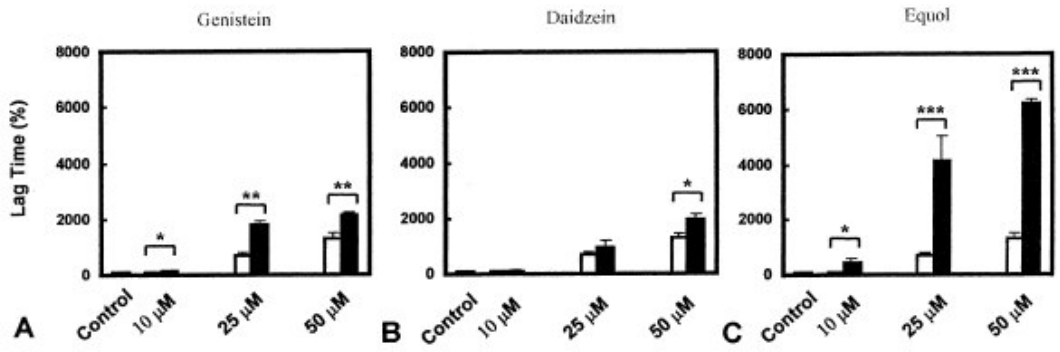

Fig. 6.3 % lag time figures in delaying LDL oxidation for genistein, daidzein and equol in the presence of 50 μM ascorbic acid [236]

De Souza *et al.* performed synergistic studies that focused on looking at solutions of copper, iron, aluminium and zinc with flavonoids such as quercetin. They compared 0.0001 M flavonoid metal chelates and 0.0001 M ascorbic acid solutions and found overall that the antioxidant properties of the chelates could be boosted by up to 50 %.

For example, in the case of Zn(II)Quercetin, it was found that the DPPH scavenging activity was boosted from 64.24 % to 100 % [8].

Wang *et al.* looked at the synergetic effect of metal ions with genistein on the enzyme α-glucosidase, a carbohydrate metaboliser. Inhibition of this enzyme was desired as a means of preventing the glycolysation of HIV (human immunodeficiency virus) type 1 virus, a route to propagation of the virus in the body. They found that α-glucosidase activity was inhibited when metal ions and genistein were added together with IC50 values as low as 1.33 μM for Cu/Genistein solutions. This proved to be much lower than the IC50 values that were achievable using Genistein alone i.e. 18.3 μM and the most inhibitory metal Cu^{2+} at 2.28 μM [235].

6.2 Aims

- To use DPPH inhibition assay to identify the antioxidant activity of stoichiometric mixes of metals and isoflavones
- To use DPPH inhibition assay to identify the antioxidant activity of synthesized isoflavone metal chelates from chapter 5
- To use DPPH inhibition assay for both liquid and solid samples of isoflavone metal chelates with 0.02 mM ascorbic acid for synergistic studies

6.3 Experimental

6.3.1 Chemicals

Genistein was from LC LABS (Woburn, MA, USA), Biochanin A and 2,2-diphenyl-1-picrylhydrazyl were from Sigma-Aldrich Ireland (Dublin, Ireland). The metal salts of $Fe(III)(NO_3)_3.9H_2O$ were from Riedel de Haen and $Cu(II)(NO_3)_2.3H_2O$ from Merck. Methanol was from Merck although purchased through Lennox Laboratory Supplies (Dublin, Ireland)

6.3.2 Instrument

Varian Cary 50 Scan Dual Beam UV/Vis spectrophotometer,
Quartz UV/Vis low volume cuvettes.

The UV/Vis scan parameters were set to 200-700 nm with a medium scan speed or a scan rate of 600 nm/min with baseline correction using makeup solution for sample sets. All files were saved in ASCII format to aid data collation and interpretation.

6.3.3 Method

6.3.3.1 Stock Solution makeup:

Antioxidants (isoflavones, isoflavone chelates, quercetin and ascorbic acid) were made up to 10 mM by dissolving the appropriate amount of isoflavone e.g. 27 mg of Genistein in a 10 mL volumetric flask made up to the mark with methanol. The metal solutions of the iron and copper nitrate salts were made up to 25 mM respectively by dissolving the appropriate amount of metal salt in a 20 mL volumetric flask made up to the mark with methanol e.g. 120.8 mg of $Cu(II)(NO_3)_2.3H_2O$.

6.3.3.2 DPPH inhibition assay for Liquid Samples:

The DPPH inhibition assay was modified from the one suggested by Yamaguchi *et al.* [232] A 1000 ppm solution of DPPH was prepared by dissolving 10 mg of DPPH in 10 ml of methanol. Subsequently, a 40 ppm solution was prepared by transferring 2 ml of the 1000 ppm solution to a 50 ml volumetric flask and filling it up to the mark with methanol. 2 ml of antioxidant solution was pippetted into a 10 ml volumetric flask followed by makeup to the mark with 40 ppm DPPH solution (8 ml). A DPPH blank was made additionally with 2 ml of methanol made up with 40 ppm DPPH solution in a 10ml volumetric flask. All solutions were prepared in triplicate. The solutions were left incubate in a dark cupboard for 1 h. The solutions were scanned on a Cary 50 UV/Vis spectrophotometer under parameters as detailed in section 6.2.2. All the absorbance values at 515 nm were collated and tabulated where DPPH inhibition was determined.

6.3.3.3 DPPH inhibition assay for Solid Samples:

The DPPH inhibition assay was modified from the one suggested by Yamaguchi *et al.* [232] A 1000 ppm solution of DPPH was prepared by dissolving 10 mg of DPPH in 10 ml of methanol. Subsequently, a 40 ppm solution was prepared by transferring 2 ml of the 1000 ppm solution to a 50 ml volumetric flask and filling it up to the mark with methanol. 2 ml of antioxidant solution was pippetted into a 10 ml volumetric

flask followed by makeup to the mark with 40 ppm DPPH solution (8 ml). A DPPH blank was made additionally with 2 ml of methanol made up with 40 ppm DPPH solution in a 10 ml volumetric flask. All solutions were prepared in triplicate. The solutions were left to incubate in a dark cupboard for 1 h. The solutions were scanned on a Cary 50 UV/Vis spectrophotometer under parameters described in section 6.2.2. All the absorbance values at 515 nm were collated and tabulated where DPPH inhibition was determined.

6.4 Results and Discussion

The following sections deal with the antioxidant activity of isoflavone metal chelates. The area of interest is to see if any modulation in antioxidant activity occurs with the isoflavones when chelated. It is expected that the stoichiometric mixes of the metals should show similar antioxidant activity to that of the synthesized chelates. Seeing antioxidant or prooxidant activity of any kind would show some of the first characterizations of isoflavone metal chelates for antioxidant activity making it a novel study in comparison to literature viewed to date.

6.4.1 DPPH UV/Vis spectra of samples

The DPPH assays were collected via spectral acquisition as opposed to just absorbance determinations at 515 nm or the free radical peak (refer to fig. 6.4). This spectral acquisition could account for any hypsochromic or bathochromic shifts of the peak at 515 nm and eliminate absorbance variations due to wavelength shifting. Fig. 6.3 shows a DPPH study with Fe(III) and Cu(II) chelates of genistein and their salts at 1.0 mM concentrations.

Included in the diagram is the DPPH blank for reference purposes. The concentration of DPPH in the blank was 32 ppm (0.08 mM) adjusting for the dilution of the methanol. The absorbance at 515 nm is around 0.8 a.u. (absorbance units). Genistein shows a peak of lower absorbance at 515 nm corresponding to 0.77 a.u. The lower absorbance would indicate it has antioxidant activity as it is reducing the intensity of the radical peak or reducing the radical form of DPPH. This has been observed before with studies of genistein in other types of antioxidant assays yielding appreciable antioxidant activity against free radical species such as peroxides [203,237].

Cu(II) genistein shows even lower absorbance with an average of 0.51 a.u. indicating that it has an antioxidant activity greater than that of genistein on its own. Cu(II) nitrate salt shows little or no reduction of DPPH with an absorbance of 0.81 a.u. overall, the same absorbance as the DPPH blank. Cu(II) is known to chelate with DPPH when reduced to Cu(I) and in certain solvent conditions e.g. chloroform [238] but the lack of wavelength shifting in this instance would not support any chelation

and indicates that the Cu(II) itself is not responsible for any decrease in antioxidant activity observed.

The Fe(III) genistein chelate shows an extremely high absorbance at 1.89 a.u. This trend has been found in other studies.The Fe(III) nitrate salt shows a hypsochromic shift from 515 nm to 494 nm. This would allude to chelation taking place between the DPPH and the free Fe(III). This was further confirmed based on experimental observation which showed that upon addition of Fe(III), the DPPH changed from a purple to a lighter red purple. This was observed by Themelis *et al.* where Fe(III) species were detected using DPPH as a chelation agent. Although DPPH normally binds better with Fe(II) species, the hour incubation time in this assay may have contributed to its ability to bind with DPPH effectively [239]. This effect highlights the importance of spectral acquisition as opposed to single wavelength absorbance determinations as it accounts for "false positives" for DPPH inhibition.

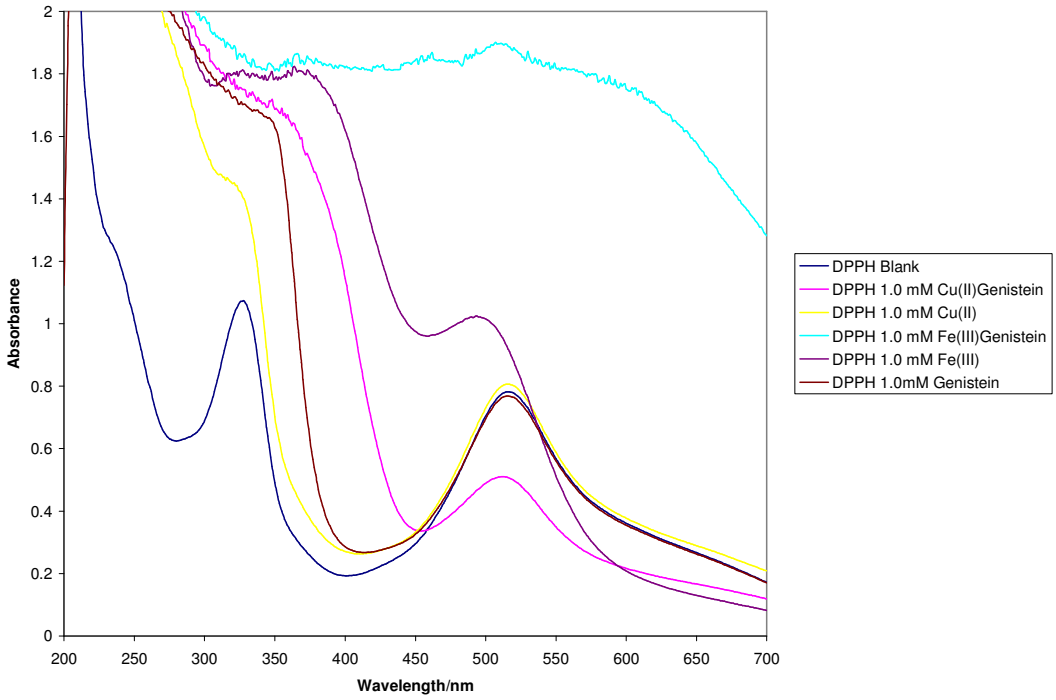

Fig. 6.4 DPPH inhibition plots with genistein, its copper and iron chelates and metal nitrate salts.

6.4.2 DPPH inhibition liquid samples

The DPPH liquid sample studies show that there are reproducible results when stoichiometric concentrations of sample are mixed with each other. The concentration of the isoflavones was maintained at 0.25, 0.5 and 1.0 mM amounts as this was the antioxidant component of the mixture and keeping it consistent would allow greater comparability of the liquid results. The DPPH inhibition studies began first with the use of 2 positive controls namely ascorbic acid and quercetin. Ascorbic acid was selected as it is one of the most powerful polyphenolic antioxidants known [8,240] and quercetin was selected as it is the most powerful known flavonoid with antioxidant properties [8,241]. These showed a relatively complete inhibition of the DPPH solution around 95 to 97 % after an hour incubation period.

The isoflavones biochanin A and genistein showed markedly reduced DPPH inhibition levels indicating significantly lower antioxidant ability (refer to fig. 6.5) from 3.64 to 10.00 % depending on the concentration. This correlates with literature where mild radical scavenging activity has been observed for isoflavones in DPPH assays [242]. Q. Guo *et al.* commented that isoflavones did not have any direct free scavenging activity for DPPH in conjunction with E.S.R studies [243] but did not quote any solvent conditions, an important factor in DPPH studies as it can become DPPH-H in solvents such as ethanol [239].

The Cu(II) chelates showed a 100% increase in antioxidant activity versus the isoflavones from 14 to 32 %. This confirms that Cu(II) does modulate antioxidant activity of isoflavones. This trend is reflected in increasing stoichiometric concentrations of the chelates. Cu(II) chelates of flavonoids in general demonstrate this ability as described by De Souza *et al.* in their own DPPH studies, where they found modulation of DPPH inhibition of 14.66% for rutin and 24.70% for the copper complex of rutin [8]. The Fe(III) chelates show pro-oxidant activity with little or no inhibition, around 0 to 3.3 %, at the lower concentrations with marked increase in pro-oxidant activity or DPPH promotion with increasing concentrations, approx. -21 % to -72 %. Iron flavonoid chelates have also been found in the literature to exhibit little effect overall on antioxidant acitivty [228] but it has been proven with iron chelates that they can stimulate pro-oxidant activity or production of OH radicals in Fenton type reactions [244].

The Cu(II) nitrate salt is showing little or no DPPH inhibition, around 0 to -3 %, but in this instance with no wavelength shifting and thus nothing to confirm this observation. The slight variations are most likely due to statistical error rather than any tangible effect on the DPPH. The Fe(III) nitrate salt shows some degree of inhibition, in the range of 14 to -3 %, but this has been attributed as a false positive. This is because the free Fe(III) ions are binding with the DPPH causing a blue shift of the DPPH spectrum and giving the impression of lowering the absorbance at 515 nm. This was also reflected in an apparent colour change of the DPPH solution to a purple red colour. (Refer to Fig. 6.6) The results show good reproducibility for higher concentration studies as the inhibition levels are substantially higher.

The RSD values become rather high at lower inhibition values (Refer to Table 6.1). The error bars in fig. 6.5 are quite small overall and would give confidence to the integrity of the results.

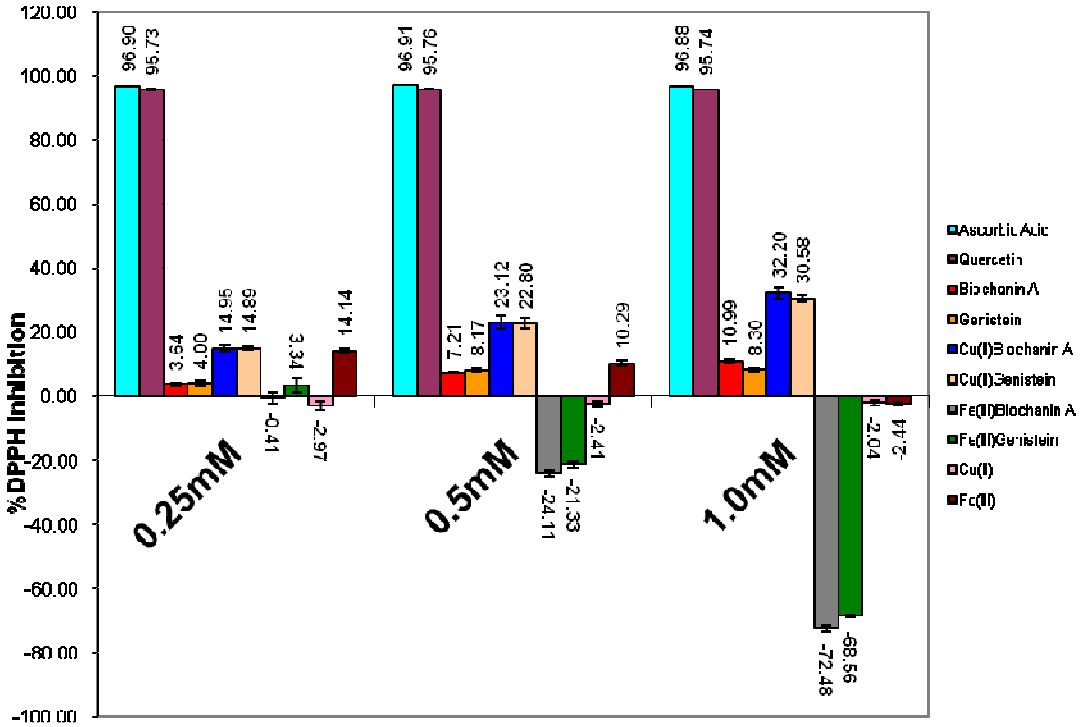

Fig. 6.5 DPPH inhibition studies of liquid samples. Concentrations are indicative of isoflavone concentration. Concentrations of metals are of stoichiometric amounts e.g. 0.25 mM genistein versus 0.125 mM Cu(II) (Standard deviation based on n=3 replicates)

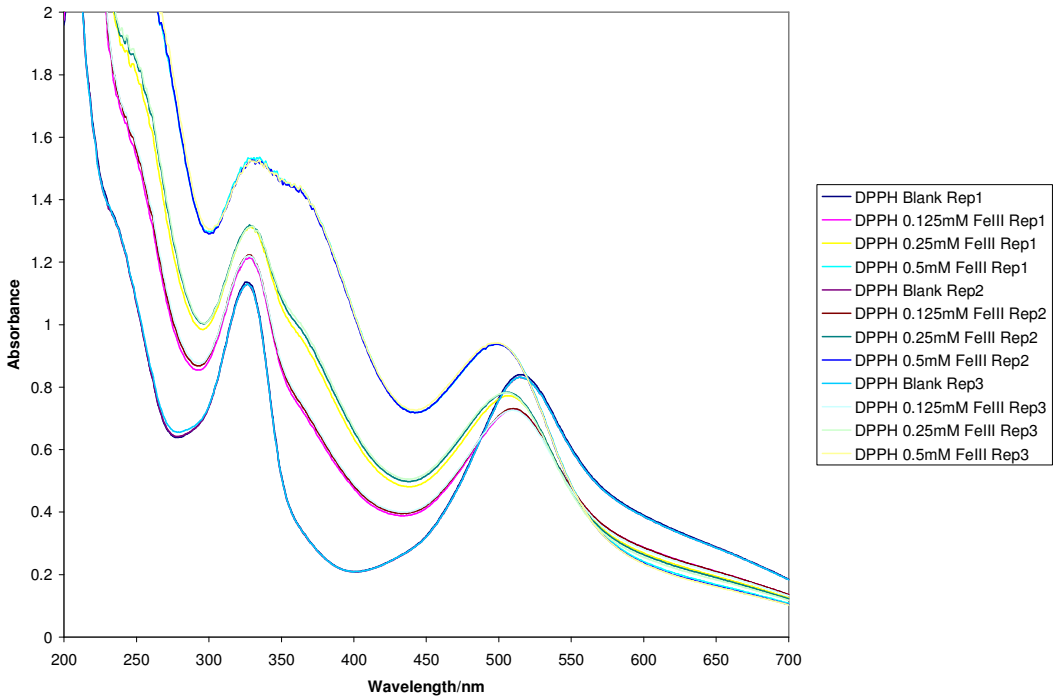

Fig. 6.6 DPPH inhibition study for Fe(III). DPPH with blue shifting increasing with Fe(III) concentration from 515 nm to 497 nm at concentrations of 0.125 to 0.5 mM Fe(III). Blank included for comparison purposes

Table 6.1 DPPH liquid samples studies of isoflavones, isoflavone chelates, metal salts and antioxidant controls (Standard deviation based on n=3 replicates)

Sample name	%DPPH Inhibition Rep1	%DPPH Inhibition Rep2	%DPPH Inhibition Rep3	%DPPH Inhibition Average	STDEV	RSD
DPPH 0.25mM Ascorbic Acid	96.91	97.00	96.78	96.90	0.11	0.11
DPPH 0.50mM Ascorbic Acid	96.92	96.99	96.84	96.91	0.08	0.08
DPPH 1.0mM Ascorbic Acid	96.94	96.83	96.86	96.88	0.06	0.06
DPPH 0.25mM Quercetin	95.63	95.50	96.07	95.73	0.30	0.31
DPPH 0.50mM Quercetin	95.59	95.82	95.88	95.76	0.15	0.16
DPPH 1.0mM Quercetin	95.75	95.65	95.83	95.74	0.09	0.09
DPPH 0.25mM Biochanin A	4.08	3.13	3.72	3.64	0.48	13.22
DPPH 0.5mM Biochanin A	7.47	6.79	7.37	7.21	0.37	5.09
DPPH 1.0mM Biochanin A	10.55	11.46	10.95	10.99	0.45	4.13
DPPH 0.25mM Genistein	3.08	4.39	4.54	4.00	0.80	20.03
DPPH 0.5mM Genistein	7.42	8.52	8.59	8.17	0.66	8.04
DPPH 1.0mM Genistein	7.73	8.66	8.51	8.30	0.50	6.07
DPPH 0.125mM Cu(II) vs 0.25mM BioA	13.89	15.63	15.33	14.95	0.93	6.24
DPPH 0.25mM Cu(II) vs 0.5mM BioA	20.96	23.88	24.53	23.12	1.91	8.24
DPPH 0.5mM Cu(II) vs 1.0mM BioA	30.38	32.45	33.77	32.20	1.71	5.31
DPPH 0.125mM Cu(II) vs 0.25 mM Genistein	14.48	14.72	15.47	14.89	0.51	3.46
DPPH 0.25mM Cu(II) vs 0.5 mM Genistein	21.20	22.72	24.47	22.80	1.63	7.16
DPPH 0.5mM Cu(II) vs 1.0 mM Genistein	29.53	30.47	31.74	30.58	1.11	3.64
DPPH 0.25mM Genistein vs 0.125mM FeIII	-1.68	-1.21	1.64	-0.41	1.80	434.82
DPPH 0.5mM Genistein vs 0.25mM FeIII	-24.84	-24.46	-23.02	-24.11	0.96	3.99
DPPH 1.0mM Genistein vs 0.50mM FeIII	-73.24	-73.13	-71.08	-72.48	1.22	-1.68
DPPH 0.25mM Biochanin A vs 0.125mM FeIII	1.75	2.43	5.84	3.34	2.19	65.71
DPPH 0.5mM Biochanin A vs 0.25mM FeIII	-20.73	-22.17	-21.08	-21.33	0.75	3.51
DPPH 1.0mM Biochanin A vs 0.5mM FeIII	-69.04	-68.51	-68.14	-68.56	0.45	-0.66
DPPH 0.125mM Cu(II)	-3.69	-1.40	-3.84	-2.97	1.36	-45.87
DPPH 0.25mM Cu(II)	-3.37	-1.77	-2.08	-2.41	0.85	-35.11
DPPH 0.5mM Cu(II)	-2.71	-0.99	-2.41	-2.04	0.92	-45.22
DPPH 0.125mM FeIII	14.68	13.46	14.29	14.14	0.62	4.40
DPPH 0.25mM FeIII	11.27	9.49	10.13	10.29	0.90	8.76
DPPH 0.5mM FeIII	-1.97	-2.71	-2.64	-2.44	0.41	-16.77

6.4.3 DPPH liquid samples investigated using DPPH inhibition ascorbic acid synergism

The DPPH liquid ascorbic acid synergism studies reveal some interesting trends. The antioxidant properties of the isoflavone ligands are boosted in the presence of ascorbic acid by 38%, i.e. in the range of 45 to 63 %, indicating synergistic interaction (Refer to Fig. 6.7). The synergistic interaction of ascorbic acid with genistein and daidzein has been reported by Hwant *et al.* in relation to in vitro determinations of LDL oxidation and they found low antioxidant activity for the isoflavones [236].

The Cu(II) chelates show an enhancement of antioxidant properties but do not have the same synergistic interaction as the free isoflavones as they are around 8% lower or in the inhibition range of 33 to 48 %. It is not uncommon for ascorbic acid to bind to Cu(II) chelates. It forms the principle behind a modern antioxidant technique called the Cupric Reducing Antioxidant Capacitiy or "CUPRAC" method whereby a Cu(II)-neocuproine chelate can interact with antioxidants such as ascorbic acid [245].

The Fe(III) chelates show markedly reduced pro-oxidant tendencies with the lower concentration of 0.25 mM showing antioxidant activity albeit reduced in comparison to the other liquid samples by about 20% or in the inhibition range of 20 to -93 %. This was not observed by de Souza *et al.* in their experimental work where they saw a boosting of antioxidant activity of the iron chelate, but the individual antioxidant activities of the iron chelates themselves were quite high before the addition of ascorbic acid [8].

The Cu(II) salts show little or no inhibition in the range of -2.42 to -2.02 %. This is not as expected as the ascorbic acid should show some sort of inhibition. This may have been due to free Cu(II) ions catalyzing the oxidation of the ascorbic acid to such an extent that no antioxidant activity can be seen for Cu(II) ions with ascorbic acid [246]. This would account for the lowered DPPH inhibition of the Cu(II) chelates versus the free isoflavones.

The Fe(III) salts are showing marked antioxidant properties but the inhibition levels decrease with increasing concentrations of Fe(III) in the range of -24.80 to 7.96 %.

This points to some pro-oxidant modulation of the ascorbic acid in the presence of the Fe(III) ions. Normally in the presence of ascorbic acid, Fe(III) can be modulated by ascorbic acid to show enhanced protection against pro-oxidant effects such as lipid induced peroxidation in iron overloaded blood [247].

The RSD values for the data is within acceptable limits for the higher inhibition values but again gets quite high when dealing with low inhibition in general in the 10 to 20 % region (with the exception of Fe(III)biochanin A) but the error bars in general are quite small (Refer to Table 6.2).

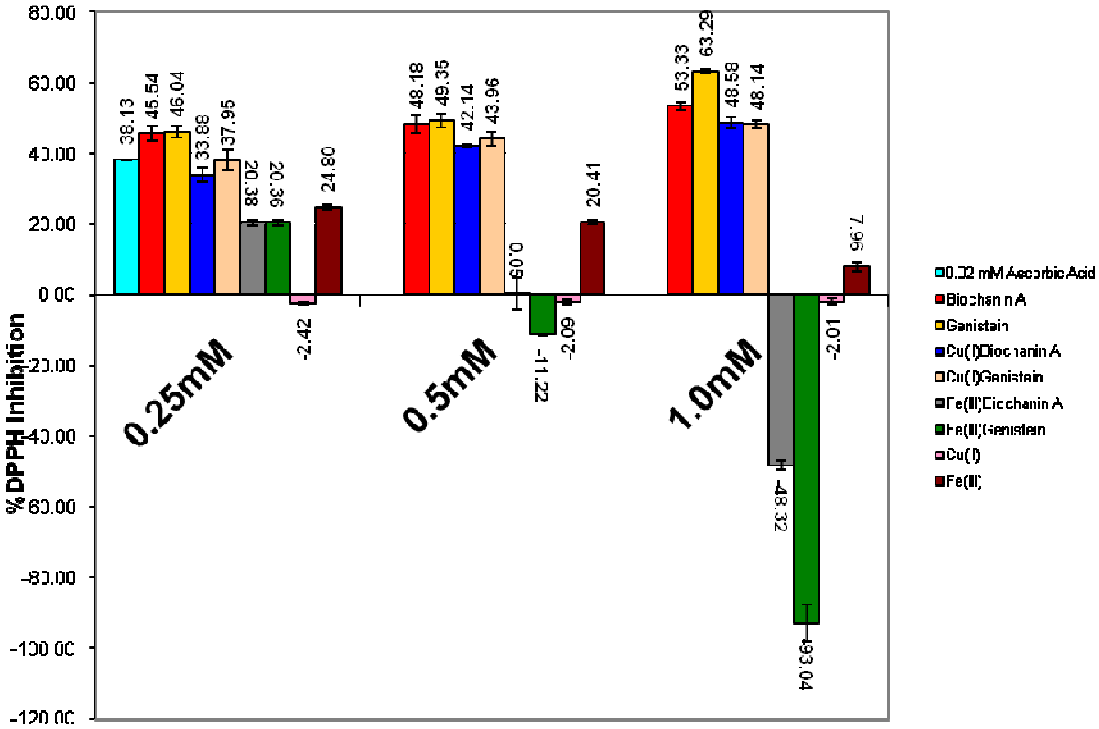

Fig. 6.7 DPPH ascorbic acid synergism inhibition studies of liquid samples. Concentrations indicative of isoflavone concentration. Concentrations of metals are of stoichiometric concentration e.g. 0.25 mM Genistein versus 0.125 mM Cu(II) (Standard deviation based on n=3 replicates)

Table 6.2 DPPH ascorbic acid synergism solid samples studies of isoflavones and isoflavone chelates,.

Sample name	%DPPH Inhibition Rep1	%DPPH Inhibition Rep2	%DPPH Inhibition Rep3	%DPPH Inhibition Average	STDEV	RSD
DPPH 0.25mM Biochanin A with 0.02mM Ascorbic acid	47.28	46.13	43.21	45.54	2.10	4.61
DPPH 0.5mM Biochanin A with 0.02mM Ascorbic acid	47.97	50.82	45.73	48.18	2.55	5.30
DPPH 1.0mM Biochanin A with 0.02mM Ascorbic acid	53.41	52.05	54.54	53.33	1.25	2.34
DPPH 0.25mM Genistein with 0.02mM Ascorbic acid	44.30	46.35	47.47	46.04	1.61	3.49
DPPH 0.5mM Genistein with 0.02mM Ascorbic acid	49.72	47.27	51.05	49.35	1.92	3.89
DPPH 1.0mM Genistein with 0.02mM Ascorbic acid	63.08	63.07	63.72	63.29	0.37	0.59
DPPH 0.125mM Cu(II) versus 0.25mM Biochanin Awith 0.02mM Ascorbic Acid	31.35	34.90	35.38	33.88	2.20	6.49
DPPH 0.25mM Cu(II) versus 0.5mM Biochanin Awith 0.02mM Ascorbic Acid	42.14	41.95	42.32	42.14	0.18	0.44
DPPH 0.5mM Cu(II) versus 1.0mM Biochanin Awith 0.02mM Ascorbic Acid	46.75	49.18	49.81	48.58	1.62	3.33
DPPH 0.25mM Cu(II) with 0.02mM Ascorbic Acid	35.33	37.36	41.17	37.95	2.96	7.81
DPPH 0.5mM Cu(II) with 0.02mM Ascorbic Acid	42.09	43.85	45.94	43.96	1.93	4.38
DPPH 1.0mM Cu(II) with 0.02mM Ascorbic Acid	47.03	48.12	49.26	48.14	1.11	2.31
DPPH 0.25mM Biochanin A vs 0.125mM FeIII with 0.02mM Ascorbic acid	20.24	21.20	19.70	20.38	0.76	3.73
DPPH 0.5mM Biochanin A vs 0.25mM FeIII with 0.02mM Ascorbic acid	-4.67	0.51	4.31	0.05	4.51	9004.28
DPPH 1.0mM Biochanin A vs 0.5mM FeIII with 0.02mM Ascorbic acid	-49.70	-47.54	-47.73	-48.32	1.20	-2.48
DPPH 0.25mM Genistein vs 0.125mM FeIII with 0.02mM Ascorbic acid	21.07	19.54	20.48	20.36	0.77	3.79
DPPH 0.5mM Genistein vs 0.25mM FeIII with 0.02mM Ascorbic acid	-11.17	-11.41	-11.09	-11.22	0.17	-1.49
DPPH 1.0mM Genistein vs 0.5mM FeIII with 0.02mM Ascorbic acid	-87.33	-94.83	-96.95	-93.04	5.05	-5.43
DPPH 0.125mM Cu(II) with 0.02mM Ascorbic Acid	-2.82	-2.24	-2.20	-2.42	0.35	-14.38
DPPH 0.25mM Cu(II) with 0.02mM Ascorbic Acid	-2.44	-2.54	-1.28	-2.09	0.70	-33.43
DPPH 0.5mM Cu(II) with 0.02mM Ascorbic Acid	-2.15	-2.59	-1.28	-2.01	0.67	-33.20
DPPH 0.125mM FeIII vs 0.02mM Ascorbic Acid	24.09	25.23	25.09	24.80	0.62	2.50
DPPH 0.25mM FeIII vs 0.02mM Ascorbic Acid	20.70	19.67	20.86	20.41	0.64	3.16
DPPH 0.5mM FeIII vs 0.02mM Ascorbic Acid	9.17	6.61	8.11	7.96	1.28	16.13
DPPH 0.02mM Ascorbic acid	37.75	39.52	37.13	38.13	1.24	3.24

6.4.4 DPPH inhibition solid samples

The DPPH solid sample assays used molar concentrations of the isoflavone metal chelate samples as determined relative to their molecular formulae in the previous characterisation chapter. The experimental model is similar to that used in the liquid sample studies with the use of positive controls, free isoflavones, isoflavone metal chelates and metal nitrate salts. The trends are also similar but with a few key differences. The genistein and biochanin A isoflavones are still substantially weaker in comparison to the ascorbic acid and quercetin controls (Refer to Fig. 6.8).

The copper chelates, however, show notably enhanced antioxidant properties with an improvement of a few percent over that seen in the liquid studies in the range of 14 to 34 %. The iron chelates also show greater pro-oxidant activity with pro-oxidant acitivity visible as low as 0.25 mM in the range of -23 to -144 %. Additionally, pro-oxidant activity seems to be higher in the case of Fe(III) biochanin A than that of Fe(III) genistein. This trend can be seen for the copper chelates as well with the Cu(II) genistein having greater antioxidant activity than the Cu(II) biochanin A.

The Cu(II) nitrate salt shows little or no inhibition (-0.30 to -1.57 %) as was observed in the previous liquid sample studies, albeit this study would have had greater molar concentrations than that in the liquid studies. The Fe(III) nitrate salt shows DPPH inhibition (17 to -15 %) in the lower concentrations followed by DPPH promotion in the higher 1.0 mM concentration. This was similar to that observed in the liquid studies where the Fe(III) salt is forming a chelate with DPPH. The promotion of antioxidant activity of flavonoids using copper has been reported in numerous publications but to the authors knowledge, this is the first reporting of antioxidant activity of Cu(II) isoflavone chelates. [9,248,249].

The reproducibility of the solid sample studies is acceptable with most figures in the 0-10 % RSD range except for some of the small DPPH inhibition figures. This is confirmed by the small error bars seen throughout the plots giving good confidence for the results in general (Refer to Table 6.3).

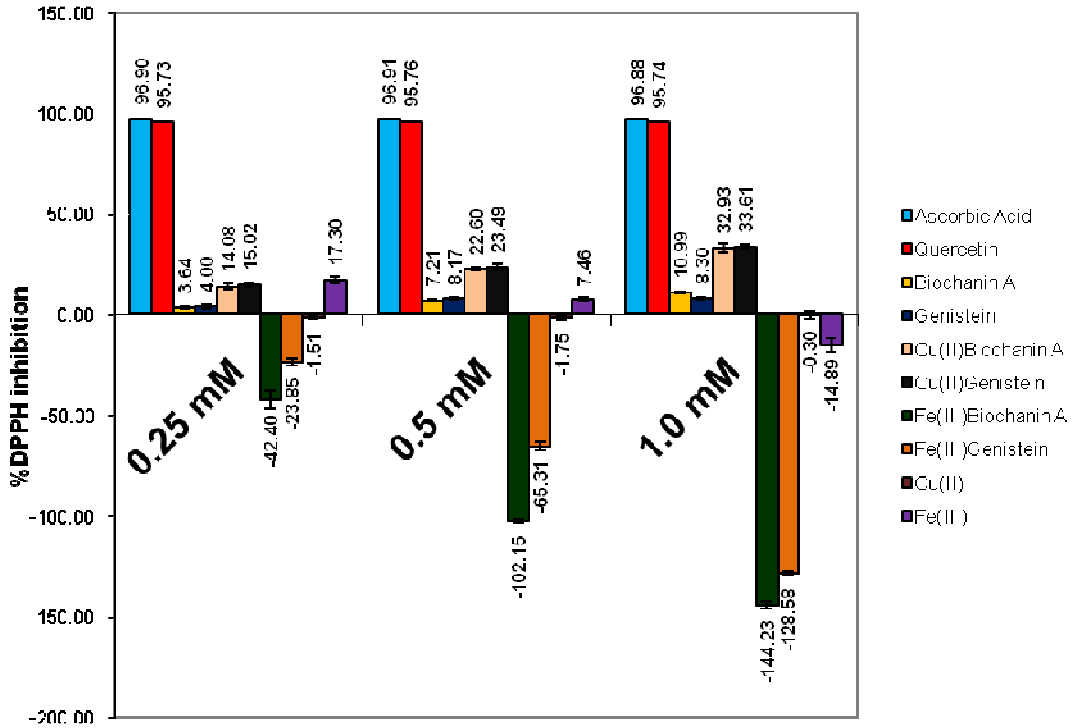

Fig. 6.8 The DPPH inhibition plots of 0.25, 0.5 and 1.0 mM concentrations of isoflavones and their metal chelates (Standard deviation based on n=3 replicates)

Table 6.3 DPPH liquid samples studies of 0.25 to 1.0 mM concentrations of isoflavones, isoflavone chelates, metal salts and antioxidant controls

Sample name	%DPPH Inhibition Rep1	%DPPH Inhibition Rep2	%DPPH Inhibition Rep3	%DPPH Inhibition Average	STDEV	RSD
DPPH 0.25 mM Ascorbic Acid	96.91	97.00	96.78	96.90	0.11	0.11
DPPH 0.50 mM Ascorbic Acid	96.92	96.99	96.84	96.91	0.08	0.08
DPPH 1.0 mM Ascorbic Acid	96.94	96.83	96.86	96.88	0.06	0.06
DPPH 0.25 mM Quercetin	95.63	95.50	96.07	95.73	0.30	0.31
DPPH 0.50 mM Quercetin	95.59	95.82	95.88	95.76	0.15	0.16
DPPH 1.0 mM Quercetin	95.75	95.65	95.83	95.74	0.09	0.09
DPPH 0.25 mM Biochanin A	4.08	3.13	3.72	3.64	0.48	13.22
DPPH 0.5 mM Biochanin A	7.47	6.79	7.37	7.21	0.37	5.09
DPPH 1.0 mM Biochanin A	10.55	11.46	10.95	10.99	0.45	4.13
DPPH 0.25 mM Genistein	3.08	4.39	4.54	4.00	0.80	20.03
DPPH 0.5 mM Genistein	7.42	8.52	8.59	8.17	0.66	8.04
DPPH 1.0 mM Genistein	7.73	8.66	8.51	8.30	0.50	6.07
DPPH 0.25 mM Cu(II)Biochanin A	13.87	14.47	13.09	14.08	1.56	11.05
DPPH 0.5 mM Cu(II)Biochanin A	20.71	22.32	23.85	22.60	0.67	2.98
DPPH 1.0 mM Cu(II)Biochanin A	30.52	31.37	33.62	32.93	2.27	6.89
DPPH 0.25 mM Cu(II)Genistein	14.04	13.39	12.98	15.02	1.11	7.41
DPPH 0.5 mM Cu(II)Genistein	22.04	21.94	23.04	23.49	1.89	8.06
DPPH 1.0 mM Cu(II)Genistein	29.83	32.12	34.48	33.61	1.14	3.40
DPPH 0.25 mM Fe(III)Genistein	-47.23	-41.32	-38.64	-42.40	4.40	-10.37
DPPH 0.5 mM Fe(III)Genistein	-102.58	-102.40	-101.49	-102.15	0.59	-0.57
DPPH 1.0 mM Fe(III)Genistein	-144.49	-142.41	-145.80	-144.23	1.71	-1.19
DPPH 0.25 mM Fe(III)Biochanin A	-25.73	-22.43	-23.40	-23.85	1.70	-7.11
DPPH 0.5 mM Fe(III)Biochanin A	-66.57	-66.48	-62.88	-65.31	2.11	-3.23
DPPH 1.0 mM Fe(III)Biochanin A	-129.54	-127.43	-128.77	-128.58	1.07	-0.83
DPPH 0.25 mM Cu(II)	-1.09	-2.45	-0.99	-1.51	0.81	-54.05
DPPH 0.5 mM Cu(II)	-1.81	-2.63	-0.80	-1.75	0.91	-52.31
DPPH 1.0 mM Cu(II)	1.41	-2.51	0.21	-0.30	2.01	-681.70
DPPH 0.25 mM Fe(III)	16.51	16.01	19.38	17.30	1.82	10.50
DPPH 0.5 mM Fe(III)	7.46	6.20	8.71	7.46	1.26	16.83
DPPH 1.0 mM Fe(III)	-15.43	-18.03	-11.20	-14.89	3.45	-23.14

6.4.5 DPPH inhibition solid samples ascorbic acid synergism

The ascorbic acid synergism studies of the solid samples again are quite similar to what was observed for the liquid DPPH inhibition studies with ascorbic acid. The experimental design is quite similar to that of the liquid samples except it is using specific molar concentrations of solid. The ascorbic acid shows a substantial improvement in antioxidant activity of the free isoflavone ligands (Refer to Fig. 6.9).

The Cu(II) chelates for the solid samples again show the trend of marked reduction in antioxidant activity relative to the isoflavone ligands in the region of 33 to 47 %. The Fe(III) chelates afterwards show notably reduced pro-oxidant behaviour in the presence of ascorbic acid as noted in the DPPH inhibition studies from -6 to -148 %. The Cu(II) salts show complete inhibition from 0.61 to 2.44 % of the antioxidant activity of the ascorbic acid giving further evidence as to why the Cu(II) chelates show poorer antioxidant properties in the presence of ascorbic acid. The Fe(III) nitrate salts again shows antioxidant activity but seem to inhibit the ascorbic acid, from 23 to -7 %. This would suggest that it is having some pro-oxidant effect when in the presence of the ascorbic acid.

The RSD values for the data are good except again when dealing with very small inhibition values where it can be as high 164.75% but the standard deviation is acceptable overall as reflected in the small error bars for the bulk of the data (Refer to Table 6.4). The pro-oxidant activity of iron with biochanin A has been previously noted in antioxidant assays in literature [250].

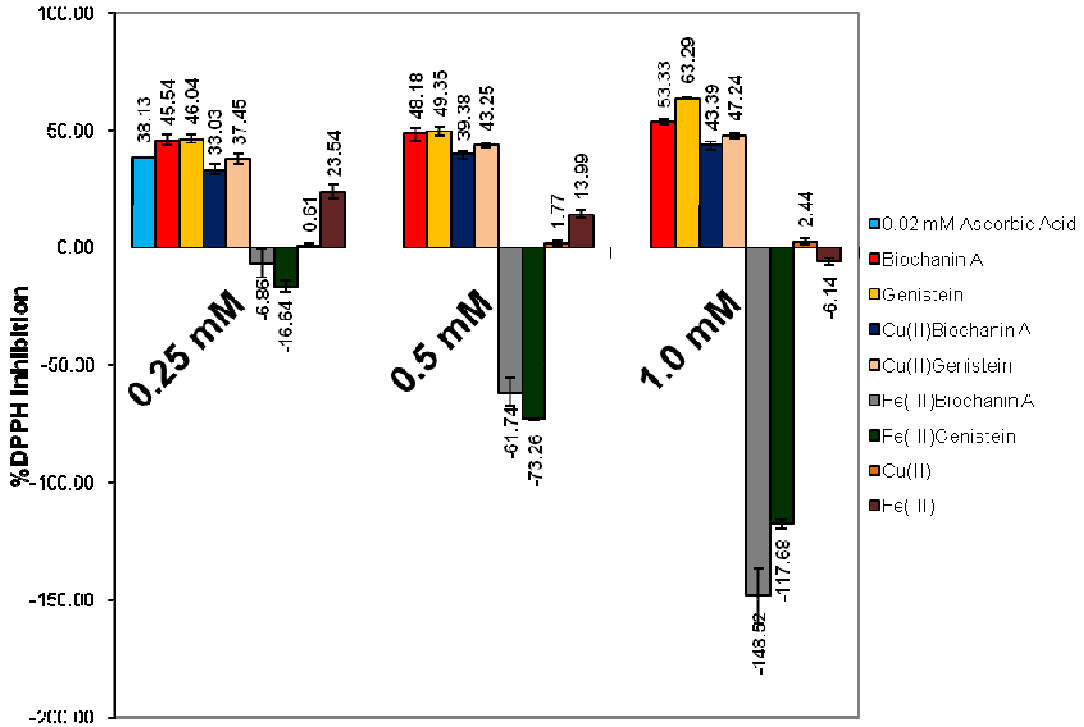

Fig. 6.9 DPPH inhibition plots of isoflavone and metal chelates with 0.02 mM Ascorbic Acid (Note: First data bar is for 0.02 mM ascorbic acid). (Standard deviation based on n=3 replicates)

Table 6.4 DPPH ascorbic acid synergism liquid samples studies of 0.25 to 1.0 mM concentrations of isoflavones, isoflavone chelates, metal salts and antioxidant controls

Sample name	%DPPH Inhibition Rep1	%DPPH Inhibition Rep2	%DPPH Inhibition Rep3	%DPPH Inhibition Average	STDEV	RSD
DPPH 0.25 mM Biochanin A with 0.02 mM Ascorbic acid	47.28	46.13	43.21	45.54	2.10	4.61
DPPH 0.5 mM Biochanin A with 0.02 mM Ascorbic acid	47.97	50.82	45.73	48.18	2.55	5.30
DPPH 1.0 mM Biochanin A with 0.02 mM Ascorbic acid	53.41	52.05	54.54	53.33	1.25	2.34
DPPH 0.25 mM Genistein with 0.02 mM Ascorbic acid	44.30	46.35	47.47	46.04	1.61	3.49
DPPH 0.5 mM Genistein with 0.02 mM Ascorbic acid	49.72	47.27	51.05	49.35	1.92	3.89
DPPH 1.0 mM Genistein with 0.02 mM Ascorbic acid	63.08	63.07	63.72	63.29	0.37	0.59
DPPH 0.25 mM Cu(II)Biochanin A solid with 0.02 mM Ascorbic Acid	30.01	31.67	35.26	33.03	2.06	6.23
DPPH 0.5 mM Cu(II)Biochanin A solid with 0.02 mM Ascorbic Acid	35.79	38.10	40.88	39.38	1.52	3.86
DPPH 1.0 mM Cu(II)Biochanin A solid with 0.02 mM Ascorbic Acid	41.17	44.19	45.52	43.39	1.60	3.70
DPPH 0.25 mM Cu(II)Genistein solid with 0.02 mM Ascorbic Acid	27.23	32.68	35.99	37.45	2.30	6.14
DPPH 0.5 mM Cu(II)Genistein solid with 0.02 mM Ascorbic Acid	36.52	37.72	38.76	43.25	0.96	2.22
DPPH 1.0 mM Cu(II)Genistein solid with 0.02 mM Ascorbic Acid	40.02	40.58	41.88	47.24	1.03	2.19
DPPH 0.25 mM Fe(III)Biochanin A with 0.02 mM Ascorbic Acid	-14.04	-3.44	-3.09	-6.86	6.23	-90.78
DPPH 0.5 mM Fe(III)Biochanin A with 0.02 mM Ascorbic Acid	-68.88	-58.48	-57.85	-61.74	6.19	-10.03
DPPH 1.0 mM Fe(III)Biochanin A with 0.02 mM Ascorbic Acid	-161.77	-139.99	-143.80	-148.52	11.63	-7.83
DPPH 0.25 mM Fe(III)Genistein with 0.02 mM Ascorbic Acid	-19.57	-14.76	-15.59	-16.64	2.57	-15.43
DPPH 0.5 mM Fe(III)Genistein with 0.02 mM Ascorbic Acid	-73.02	-73.08	-73.70	-73.26	0.38	-0.51
DPPH 1.0 mM Fe(III)Genistein with 0.02 mM Ascorbic Acid	-115.82	-117.35	-119.85	-117.68	2.03	-1.73
DPPH 0.25 mM Cu(II) with 0.02 mM Ascorbic Acid	-0.48	1.50	0.82	0.61	1.01	164.75
DPPH 0.5 mM Cu(II) with 0.02 mM Ascorbic Acid	0.99	3.04	1.27	1.77	1.11	62.80
DPPH 1.0 mM Cu(II) with 0.02 mM Ascorbic Acid	2.84	3.29	1.19	2.44	1.11	45.47
DPPH 0.25 mM Fe(III) solid with 0.02 mM Ascorbic Acid	21.21	22.61	26.81	23.54	2.92	12.38
DPPH 0.5 mM Fe(III) solid with 0.02 mM Ascorbic Acid	13.92	12.38	15.66	13.99	1.64	11.74
DPPH 1.0 mM Fe(III) solid with 0.02 mM Ascorbic Acid	-5.37	-7.90	-5.13	-6.14	1.53	-25.01
DPPH 0.02 mM Ascorbic acid	37.75	39.52	37.13	38.13	1.24	3.24

6.5 Conclusion

The isoflavones metal chelates studied in this chapter have been shown to modulate antioxidant activity in comparison to that of isoflavones. The DPPH inhibition assay showed the prooxidant acitivty for the iron chelates and the antioxidant activity for the copper chelates. The presence of ascorbic acid within the assay for the liquid and solid samples confirmed that this antioxidant does not work synergistically with the copper chelates but did show some synergism with the iron chelates.

Isoflavones are weak antioxidants overall in comparison to positive controls, quercetin and ascorbic acid, showing DPPH inhibition of 95 to 97 % for quercetin and ascorbic acid and 4 to 11% for isoflavones biochanin A and genistein. The isoflavones show a synergistic effect with ascorbic acid giving DPPH values of 43 to 67 %. This shows that the antioxidant properties of isoflavones can be enhanced under the right conditions.

Cu(II) chelates overall showed a clear boost in antioxidant activity with respect to the free isoflavones with increasing antioxidant activity correlating with increasing concentration. The Cu(II) chelates of biochanin A and genistein show inhibition values in the region of 13 to 35 % in the liquid studies of the Cu(II) chelates. The Cu(II) chelate liquid studies in the ascorbic acid synergism studies revealed an increase in DPPH inhibition but were shown to be lower in comparison overall to the DPPH inhibition values of free isoflavones.

Fe(III) chelates showed heightened pro-oxidant activity in comparison to the free isoflavones. The pro-oxidant activity seems to be larger than the antioxidant activity of the Cu(II) chelates. The liquid and solid sample studies show increasing pro-oxidant activity with increasing concentration of iron chelate. The ascorbic acid synergism studies with the iron chelates show a reduction of pro-oxidant activity in the lower concentrations but this synergistic effect is not observed at 1.0 mM concentrations.

Cu(II) shows no modulation of DPPH inhibition overall but this is not to say it does not show some degree of interference with the antioxidant properties of ascorbic acid

in the synergism studies. Fe(III)nitrate salt show chelation with DPPH overall leading to the blue shifting of the radical peak from 515 nm to 492 nm. This may lead to false DPPH inhibition results being recorded.

Overall, the results collated here for the iron and copper chelates of biochanin A and Genistein are novel and have not been reported in any other literature to the knowledge of this author. This could lead to further understanding of how transition metal species such as Cu(II) and Fe(III) could affect soya isoflavones. It may also prove useful for predicting possible effects *in vivo* when using isoflavones for iron and copper disorders such as iron induced lipid peroxidation and Wilson's disease respectively.

Chapter 7: Conclusions and Future Work

7.1 Conclusion

7.1.1 FTIR analysis of foodstuffs and soil for the presence of germanium(IV) compounds and the identification of sample components

The FTIR analysis of foodstuffs for germaniun sesquioxide revealed that it could not be adequately distinguished from interferences due to presence of lipids, proteins and carbohydrates. The primary interference was from the C-O-C band associated with polysaccharides, mainly cellulose. There was a possibility for the identification of organic germanium compounds based on the analysis of the Ge-C band, which seemed to be free from interferences from foods based on the bands collated from the literature.

The FTIR analysis of soils for germanium sesquioxide revealed that it could not be distinguished due to interferences from the inorganic fraction of the soil, mainly from the Si-O band associated with a number of silicon based compounds such as silica and silicates. The other interferent was determined to be the C-O-C band from the cellulose of decaying plant matter present in the organic fraction of the soil.

The novelty of this study is that it is the first study of its kind to use FTIR spectroscopy to try and assign interferences for the identification of a Ge(IV) compound in foods and soils. The analysis of the soil for germanium sesquioxide is completely novel and has not been recorded in the literature so far.

7.1.2 Atomic absorption spectroscopy of Ge, Cu, Pb and Fe levels in foods and soils

The use of Atomic Absorption Spectroscopy (AAS) has identified that the levels of copper, lead and iron are satisfactory for soils in the Santry/Glasnevin area with respect to values given by the EPA. (Refer to section 3.4.1) The germanium levels were found to be 50 times higher than the average of 0.3-2.4 μg/g. The lack of an SRM for Ge made it difficult to assess if the values obtained for Ge were outside acceptable recovery limits. High RSD levels were observed between the digestions of the soil samples. The analysis of Cu, Pb, Ge and Fe in soils around the Santry/Glasnevin area is novel and has not been reported before in literature. The data may be useful for establishing environmental quality relative to the element studied.

The use of AAS in foods has identified that the levels of copper, iron and lead in food are within acceptable parameters for all of the foods studied. The Ge levels in the studied food were higher than that found by previous work carried out by this group by a factor of 10 [31]. This may be due to complications with interferents from sample digestion or complications with the GFAAS. The results for copper and iron levels in food will be of use in future stages of the research where the establishment of a relationship between total metal content in food and the percentage of metal sequestered by biomolecules present in the food samples can be established.

7.1.3 UV/Vis determinations of the stoichiometry of isoflavone metal chelates with Cu(II), Fe(III) and Ge(IV) compounds

Biochanin A and genistein showed chelation with Cu(II) and Fe(III) at a pH range of 4.0 – 9.0. Biochanin A and genistein did not chelate with Cd(II), Co(II), Pb(II), Ni(II), Zn(II), GeO_2 and germanium sesquioxide based on UV/Vis spectroscopy. Daidzein did not chelate with any of the studied metals whatsoever. These results represent the first successful chelation of Cu(II) and Fe(III) with genistein and Cu(II) with biochanin A. It is also the first attempt to assess if isoflavones can chelate with Ge(IV) compounds.

The chelation of biochanin A and genistein with Cu(II) over a pH range of 4.0-9.0 yielded M/L values of 1:1 and 1:2. The chelation of biochanin A and genistein with Cu(II) over a pH range of 4.0-9.0 yielded M/L values of 1:2 and 1:1. These are the first reported stoichiometries for biochanin A and genistein with Cu(II) and Fe(III) and have broad implications for the understanding of the interactions of these metals with isoflavones from an *in vitro* perspective.

The work done with isoflavone metal chelates is promising and is a good basis for a project based on flavonoid metal chelate research. It would also be interesting to further characterise these complexes and assess their presence in the foods studied so far in this project. The establishment of the health benefits of flavonoid metal chelates may also be of interest.

7.1.4 Synthesis and characterisation of isoflavone metal chelates

This study shows the partial structural characterisation and assessment of the antioxidant characteristics of isoflavone metal chelates. Isoflavones were found to bind with Cu(II) and Fe(III) with stoichiometries of 1:2 M/L ratios in methanol. Specifically, the isoflavones, biochanin A and genistein bind with Cu(II) and Fe(III) whereas daidzein was found not to chelate with any of the metals based upon UV/Vis studies. Further characterisation of the synthesised Cu(II) and Fe(III) chelates via FTIR, ESI-MS, TGA and elemental analysis confirmed the 1:2 M/L stoichiometries, indicating that the metals were binding at the 4-keto and 5-OH site of biochanin A and genistein and indicated the presence of chelated water.

The work here represents the first attempt at structural characterisation of Cu(II) genistein and Fe(III) isoflavone chelates of genistein and biochanin A. Full structural characterisation would only be possible using X-ray crystallography, if successful crystals were grown. Another area of the synthesis, where improvement is needed, was the purity levels of the synthesised isoflavone metal chelates but this can be recitified in future with better established methods such as the one described by Chen *et al.* [96] who managed to synthesise the chelates to a purity greater than 95 %.

7.1.5 Characterisation of antioxidant properties of flavonoid metal chelates using the DPPH inhibition assay

Isoflavones are weak antioxidants overall in comparison to the positive controls quercetin and ascorbic acid. These antioxidants are much greater in terms of overall antioxidant activity to the extent of showing 100 % inhibition for most of the studies.

Cu(II) chelates overall showed a clear boost in antioxidant activity with respect to the free isoflavones with increasing antioxidant activity correlating with increasing concentration. Fe(III) chelates showed heightened pro-oxidant activity in comparison to the free isoflavones. The pro-oxidant activity seems to be higher in scale than that of the antioxidant activity of the Cu(II) chelates.

The ascorbic acid synergism studies with the iron chelates show a reduction of pro-oxidant activity in the lower concentrations but this synergistic effect is not observed at 1.0 mM concentrations. The copper chelates with ascorbic acid show heightened antioxidant activity but do seem to inhibit the antioxidant activity of the ascorbic acid itself by an order of a few DPPH inhibition % units.

Cu(II) shows no modulation of DPPH inhibition overall but this is not to say it does not have some degree of interference with the antioxidant properties of ascorbic acid in the synergism studies. The Fe(III) nitrate salt shows chelation with DPPH additionally so any modifications in DPPH inhibition due to Fe(III) are questionable.

7.2 Future Work

The continuation of the research into the area of flavonoid metal chelate research is possible. The key area is to identify chelates with other transition metal species such as Cd(II) and Co(II). The UV/Vis studies (refer to chapter 4) previously showed no chelation but this cannot be used as an affirmative indicator without more indepth analysis via mass spectrometry.

Additionally, the work done in this project does show novelty in relation to the investigation of the stoichiometries of isoflavone metal chelates. The stoichiometry studies on chelation of copper and iron with isoflavones genistein and biochanin A disagreed with previously performed work in the field by Lurdes Mira *et al.*, who said that copper and iron atoms did not chelate with the isoflavones daidzein and genistein. [9]

The main areas that need to be considered in future work can be addressed by considering the nature of flavonoid metal chelates and how they interact with food. Also, this project has so far not addressed the antioxidant/therapeutic abilities of the compounds investigated. Thus, the future work areas can be refined as:

- The examination of metal stressing on soya products within isoflavone containing foods
- The investigation of germanium flavonoid chelates
- The investigation of other isoflavone metal chelates with other transition metal species

7.2.1 The examination of metal stressing on soya products with isoflavone containing foods

The effect of metals on the antioxidant properties was previously looked at for the isoflavone metal chelates in this project. It was seen that the metals influenced the antioxidant properties of the in a negative or a positive fashion. With these effects in mind, it would be interesting to look at the effect of metal stressing upon isoflavone containing foodstuffs using copper and iron with a possibility of including other biologically relevant transition metal species.

The effect of metal stressing upon flavonoids in foods has been documented by Lachman *et al.* where the effect of cadmium on flavonoid content in young barley was examined. The group found the flavonoid content was reduced with the highest found in the leaves then shoots then roots upon comparison to the control barley. It was hypothesised that the flavonoids were chelating with the free flavonoids and thus reducing the overall flavonoid content [251].

The studies could be extended by stressing with micromolar quantities of metal species, soybean products with a view to looking at processed varieties and if possible, trying to grow the soybean in tandem with the metals to see the effects of metal stressing over time and to identify where the greatest concentrations of metal are within the soy bean plant [182]. An examination of the effect of spiking the foods with isoflavones may also yield some interesting results [62].

7.2.2 The investigation of germanium flavonoid chelates

The making of germanium flavonoid chelates had been done previously by McMahon *et al.* [104]in relation to a novel way of complexing germanium c little or no UV/Vis spectrum. This group has done some mole ratio work with flavonoid metal chelates with germanium dioxide and germanium sesquioxide complexation with quercetin. It was found that the stoichiometry of the complexes were 1:1 at a pH of 8.0 in a 50:50 MeOH:Water solution. It was hypothesised that the chelation took place at the catechol site of the compound and may account for why the compounds never bound with the genistein, daidzein and biochanin A isoflavones as they did not possess this site.

There has not been much research performed into the area of germanium flavonoid compounds and as such it seems to be an exploitable area for research [207]. The properties of organic germanium compounds are well documented for antioxidant and immunomodulatory properties and so are flavonoids. It is proposed that synthesis and characterisation of flavonoid germanium complexes should be investigated for quercetin with germanium dioxide and germanium sesquioxide. The free radical savenging abilities of germanium compounds combined with that of flavonoids could lead to greatly improved antioxidant compounds.

7.2.3 The investigation of other isoflavones with other transition metal species

This thesis mainly concentrated on the interactions between copper and iron complexes whereas Chen *et al.* [200] have remarked successful chelation with other types of compounds including Zn(II), Cu(II), Ni(II), Co(II) and Mn(II) compounds of biochanin A or 4'-methoxy-5,7-dihydroxy-isoflavone. The group also achieved higher purity levels of 95 % or greater for most compounds.

It is proposed that future isoflavone chelates may be synthesised via this method as it shows better purity levels overall. There are differences in terms of temperatures utilised i.e. 40 ^{0}C for 1 h and 60 ^{0}C for 12 hours as opposed to the 15 min dissolution of the isoflavone ligand followed by the addition and stirring of the metal salt for an additional 90 min. The solvent utilised was ethanol as opposed to methanol also. The samples solids were also washed with ethanol [96].

To accomplish what has been described by Chen *et al.* [96], redoing the mole ratio and job plot determinations within ethanol may be an option for the copper and iron species with genistein and biochanin A. Synthesis of genistein metal chelates based upon Zn(II), Co(II), Ni(II) and Mn(II) would be of interest for this group as their antioxidant and other biological properties have not been assessed.

Literature Cited

1. Feng, Yi, Wu, Zhaohui, Zhou, Xuezhong, Zhou, Zhongmei, and Fan, Weiyu. Knowledge discovery in traditional Chinese medicine: State of the art and perspectives. Artificial Intelligence in Medicine 38[3], 219-236. 1-11-2006.

2. Coleman CI, Hebert JH, Reddy P. 2003. The effects of Panax ginseng on quality of life. *Journal of Clinical Pharmacy and Therapeutics* 28:5-15.

3. Fuente MDL, Victor V. 2000. Anti-oxidants as modulators of immune function. *Immunology and Cell Biology* 78:49-54.

4. Hughes DA. 2000. Dietary antioxidants and human immune function. *Nutrition Bulletin* 25:35-41.

5. Scheibmeir HD, Christensen K, Whitaker SH, Jegaethesan J, Clancy R, Pierce JD. 2005. A review of free radicals and antioxidants for critical care nurses. *Intensive and Critical Care Nursing* 21:24-28.

6. Gupta P, Su Zz, Lebedeva IV, Sarkar D, Sauane M, Emdad L, Bachelor MA, Grant S, Curiel DT, Dent P, Fisher PB. 2006. mda-7/IL-24: Multifunctional cancer-specific apoptosis-inducing cytokine. *Pharmacology & Therapeutics* 111:596-628.

7. Ladik J. 2000. Towards a unified theory of cancer initiation in the cell. *Journal of Molecular Structure: THEOCHEM* 504:1-11.

8. De Souza RFV, De Giovani WF. 2004. Antioxidant properties of complexes of flavonoids with metal ions. *Redox Rep* 9:97-104.

9. Mira L, Fernandez MT, Santos M, Rocha R, ncio MH, Jennings KR. 2002. Interactions of Flavonoids with Iron and Copper Ions: A Mechanism for their Antioxidant Activity. *Free Radical Res* 36:1199-1208.

10. Malesev D, Kuntic V. 2007. Investigation of metal-flavonoid chelates and the determination of flavonoids via metal-flavonoid complexing reactions. *J Serb Chem Soc* 72:921-939.

11. Bartlett H, Eperjesi F. 2004. An ideal ocular nutritional supplement? *Ophthalmic and Physiological Optics* 24:339-349.

12. Kaur C, Kapoor HC. 2001. Antioxidants in fruits and vegetables - the millennium's health. *International Journal of Food Science and Technology* 36:703-725.

13. Asai, K. Miracle Cure Organic Germanium. 1980. Tokyo, Japan Publications, Inc.

14. McKevith B, Kelly C, Stanner S, Hughes J, Buttriss J. 2003. The Food Standards Agency's antioxidants in food programme - a summary. *Journal of Human Nutrition and Dietetics* 16:257-263.

15. Rodriguez-Bernaldo de Quiros A, Costa HS. 2006. Analysis of carotenoids in vegetable and plasma samples: A review. *Journal of Food Composition and Analysis* 19:97-111.

16. Ewen JG, Surai P, Stradi R, Moller AP, Vittorio B, Griffiths R, Armstrong DP. 2006. Carotenoids, colour and conservation in an endangered passerine, the hihi or stitchbird (Notiomystis cincta). *Animal Conservation* 9:229-235.

17. Cesarini JP, Michel L, Maurette JM, Adhoute H, Bejot M. 2003. Immediate effects of UV radiation on the skin: modification by an antioxidant complex containing carotenoids. *Photodermatology, Photoimmunology and Photomedicine* 19:182-189.

18. Linan-Cabello MA, Medina-Zendejas R, Sanchez-Barajas M, Mena Herrera A. 2004. Effects of carotenoids and retinol in oocyte maturation of crayfish Cherax quadrucarinatus. *Aquaculture Research* 35:905-911.

19. Colgan HA, Floyd S, Noone EJ, Gibney MJ, Roche HM. 2004. Increased intake of fruit and vegetables and a low-fat diet, with and without low-fat plant sterol-enriched spread consumption: effects on plasma lipoprotein and carotenoid metabolism. *Journal of Human Nutrition and Dietetics* 17:561-569.

20. Porat Y, Abramowitz A, Gazit E. 2006. Inhibition of Amyloid Fibril Formation by Polyphenols: Structural Similarity and Aromatic Interactions as a Common Inhibition Mechanism. *Chemical Biology & Drug Design* 67:27-37.

21. Boveris Albe, Valdez Laur, Alvarez Silv. 2002. Inhibition by Wine Polyphenols of Peroxynitrite-Initiated Chemiluminescence and NADH Oxidation. *Annals of the New York Academy of Sciences* 957:90-102.

22. Yahiro K, Shirasaka D, Tagashira M, Wada A, Morinaga N, Kuroda F, Choi O, Inoue M, Aoyama N, Ikeda M, Hirayama T, Moss J, Noda M. 2005. Inhibitory Effects of Polyphenols on Gastric Injury by Helicobacter pylori VacA Toxin. *Helicobacter* 10:231-239.

23. Madhan B, Subramanian V, Rao JR, Nair BU, Ramasami T. 2005. Stabilization of collagen using plant polyphenol: Role of catechin. *International Journal of Biological Macromolecules* 37:47-53.

24. Ivanova E, Toshkova R, Serkedjieva J. 2005. A plant polyphenol-rich extract restores the suppressed functions of phagocytes in influenza virus-infected mice. *Microbes and Infection* 7:391-398.

25. Denny BJ, Lambert PA, West PWJ. 2002. The flavonoid galangin inhibits the L1 metallo-beta-lactamase from Stenotrophomonas maltophilia. *FEMS Microbiology Letters* 208:21-24.

26. Aherne SA, O'Brien NM. 2002. Dietary flavonols: chemistry, food content, and metabolism. *Nutrition* 18:75-81.

27. Croft KD. 1998. The Chemistry and Biological Effects of Flavonoids and Phenolic Acidsa. *Annals of the New York Academy of Sciences* 854:435-442.

28. Kostyuk VA, Potapovich AI, Vladykovskaya EN, Korkina LG, Afanas'ev IBA. 2001. Influence of Metal Ions on Flavonoid Protection against Asbestos-Induced Cell Injury. *Arch Biochem Biophys* 385:129-137.

29. Bucki R, Pastore JJ, Giraud F, Sulpice JC, Janmey PA. 2003. Flavonoid inhibition of platelet procoagulant activity and phosphoinositide synthesis. *Journal of Thrombosis and Haemostasis* 1:1820-1828.

30. Goodman S. 1988. Therapeutic effects of organic Germanium. *Medical Hypotheses* 26:207-215.

31. McMahon M, Regan F, Hughes H. 2006. The determination of total germanium in real food samples including Chinese herbal remedies using graphite furnace atomic absorption spectroscopy. *Food Chem* 97:411-417.

32. Yu KW, Murthy HN, Jeong CS, Hahn EJ, Paek KY. 2005. Organic germanium stimulates the growth of ginseng adventitious roots and ginsenoside production. *Process Biochemistry* 40:2959-2961.

33. Tsutsumi Y, Tanaka J, Kanamori H, Musashi M, Minami H, Fukushima A, Yamato H, Ehira N, Kawamura T, Obara S, Ogura N, Asaka M, Imamura M, Masauzi N. 2004. Effectiveness of propagermanium treatment in multiple myeloma patients. *European Journal of Haematology* 73:397-401.

34. Lee JH, Kim KW, Yoon MY, Lee JY, Kim CJ, Sim SS. 2005. Anti-inflammatory effect of germanium-concentrated yeast against paw oedema is related to the inhibition of arachidonic acid release and prostaglandin E2 production in RBL 2H3 cells. *Autonomic and Autacoid Pharmacology* 25:129-134.

35. LeMaster DM, Minnich M, Parsons PJ, Anderson JS, Hernandez G. 2006. Tetrathiolate coordination of germanium(IV) in a protein active site. *J Inorg Biochem* 100:1410-1412.

36. Hertog MGL, Hollman PCH, Katan MB. 1992. Content of potentially anticarcinogenic flavonoids of 28 vegetables and 9 fruits commonly consumed in the Netherlands. *J Agric Food Chem* 40:2379-2383.

37. Podsedek A. 2007. Natural antioxidants and antioxidant capacity of Brassica vegetables: A review. *LWT - Food Science and Technology* 40:1-11.

38. Tripathi R, Mohan H, Kamat JP. 2007. Modulation of oxidative damage by natural products. *Food Chem* 100:81-90.

39. Shamberger RJ. 1981. Selenium in the environment. *The Science of The Total Environment* 17:59-74.

40. Buttriss JL, Hughes J, Kelly CNM, Stanner S. 2002. Antioxidants in food: a summary of the review conducted for the Food Standards Agency. *Nutrition Bulletin* 27:227-236.

41. Attele AS, Wu JA, Yuan CS. 1999. Ginseng pharmacology: Multiple constituents and multiple actions. *Biochemical Pharmacology* 58:1685-1693.

42. Schlag EM, McIntosh MS. 2006. Ginsenoside content and variation among and within American ginseng (Panax quinquefolius L.) populations. *Phytochemistry* 67:1510-1519.

43. Feng-Jie L, Ai-Hua Z, Yong-Hua X, Lian-Xue Z. 2010. Allelopathic effects of ginsenosides on in vitro growth and antioxidant enzymes activity of ginseng callus. *Allelopathy Journal* 26:13-22.

44. Chang CH, Lin HY, Chang CY, Liu YC. 2006. Comparisons on the antioxidant properties of fresh, freeze-dried and hot-air-dried tomatoes. *Journal of Food Engineering* 77:478-485.

45. Toor RK, Savage GP. 2005. Antioxidant activity in different fractions of tomatoes. *Food Research International* 38:487-494.

46. Dewanto V, Wu X, Adom KK, Liu RH. 2002. Thermal Processing Enhances the Nutritional Value of Tomatoes by Increasing Total Antioxidant Activity. *J Agric Food Chem* 50:3010-3014.

47. Melindez-Martinez AJ, Fraser PD, Bramley PM. 2010. Accumulation of health promoting phytochemicals in wild relatives of tomato and their contribution to in vitro antioxidant activity. *Phytochemistry* 71:1104-1114.

48. Wongmekiat O, Thamprasert K. 2005. Investigating the protective effects of aged garlic extract on cyclosporin-induced nephrotoxicity in rats. *Fundamental and Clinical Pharmacology* 19:555-562.

49. Navas PB, Carrasquero-Duran A, Flores I. 2006. Effect of black tea, garlic and onion on corn oil stability and fatty acid composition under accelerated oxidation. *International Journal of Food Science and Technology* 41:243-247.

50. Balasenthil S, Arivazhagan S, Ramachandran CR, Nagini S. 1999. Effects of Garlic on 7,12-Dimethylbenz[a]anthracene-Induced Hamster Buccal Pouch Carcinogenesis. *Cancer Detection & Prevention* 23:534-538.

51. McNulty CAM, Wilson MP, Havinga W, Johnston B, O'Gara EA, Maslin DJ. 2001. A Pilot Study to Determine the Effectiveness of Garlic Oil Capsules in the Treatment of Dyspeptic Patients with Helicobacter pylori. *Helicobacter* 6:249-253.

52. Naznin MT, Maeda T, Morita N. 2010. Antioxidant Functions of E AND Z-Ajoene Derived from Japanese Garlic. *International Journal of Food Properties* 13:821-829.

53. Shon MY, Choi SD, Kahng GG, Nam SH, Sung NJ. 2004. Antimutagenic, antioxidant and free radical scavenging activity of ethyl acetate extracts from white, yellow and red onions. *Food and Chemical Toxicology* 42:659-666.

54. Zurada JM, Kriegel D, Davis IC. 2006. Topical treatments for hypertrophic scars. *Journal of the American Academy of Dermatology* 55:1024-1031.

55. Santas J, Almajano MP, Carbo R. 2010. Antimicrobial and antioxidant activity of crude onion (Allium cepa, L.) extracts. *International Journal of Food Science and Technology* 45:403-409.

56. Fournier DB, Erdman JW, Gordon GB. 1998. Soy, its components, and cancer prevention: a review of the in vitro, animal, and human data. *Cancer Epidemiology Biomarkers & Prevention* 7:1055-1065.

57. Murphy PA, Song T, Buseman G, Barua K. 1997. Isoflavones in Soy-Based Infant Formulas. *J Agric Food Chem* 45:4635-4638.

58. Khetarpaul N, Grewal RB, Goyal R, Garg R. 2004. Development of partially defatted soy flour and dhal. *Food Chem* 87:355-359.

59. Achouri A, Boye JI, Belanger D. 2005. Soybean isoflavones: Efficacy of extraction conditions and effect of food type on extractability. *Food Research International* 38:1199-1204.

60. Singh HB, Singh BN, Singh SP, Nautiyal CS. 2010. Solid-state cultivation of Trichoderma harzianum NBRI-1055 for modulating natural antioxidants in soybean seed matrix. *Bioresource Technology* 101:6444-6453.

61. Suhaj M. 2006. Spice antioxidants isolation and their antiradical activity: a review. *Journal of Food Composition and Analysis* 19:531-537.

62. Luthria DL, Biswas R, Natarajan S. Comparison of extraction solvents and techniques used for the assay of isoflavones from soybean. *Food Chem* In Press, Corrected Proof.

63. Murphy PA, Barua K, Hauck CC. 2002. Solvent extraction selection in the determination of isoflavones in soy foods. *Journal of Chromatography B* 777:129-138.

64. Li BB, Smith B, Hossain M. 2006. Extraction of phenolics from citrus peels: II. Enzyme-assisted extraction method. *Separation and Purification Technology* 48:189-196.

65. Owen RW, Haubner R, Mier W, Giacosa A, Hull WE, Spiegelhalder B, Bartsch H. 2003. Isolation, structure elucidation and antioxidant potential of the major phenolic and flavonoid compounds in brined olive drupes. *Food and Chemical Toxicology* 41:703-717.

66. Dopico-Garcia MS, Lopez-Vilarino JM, Gonzalez-Rodriguez MV. 2005. Determination of antioxidants by solid-phase extraction method in aqueous food simulants. *Talanta* 66:1103-1107.

67. Juntachote T, Berghofer E, Bauer F, Siebenhandl S. 2006. The application of response surface methodology to the production of phenolic extracts of lemon grass, galangal, holy basil and rosemary. *International Journal of Food Science and Technology* 41:121-133.

68. Bezerra MA, Santelli RE, Oliveira EP, Villar LS, Escaleira LA. 2008. Response surface methodology (RSM) as a tool for optimization in analytical chemistry. *Talanta* 76:965-977.

69. Santoso J, Yoshie-Stark Y, Suzuki T. 2004. Anti-oxidant activity of methanol extracts from Indonesian seaweeds in an oil emulsion model. *Fisheries Science* 70:183-188.

70. Row KH, Jin Y. 2006. Recovery of catechin compounds from Korean tea by solvent extraction. *Bioresource Technology* 97:790-793.

71. Ferruzzi MG, Green RJ. 2006. Analysis of catechins from milk-tea beverages by enzyme assisted extraction followed by high performance liquid chromatography. *Food Chem* 99:484-491.

72. Sudjaroen Y, Haubner R, Wurtele G, Hull WE, Erben G, Spiegelhalder B, Changbumrung S, Bartsch H, Owen RW. 2005. Isolation and structure elucidation of phenolic antioxidants from Tamarind (Tamarindus indica L.) seeds and pericarp. *Food and Chemical Toxicology* 43:1673-1682.

73. Salo-Vaananen P, Ollilainen V, Mattila P, Lehikoinen K, Salmela-Molsa E, Piironen V. 2000. Simultaneous HPLC analysis of fat-soluble vitamins in selected animal products after small-scale extraction. *Food Chem* 71:535-543.

74. Bruggemann O, Visnjevski A, Burch R, Patel P. 2004. Selective extraction of antioxidants with molecularly imprinted polymers. *Anal Chim Acta* 504:81-88.

75. Rochfort S, Caridi D, Stinton M, Trenerry VC, Jones R. 2006. The isolation and purification of glucoraphanin from broccoli seeds by solid phase extraction and preparative high performance liquid chromatography. *Journal of Chromatography A* 1120:205-210.

76. Chen LJ, Zhao X, Plummer S, Tang J, Games DE. 2005. Quantitative determination and structural characterization of isoflavones in nutrition supplements by liquid chromatography-mass spectrometry. *Journal of Chromatography A* 1082:60-70.

77. Yang S, Zhou X, Xu Y. 2005. Determination of Genistein and Daidzein in Human Plasma by Liquid Chromatography and Tandem Mass Spectrometry. *Journal of Liquid Chromatography & Related Technologies* 27:481-499.

78. Pereira RMS, Andrades NED, Paulino N, Sawaya ACHF, Eberlin MN, Marcucci MC, Favero GM, Novak EM, Bydlowski SP. 2007. Synthesis and characterization of a metal complex containing naringin and Cu, and its antioxidant, antimicrobial, antiinflammatory and tumor cell cytotoxicity. *Molecules* 12:1352-1366.

79. Deng HT, Van Berkel GJ. 1998. Electrospray mass spectrometry and UV/visible spectrophotometry studies of Aluminum(III)-flavonoid complexes. *J Mass Spectrom* 33:1080-1087.

80. Fernandez MT, Mira ML, Florencio MH, Jennings KR. 2002. Iron and copper chelation by flavonoids: an electrospray mass spectrometry study. *J Inorg Biochem* 92:105-111.

81. Gallignani M, Brunetto MdR. 2004. Infrared detection in flow analysis -- developments and trends (review). *Talanta* 64:1127-1146.

82. Torreggiani A, Tamba M, Trinchero A, Bonora S. 2005. Copper(II)-Quercetin complexes in aqueous solutions: spectroscopic and kinetic properties. *J Mol Struct* 744-747:759-766.

83. Mello LD, Pereira RMS, Sawaya ACHF, Eberlin MN, Kubota LT. 2007. Electrochemical and spectroscopic characterization of the interaction between DNA and Cu(II)-naringin complex. *Journal of Pharmaceutical and Biomedical Analysis* 45:706-713.

84. de Souza RFV, Sussuchi EM, De Giovani WF. 2003. Synthesis, electrochemical, spectral, and antioxidant properties of complexes of flavonoids with metal ions. *Synth React Inorg Met -Org Chem* 33:1125-1144.

85. Torreggiani A, Trinchero A, Tamba M, Taddei P. 2005. Raman and pulse radiolysis studies of the antioxildant properties of quercetin: Cu(II) chelation and oxidizing radical scavenging. *J Raman Spectrosc* 36:380-388.

86. Souza RFV, De Giovani WF. 2005. Synthesis, spectral and electrochemical properties of Al(III) and Zn(II) complexes with flavonoids. *Spectrochim Acta, Part A* 61:1985-1990.

87. Torreggiani A, Jurasekova Z, Sanchez-Cortes S, Tamba M. 2008. Spectroscopic and pulse radiolysis studies of the antioxidant properties of (+)catechin: metal chelation and oxidizing radical scavenging. *J Raman Spectrosc* 39:265-275.

88. Liggins J, Bluck LJC, Runswick S, Atkinson C, Coward WA, Bingham SA. 2000. Daidzein and genistein content of fruits and nuts. *J Nutr Biochem* 11:326-331.

89. Klejdus B, Mikelova R, Petrlova J, Potesil D, Adam V, Stiborova M, Hodek P, Vacek J, Kizek R, Kuban V. 2005. Evaluation of Isoflavone Aglycon and Glycoside Distribution in Soy Plants and Soybeans by Fast Column High-Performance Liquid Chromatography Coupled with a Diode-Array Detector. *J Agric Food Chem* 53:5848-5852.

90. Jungbluth G, Ruhling I, Ternes W. 2000. Oxidation of flavonols with Cu(II), Fe(II) and Fe(III) in aqueous media. *Journal of the Chemical Society-Perkin Transactions 2* 1946-1952.

91. Weber G. 1988. HPLC with electrochemical detection of metal-flavonoid-complexes isolated from food. *Chromatographia* 26:133-138.

92. Zhang Dq, Ni ZM. 1996. Separation and determination of trace inorganic germanium in [beta]-carboxyethylgermanium sesquioxide by filtration chromatography and hydride generation-graphite furnace atomic absorption spectrometry. *Anal Chim Acta* 330:53-58.

93. Leopoldini M, Russo N, Chiodo S, Toscano M. 2006. Iron Chelation by the Powerful Antioxidant Flavonoid Quercetin. *J Agric Food Chem* 54:6343-6351.

94. Davis BD, Brodbelt JS. 2004. Determination of the glycosylation site of flavonoid monoglucosides by metal complexation and tandem mass spectrometry. *Journal of the American Society for Mass Spectrometry* 15:1287-1299.

95. Leopoldini M, Russo N, Chiodo S, Toscano M. 2006. Iron Chelation by the Powerful Antioxidant Flavonoid Quercetin. *J Agric Food Chem* 54:6343-6351.

96. Chen X, Tang LJ, Sun YN, Qiu PH, Liang G. 2010. Syntheses, characterization and antitumor activities of transition metal complexes with isoflavone. *J Inorg Biochem* 104:379-384.

97. Coward L, Barnes NC, Setchell KDR, Barnes S. 1993. Genistein, daidzein, and their .beta.-glycoside conjugates: antitumor isoflavones in soybean foods from American and Asian diets. *J Agric Food Chem* 41:1961-1967.

98. Dixon RA, Ferreira D. 2002. Genistein. *Phytochemistry* 60:205-211.

99. Mazur W. 1998. 11 Phytoestrogen content in foods. *Bailliere's Clinical Endocrinology and Metabolism* 12:729-742.

100. Zhang LN, Cao P, Tan SH, Gu W, Shi L, Zhu HL. Synthesis and antimicrobial activities of 7-O-modified genistein derivatives. *European Journal of Medicinal Chemistry* In Press, Corrected Proof.

101. Swain JH, Alekel DL, Dent SB, Peterson CT, Reddy MB. 2002. Iron indexes and total antioxidant status in response to soy protein intake in perimenopausal women. *Am J Clin Nutr* 76:165-171.

102. Moridani MY, Pourahmad J, Bui H, Siraki A, O'Brien PJ. 2003. Dietary flavonoid iron complexes as cytoprotective superoxide radical scavengers. *Free Radical Biol Med* 34:243-253.

103. Kostyuk VA, Potapovich AI, Kostyuk TV, Cherian MG. 2007. Metal complexes of dietary flavonoids: Evaluation of radical scavenger properties and protective activity against oxidative stress in vivo. *Cellular and Molecular Biology* 53:62-69.

104. McMahon M. 2006. The Development of Novel Methods of Metal Determination with Emphasis on Germanium. Dublin City University; Waterford Institute of Technology.

105. Kaplan BJ, Andrus GM, Parish WW. 2004. Germane facts about germanium sesquioxide: II. Scientific error and misrepresentation. *Journal of Alternative and Complementary Medicine* 10:345-348.

106. Gerber GB, Leonard A. 1997. Mutagenicity, carcinogenicity and teratogenicity of germanium compounds. *Mutation Research/Reviews in Mutation Research* 387:141-146.

107. Thomas DW, Mahmood T, Lindahl CB. 2000. *Germanium and Germanium Compounds*. John Wiley & Sons, Inc..

108. Rochow EG. 1947. Organic Compounds of Germanium. The Direct Synthesis from Elementary Germanium. *J Am Chem Soc* 69:1729-1731.

109. Nagata N, Yoneyama T, Yanagida K, et a. 1985. Accumulation of germanium in the tissues of a long-term user of germanium preparation died of acute renal failure. *J Toxicol Sci* 10:333-341.

110. Okuda S, Kiyama S, Oh Y, et a. 1987. Persistent renal dysfunction induced by chronic intake of germanium-containing compounds. *Curr Ther Res , Clin Exp* 41:265-275.

111. Kaplan BJ, Parish WW, Andrus GM, Simpson JSA, Field CJ. 2004. Germane facts about germanium sesquioxide: I. Chemistry and anticancer properties. *Journal of Alternative and Complementary Medicine* 10:337-344.

112. Tsutsui M, Kakimoto N, Axtell DD, Oikawa H, Asai K. 1976. Crystal structure of "carboxyethylgermanium sesquioxide". *J Am Chem Soc* 98:8287-8289.

113. Lai YW, Kemsley EK, Wilson RH. 1994. Potential of Fourier Transform Infrared Spectroscopy for the Authentication of Vegetable Oils. *J Agric Food Chem* 42:1154-1159.

114. Abbott TP, Nabetani H, Sessa DJ, Wolf WJ, Liebman MN, Dukor RK. 1996. Effects of Bound Water on FTIR Spectra of Glycinin. *J Agric Food Chem* 44:2220-2224.

115. Lachenmeier DW. 2007. Rapid quality control of spirit drinks and beer using multivariate data analysis of Fourier transform infrared spectra. *Food Chem* 101:825-832.

116. Dogan A, Siyakus G, Severcan F. 2007. FTIR spectroscopic characterization of irradiated hazelnut (Corylus avellana L.). *Food Chem* 100:1106-1114.

117. Verma SK, Deb MK. 2007. Nondestructive and rapid determination of nitrate in soil, dry deposits and aerosol samples using KBr-matrix with diffuse

reflectance Fourier transform infrared spectroscopy (DRIFTS). *Anal Chim Acta* 582:382-389.

118. Viscarra Rossel RA, Walvoort DJJ, McBratney AB, Janik LJ, Skjemstad JO. 2006. Visible, near infrared, mid infrared or combined diffuse reflectance spectroscopy for simultaneous assessment of various soil properties. *Geoderma* 131:59-75.

119. McBratney AB, Minasny B, Viscarra Rossel R. 2006. Spectral soil analysis and inference systems: A powerful combination for solving the soil data crisis. *Geoderma* 136:272-278.

120. Kakimoto, N. Method for maintaining freshness of vegetables by increasing germanium content. [4,849,236]. 18-7-1989.

121. Linker R, Weiner M, Shmulevich I, Shaviv A. 2006. Nitrate Determination in Soil Pastes using Attenuated Total Reflectance Mid-infrared Spectroscopy: Improved Accuracy via Soil Identification. *Biosystems Engineering* 94:111-118.

122. Calderon FJ, McCarty GW, Reeves III JB. 2006. Pyrolisis-MS and FT-IR analysis of fresh and decomposed dairy manure. *Journal of Analytical and Applied Pyrolysis* 76:14-23.

123. Changwen D, Guiqin Z, Jianmin Z, Huoyan W, Xiaoqin C, Yuanhua D, Hui W. 2010. Characterization of animal manures using mid-infrared photoacoustic spectroscopy. *Bioresource Technology* 101:6273-6277.

124. Du C, Zhou J. 2009. Evaluation of soil fertility using infrared spectroscopy: a review. *Environmental Chemistry Letters* 7:97-113.

125. Cox RJ, Peterson HL, Young J, Cusik C, Espinoza EO. 2000. The forensic analysis of soil organic by FTIR. *Forensic Science International* 108:107-116.

126. Kacurkov M, Wilson RH. 2001. Developments in mid-infrared FT-IR spectroscopy of selected carbohydrates. *Carbohydrate Polymers* 44:291-303.

127. Schulz H, Baranska M. 2007. Identification and quantification of valuable plant substances by IR and Raman spectroscopy. *Vibrational Spectroscopy* 43:13-25.

128. Yang H, Irudayaraj J, Paradkar MM. 2005. Discriminant analysis of edible oils and fats by FTIR, FT-NIR and FT-Raman spectroscopy. *Food Chem* 93:25-32.

129. Downey G. 1998. Food and food ingredient authentication by mid-infrared spectroscopy and chemometrics. *TrAC Trends in Analytical Chemistry* 17:418-424.

130. Cerna M, Barros AS, Nunes A, Rocha SM, Delgadillo I, Copikova J, Coimbra MA. 2003. Use of FT-IR spectroscopy as a tool for the analysis of polysaccharide food additives. *Carbohydrate Polymers* 51:383-389.

131. Palma M, Barroso CG. 2002. Application of FT-IR spectroscopy to the characterisation and classification of wines, brandies and other distilled drinks. *Talanta* 58:265-271.

132. Kakimoto N, Akiba M, Takada T. 1985. Organogermanium Compounds .2. A Simple Synthesis of Substituted 3-Trichlorogermylpropanoic Acids and Esters by Regioselective Hydrogermylation. *Synthesis-Stuttgart* 272-274.

133. Schulz H, Baranska M. Identification and quantification of valuable plant substances by IR and Raman spectroscopy. *Vibrational Spectroscopy* In Press, Corrected Proof.

134. Belton PS, Kemsley EK, McCann MC, Ttofis S, Wilson RH, Delgadillo I. 1995. The identification of vegetable matter using Fourier Transform Infrared Spectroscopy. *Food Chem* 54:437-441.

135. Badr El-Din NK. 2004. Protective role of sanumgerman against [gamma]-irradiation-induced oxidative stress in Ehrlich carcinoma-bearing mice. *Nutrition Research* 24:271-291.

136. Coimbra MA, Barros An, Rutledge DN, Delgadillo I. 1999. FTIR spectroscopy as a tool for the analysis of olive pulp cell-wall polysaccharide extracts. *Carbohydrate Research* 317:145-154.

137. Simmonds RJ. 1992. *Chemistry of Biomolecules: An Introduction*. The Royal Society of Chemistry.

138. Lehninger AL, Nelson DL, Cox MM. 1993. *Principles of Biochemistry*. Worth Publishers.

139. Skoog DA, West DM, Holler J. 1996. *Fundamentals of Analytical Chemistry*. Saunders College Publishing.

140. Voet D, Voet JG. 1995. *Biochemistry*. John Wiley & Sons, Inc..

141. Lacroix M, Le TC, Ouattara B, Yu H, Letendre M, Sabato SF, Mateescu MA, Patterson G. 2002. Use of [gamma]-irradiation to produce films from whey, casein and soya proteins: structure and functionals characteristics. *Radiation Physics and Chemistry* 63:827-832.

142. Sewell SL, Rutledge RD, Wright DW. 2008. Versatile biomimetic dendrimer templates used in the formation of TiO2 and GeO2. *Dalton Trans* 3857-3865.

143. Gaudenzi S, Furfaro MG, Pozzi D, Silvestri I, Congiu Castellano A. 2003. Cell-metal interaction studied by cytotoxic and FT-IR spectroscopic methods. *Environmental Toxicology and Pharmacology* 14:51-59.

144. Guillen MD, Cabo N. 1997. Infrared spectroscopy in the study of edible oils and fats. *J Sci Food Agric* 75:1-11.

145. Zagonel GF, Peralta-Zamora P, Ramos LP. 2004. Multivariate monitoring of soybean oil ethanolysis by FTIR. *Talanta* 63:1021-1025.

146. Mossoba M, Kramer J, Milosevic V, Milosevic M, Azizian H. 2007. Interference of Saturated Fats in the Determination of Low Levels of trans Fats (below 0.5%) by Infrared Spectroscopy. *Journal of the American Oil Chemists' Society* 84:339-342.

147. Hassett JJ, Banwart WL. 1992. *Soils & Their Environment*. Prentice-Hall Inc..

148. Killham K. 1999. *Soil Ecology*. Cambridge University Press.

149. Szumera M, Waclawska I, Mozgawa W, Sitarz M. 2005. Spectroscopic study of biologically active glasses. *J Mol Struct* 744-747:609-614.

150. Schulz H, Baranska M. Identification and quantification of valuable plant substances by IR and Raman spectroscopy. *Vibrational Spectroscopy* In Press, Corrected Proof.

151. Linker R, Shmulevich I, Kenny A, Shaviv A. 2005. Soil identification and chemometrics for direct determination of nitrate in soils using FTIR-ATR mid-infrared spectroscopy. *Chemosphere* 61:652-658.

152. Soylak M, Saracoglu S, Tuzen M, Mendil D. 2005. Determination of trace metals in mushroom samples from Kayseri, Turkey. *Food Chem* 92:649-652.

153. Demirizen Dile, Aksoy Ahme. 2006. Heavy metal levels in vegetables in Turkey are within safe limits for Cu, Zn, Ni and exceeded for Cd AND Pb. *Journal of Food Quality* 29:252-265.

154. Fukushi K, Takeda S, Chayama K, Wakida SI. 1999. Application of capillary electrophoresis to the analysis of inorganic ions in environmental samples. *Journal of Chromatography A* 834:349-362.

155. Jinhui S, Kui J. 1995. Adsorptive complex catalytic polarographic determination of germanium in soils and vegetables. *Anal Chim Acta* 309:103-109.

156. Ebdon L, Evans EH, Fisher AS, ill SJ. 1998. *An Introduction to Analytical Atomic Spectrometry*. John Wiley & Sons Ltd..

157. McGrath D. Soil and Herbage Heavy Metal/Trace Element Variability and Relationships at Farm and Regional Level. Teagasc.

158. Lopez-Garcia I, Campillo N, rnau-Jerez I, Hernandez-Cordoba M. 2005. Electrothermal atomic absorption spectrometric determination of germanium in soils using ultrasound-assisted leaching. *Anal Chim Acta* 531:125-129.

159. Gomez-Ariza JL, Garcia-Barrera T, Lorenzo F, Bernal V, Villegas MJ, Oliveira V. 2004. Use of mass spectrometry techniques for the characterization of metal bound to proteins (metallomics) in biological systems. *Anal Chim Acta* 524:15-22.

160. Hseu ZY. 2004. Evaluating heavy metal contents in nine composts using four digestion methods. *Bioresource Technology* 95:53-59.

161. Hoenig M, de Kersabiec AM. 1996. Sample preparation steps for analysis by atomic spectroscopy methods: present status. *Spectrochimica Acta Part B: Atomic Spectroscopy* 51:1297-1307.

162. Hseu ZY, Chen ZS, Tsai CC, Tsui CC, Cheng SF, Liu CL, Lin HT. 2002. Digestion methods for total heavy metals in sediments and soils. *Water Air and Soil Pollution* 141:189-205.

163. Gaudino S, Galas C, Belli M, Barbizzi S, de Zorzi P, Jacimovic R, Jeran Z, Pati A, Sansone U. 2007. The role of different soil sample digestion methods on trace elements analysis: a comparison of ICP-MS and INAA measurement results. *Accreditation and Quality Assurance* 12:84-93.

164. Micó C, Peris M, nchez J, Recatalá L. 2008. Trace Element Analysis via Open-Vessel or Microwave-Assisted Digestion in Calcareous Mediterranean Soils. *Communications in Soil Science and Plant Analysis* 39:890-904.

165. Alvarado J, Leon LE, Lopez F, Lima C. 1988. Comparison of Conventional and Microwave Wet Acid Digestion Procedures for the Determination of Iron, Nickel and Vanadium in Coal by Electrothermal Atomization Atomic-Absorption Spectrometry. *Journal of Analytical Atomic Spectrometry* 3:135-138.

166. Ekholm P, Reinivuo H, Mattila P, Pakkala H, Koponen J, Happonen A, Hellstrom J, Ovaskainen ML. 2007. Changes in the mineral and trace element contents of cereals, fruits and vegetables in Finland. *Journal of Food Composition and Analysis* 20:487-495.

167. Dolan SP, Capar SG. 2002. Multi-element Analysis of Food by Microwave Digestion and Inductively Coupled Plasma-Atomic Emission Spectrometry. *Journal of Food Composition and Analysis* 15:593-615.

168. Erdogan S, Erdemoglu SB, Kaya S. 2006. Optimisation of microwave digestion for determination of Fe, Zn, Mn and Cu in various legumes by flame atomic absorption spectrometry. *J Sci Food Agric* 86:226-232.

169. Winefordner JD, Fitzgerald JJ, Omenetto N. 1975. Review of Multielement Atomic Spectroscopic Methods. *Applied Spectroscopy* 29:369-385.

170. Zheng N, Wang Q, Zheng D. 2007. Health risk of Hg, Pb, Cd, Zn, and Cu to the inhabitants around Huludao Zinc Plant in China via consumption of vegetables. *Science of The Total Environment* 383:81-89.

171. Nikkarinen M, Mertanen E. 2004. Impact of geological origin on trace element composition of edible mushrooms. *Journal of Food Composition and Analysis* 17:301-310.

172. Scherz H, Kirchhoff E. 2006. Trace elements in foods: Zinc contents of raw foods--A comparison of data originating from different geographical regions of the world. *Journal of Food Composition and Analysis* 19:420-433.

173. Mahmut C, Eiliv S, Marina VF, Torill ES, Svetlana D. 2006. Heavy Metal Pollution of Surface Soil in the Thrace Region, Turkey. *Environmental Monitoring and Assessment* V119:545-556.

174. Rucandio I, Petit D. 1999. Determination of cadmium in coal fly ash, soil and sediment samples by GFAAS with evaluation of different matrix modifiers. *Fresenius' Journal of Analytical Chemistry* V364:541-548.

175. Bacon JR, Hewitt IJ. 2005. Heavy metals deposited from the atmosphere on upland Scottish soils: Chemical and lead isotope studies of the association of metals with soil components. *Geochimica et Cosmochimica Acta* 69:19-33.

176. Legrand P, Turmel MC, Sauve S, Courchesne F. 2005. Speciation and bioavailability of trace metals (Cd, Cu, Ni, Pb, Zn) in the rhizosphere of contaminated soils. In Huang PM, Gobran GR, eds, *Biogeochemistry of Trace Elements in the Rhizosphere*, Elsevier, Amsterdam, pp 261-299.

177. Tao S, Liu WX, Chen YJ, Cao J, Li BG, Xu FL. 2005. Fractionation and bioavailability of copper, cadmium and lead in rhizosphere soil. In Huang PM, Gobran GR, eds, *Biogeochemistry of Trace Elements in the Rhizosphere*, Elsevier, Amsterdam, pp 313-336.

178. Brogan J, Crowe M, Carty G. Towards setting environmental quality objectives for soil, *Devloping a Soil Protection Strategy for Ireland.* Environmental Protection Agency Ireland.

179. Kabata-Pendias A, Pendias H. 2002. *Trace Elements in Soils and Plants*. CRC Press.

180. He ZL, Yang XE, Stoffella PJ. 2005. Trace elements in agroecosystems and impacts on the environment. *Journal of Trace Elements in Medicine and Biology* 19:125-140.

181. Chatterjee C, Gopal R, Dube BK. 2006. Impact of iron stress on biomass, yield, metabolism and quality of potato (Solanum tuberosum L.). *Scientia Horticulturae* 108:1-6.

182. Xiong ZT. 1998. Lead Uptake and Effects on Seed Germination and Plant Growth in a Pb Hyperaccumulator Brassica pekinensis Rupr. *Bull Environ Contam Toxicol* 60:285-291.

183. Motto HL, Daines RH, Chilko DM, Motto CK. 1970. Lead in soils and plants: its relation to traffic volume and proximity to highways. *Environ Sci Technol* 4:231-237.

184. Brun LA, Maillet J, Hinsinger P, Pepin M. 2001. Evaluation of copper availability to plants in copper-contaminated vineyard soils. *Environmental Pollution* 111:293-302.

185. Guo TR, Zhang GP, Zhang YH. 2007. Physiological changes in barley plants under combined toxicity of aluminum, copper and cadmium. *Colloids and Surfaces B: Biointerfaces* 57:182-188.

186. Dietary Reference Intakes (DRIs): Recommended Dietary Allowances and Adequate Intakes, Vitamins.

187. Yang Ll, Zhang Dq. 2002. Direct determination of germanium in botanical samples by graphite furnace atomic absorption spectrometry with palladium-zirconium as chemical modifier. *Talanta* 56:1123-1129.

188. Tao SH, Bolger PM. 1997. Hazard Assessment of Germanium Supplements. *Regulatory Toxicology and Pharmacology* 25:211-219.

189. Swennen B, Mallants A, Roels HA, Buchet JP, Bernard A, Lauwerys RR, Lison D. 2000. Epidemiological survey of workers exposed to inorganic germanium compounds. *Occup Environ Med* 57:242-248.

190. Mainwaring MG, Poor C, Zander DS, Harman E. 2000. Complete Remission of Pulmonary Spindle Cell Carcinoma After Treatment With Oral Germanium Sesquioxide. *Chest* 117:591-593.

191. Tarwadi K, Agte V. 2005. Antioxidant and micronutrient quality of fruit and root vegetables from the Indian subcontinent and their comparative performance with green leafy vegetables and fruits. *J Sci Food Agric* 85:1469-1476.

192. Fraga CG, Oteiza PI. 2002. Iron toxicity and antioxidant nutrients. *Toxicology* 180:23-32.

193. Ahamed M, Siddiqui MKJ. 2007. Low level lead exposure and oxidative stress: Current opinions. *Clinica Chimica Acta* 383:57-64.

194. Maduabuchi JMU, Nzegwu CN, Adigba EO, Aloke RU, Ezomike CN, Okocha CE, Obi E, Orisakwe OE. 2006. Lead and cadmium exposures from canned and non-canned beverages in Nigeria: A public health concern. *Science of The Total Environment* 366:621-626.

195. Ali M, Hahn EJ, Paek KY. 2006. Copper-induced changes in the growth, oxidative metabolism, and saponin production in suspension culture roots of Panax ginseng in bioreactors. *Plant Cell Reports* 25:1122-1132.

196. Tuzen M, Sesli E, Soylak M. 2007. Trace element levels of mushroom species from East Black Sea region of Turkey. *Food Control* 18:806-810.

197. Uriu-Adams JY, Keen CL. 2005. Copper, oxidative stress, and human health. *Mol Aspects Med* 26:268-298.

198. Bings NH, Bogaerts A, Broekaert JüAC. 2010. Atomic Spectroscopy: A Review. *Anal Chem* 82:4653-4681.

199. Jurd L, Geissman TA. 1956. Absorption Spectra of Metal Complexes of Flavonoid Compounds. *J Org Chem* 21:1395-1401.

200. Chen X, Tang LJ, Sun YN, Qiu PH, Liang G. 2010. Syntheses, characterization and antitumor activities of transition metal complexes with isoflavone. *J Inorg Biochem* 104:379-384.

201. Panhwar QK, Memon S, Bhanger MI. 2010. Synthesis, characterization, spectroscopic and antioxidation studies of Cu(II)-morin complex. *J Mol Struct* 967:47-53.

202. Birjees Bukhari S, Memon S, Mahroof Tahir M, Bhanger MI. 2008. Synthesis, characterization and investigation of antioxidant activity of cobalt-quercetin complex. *J Mol Struct* 892:39-46.

203. Record IR, Dreosti IE, McInerney JK. 1995. The antioxidant activity of genistein in vitro. *J Nutr Biochem* 6:481-485.

204. Liggins J, Bluck LJC, Coward WA, Bingham SA. 1998. Extraction and Quantification of Daidzein and Genistein in Food. *Anal Biochem* 264:1-7.

205. Cao G, Sofic E, Prior RL. 1997. Antioxidant and Prooxidant Behavior of Flavonoids: Structure-Activity Relationships. *Free Radical Biol Med* 22:749-760.

206. Wallace, Robert G. and Burong, Willfrits G. Extraction of flavonoids. [20030147980]. 2003. United States.

207. Garcia-Campana AM, Barrero FA, Gonzalez AL, Ceba MR. 2001. Non-ionic micellar solubilization -- spectrofluorimetric determination of trace of germanium(IV) with quercetin in real samples. *Anal Chim Acta* 447:219-228.

208. Zielonka J, Gebicki J, Grynkiewicz G. 2003. Radical scavenging properties of genistein. *Free Radical Biol Med* 35:958-965.

209. Cotton AF, Wilkinson G, Gaus PL. 1995. *Basic Inorganic Chemistry*. John Wiley & Sons, Inc..

210. G.Svehla. 1996. *Vogel's Qualitative Inorganic Analysis*. Longman.

211. Keung WM. 2001. Biogenic aldehyde(s) derived from the action of monoamine oxidase may mediate the antidipsotropic effect of daidzin. *Chemico-Biological Interactions* 130-132:919-930.

212. Kuo SM, Leavitt PS, Lin CP. 1998. Dietary flavonoids interact with trace metals and affect metallothionein level in human intestinal cells. *Biol Trace Elem Res* 62:135-153.

213. Ferrer E, Salinas Ma, Correa Ma, Naso L, Barrio D, Etcheverry S, Lezama L, Rojo T, Williams P. 2006. Synthesis, characterization, antitumoral and osteogenic activities of quercetin vanadyl(IV) complexes. *Journal of Biological Inorganic Chemistry* 11:791-801.

214. Bukhari SB, Memon S, Mahroof-Tahir M, Bhanger MI. 2009. Synthesis, characterization and antioxidant activity copper-quercetin complex. *Spectrochim Acta, Part A* 71:1901-1906.

215. Ungar Y, Osundahunsi OF, Shimoni E. 2003. Thermal Stability of Genistein and Daidzein and Its Effect on Their Antioxidant Activity. *J Agric Food Chem* 51:4394-4399.

216. Mingxiong Tan, Jinchan Zhu, Yingming Pan, Zhenfeng Chen, Hong Liang, Huagang Liu, Hengshan Wang. 2009. Synthesis, Cytotoxic Activity, and DNA Binding Properties of Copper (II) Complexes with Hesperetin, Naringenin, and Apigenin. *Bioinorg Chem Appl* 2009.

217. Nowak D, Ku+¦niar A, Kopacz M. 2010. Solid complexes of iron(II) and iron(III) with rutin. *Structural Chemistry* 21:323-330.

218. Satterfield M, Brodbelt JS. 2000. Enhanced Detection of Flavonoids by Metal Complexation and Electrospray Ionization Mass Spectrometry. *Anal Chem* 72:5898-5906.

219. Ni Y, Du S, Kokot S. 2007. Interaction between quercetin-copper(II) complex and DNA with the use of the Neutral Red dye fluorophor probe. *Anal Chim Acta* 584:19-27.

220. Bodini ME, Copia G, Tapia R, Leighton F, Herrera L. 1999. Iron complexes of quercetin in aprotic medium. Redox chemistry and interaction with superoxide anion radical. *Polyhedron* 18:2233-2239.

221. Fleck M, Petrosyan AM. 2009. Comments on papers reporting IR-spectra and other data of alleged L-alanine alaninium nitrate and L-alanine sodium nitrate crystals. *Crystal Research and Technology* 44:769-772.

222. El Hajji H, Nkhili E, Tomao V, Dangles O. 2006. Interactions of quercetin with iron and copper ions: Complexation and autoxidation. *Free Radical Res* 40:303-320.

223. Le Nest G, Caille O, Woudstra M, Roche S, Guerlesquin F, Lexa D. 2004. Zn-polyphenol chelation: complexes with quercetin, (+)-catechin, and derivatives: I optical and NMR studies. *Inorganica Chimica Acta* 357:775-784.

224. Teixeira S, Siquet C, Alves C, Boal I, Marques MP, Borges F, Lima JLFC, Reis S. 2005. Structure-property studies on the antioxidant activity of flavonoids present in diet. *Free Radical Biol Med* 39:1099-1108.

225. Kumamato M, Sonda T, Nagayama K, Tabata M. 2001. Effects of pH and Metal Ions on Antioxidative Activities of Catechins. *Bioscience, Biotechnology, and Biochemistry* 65:126-132.

226. Halliwell B. 1995. Antioxidant characterization : Methodology and mechanism. *Biochemical Pharmacology* 49:1341-1348.

227. Arora A, Nair MG, Strasburg GM. 1998. Antioxidant Activities of Isoflavones and Their Biological Metabolites in a Liposomal System. *Arch Biochem Biophys* 356:133-141.

228. van Acker SABE, van Balen GP, van den Berg D-J, Bast A, van der Vijgh WJF. 1998. Influence of iron chelation on the antioxidant activity of flavonoids. *Biochemical Pharmacology* 56:935-943.

229. Chen W, Sun S, cao W, Liang Y, Song J. 2009. Antioxidant property of quercetin-Cr(III) complex: The role of Cr(III) ion. *J Mol Struct* 918:194-197.

230. Parejo I, Codina C, Petrakis C, Kefalas P. 2000. Evaluation of scavenging activity assessed by Co(II)/EDTA-induced luminol chemiluminescence and DPPH+ (2,2-diphenyl-1-picrylhydrazyl) free radical assay. *Journal of Pharmacological and Toxicological Methods* 44:507-512.

231. Huang D, Ou B, Prior RL. 2005. The Chemistry behind Antioxidant Capacity Assays. *J Agric Food Chem* 53:1841-1856.

232. Yamaguchi T, Takamura H, Matoba T, Terao J. 1998. HPLC method for evaluation of the free radical-scavenging activity of foods by using 1,1-diphenyl-2-picrylhydrazyl. *Biosci Biotechnol , Biochem* 62:1201-1204.

233. Etcheverry S, Ferrer E, Naso L, Rivadeneira J, Salinas V, Williams P. 2008. Antioxidant effects of the VO(IV) hesperidin complex and its role in cancer chemoprevention. *Journal of Biological Inorganic Chemistry* 13:435-447.

234. R.J.Hamilton, J.C.Allen. 1999. *Rancidity In Foods.* Aspen.

235. Wang Y, Ma L, Li Z, Du Z, Liu Z, Qin J, Wang X, Huang Z, Gu L, Chen ASC. 2004. Synergetic inhibition of metal ions and genistein on [alpha]-glucosidase. *FEBS Lett* 576:46-50.

236. Hwang J, Sevanian A, Hodis HN, Ursini F. 2000. Synergistic inhibition of LDL oxidation by phytoestrogens and ascorbic acid. *Free Radical Biol Med* 29:79-89.

237. Foti P, Erba D, Riso P, Spadafranca A, Criscuoli F, Testolin G. 2005. Comparison between daidzein and genistein antioxidant activity in primary and cancer lymphocytes. *Arch Biochem Biophys* 433:421-427.

238. Leh F, Wan JKS. 1972. Organic Free-Radical and Metal-Complexes - 2,2-Diphenyl-1-Picrylhydrazyl with Cu(I). *Canadian Journal of Chemistry* 50:999-&.

239. Themelis D, Tzanavaras P, Kika F, Sofoniou M. 2001. Flow-injection manifold for the simultaneous spectrophotometric determination of Fe(II) and Fe(III) using 2,2'-dipyridyl-2-pyridylhydrazone and a single-line double injection approach. *Fresenius' Journal of Analytical Chemistry* 371:364-368.

240. Wu Y, Wang D. 2008. Structural Characterization and DPPH Radical Scavenging Activity of an Arabinoglucogalactan from Panax notoginseng Root. *J Nat Prod* 71:241-245.

241. Gao Z, Huang K, Yang X, Xu H. 1999. Free radical scavenging and antioxidant activities of flavonoids extracted from the radix of Scutellaria baicalensis Georgi. *Biochimica et Biophysica Acta (BBA) - General Subjects* 1472:643-650.

242. Kao TH, Chen BH. 2006. Functional Components in Soybean Cake and Their Effects on Antioxidant Activity. *J Agric Food Chem* 54:7544-7555.

243. Guo Q, Rimbach G, Moini H, Weber S, Packer L. 2002. ESR and cell culture studies on free radical-scavenging and antioxidant activities of isoflavonoids. *Toxicology* 179:171-180.

244. Halliwell B. 1978. Superoxide-dependent formation of hydroxyl radicals in the presence of iron chelates: Is it a mechanism for hydroxyl radical production in biochemical systems? *FEBS Lett* 92:321-326.

245. Apak R, Guclu K, Ozyurek M, Karademir SE. 2004. Novel Total Antioxidant Capacity Index for Dietary Polyphenols and Vitamins C and E, Using Their Cupric Ion Reducing Capability in the Presence of Neocuproine: CUPRAC Method. *J Agric Food Chem* 52:7970-7981.

246. Dekker AO, Dickinson RG. 1940. Oxidation of Ascorbic Acid by Oxygen with Cupric Ion as Catalyst. *J Am Chem Soc* 62:2165-2171.

247. Berger TM, Polidori MC, Dabbagh A, Evans PJ, Halliwell B, Morrow JD, Roberts LJ, Frei B. 1997. Antioxidant activity of vitamin C in iron-overloaded human plasma. *J Biol Chem* 272:15656-15660.

248. Botelho FV, varez-Leite JI, Lemos VS, Pimenta AMC, Calado HDR, Matencio T, Miranda CT, Pereira-Maia EC. 2007. Physicochemical study of floranol, its copper(II) and iron(III) complexes, and their inhibitory effect on LDL oxidation. *J Inorg Biochem* 101:935-943.

249. Gonzalez-Alvarez M, Alzuet G, Garcia-Gimenez JL, Macias B, Borras J. 2005. Biological activity of flavonoids copper complexes. *Z Anorg Allg Chem* 631:2181-2187.

250. Caillet S, Yu H, Lessard S, Lamoureux G, Ajdukovic D, Lacroix M. 2007. Fenton reaction applied for screening natural antioxidants. *Food Chem* 100:542-552.

251. Dudjak J, Lachman J, Miholova D, Kolihova D, Pivec V. 2004. Effect of cadmium on polyphenol content in young barley plants (Hordeum vulgare L.). *Plant Soil and Environment* 50:471-477.

APPENDIX 1: Paper publication